Università
di Genova

**Ph.D. program in Biotechnology in Translational Medicine**

**Curriculum: Cellular and Molecular Biotechnology**

**XXXVI CYCLE**

Doctoral thesis

# *Evaluation of metabolic and molecular alterations in Fanconi Anemia*


Author: Dr. Nadia Bertola

Coordinator: Prof. Paolo Malatesta

Tutor: Prof. Silvia Ravera

## Summary

# 1 Abstract

This thesis investigates the multifaceted metabolic landscape of Fanconi Anemia (FA), a rare genetic disorder characterized by defective DNA repair mechanisms. Through several analyses, it uncovers mitochondrial dysfunction in FA cells, resulting in impaired oxidative phosphorylation and heightened oxidative stress. The altered aerobic metabolism is associated with unbalanced mitochondrial dynamics, characterized by increased fission and decreased fusion. The study also reveals the ineffectiveness of antioxidant defenses in FA cells, which exacerbates cellular damage accumulation and contributes to the onset of aplastic anemia, a leading cause of mortality in FA patients. By targeting diverse metabolic pathways, including but not limited to histone deacetylase inhibition, mitochondrial fission inhibition, and antioxidant interventions, this study identifies potential therapeutic strategies to mitigate mitochondrial dysfunction, reduce oxidative stress, and delay aplastic anemia onset. Moreover, it delves into the inflammatory aspects of FA, revealing associations between oxidative stress, mitochondrial dysfunction, and systemic inflammation. Furthermore, the investigation extends to FA-associated head and neck squamous cell carcinomas, highlighting metabolic similarities with FA cells and suggesting novel therapeutic strategies for the management of this tumor in FA patients. Additionally, the study explores Schwachman-Diamond Syndrome, another rare genetic disease that results in aplastic anemia, revealing mitochondrial abnormalities and oxidative stress management challenges shared with those observed in FA. Through antioxidant interventions, mitochondrial function is restored, confirming the potential of antioxidant therapies in mitigating cellular damage in diseases causing aplastic anemia. Overall, this study underscores the importance of targeting mitochondrial dysfunctions, oxidative stress, inflammation, and mitochondrial dynamics to improve outcomes in FA, SDS, and related conditions, paving the way for personalized therapeutic interventions tailored to the unique genetic and metabolic features of affected patients. In conclusion, this thesis represents a paradigm shift in the study of FA, traditionally centered on DNA repair defects, by elucidating the multifactorial nature of the disease and the significance of metabolic dysfunctions. By unveiling profound mitochondrial abnormalities, inadequate antioxidant responses, and systemic inflammation, this research expands our understanding of FA pathogenesis beyond DNA repair deficiencies. Consequently, it pioneers innovative therapeutic strategies targeting metabolic pathways to mitigate cellular damage and delay disease progression.

# 2 Introduction

## 2.1 Fanconi Anemia

### 2.1.1 Clinical Features

Fanconi Anemia (FA) is a rare genetic syndrome, with an expected prevalence at birth of 1-5 in 160,000 individuals worldwide (ORPHA:84). It is associated with a variety of clinical manifestations, first described by pediatrician Guido Fanconi in 1927 [1]. The phenotype is characterized by low birth weight, microphthalmia, hypogonadism, congenital internal organs malformations, skeletal abnormalities (thumb and radius deformity), developmental defects, hearing failure, skin hypo- or hyper-pigmentation, and metabolic dysfunction susceptibility (e.g., diabetes and dyslipidemia). However, these anomalies can differ in extent or severity or may not be present [2], [3]. Progressive bone marrow failure (BMF) and the resulting aplastic anemia are the primary causes of morbidity and mortality in FA patients, with a 5000-fold increased risk compared to the general population [4]. BMF typically arises at a median age of 7 years [5], [6], and International Fanconi Anemia Registry (IFAR) and German Fanconi Anemia Registry (GEFA) clinical data indicate that nearly all FA patients will develop BMF by the age of 40 [7], [8]. The diagnosis is usually made after observing signs of pancytopenia (significant count reduction of platelets and red and white blood cells) [3]. Nevertheless, there are cases where the condition might not become apparent until adolescence or early adulthood, a period when the likelihood of developing acute myeloid leukemia (AML) and myelodysplastic syndromes (MDS) becomes particularly elevated [9]. As patients transition into adulthood, they face an increased susceptibility to the emergence of solid malignancies, the most common of which is squamous cell carcinoma within the oral cavity, namely Head and Neck Squamous Cell Carcinoma (HNSCC) [10]. When a diagnosis cannot be formulated based on clinical signs or pancytopenia, it is typically established only upon the onset of BMF [3]. However, early clinical diagnosis of the disease remains an ongoing challenge, highlighting the need for increased awareness among pediatricians and physicians of the clinical features associated with this syndrome, as well as the necessity of conducting prenatal or newborn testing to identify this condition promptly.

### 2.1.2 Genetic and molecular characteristics

Proteins encoded by FANC genes are involved in DNA repair processes and genomic stability. Precisely, they form a multi-subunit ubiquitin ligase complex involved in DNA interstrand crosslink (ICL) repair [11], [12], better described in Figure 1. Currently, a total of 22 genes associated with this DNA-repair pathway have been identified, also referred to as the FA/BRCA pathway (Figure 1 and Table 1) [13], [14]. More than 90% of patients present mutations within FANCA, FANCC, FANCG, or FANCD2 genes [4], [11], [15]. In most cases, the disease presents as autosomal recessive, with FANCA being the most frequently mutated gene worldwide, accounting for about two-thirds of cases [16], [17]. However, exceptions exist, such as FANCB, which exhibits X-linked inheritance [18], and

mutations in RAD51/FANCR, which have a dominant negative effect [19]. Pathogenic variants have been described in all 22 known FANC genes, resulting in different complementation groups [20]. The severity of the disease will be partially determined by the patient's specific complementation group and the inherited pathogenic genetic variants. Among these variants, biallelic mutations in FANC genes have been reported, which mutations have been associated with cancer predisposition, such as mutations in FANCD1 (BRCA2) and FANCN (PALB2), often found in AML, ovarian cancer, and neuroblastoma. Mutations in the remaining complementation groups have been primarily linked to AML and HNSCC [13], [21].

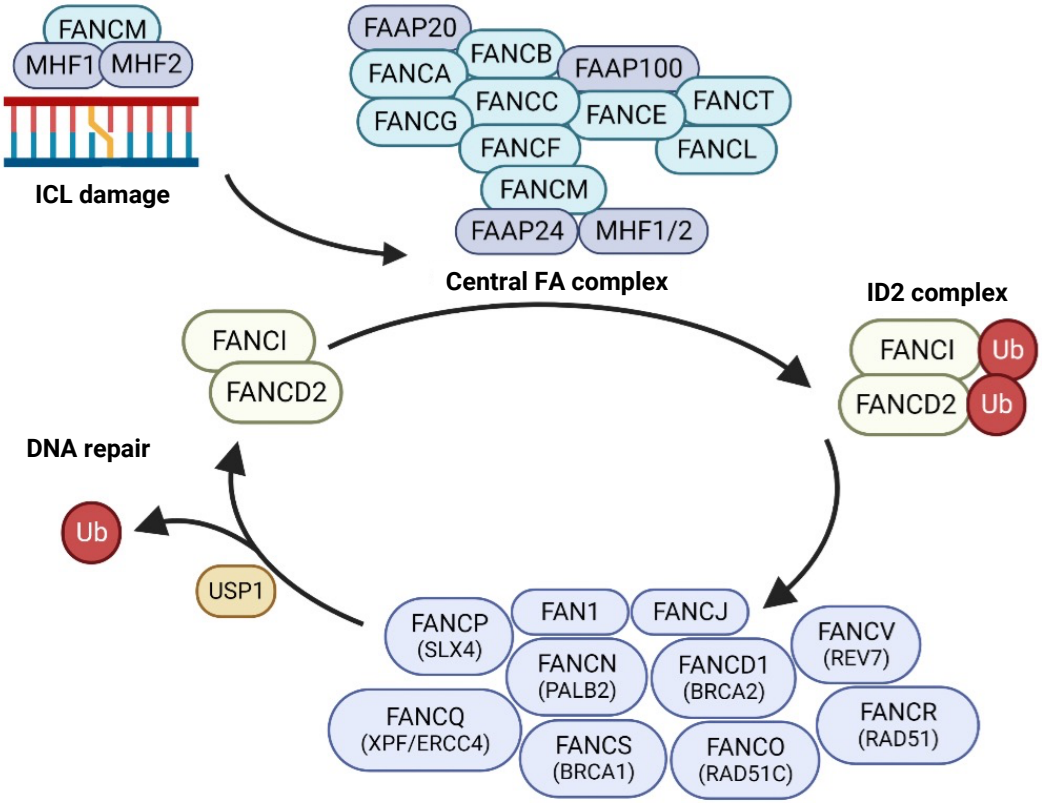


Figure 1 Scheme of DNA damage repair through the FA pathway. The FANCM-MHF1-MHF2 complex initially recognizes ILC damage. Activation of FANCM leads to recruitment, assembly, and phosphorylation of the central FA complex, composed of proteins FANCA, FANCB, FANCC, FANCE, FANCF, FANCG, FANCL, FANCM, FAAP20, FAAP24, and FAAP100. The central complex's role is to ensure activation of the E3 ubiquitin ligase for mono-ubiquitination of the ID2 complex, comprised of FANCD2 and FANCI proteins. This complex acts as the central hub of the FA pathway, promoting the recruitment of nucleases like FANCP, FANCQ, and FAN1 and facilitating final repair at the DNA damage site through homologous recombination. Pathway inactivation occurs through de-ubiquitination of the ID2 complex by the activity of the USP1 protein [13].

DNA ICLs occur when various exogenous or endogenous agents (e.g., mitomycin C, cisplatin; metabolic derivatives like acetaldehyde, formaldehyde, and malondialdehyde) react with two DNA nucleotides, forming a covalent bond between nucleotides on opposing DNA strands; this prevents the progression of DNA replication and transcription molecular machinery, blocking cells in G2/M phase. FANC genes mutations prevent the FANC-

associated repair system from properly repairing the damage caused by ICLs, resulting in genomic instability and chromosomal aberrations [22], [23].

| | | Gene | Alias | Frequency (%) | Molecular function |
|---|---|---|---|---|---|
| Mutated genes in FA patients | Central FA complex | FANCA | | 64 | Subcomplex with FANCG and FAAP20* |
| | | FANCB | | 2 | Subcomplex with FAAP100* and FANCL |
| | | FANCC | | 12 | Ternary complex with FANCE, FANCF, and FANCD2 |
| | | FANCE | | 1 | Central FA complex |
| | | FANCF | | 2 | Required for interaction between FANCA, FANCC, and FANCE |
| | | FANCG | XRCC9 | 8 | Subcomplex with FANCA and FAAP20*; complex with BRCA2, XRCC3 and FANCD2 |
| | | FANCL | | 0.4 | RING domain-containing ubiquitin E3 ligase |
| | | FANCM | | 0.1 | Damage recognition point; activation control and recruitment of the central FA complex |
| | | FANCT | UBE2T | 0.1 | Ubiquitin E2 ligase conjugation |
| | ID2 complex | FANCD2 | | 4 | ID2 complex; involved in ICL removal; multiple regulatory functions |
| | | FANCI | | 1 | ID2 complex; recruitment of components for ICL cleavage and damage repair |
| | FA/Homologous Recombination | FANCD1 | BRCA2 | 2 | HR; stimulation of RAD51 recombinase; stabilization of replication forks |
| | | FANCJ | BRIP1 | 2 | Interaction with BRCA1 to promote HR and inhibit TLS; ATPase and helicase activity |
| | | FANCN | PALB2 | 0.4 | HR; stimulation of RAD51 recombinase; stabilization of replication forks; link between BRCA1 and BRCA2 |
| | | FANCO | RAD51C | 0.1 | HR; homolog of RAD51 |
| | | FANCP | SLX4 | 0.5 | Main structural support and regulation of nucleases ERCC1-XPF, MUS81-EME1/2, and SLX1 during ICL cleavage |
| | | FANCR | RAD51 | rare | HR; stabilization of replication forks |
| | | FANCS | BRCA1 | 0.1 | HR; facilitates RAD51 activity along with BRCA2 and PALB2 |
| | | FANCU | XRCC2 | 0.1 | HR |
| | Recent | FANCV | REV7/ MAD2L2 | one patient | TLS polymerase activity, restoration of the fork after ICL cleavage |
| | | FANCW | RFWD3 | one patient | Ubiquitin E3 ligase activity for the regulation of RAD51 displacement during HR and ICL repair |
| | | FANCQ | ERCC4, XPF | 0.1 | Catalytic subunit during ICL cleavage; NER endonuclease |

Table 1 Classification of FA genes and their molecular functions. Abbreviations: FAAP: Fanconi anemia-associated proteins; HR: homologous recombination; ICL: interstrand crosslinks; NER: nucleotide excision repair; TLS: translesion synthesis. *FAAP genes are essential for ICL repair, but to date, no patients with biallelic mutations have been reported. Table adapted from [20], [24]. Each gene's (%) frequencies are estimates based on global data but may vary by country.

### 2.1.3 Treatment and Prevention

Currently, bone marrow transplantation (BMT) is the principal therapeutic approach for FA patients who develop severe aplastic anemia resulting from BMF, as well as MDS or AML [25]. However, BMT must be carefully evaluated in FA patients, as the transplant recipient

needs to undergo a conditioning regimen, which involves high-dose chemotherapy and/or radiation therapy to eliminate the existing bone marrow cells and suppress the immune system to prevent rejection of the donor cells. As described in the previous paragraph, the defect in the ICL repair system makes FA patients highly susceptible to DNA damage, and subjecting them to the pre-transplant conditioning regimen can be highly detrimental and further increase the predisposition to developing cancer.

To date, the primary available chemo-preventive treatment includes the administration of oral androgens like oxymetholone, capable of improving red blood cell and platelet counts in approximately 50% of FA patients, alone or in combination with a granulocyte colony-stimulating factor, which can enhance neutrophil counts. However, despite the possibility of delaying BMF, all these treatments come with potential associated toxicity [26], [27].

For this reason, other approaches for preventing BMF are being explored. Since various studies have demonstrated that the high sensitivity of hematopoietic progenitors to reactive oxygen species (ROS) is a critical factor in the pathogenesis of BMF in FA, therapy with antioxidant compounds is being explored. Specifically, quercetin, a natural and abundant antioxidant flavonoid, has been shown to be safe in the long term, well-tolerated, and capable of stabilizing blood levels in FA patients [28]. Moreover, in recent years, new strategies based on gene therapy have been developed, focusing on correcting the genetic defect in the patient's hematopoietic stem cells: this is achieved by introducing functional copies of the affected FANC gene using lentiviral vectors [29]. Other strategies, such as CRISPR/Cas9-mediated gene editing, have shown preclinical effectiveness in correcting the effects of truncating mutations. This technology allows targeted cuts near the mutation site and the reading frame to be repaired through non-homologous end-joining (NHEJ). This process has the potential to restore functional protein expression. While not suitable for all genetic diseases, it has been successful in FA cases, where corrected hematopoietic stem cells showed a proliferative advantage over uncorrected cells and improved survival when treated with mitomycin C [30], an alkylating drug causing DNA crosslink commonly used in FA diagnosis due to its capability to reveal DNA ICL damage hypersensitivity [31]. Despite the development of new strategies, BMT remains the first-line treatment for BMF in FA.

### 2.2 Metabolic dysfunctions

While the defective DNA repair system has been considered the main molecular hallmark of FA for decades, recent research has revealed other significant molecular mechanisms contributing to the disease pathogenesis: FA is also characterized by substantial metabolic alterations contributing to its pathogenesis and clinical manifestations. Specifically, FA metabolic dysfunctions appear to be related to mitochondria, essential double-membrane cellular organelles involved in energy production, regulation of cell death processes, calcium homeostasis, and signaling pathways. Mitochondria are also the cellular compartment home to the pyruvate dehydrogenase complex, citric acid cycle enzymes, as well as fatty acid β-oxidation, and amino acid oxidation pathways, which are all the nutrient

oxidation pathways except for glycolysis, which occurs in the cytosol. The metabolic alterations in FA extend beyond specific pathways and involve overall cellular metabolism. FA cells display an imbalance between energy production and consumption, leading to cellular energy depletion. This deficit affects various cellular processes, including DNA repair and replication, cell cycle progression, and overall cell growth and survival. The disrupted cellular metabolism in FA contributes to the disease phenotype, such as BMF and cancer predisposition [32].

### 2.2.1 Mitochondrial functional defects

The mitochondrial respiratory chain, also known as the electron transport chain (ETC), is a critical component of cellular energy production via oxidative phosphorylation (OxPhos), being responsible for generating the majority of ATP (adenosine triphosphate), the primary cells' energy source. ETC is composed of five protein complexes (Complex I, II, III, IV, and $F_oF_1$ ATP synthase) and two electron carriers (coenzyme Q or CoQ and cytochrome c), which are embedded within the inner mitochondrial membrane [33]. Figure 2 represents a schematic representation of the ECT and the electron flow through it, better described below.

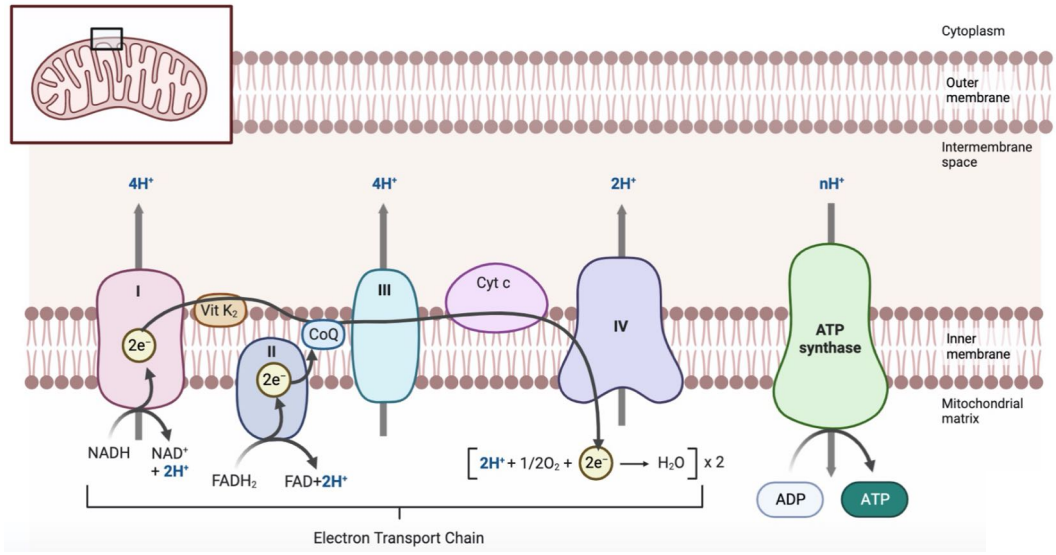


Figure 2 Schematic representation of the Electron Transport Chain and the electron flow through it.

The ATP production process begins with the electrons transfer from high-energy electron donors, such as NADH (Nicotinamide Adenine Dinucleotide) and $FADH_2$ (Flavin Adenine Dinucleotide), derived from catabolic pathways like fatty acid β-oxidation and tricarboxylic acid (TCA) cycle. NADH donates its electrons to Complex I (also known as NADH dehydrogenase), while $FADH_2$ donates its electrons to Complex II (also called succinate dehydrogenase). This process produces $NAD^+$ and FAD, which can be used again in other metabolic reactions. Complex I and II are electron carriers, both passing electrons to CoQ, a more mobile electron carrier. As electrons flow through these complexes, protons ($H^+$) are pumped across the inner mitochondrial membrane from the mitochondrial matrix to the intermembrane space. Next, electrons are transferred from CoQ to Complex III (also known

as cytochrome c oxidoreductase). Here, the electrons pass through several carrier proteins, ultimately leading to the transfer of electrons to cytochrome c (cyt c), another mobile carrier. Electrons are then transferred from cyt c to Complex IV (cytochrome oxidase). In this last step, oxygen ($O_2$) serves as the final electron acceptor and is combined with four electrons and four protons to form water ($H_2O$). The transfer of electrons through Complexes I, III, and IV causes the pumping of protons ($H^+$) across the inner mitochondrial membrane, creating a proton gradient, representing a significant potential energy source. Protons flow back into the mitochondrial matrix through the $F_oF_1$ ATP synthase, driving the rotation of a portion of the complex and catalyzing the bond between ADP (adenosine diphosphate) and inorganic phosphate to form ATP [34]. This process is highly efficient and produces large amounts of ATP, which the cell can use to sustain cellular functions and respond to the cell's energy demands [33]. The Phosphorylation to Oxygen ratio (P/O ratio) is a critical concept in bioenergetics that quantifies OxPhos efficiency. It provides insight into how efficiently the ECT couples the transfer of electrons to the synthesis of ATP. Specifically, it represents the number of ATP molecules synthesized per pair of electrons transferred through the ETC and used to reduce oxygen molecules to water. The theoretical maximum P/O ratio can be calculated based on the stoichiometry of the ETC complexes and the structure of the $F_oF_1$ ATP synthase. Efficient mitochondria with a coupled ECT have a P/O value of around 2.5 or 1.5 when pathways led respectively by complexes I or II are activated. A P/O ratio lower than these values suggests that mitochondria's ECT are uncoupled, and therefore, the oxygen is not entirely used for energy production but contributes to reactive oxygen species (ROS) production [35].

One of the critical aspects of mitochondrial dysfunction in FA is the defective ETC, specifically the impaired electron transport between respiratory Complexes I and III, uncoupling the ECT and disrupting the normal OxPhos process. The disrupted electron flow leads to reduced ATP production via OxPhos and a compensatory metabolic shift from aerobic respiration to anaerobic glycolysis. Consequently, FA cells experience energy deficits, which can affect various cellular processes requiring ATP, including DNA repair and replication, cell division, and overall cell growth [36], [37].

### 2.2.2 Uncoupling proteins

Uncoupling proteins (UCPs) are a family of mitochondrial inner membrane transporters that play a significant role in regulating energy metabolism and heat production in various tissues. The primary function of UCPs is to uncouple ECT, therefore, oxygen consumption from ATP synthesis. By allowing protons to re-enter the mitochondrial matrix without passing through ATP synthase, UCPs dissipate the proton gradient generated during the electron transport chain [38]. UCP1, prevalent in brown adipose tissue, is specialized for non-shivering thermogenesis, dissipating energy as heat: this is vital for maintaining body temperature in cold environments and newborns [39].

UCP2 and UCP3 are found in various tissues, including muscle, adipose tissue, and liver.

They are implicated in regulating energy balance, lipid metabolism, and glucose homeostasis. UCP2 has also been proposed to prevent excessive ROS production by dissipating the proton gradient and modulating mitochondrial membrane potential, thereby reducing the likelihood of electron leakage from the respiratory chain [40], [41], [42].

UCP2 is also considered a significant player in various pathological conditions, as it can influence cellular metabolism, energy balance, and ROS regulation, all contributing to disease progression. In cancer, UCP2 is implicated in metabolic reprogramming, as affecting the balance between glycolysis and OxPhos may provide a survival advantage to cancer cells, enabling them to thrive under stressful conditions. Furthermore, its ability to modulate ROS production by impacting mitochondrial membrane potential could influence oxidative stress levels within cancer cells. Indeed, moderate ROS are essential for cellular signaling, promoting cellular proliferation and survival, and potentially maintaining cells' viability under metabolic stress, such as nutrient deprivation or hypoxia.

Additionally, UCP2 has been linked to cancer metastasis and invasion. Its association with epithelial-mesenchymal transition (EMT), a critical step in metastasis, suggests that UCP2 could contribute to cancer's ability to spread to other parts of the body [43], [44], [45].

While the precise role of UCP2 is still the subject of active investigation, it holds promise as a key player in metabolic health and disease. UCP1's established role in thermogenesis contrasts with the complexity surrounding the functions of other UCPs in various tissues. Exploring UCP2 in the context of cancer reveals its potential as a therapeutic target for conditions involving dysregulation of mitochondrial metabolism.

### 2.2.3 Mitochondrial morphological defects

Mitochondria have always been described as individual organelles within cells. However, in living cells, they are fused to form a mitochondrial reticulum that increases oxidative phosphorylation efficiency. The mitochondrial reticulum is continuously remodeled through mitochondrial dynamics, composed of the processes of mitochondrial fusion and fission that play crucial roles in maintaining mitochondria's morphology, distribution, and function within cells. Moreover, these processes are essential to respond to cellular energy needs and for the elimination of depolarized or damaged mitochondria via selective autophagic removal (mitophagy) [46], [47], [48]. Dysregulation of mitochondrial dynamics has been implicated in various diseases, including neurodegenerative disorders, cardiovascular diseases, and cancer [49], [50]. Figure 3 represents a schematic representation of mitochondrial dynamics, better described below.

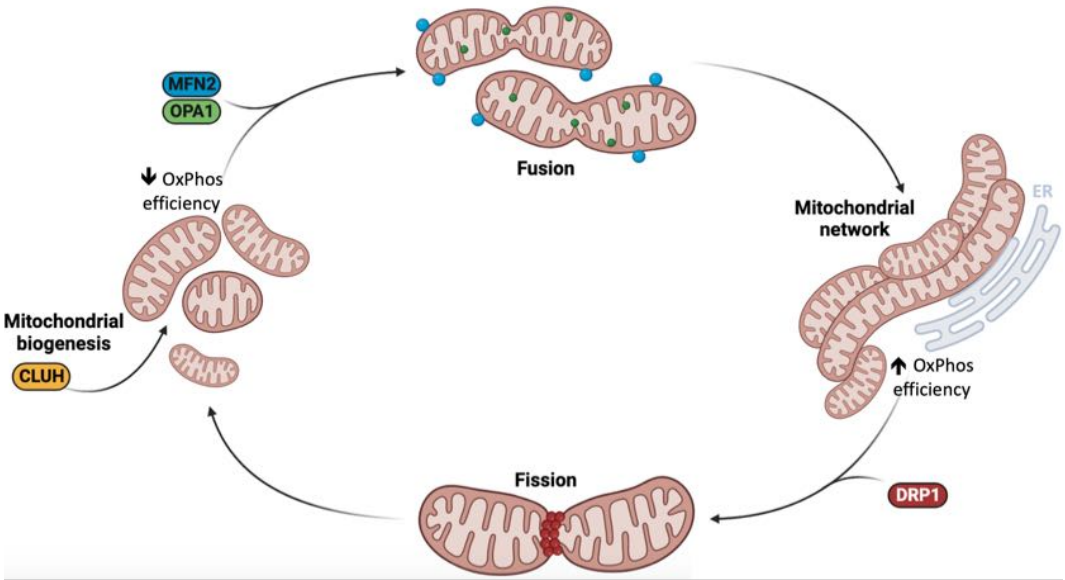


Figure 3 Mitochondrial dynamics schematic representation

Mitochondrial fusion involves merging two or more individual mitochondria to form a single, interconnected organelle. This process is facilitated by several proteins, including Mitofusins (MFN1 and MFN2) and OPA1 (Optic Atrophy 1). MFN proteins are found in the outer mitochondrial membrane and mediate the fusion of adjacent mitochondria. In contrast, OPA1, located in the inner mitochondrial membrane, is involved in the fusion of the mitochondrial cristae [46]. This process is essential for maintaining mitochondrial function and integrity: it allows the exchange of mitochondrial DNA (mtDNA), protein complexes, metabolites, and ions between mitochondria. It also helps to repair damaged mitochondria by combining healthy and damaged portions, rescuing their functions [48].

Mitochondrial fission consists of the opposite process by which a single mitochondrion divides into two or more smaller mitochondria. The main protein involved in this process is Dynamin-related protein 1 (DRP1), recruited from the cytosol to the mitochondrial outer membrane. DRP1 forms a spiral around the mitochondria and constricts them until fission occurs. Fission is essential for several cellular functions, including distributing mitochondria throughout the cell, segregating dysfunctional or depolarized mitochondria for mitophagic degradation, and facilitating apoptosis by generating small, fragmented mitochondria that release pro-apoptotic factors [46].

The balance between mitochondrial fusion and fission is tightly regulated and responsive to various cellular signals and stresses. It is influenced by post-translational modifications, such as phosphorylation and ubiquitination, and changes in cellular energy status and redox balance. Additionally, several signaling pathways, including the mammalian target of rapamycin (mTOR) pathway, play crucial roles in governing mitochondrial dynamics [51]. A disruption of this balance has been associated with various diseases, as impaired fusion or excessive fission can lead to fragmented and dysfunctional mitochondria, which are related to cellular dysfunction and apoptosis. Defects in mitochondrial fusion or fission have also been linked to abnormal accumulation of damaged mitochondria and the generation

of reactive oxygen species (ROS), contributing to cell death. In cancer, altered mitochondrial dynamics can impact tumor cell metabolism, growth, and resistance to therapy. Cancer cells often display increased fission, leading to fragmented mitochondria that promote a shift towards aerobic glycolysis (the Warburg effect) and enhanced cell proliferation [47], [50].

Understanding the intricate processes of mitochondrial dynamics is essential for gaining insights into cellular physiology and the pathogenesis of various diseases linked to dysregulated mitochondrial function, including FA, where these aspects have not been investigated before and where modulating mitochondrial dynamics could be a novel and promising therapeutic strategy [52], [53].

### 2.2.4 Autophagy and Mitophagy

Autophagy is a complex and highly regulated process strictly correlated with mitochondrial and membrane dynamics [54]. It involves the degradation of cellular components through the formation of specialized double-membrane vesicles called autophagosomes. These autophagosomes engulf a portion of cytoplasm, organelles, or protein aggregates and then fuse with lysosomes, which contain enzymes capable of breaking down the sequestered material. This degradation process provides cells with essential nutrients and helps to maintain cellular homeostasis [55]. Figure 4 is a schematic representation of autophagy, described in detail below.

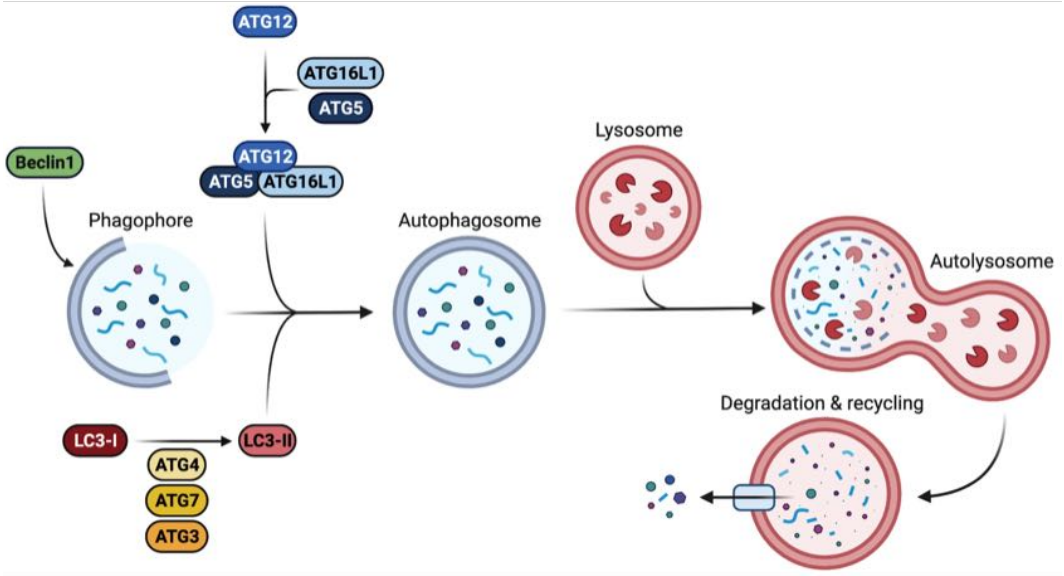


Figure 4 Autophagy schematic representation

Autophagy begins with the initiation of a structure called the phagophore or isolation membrane. This process is controlled by a complex network of autophagy-related genes (Atg genes) that regulate the assembly of protein complexes involved in autophagosome formation. The phagophore forms and elongates through the action of protein complexes recruited to specific subcellular locations. The class III phosphatidylinositol 3-kinase (PI3K) complex, including Beclin 1 [56], [57], is a crucial regulator of this nucleation step. The

phagophore expands around the targeted cargo, forming a double-membrane vesicle called an autophagosome and activating the LC3 protein [58]. The autophagosome then undergoes maturation, during which its outer membrane fuses with lysosomes. Lysosomes are membrane-bound organelles containing various hydrolytic enzymes. Once the autophagosome fuses with a lysosome, the contents of the autophagosome are exposed to the acidic and enzymatic environment within the lysosome: this leads to the degradation of the sequestered material into smaller molecules, such as amino acids, fatty acids, and sugars. These breakdown products are then transported from the lysosome and made available for cellular processes, including energy production and biosynthesis [59], [60].

Autophagy serves several critical cellular functions, allowing cells to adapt to various stress conditions by removing damaged or dysfunctional organelles, misfolded proteins, and protein aggregates, thus preventing cellular oxidative damage and toxicity and recycling cellular components to generate energy and maintain essential functions. Autophagy is also involved in processes such as embryonic development, tissue remodeling, and differentiation and participates in the elimination of intracellular pathogens and the presentation of antigens to immune cells. Several studies have correlated autophagy to cellular metabolism and mitochondria [61], [62]. Moreover, its dysregulation has been implicated in aging and various diseases, including neurodegenerative disorders, cancer, and metabolic diseases [63], [64], [65].

The selective autophagic elimination process of damaged, depolarized, or dysfunctional mitochondria is called mitophagy. It is a critical cellular process that maintains mitochondrial quality control, ensures the proper functioning of cells, and prevents the accumulation of dysfunctional mitochondria that can lead to oxidative stress, energy depletion, and various diseases [66].

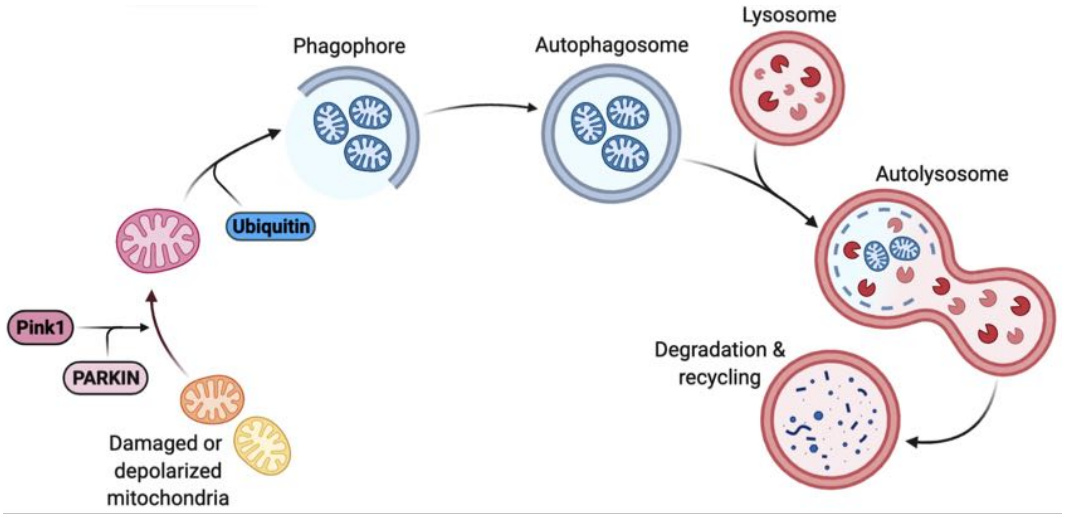


Figure 5 Mitophagy schematic representation

The process of mitophagy, schematically represented in Figure 5, involves several key steps, starting with recognizing and targeting damaged mitochondria. When mitochondria are damaged, PINK1 (PTEN-induced kinase 1) accumulates on their outer membrane,

recruiting Parkin, an E3 ubiquitin ligase enzyme. Parkin tags the damaged mitochondria with ubiquitin molecules, which act as signals for recognition and capture by the autophagosome, a double-membrane vesicle derived from a specialized membrane structure called the phagophore that engulfs cellular components for degradation. The autophagosome containing the damaged mitochondria fuses with lysosomes, cellular organelles filled with lytic enzymes, forming an autolysosome. Lysosomal enzymes break down the damaged mitochondria through enzymatic degradation within the autolysosome, releasing amino acids, fatty acids, and other building blocks that can be recycled by the cell to build new cellular components [66], [67].

Mitophagy is a finely regulated process that ensures a balance between removing damaged mitochondria and preserving healthy ones. Dysregulation of mitophagy has been implicated in various diseases, including neurodegenerative disorders (i.e., Parkinson's disease), cancer, and metabolic diseases. Understanding mitophagy has significant implications for developing therapies to target diseases that involve mitochondrial dysfunction and oxidative stress, such as FA.

### 2.2.5 FA metabolic shift toward glycolysis

Glycolysis is a central pathway in cellular metabolism that converts glucose into pyruvate, generating ATP and NADH in the process [68]. In FA, the defective mitochondrial electron transport and subsequent impaired OxPhos lead to an increased reliance on glycolysis for ATP production, even in oxygen presence, possibly as a compensatory response to the energy deficit caused by the dysfunctional mitochondria [69]. While glycolysis provides a rapid source of ATP, it is less efficient than OxPhos in generating energy [68], as shown in Figure 6. Moreover, relying on glycolysis for energy production is a hallmark of various cancer cells [70].

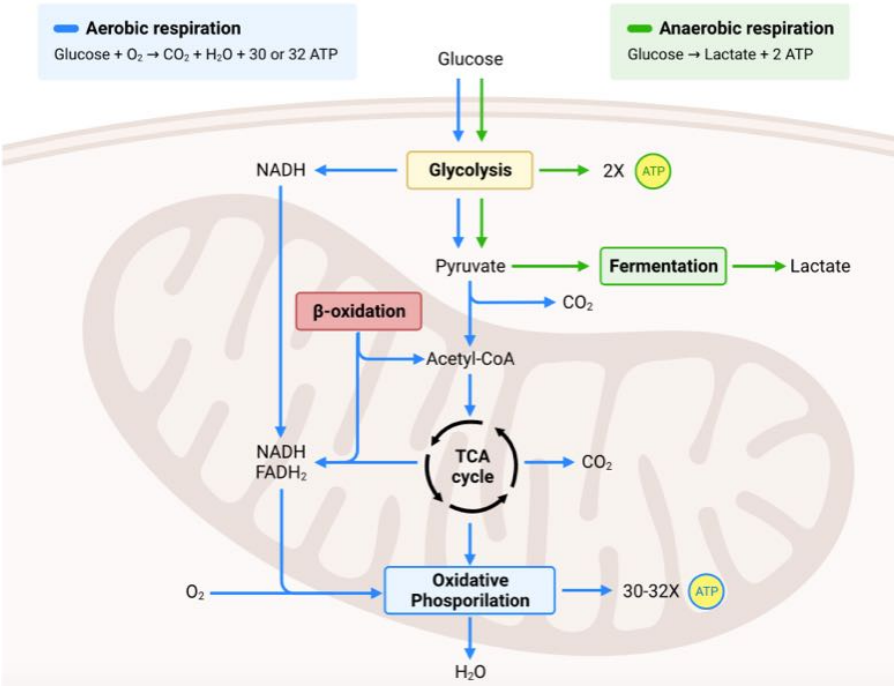


Figure 6 Glycolysis vs oxidative phosphorylation for ATP production

In FA, this altered metabolism is linked to increased lactate production and decreased cellular energy levels, potentially contributing to the bone marrow failure observed in FA patients. This shift towards glycolysis also leads to the accumulation of glycolytic intermediates, which can be used in alternative metabolic pathways, such as the pentose phosphate pathway and *de novo* fatty acid synthesis, further contributing to metabolic dysregulation. Moreover, lactate fermentation, a consequence of enhanced glycolysis, contributes to an acidic microenvironment, creating a favorable environment for cancer development and progression [69]. Additionally, the shift toward glycolysis may contribute to the observed metabolic abnormalities in FA, including insulin resistance and dyslipidemia. The dysregulated glycolysis and subsequent metabolic alterations may underlie the clinical manifestations of FA, such as the development of obesity and other metabolic dysfunctions.

### 2.2.6 The tricarboxylic acid cycle

The tricarboxylic acid (TCA) cycle, or the citric acid or Krebs cycle, is a central metabolic pathway that plays a crucial role in cellular aerobic respiration. It takes place in the mitochondria and involves the oxidation of acetyl-CoA, a two-carbon compound derived from carbohydrates, fats, and proteins catabolism, to generate ATP and reduced coenzymes [68], as schematized in Figure 7 and explained in detail below.

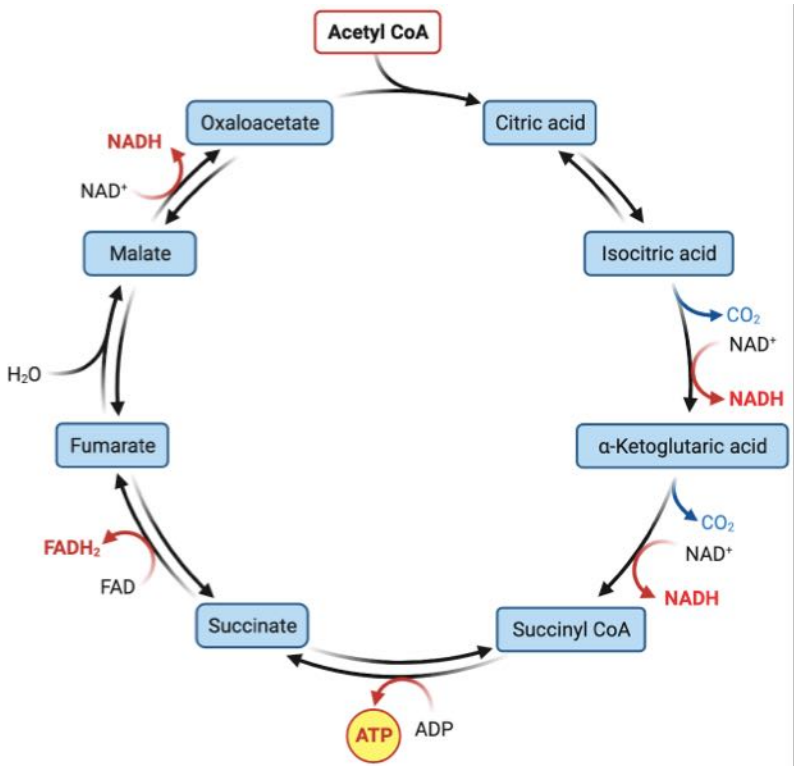


Figure 7 TCA cycle schematic representation

The cycle begins with the entry of acetyl-CoA into the cycle, which is combined with a four-carbon compound, the oxaloacetate, to form citrate. Then, citrate undergoes a series of enzyme-catalyzed reactions, leading to its isomerization into isocitrate. Isocitrate is then

oxidized and decarboxylated, resulting in the release of carbon dioxide ($CO_2$) and NADH and the formation of α-ketoglutarate, which undergoes further oxidation and decarboxylation, releasing another $CO_2$ molecule and producing succinyl-CoA. A high-energy phosphate group is then transferred from succinyl-CoA to ADP, forming ATP and resulting in the formation of succinate. Succinate is oxidized to fumarate, and $FADH_2$ is produced in this step, where the enzyme succinate dehydrogenase also contributes to the transfer of electrons to the ETC for further energy production. Fumarate is hydrated to form malate, which is then oxidized to oxaloacetate, completing the cycle. NADH is produced in this step, and oxaloacetate can then combine with another acetyl-CoA to begin the cycle again [33].

The TCA cycle is a fundamental part of cellular metabolism, connecting various metabolic pathways and playing a central role in maintaining cells' energy needs. It generates high-energy electrons in the form of the reducing equivalents NADH and $FADH_2$, crucial for OxPhos and to keep the redox balance. Moreover, it provides intermediates that can be used to synthesize various molecules, including amino acids, nucleotides, and fatty acids [68].

### 2.2.7 Fatty acid metabolism dysfunction

Fatty acid metabolism is closely interconnected with mitochondrial function, as fatty acid oxidation (β-oxidation) occurs in the mitochondria and produces NADH and $FADH_2$, essential for OxPhos function [33]. In FA, dysfunctional mitochondrial metabolism disrupts β-oxidation and leads to the accumulation of acetyl-CoA, a central molecule in cellular metabolism. It is generated from various sources, including the breakdown of glucose via glycolysis and the breakdown of fatty acids through β-oxidation. The accumulation of acetyl-CoA promotes fatty acid synthesis, and the excessive influx of fatty acid into cells can overwhelm mitochondria's capacity to oxidize them for energy production. This imbalance can lead to incomplete oxidation, accumulation of intermediates, and impaired ATP production. As a result, to store these excess fatty acids, cells form lipid droplets, one of the characteristic features of FA cells. While this can be a protective mechanism, excessive lipid droplet accumulation can lead to cellular dysfunction and contribute to lipotoxicity. Lipotoxicity triggers a series of molecular consequences, including impaired fatty acid oxidation, mitochondrial dysfunctions, oxidative stress, inflammation, insulin resistance, and endoplasmic reticulum stress, which can also trigger the Unfolded Protein Response (UPR). Moreover, lipotoxicity can affect the composition and function of cell membranes, potentially impacting various cellular processes other than triggering apoptosis and impairing autophagy. These disruptions collectively contribute to cellular damage and dysfunction, rendering lipotoxicity a pivotal factor in the development of various metabolic disorders and providing insights into the intricate interplay between lipid metabolism and cellular stress responses. In FA, this vicious cycle of dysfunctional fatty acid metabolism and impaired mitochondrial function can contribute to some of the clinical manifestations of the disease, such as insulin resistance and dyslipidemia, as the

accumulation of lipids and dysfunctional fatty acid metabolism can lead to changes in insulin signaling and lipid homeostasis.

### 2.2.8 Roles of FANC proteins in mitochondria and their relationship between mitochondrial and nuclear functions

The intricate interplay between mitochondrial and nuclear functions is crucial for maintaining cellular homeostasis and genomic stability. Within this context, the FA pathway emerges as a key player in orchestrating responses to genotoxic stress and oxidative challenges.

The FANCG protein exhibits a dual role: one in nuclear DNA damage repair and another in mitochondrial oxidative stress management. In detail, FANCG plays a pivotal role in protecting mitochondria from oxidative stress, as evidenced by its interaction with peroxiredoxin 3 (PRDX3) [71]. It has been found that a mutation in FANCG, resulting in the conversion of arginine at position 22 to proline, leads to a mutant protein (hFANCGR22P) that loses its mitochondrial localization and capacity to safeguard mitochondria from oxidative stress [72]. Furthermore, specific mutations, such as G546R in FANCG, disrupt this interaction, while proteolytic cleavage of PRDX3, observed in various FA subtypes (A, C, and G), underscores defects in PRDX3 integrity maintenance [71]. Cleavage or overoxidation of PRDX3 can elevate ROS levels within mitochondria, triggering apoptosis and compromising mitochondrial function and structure. The incorrect localization of PRDX3 in FANCG cells correlates with distorted mitochondrial structures, indicating an impaired mitochondrial function in FA patients. Moreover, reduced mitochondrial peroxidase activity, observed in FA cells from different subtypes, heightens sensitivity to oxidative stress [71]. Overexpression of PRDX3 restores survival in FANCG mutant cells under oxidative stress, illustrating PRDX3's critical role in mitigating oxidative damage. The intricate relationship between mitochondrial and nuclear functions, mediated by proteins like FANCG and PRDX3, underscores the broader implications of mitochondrial dysfunction on cellular health and responses to genotoxic stressors, such as mitomycin C (MMC) in FA [71].

FANCG mutations also impact the function of frataxin (FXN), an essential protein involved in mitochondrial iron-sulfur cluster biogenesis. The subsequent downregulation of FXN leads to iron deficiency, impacting the function of the FA protein FANCJ, an iron-sulfur-containing helicase crucial for DNA repair [72]. This underscores the significance of mitochondrial health in maintaining genomic stability and highlights the intricate relationship between mitochondrial and nuclear functions in FA.

The Fanconi pathway is crucial for preserving genome stability and preventing cancer-associated rearrangements at common fragile sites (CFSs). Among its key components, FANCD2 plays a pivotal role in coordinating replication and transcription processes to mitigate genomic instability. Moreover, FANCD2 exhibits non-canonical functions in regulating mitochondrial activity and redox metabolism. Research indicates its interaction with mitochondrial nucleoid components, modulation of mitochondrial gene expression,

and impact on energy metabolism. Additionally, FANC proteins participate in mitophagy, essential for maintaining mitochondrial quality. The intricate relationship between the FA pathway and mitochondrial function involves FANCD2's role in regulating mitochondrial energy metabolism through interactions with specific mitochondrial proteins. Dysfunctions in this pathway can disrupt mitochondrial function, affecting cellular metabolism and contributing to the FA cellular phenotype. FANCD2 plays a role in coordinating nuclear and mitochondrial activities to prevent genome instability, attenuating CFS gene transcription, promoting CFS stability, and dampening the activation of the mitochondrial stress response preventing the dysfunction and modulating the antioxidant response. In summary, the FA pathway, notably via FANCD2, not only preserves genome stability but also engages in crosstalk with mitochondrial processes, emphasizing the interconnectedness of nuclear functions in DNA repair and mitochondrial homeostasis maintenance [73].

Moreover, FANCD2 was also demonstrated to play a critical role in mitigating the toxic effects of naturally produced aldehydes in mice, highlighting the importance of DNA repair mechanisms in counteracting endogenous threats to genome stability [74]. Specifically, the FA DNA repair pathway, involving FANCD2, protects against acetaldehyde-induced genotoxicity, a by-product of ethanol metabolism known to cause DNA damage and developmental issues, bone marrow failure, and cancer predisposition. Disrupting Aldh2, an enzyme involved in acetaldehyde catabolism, in combination with FANCD2 deficiency in mice, leads to increased sensitivity to ethanol exposure in utero and rapid bone marrow failure postnatally. Additionally, these mice spontaneously develop acute leukemia, further emphasizing the importance of FANC proteins in safeguarding against aldehyde-induced genotoxicity and maintaining genome stability [74].

A study conducted on Indian FA patients revealed changes in mtDNA number, variations in mtDNA, downregulation of mtDNA complex-I and complex-III encoding genes, and deregulation of mitophagy genes as robust biomarkers for impaired mitochondrial functions in FA [75]. Additionally, a decreased mitochondrial membrane potential, low ATP production, and impaired oxygen consumption rate in FA mitochondria were demonstrated [75].

Moreover, defective respiration through Complex I, diminished ATP production, and metabolic sufferance have been observed in FANCA mutants, with N-acetyl cysteine treatment restoring oxygen consumption to normal levels [75]. Genetic deletion of FANCC has been associated with impaired autophagic clearance of damaged mitochondria, resulting in phenotypes like bone marrow failure and increased susceptibility to viral encephalitis. The study underscores the importance of comprehending mitochondrial dysfunction in FA pathogenesis through biomarker studies on mitochondrial DNA variations and impaired mitophagy in FA patients. These findings suggest that mitochondrial alteration contributes to the pathogenesis of FA, emphasizing the importance of studying mtDNA variations, oxidative phosphorylation efficiency, and mitophagy gene regulation to track the deterioration of mitochondrial-associated phenotypes in FA patients. Furthermore,

the study sheds light on how different FANC proteins influence mitochondrial functions and their impact on the development of FA-associated phenotypes like bone marrow failure and susceptibility to viral infections [75].

In summary, the roles of FANC proteins in both mitochondrial and nuclear functions are intricately interconnected, emphasizing their vital contribution to cellular homeostasis and genomic stability. Through their involvement in DNA repair, oxidative stress management, and regulation of mitochondrial activity, FANC proteins play essential roles in safeguarding mitochondrial integrity and maintaining cellular health. The dysregulation of these processes can lead to mitochondrial dysfunction, contributing to the pathogenesis of FA and other associated phenotypes.

### 2.2.9 Oxidative stress and antioxidant defenses

Oxidative stress is characterized by an imbalance between reactive oxygen species (ROS) production and cellular antioxidant defenses able to neutralize or detoxify them. ROS are highly reactive oxygen-containing molecules produced as by-products of aerobic metabolism in mitochondria. Physiologically, 0.2-2% of oxygen is converted into ROS, which would already be enough to create cellular damage if not balanced. ROS play essential roles in cell signaling and various physiological processes, as they can act as secondary messengers in redox signaling pathways, influencing processes such as cell proliferation, differentiation, apoptosis, immune responses, and gene expression. ROS-mediated signaling can promote adaptive responses in specific contexts and contribute to cellular adaptation and survival. However, when ROS levels exceed the cellular antioxidant defense capacity, they can cause damage to cellular components, including membranes, lipids, proteins, and DNA, leading to genotoxic stress and DNA double-strand breaks. This oxidative damage can lead to cellular dysfunction and the development of various diseases, including cancer, neurodegenerative disorders, cardiovascular diseases, and metabolic syndromes.

In FA, the defective electron transport between respiratory complexes I and III leads to an electron leakage, which originates a higher amount of ROS. Electrons reacting with molecular oxygen produce superoxide radicals ($^{\bullet}O_2^-$) that can be converted into even more reactive hydroxyl radicals ($^{\bullet}OH$) and hydrogen peroxide ($H_2O_2$) through various enzymatic and non-enzymatic reactions.

Antioxidant defenses are a complex network of enzymatic and non-enzymatic systems that work together to protect cells from oxidative damage caused by ROS and maintain cellular redox homeostasis. The main antioxidant enzymes include catalase, superoxide dismutase (SOD), and glutathione peroxidase. Non-enzymatic antioxidants include vitamins C and E, glutathione (continuously restored to its reduced form by the enzyme glutathione reductase), and other molecules that can directly scavenge ROS and stabilize free radicals. Defective DNA repair, dysfunctional mitochondria, and increased oxidative stress production create a vicious cycle in FA. Understanding the intricate relationship between oxidative stress and antioxidant defenses in FA is essential for developing targeted

therapeutic strategies to alleviate oxidative damage and improve the overall cellular function in FA patients. Enhancing antioxidant defenses and reducing oxidative stress may mitigate the adverse effects of DNA damage and genomic instability, potentially providing new avenues for treating and managing Fanconi Anemia.

## 2.3 Head and Neck Cancer

### 2.3.1 General population: prevalence, mortality, risk factors, and histological and molecular features.

Head and neck cancer (HNC) refers to a group of malignant neoplasms affecting the upper digestive and respiratory tracts. These cancers are categorized by anatomical region and are classified as cancers of the oral cavity (tongue, inner lining/mucosa of cheeks and lips, mouth floor, palate), pharynx (nasopharynx, oropharynx, hypopharynx), larynx, salivary glands, nasal cavities, and paranasal sinuses [76].

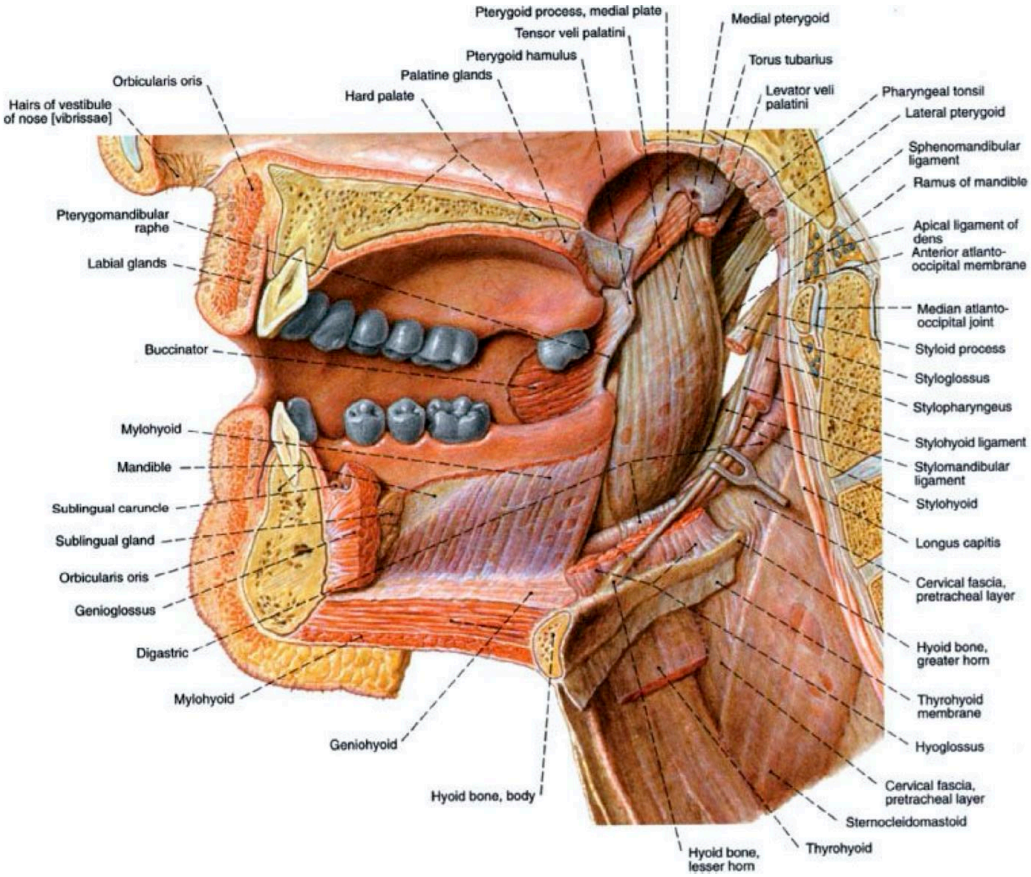


Figure 8 Anatomy of the oral cavity. The anatomical regions where HNSSC most frequently originates are visible in this image.

The International Agency for Research on Cancer (IARC: GLOBOCAN 2020) reports an annual global HNC diagnosis of over 930,000 people worldwide, constituting 5% of yearly cancer diagnoses, with an anticipated 30% rise by 2030. HNC prevalence is 2 to 4 times higher in men than in women. Survival rates depend on the disease stage, with advanced cases (70% of new diagnoses) showing 5-year survival rates of 50-60% [77]. Various epidemiological studies have identified several risk factors, including tobacco and/or alcohol consumption, age, exposure to environmental pollutants, infection by different viral agents, poor dental hygiene, a vegetable-deficient diet, and certain genetic disorders like FA. Notably, alcohol and tobacco together account for approximately 75% of HNC cases and raise the risk by 35 times [78]. Viral infections, including HPV and Epstein-Barr virus,

are significant contributors to HNC development. HPV-positive tumors account for 25% of total HNSCCs (head and neck squamous cell carcinomas) and represent a distinct clinical, pathological, and molecular entity from HPV-negative tumors. Unlike HPV-negative HNCs associated with tobacco and alcohol, HPV-positive HNCs are linked to specific sexual practices, particularly oral sex, and are typically located in the oropharynx [77], [79].

| | Global data (2020) | |
|---|---|---|
| | **New cases** | **Deaths** |
| Lip and Oral Cavity | 377,713 | 177,757 (47%) |
| Nasopharynx | 133,354 | 80,008 (60%) |
| Oropharynx | 98,412 | 48,143 (49%) |
| Hypopharynx | 84,254 | 38,599 (46%) |
| Larynx | 184,615 | 99,840 (54%) |
| Salivary Glands | 53,583 | 22,778 (42%) |
| TOTAL | 931,931 | 467,125 (50%) |

Table 2 Incidence and Mortality of Head and Neck Cancer. Incidence and mortality data for HNC worldwide, as reported in the IARC GLOBOCAN 2020 report.

The diagnosis of HNSCC remains a significant challenge, with early detection being crucial for improving patient survival and quality of life. However, the diverse anatomical locations and accessibility for visualization make accurate diagnosis problematic. Oral cavity tumors are often identified through visible symptoms like ulcers, impacting essential functions like eating or speaking. In contrast, diagnosing laryngeal or pharyngeal tumors relies on detecting clinical symptoms, ranging from voice changes to advanced indicators such as dysphagia, odynophagia, otalgia, dyspnea, or airway obstruction.

Regarding histopathological characteristics, over 95% of these tumors manifest as head and neck squamous cell carcinomas (HNSCC) [77], while the remaining percentage includes sarcomas, adenocarcinomas, melanomas, or unspecified tumors. HNSCCs originate from mucosal epithelial squamous cells, and their progression ranges from an increase in cell numbers in the tissue to hyperplasia to morphological changes in these cells and their spread to other tissues, leading to invasive carcinomas [80]. Notably, changes in keratin expression, including increased K5/K10 and decreased K4/K13, offer potential as prognostic indicators [81]. Molecular biomarkers like CD44, CD133, and ALDH1, linked to enhanced invasion and metastasis capabilities, signify a poorer clinical outcome [80]. Recent studies have demonstrated that HNSCC is highly heterogeneous, making it challenging to establish accurate prognosis and treatment planning and, from a biological perspective, identify cancer-causing genes. Molecular profiling identifies four subgroups with varied prognoses: an EGFR-associated subtype with poor prognosis and higher recurrence rates, mesenchymal and standard epithelium-like subtypes, and an antioxidant enzyme-rich subtype [82]. Additionally, location, extent, and stage contribute to the clinical prognosis.

In addition to distinct clinical-pathological and molecular characteristics, HPV-positive and HPV-negative tumors exhibit different gene expression patterns, mutational profiles, and

immune responses. HPV-positive tumors, characterized by the integration of the viral genome and the activity of E6 and E7 genes inactivating TP53 and RB1 [83], [84], [85], show a more favorable prognosis and better treatment response due to increased lymphocyte infiltrate [86]. Conversely, HPV-negative tumors, often linked to tobacco and alcohol-related DNA damage, involve mutations in genes such as TP53, CDKN2A, PTEN, FAT1, NOTCH1, and KMT2D, contributing to genetic instability and errors in DNA replication [77], [80], [87]. HNSCC metastasis, driven by altered epithelial-mesenchymal transition (EMT) processes under hypoxic conditions, involves the expression of transcription factors like ZEB1/2 and SNAIL, leading to increased vimentin expression and enhanced metastatic potential [88].

Due to the high heterogeneity of HNSCCs, treatment selection requires a multidisciplinary team involving specialists, such as clinical oncologists, maxillofacial surgeons, and radiologists, among others. Treatment selection depends on factors like tumor location, size, stage, patient's age, overall health status, and possible genetic conditions like FA. Specifically, patients with FA experience high toxicity from conventional treatments like radio/chemotherapy due to their inability to repair DNA damage, limiting treatment options. In early-stage disease diagnosis, standard treatments include surgery or radiotherapy, with a favorable prognosis. However, in most cases, diagnosis occurs in advanced stages, leading to surgery combined with postoperative radiotherapy. Enhanced understanding of HNSCC biology and immunology has led to the identification of new biomarkers or therapeutic targets for designing more effective and less toxic therapies. Recently, in cases where comorbidities prevent chemotherapy use, targeted drugs like cetuximab, a specific monoclonal antibody against EGFR, have been employed. EGFR inhibitors have demonstrated reduced side effects compared to platinum-derived therapies, and currently, cetuximab is used in combination with radiotherapy for HPV-negative HNSCC treatment [80], [89]. In 2019, the U.S. Food and Drug Administration (FDA) and the European Medicines Agency (EMA) approved the use of immune checkpoint inhibitors PD-1 pembrolizumab and nivolumab for recurrent or metastatic HNSCC and pembrolizumab as primary treatment for unresectable tumors [80], [90]. PD-1 inhibitors have proven to be more effective than conventional platinum-based therapies in second-line treatment, as well as improving survival in recurrent/metastatic HNSCC.

Regarding HNSCC prevention, reducing exposure to risk factors, primarily tobacco and alcohol consumption, and HPV vaccination for specific gender and age groups is recommended. Routine medical exams for high-risk HNSCC patients and monitoring of visible lesions or symptoms are also advised.

### 2.3.2 HNSCC in FA

Due to genomic instability, patients with FA face an elevated risk of developing cancer, with HNSCC being the most prevalent solid tumor. The estimated incidence of HNSCC associated with FA (HNSCC-FA) is 500-800-fold times higher than that in the general population and can develop even without exposure to the most common risk factor [7].

Notably, the tongue is the organ most frequently affected [91]. Moreover, the typical age of tumor onset is 30-32 years, significantly earlier than the general population's average of 60 years [7], [92], [93], [94]. The likelihood of HNSCC development is 30% by age 30 and rises to 76% by age 45 [91].

The incidence of oral lesions and HNSCC is even more significant in FA patients who have undergone BMT: this can be attributed to the pre-transplant conditioning regimen, which consists of radiotherapy or chemotherapy, resulting in DNA damage that FA patients are unable to repair [93], [95]. In such cases, the risk of developing oral premalignant lesions surpasses 90% in patients with an average age of 11 [96]. The average age of HNSCC onset in transplanted FA patients is 18 years [95], with the risk increased to 75% in patients transplanted before the age of 25 [92].

Recent studies based on genome or exome sequencing of SCCs in FA patients have identified a genomic signature associated with DNA repair defects characterized by a high number of structural variants resulting from the accumulation of DNA damage. These structural variants include small deletions, translocations, and inversions that are often interconnected, forming complex rearrangements. These studies have shown that HNSSCs-FA are not associated with HPV infection but originate from the loss of TP53, which is mutated in 85% of SCC-FA tumors [97]. Furthermore, HNSCC-FA tumors exhibit a high number of amplifications and/or deletions in various tumor suppressor genes and oncogenes. Specifically, the most frequent amplifications occur in PIK3CA (amplified in 78% of cases) and MYC (71% of cases), concurrently present in 56% of HNSSC-FA. Fanconi pathway deficiency can also lead to epithelial-mesenchymal transition (EMT), resulting in increased expression of markers such as SNAIL or vimentin, as well as heightened intrinsic inflammatory signaling in keratinocytes. These factors contribute to the aggressive nature of HNSCC in FA patients and participate in metastases development [97].

HNSCC treatment in FA patients is challenging due to poor tolerance to the conventional treatments described in the previous paragraph. Indeed, in these patients, radiation therapy causes mucositis, hematological conditions, and dysphagia as the main side effects impacting over 50% of patients. Surgery remains the primary approach, with complex ablative and reconstructive surgeries requiring careful postoperative follow-up to minimize morbidity [98].

Regarding targeted drugs, EGFR inhibitors have been tested in 10 FA patients, primarily cetuximab, alone or with other agents, for primary or recurrent FA-HNSCC. Combined use with radiation therapy showed good tolerance for primary HNSCC in FA patients [99], [100]. However, standardized clinical trials are needed to evaluate its effectiveness. In 2018, EMA designated gefitinib and afatinib as orphan drugs for FA patients based on effective tumor growth inhibition in preclinical models; however, there is currently no available clinical data. Immunotherapy's use in FA patients is cautious due to hematological conditions and BMT prevalence, which could cause or exacerbate severe graft-versus-host disease. The FDA

has not approved the use of PD-1 inhibitors for treating HNSCC-FA. Efforts towards preventive therapies include HPV-positive HNSCC vaccines; however, the incidence of HPV-associated HNSCC in FA patients is very low, making vaccination irrelevant for preventing this type of neoplasm [101], [102]. Recent studies show metformin, a widely used diabetes medication, improves hematopoiesis and peripheral blood counts and delays HNSCC in a preclinical FA mouse model. Metformin's involvement in aldehyde degradation reduces DNA damage, addressing FA patients' chromosomal instability [102].

## 3 Context and Objectives

FA is a rare genetic disorder characterized by defective DNA repair mechanisms and increased cancer susceptibility. Besides the well-known DNA repair issues, FA shows significant mitochondrial metabolic changes affecting vital cellular functions like energy production and cellular survival. Despite progress in understanding its molecular basis, FA remains a complex disease with few treatment options and high morbidity and mortality rates. This thesis seeks to underscore the complexity and multifactorial nature of the disorder exploring the complex metabolic alterations of FA and its link to HNSCC, emphasizing the need for innovative therapies to address metabolic dysfunctions and mitochondrial impairments driving FA's progression. By examining how mitochondrial dysfunction, oxidative stress, and inflammation interact in FA cells, this research aims to identify therapeutic targets and personalized treatments to improve patient outcomes and delay complications like bone marrow failure and cancer.

The primary objectives of this thesis include:

- Investigate the metabolic dysfunctions associated with FA, focusing on mitochondrial functional defects, uncoupling proteins, mitochondrial morphological defects, autophagy, mitophagy, and metabolic shifts between OxPhos and glycolysis.
- Compare the metabolic profiles of FA cells with healthy controls, studying bone marrow- and peripheral blood-derived cells, to elucidate the timing of metabolic damage manifestation.
- Assess OxPhos complexes expression, analyze mitochondrial morphological defects and mitochondrial dynamics, exploring potential treatments to prevent alteration in mitochondrial reticulum organization.
- Evaluate the effect of various antioxidant compounds in modulating mitochondrial metabolism impairment and oxidative stress, cell proliferation, and cell death in FA.
- Investigate the effects of deacetylase inhibition on antioxidant response activation in combination with oxidative insult on aerobic metabolism, cell survival, and mitochondrial dynamics.
- Explore the role of miRNA in FA pathogenesis, aiming to understand their potential implications in disease progression.
- Explore the role of inflammation in FA, investigating its contribution to disease progression and as a potential therapeutic target to mitigate its effects on cellular metabolism and overall pathology.
- Examine the metabolic characteristics of FA-related HNSCC, focusing on energy metabolism, mitochondrial dynamics, antioxidant defenses, oxidative damage, mitochondrial dynamics, cellular proliferation, and DNA damage.
- Compare metabolic defects in Fanconi Anemia with those in Shwachman-Diamond Syndrome (SDS), particularly investigating the implications of iron metabolism in SDS metabolic defect.

This thesis addresses FA's complex and multifactorial nature, highlighting its intricate metabolic dysfunctions and its association with HNSCC. By delving into mitochondrial dysfunction, oxidative stress, inflammation, and their interplay within FA cells, this research aims to identify novel therapeutic targets and personalized treatments to improve patient outcomes. Through comprehensive analyses of metabolic alterations and comparative studies with healthy controls and related bone marrow failure syndromes like SDS, this work contributes to advancing our understanding of the multifactorial pathogenesis of FA, offering promising avenues for innovative interventions to mitigate disease progression and associated complications, such as bone marrow failure and cancer.

# 4 Materials and Methods

All chemical compounds were of the highest chemical grade (i.e., Tris-HCl, KCl, EGTA, $MgCl_2$, sulfuric acid, trichloroacetic acid, HCl) and were purchased from Sigma-Aldrich, St. Louis, MO, USA.

## 4.1 Primary cells, cell lines, and their culture conditions

Four distinct FANCA lymphoblast cell lines (Lympho FA) and three different FANCA fibroblast cell lines (Fibro FA), derived from various patients, each carrying a different mutation of the FANCA gene, were obtained from the "Cell Line and DNA Biobank from Patients affected by Genetic Diseases" (G. Gaslini Institute) - Telethon Genetic Biobank Network (Project No. GTB07001) [103]. In addition, isogenic FAcorr cell lines, generated by the same FANCA lymphoblast and fibroblast cell lines and corrected with the S11FAIN retrovirus (Lympho FAcorr and Fibro FAcorr), were employed as a control to maintain the characteristics of the FA cell lines except for the FANCA gene mutations [103].

For some of the experiments, four distinct FANCC lymphoblast cell lines (FANCC) were employed, derived from various patients, each carrying different mutations of the FANCC gene, were obtained from the "Cell Line and DNA Biobank from Patients affected by Genetic Diseases" (G. Gaslini Institute) - Telethon Genetic Biobank Network (Project No. GTB07001) [103]. Isogenic FANC corr cell lines were generated by correcting the cell lines with a retrovirus and used as a control to maintain the FA characteristics except for the FANCC gene mutations [103].

Lymphoblast cell lines were grown in RPMI-1640 medium (#21875091, GIBCO, Billings, MT, USA) containing 10% FBS (#ECS0120L, Euroclone, Milan, Italy), 100 U/mL penicillin, and 100 µg/mL streptomycin (#ECB3001D, Euroclone, Milan, Italy) at 37 °C with a 5% $CO_2$. Fibroblast cell lines were grown as a monolayer at 37 °C with a 5% $CO_2$ in DMEM high glucose with Glutamax® (#61965026, GIBCO, Billings, MT, USA), containing 10% fetal bovine serum (FBS; #ECS0120L, Euroclone, Milan, Italy), 100 U/mL penicillin, and 100 µg/mL streptomycin (#ECB3001D, Euroclone, Milan, Italy) [103].

OHSU-974-S91 (OHSU-S91) and OHSU-974-FAcorr (OHSU-FAcorr), human head and neck squamous cell carcinoma (HNSCC) cell lines, were kindly provided by Prof. Susanne Wells, Cincinnati Children's Hospital Medical Center Cincinnati, USA. Specifically, OHSU-S91 carries a FANCA gene mutation, while OHSU-FAcorr is an isogenic HNSCC cell line corrected with the functional FANCA gene inserted with a retrovirus. Cells were grown in RPMI medium supplemented with 10% fetal calf serum (#ECS0120L, Euroclone, Milan, Italy), 100 U/mL penicillin (#ECB3001D, Euroclone, Milan, Italy), and 100 µg/mL streptomycin (#ECB3001D, Euroclone, Milan, Italy) and maintained at 37 °C with a 5% $CO_2$ [104].

Primary Fanconi Anemia patient cells were part of a study approved by the institutional review board of the G. Gaslini Hospital, Genoa, Italy. According to the Declaration of Helsinki, all the subjects or their legal guardians gave written informed consent to the

investigation. 15 FA patients (6 males and 9 females) have been involved in the study. The median age was 8, ranging from 5 to 34 years old subjects.

Control samples were taken from healthy voluntary donors (HD samples; 5 males and 8 females). Primary bone marrow (BM) and peripheral blood (PB) mononuclear cells (MNCs) were isolated using Ficoll-Hipaque Plus (GE Healthcare Biosciences, Piscataway, NJ, USA) and cultured at 37 °C with a 5% $CO_2$ in RPMI supplemented with 10% fetal calf serum, glutamine, and antibiotics. For hypoxic culture conditions, cells were maintained at 3% oxygen. In several experiments, to induce BM-MNCs differentiation, samples were stimulated with 10 µg/ml phytohemagglutinin (PHA), and cultured cells were analyzed every 24 h [105].

Primary Shwachman Diamond Syndrome (SDS) cells were kindly provided by Dr. D'Amico, Tettamanti Center, Fondazione IRCCS San Gerardo dei Tintori, Monza, Italy. All patients were part of an approved study, and all the subjects, or their legal guardians, gave written informed consent to the investigation according to the Declaration of Helsinki. 11 SDS patients have been involved in the study. 11 control samples were taken from healthy voluntary donors (HD). BM mesenchymal stromal cells (MSCs) were isolated using Ficoll-Hipaque Plus (GE Healthcare Biosciences, Piscataway, NJ, USA) and cultured at 37 °C with a 5% $CO_2$ in RPMI supplemented with 10% fetal calf serum, glutamine, and antibiotics.

### 4.1.1 Treatments

In some experiments, FA and FAcorr lymphoblasts and fibroblasts cell lines were treated for 24 h with 1 µM P110 (#6897/1, Bio-Techne, Minneapolis, MN, USA), a specific inhibitor of DRP1, a protein involved in the mitochondrial fission process [106].

For other sets of experiments, the same cells were treated for 3 or 24 h with histone deacetylase inhibitors (HDACi), specifically 1 mM Valproic Acid (VPA), 10 mM b-hydroxybutyrate (OHB), or 100 nM EX257 (a specific SIRT1 inhibitor) or their combinations at the same dosages. 0.5 mM hydrogen peroxide ($H_2O_2$) was added when necessary to induce oxidative damage [107].

In other experiments, FA and FAcorr lymphoblast cell lines were treated for 48 with 10 µM quercetin, a flavonoid compound (#Q4951, Merck, Darmstadt, Germany), 5 µM C75, a fatty acid synthesis inhibitor (#C5490, Merck, Darmstadt, Germany), and 10 nM rapamycin, a specific mTOR inhibitor (#37094, Merck, Darmstadt, Germany) [108].

For experiments conducted on FANCA, FANCAcorr, FANCC, and FANCCcorr lymphoblastoid cell lines, cells were treated for 48 hours with 10 µg/ml of a TGFβ inhibitor (luspatercept, Reblozyl, Bristol Myers Squibb, Princeton, NJ, USA), 500 ng/ml of an IL1 inhibitor (Anakinra, Kineret, Amgen, Thousand Oaks, CA, USA), 500 ng/ml of an NLRP3 inhibitor (#MCC950, Sigma-Aldrich, St. Louis, MO, USA), 10 µg/ml of a TNFα inhibitor (Etanercept, Amgen, Pfizer, NY, USA), or 1 µM P110 (#6897/1, Bio-Techne, Minneapolis, MN, USA).

Finally, primary MSCs from SDS patients and HD used as controls were treated 48 hours with 0.05% dimethyl sulfoxide (DMSO) or 1 mM N-acetylcysteine (NAC).

### 4.2 RNA isolation and qRT-PCR of miR-29a-3p

RNA containing the small RNA fraction was extracted using the RNeasy Plus mini kit (Qiagen, Hilden, Germany) following a dedicated protocol. miR-29a-3p expression was evaluated using a specific TaqMan MicroRNA Assay as described by the manufacturer (Applied Biosystems, Foster City, CA, USA). Briefly, 10 ng of RNA were reverse transcribed using the TaqMan MicroRNA Reverse Transcription kit primed with the specific RT primer. Real-time PCR was performed in triplicate using the specific primers. The expression of each miRNA was normalized on the RNU44 expression.

### 4.3 FA fibroblast and lymphoblast cells transfection with miR-29a-3p

FA fibroblast cell lines were transfected with miRNA29A mimic (ThermoFisher, Waltham, MA, USA) using RNAiMAX (Invitrogen, Waltham, MA, USA) following the manufacturer's instructions. For subsequent RNA extraction, 75,000 cells grown in 6-well plates were transfected with 25 pmol of miR-29a mimic or negative control mimic using 7.5 µl of lipofectamine RNAiMAX Transfection Reagent (LF). After 24h or 48h, cells were harvested, washed with PBS, lysed, and RNA was extracted. For biochemical analysis, 500,000 cells grown in 175 $cm^2$ flasks were transfected with 437.5 pmoles of miR-29a mimic or negative control mimic using 131.25 µl LF. Cells were processed 24h or 48h post-transfection.

FA lymphoblast cell lines were transfected with miRNA29A mimic (ThermoFisher, Waltham, MA, USA) using RNAiMAX (Invitrogen, Waltham, MA, USA) according to the manufacturer's instructions. 500,000 cells grown in 6-well plates were transfected with 25 pmol of miRNA29A mimic or 25 pmol of negative control mimic using 7.5 µl LF for subsequent RNA extraction. After 24h or 48h, cells were harvested, washed with PBS, lysed, and RNA was extracted.

For subsequent biochemical analysis, 2.5 $x10^6$ and $7.5x10^6$ cells grown in 25 $cm^2$ and 75 $cm^2$ flasks, respectively, were transfected with 62.5 and 187.5 pmoles of miRNA29A mimic or negative control mimic using 18.75 µl and 56.25 µl LF, respectively. Cells were processed 24h or 48h post-transfection.

### 4.4 Catalase and glutathione reductase gene expression evaluation

RNA was extracted from lymphoblast pellets using the RNeasy mini kit (Qiagen, Hilden, Germany). To evaluate the mRNAs expression of Catalase (CAT) and Glutathione reductase (GR), 100 ng of RNA were reverse transcribed using the SuperScript VILO IV cDNA Synthesis Kit (Invitrogen, Waltham, MA, USA). Real-time PCR was performed on the cDNA using the primers-probe mix contained in the specific TaqMan Gene Expression Assays (Applied Biosystems, Foster City, CA, USA). Gene expression was normalized to the GAPDH expression. Experiments were performed in triplicate.

### 4.5 Mitomycin C (MMC) survival assay

Cells survival under mitomycin C (MMC) treatment (0, 1, 3, 10, and 33 nM) was tested as previously described in Bottega et al. [109].

### 4.6 DNA damage induction

Cells were seeded in 6-well plates and, for some experiments, were treated for 24 h with quercetin, C75, and rapamycin, as previously described. Afterwards, 2 mM hydroxyurea (HU) were added to the culture medium for 3 h. Then, cells were washed with fresh growth medium containing the protective drugs and maintained in culture for 48 h.

In the case of the OHSU-S91 and OHSU-FAcorr cell lines, which were not subjected to any treatment, the cells were seeded in 6-well plates and cultured until they reached confluence. Subsequently, the cells were treated with 2 mM hydroxyurea (HU) dissolved in an appropriate volume of fresh medium for 3 hours to induce DNA damage. For all the experiments, control cells, seeded in parallel, received only fresh medium [108].

### 4.7 Cells collection and growth curve

To harvest the cells after culture, fibroblasts, HNSCC cell lines, and HD- and SDS-MSCs, which all grow in adhesion, were detached through trypsinization for 5 minutes at 37 °C. This process followed the removal of the culture medium and a PBS wash (#14190250, ThermoFisher, Waltham, MA, USA) to eliminate any residual FBS. Subsequently, trypsin (Trypsin-EDTA 1X in PBS, #ECB3052D, Euroclone, Milan, Italy) was neutralized with the appropriate fresh culture medium, and the cells were collected.

Lymphoblastoid cell lines and HD- and FA-MNCs growing in suspension were collected directly. All cell types were centrifuged at 1,000 x g for 5 minutes to remove the growth medium and washed twice with PBS.

To assess the cellular growth rate, cells were resuspended in an appropriate volume of PBS and counted in a Burker chamber after staining with trypan blue.

### 4.8 Flow-cytometric evaluation of cell viability

Cellular viability was assessed with the propidium iodide (PI) exclusion assays. Cells were incubated for 5 min with 1 µg/mL PI (Sigma-Aldrich, St. Louis, MO, USA), and PI fluorescence was measured by flow cytometry (FACSCalibur, Becton Dickinson, Franklin Lakes, NJ, USA). Cells positive for PI fluorescence were considered dead cells [110].

### 4.9 Mitochondrial Trans Membrane Potential by Flow Cytometry

Fresh cells were washed once with the appropriate culture medium, incubated with 200 nM tetramethyl-rhodamine-methyl-ester (TMRM; Invitrogen, Waltham, MA, USA) for 10 min at 37 °C and immediately measured on a FACSCalibur flow cytometer (Becton Dickinson, Franklin Lakes, NJ, USA). To exclude the unspecific staining, the same experiments were conducted in the presence of 50 nM of Carbonyl cyanide-4-(trifluoromethoxy)-phenylhydrazone (FCCP), an uncoupling molecule. The analysis was confined to viable cells only after gating procedures based on forward- and side-scatter features. Ten thousand cells per sample were analyzed [111].

### 4.10 Oxygen consumption rate assay

Oxygen consumption rate (OCR) was measured using an amperometric electrode (Unisense Microrespiration, Unisense, Aarhus, Denmark) in a closed chamber at 25 °C.

For each experiment, 2 x $10^5$ cells were resuspended in phosphate buffer saline (PBS) and permeabilized for 1 min with 0.03 mg/mL digitonin.

To stimulate the pathways composed of complexes I, III, and IV or complexes II, III, and IV, 10 mM pyruvate plus 5 mM malate (#P4562 and #M8304, respectively, Sigma-Aldrich, St. Louis, MO, USA) or 20 mM succinate (#S7501, Sigma-Aldrich, St. Louis, MO, USA) were employed, respectively, and in both cases 0.1 mM ADP was added to initiate ATP synthesis [111], [112].

To test the cellular affinity for glucose, glutamine, and fatty acids as respiratory substrates, 3 μM BPTES (a glutaminase inhibitor [113]), 4 μM Etomoxir (a fatty acid oxidation inhibitor [114]), and 2 μM UK5099 (a mitochondrial pyruvate carrier inhibitor [115]) were added to cells resuspended in the growth medium. All data were expressed as nmol O/min/$10^6$ cells.

### 4.11 $F_oF_1$ ATP-Synthase activity assay

The $F_oF_1$ ATP-synthase (ATP Synthase) activity was evaluated by incubating 2 × $10^5$ cells at 25 °C for 10 min in a medium containing: 50 mM Tris-HCl (pH 7.4), 50 mM KCl, 1 mM EGTA, 2 mM $MgCl_2$, 0.6 mM ouabain (#O0200000, Sigma-Aldrich, St. Louis, MO, USA), 0.25 mM di(adenosine)-5-Penta-phosphate (Ap5A, an adenylate kinase inhibitor, #D1387, Sigma-Aldrich, USA), and 25 μg/mL ampicillin (#A9393, Sigma-Aldrich, St. Louis, MO, USA); then, 10 mM pyruvate plus 5 mM malate (#P4562 and #M8304, respectively, Sigma-Aldrich, St. Louis, MO, USA) or 20 mM succinate (#S7501, Sigma-Aldrich, St. Louis, MO, USA) were employed to stimulate complexes I, III, and IV or complexes II, III, and IV, respectively [116].

As for OCR evaluation, 3 μM BPTES, 4 μM Etomoxir, and 2 μM UK5099 were used for the cellular energy substrate affinity evaluation. In this case, cells were suspended in the growth medium diluted 1:1 with the solution described above. In each case, ATP synthesis was induced by adding 0.1 mM ADP. The reaction was monitored every 30 sec for 2 min with a luminometer (GloMax® 20/20Luminometer, Promega Italia, Milano, Italy), using the luciferin/luciferase chemiluminescent method (luciferin/luciferase ATP bioluminescence assay kit CLS II, Roche, Basel, Switzerland). ATP standard solutions in a concentration range between $10^{-8}$ and $10^{-5}$ M were used for calibration. Data were expressed as nmol ATP/min/$10^6$ cells [111].

### 4.12 P/O ratio

To evaluate OxPhos efficiency, the P/O ratio was determined by dividing the ATP synthesized through aerobic respiration by the oxygen consumption in the presence of respiring substrates and ADP. Efficient mitochondria have a P/O value around 2.5 when stimulated with pyruvate and malate or 1.5 when stimulated with succinate as respiring substrates, activating the pathways led respectively by complexes I or II. A P/O ratio lower than 2.5 for pyruvate and malate or lower than 1.5 for malate suggests that mitochondria are uncoupled and, therefore, oxygen is not entirely used for energy production but contributes to reactive oxygen species (ROS) production [35].

### 4.13 Microscopy Analysis

#### 4.13.1 Transmission electron microscopy

FA, FAcorr lymphoblast, and fibroblast pellets were fixed with 2.5% glutaraldehyde 0.1 M cacodylate buffer (pH 7.6) for 1h at room temperature. The post-fixation was made with 1% $OsO_4$ in cacodylate buffer for 1h, and pellets were dehydrated in an ethanol series and embedded in Epon resin. Ultrathin sections stained with uranyl-acetate and lead citrate were observed with a Jeol Jem-1011 transmission electron microscope [117].

#### 4.13.2 Confocal microscopy

Fibroblasts were cultured in chamber slides for 24 h with or without treatments (P110 or one of the HDACi). After PBS washes, cells were fixed with 0.3% paraformaldehyde (#P6148, Sigma-Aldrich, St. Louis, MO, USA) and permeabilized with 0.1% triton (#X100, Sigma-Aldrich, St. Louis, MO, USA). Cells were incubated overnight at 4 °C with the antibody against TOM20 (#42406S, Cell Signaling, Danvers, MA, USA). After PBS washes, cells were incubated for 1 h at 25 °C with the Alexa-546-conjugated anti-rabbit antiserum (#A11010, Invitrogen, Waltham, MA, USA) as a secondary antibody and DAPI to mark nuclei. After PBS wash, chamber slides were mounted in mowiol. Immunofluorescence confocal laser scanner microscopy (CLSM) imaging was performed using a laser scanning spectral confocal microscope TCS SP2 AOBS (Leica, Wetzlar, Germany), equipped with Argon ion, He–Ne 543 nm, and He–Ne 633 nm lasers. Images were acquired through an HCX PL APO CS 40×/1.25 oil UV objective and processed with Leica. Images were acquired as single transcellular optical sections. To evaluate the mitochondrial network shape, fibroblasts were scored depending on the morphology of most of their mitochondrial population as elongated or intermediated/short, following the method described in [118]

#### 4.13.3 Optical microscopy

To evaluate cell morphology, OHSU-S91 and OHSU-FAcorr cell lines were seeded in a 6-well plate and observed through an inverted optical microscope.

### 4.14 Cell homogenate preparation

After cell collection, as described in section 2.4, the cell pellets were washed twice with PBS and centrifuged. All resulting pellets were resuspended in an appropriate volume of Milli-Q water and subjected to sonication using a Microson XL Model DU-2000 (Misonix Inc., Farmingdale, NY, USA). The sonication process consisted of two rounds, each lasting 10 seconds, with a 30-second interval between rounds to prevent overheating. The total protein content in the samples was determined using the Bradford method [119].

### 4.15 Anaerobic metabolism evaluation: lactate dehydrogenase activity, glucose consumption, lactate release assays, and glycolysis rate

Lactate dehydrogenase (LDH) activity was assessed spectrophotometrically, measuring NADH oxidation at 340 nm. The assay mix contained Tris-HCl (pH 7.4), 1 mM pyruvate, and 0.2 mM NADH [111].

Glucose consumption was evaluated in the growth medium, following NADP reduction at 340 nm. The assay mix included 10 µL of growth medium, 50 mM Tris-HCl (pH 8.0), 1 mM NADP, 10 mM $MgCl_2$, and 2 mM ATP. Samples were analyzed spectrophotometrically before and after adding 4 µg of purified hexokinase plus glucose-6-phosphate dehydrogenase [69].

Lactate concentration was determined spectrophotometrically in the growth medium, following the reduction of $NAD^+$ at 340 nm. The assay mix contained 10 µL of the growth medium, 100 mM Tris-HCl (pH 8.0), and 5 mM $NAD^+$. Samples were analyzed before and after adding 4 µg of purified LDH [69].

The glycolysis rate was calculated as the percentage of actually released lactate to the theoretical lactate production, corresponding to twice the glucose concentration consumed, as in an exclusive anaerobic metabolism, one glucose molecule is converted into two lactate molecules + 2 ATP molecules.

### 4.16 Evaluation of respiratory chain complexes' enzymatic activities and electron transport between complexes I and III

For each assay, 50 µg of total protein was used. Complex I and complex II activities were assayed spectrophotometrically at 420 nm, following the ferricyanide reduction. The reaction mix contained 100 mM Tris-HCl (pH 7.4), 0.8 mM $K_3[Fe(CN)_6]$, and, respectively, 0.7 mM NADH for Complex I or 20 mM succinate for Complex II. Complex III activity was assayed following the oxidized cytochrome c (CytC) reduction at 550 nm. The reaction mix contained 100 mM Tris-HCl (pH 7.4), 0.5 mM NADH, and 0.03% oxidized CytC. Complex IV was assayed following the ascorbate-reduced-CytC oxidation at 550 nm. The reaction mix contained 100 mM Tris-HCl (pH 7.4), 50 µM antimycin A, and 0.03% CytC reduced with 3 mM ascorbic acid [120].

The electron transfer between respiratory chain complexes I and III was analyzed spectrophotometrically following the reduction of CytC at 550 nm. The reaction mix contained 100 mM Tris-HCl (pH 7.4) and 0.03% of oxidized CytC (#C2867, Sigma-Aldrich, St. Louis, MO, USA). The reaction was started with the addition of 0.7 mM NADH. If the electron transport from Complex I to Complex III is conserved, electrons pass from NADH to Complex I, then to Complex III via coenzyme Q, and finally to CytC [111].

### 4.17 Cellular energy status, ATP, and AMP intracellular content evaluation

For each assay, 50 µg of total protein was used. ATP was assayed spectrophotometrically following NADP reduction at 340 nm. The assay medium contained 100 mM Tris-HCl (pH 8.0), 0.2 mM NADP, 5 mM $MgCl_2$, and 50 mM glucose. Samples were analyzed before and after adding 3 µg of purified hexokinase plus glucose-6-phosphate dehydrogenase. AMP was assayed spectrophotometrically following NADH oxidation at 340 nm. The reaction medium contained 100 mM Tris-HCl (pH 8.0), 5 mM $MgCl_2$, 0.2 mM ATP, 10 mM phosphoenolpyruvate, 0.15 mM NADH, 10 IU adenylate kinase, 25 IU pyruvate kinase, and 15 IU of lactate dehydrogenase.

Cellular energy status was calculated as the intracellular ATP to AMP ratio, expressed in mM/mg of total protein [111], [112].

### 4.18 Lipid metabolism evaluation: lipid and acetyl-CoA concentrations and 3-ketoacyl-ACP reductase activity

Cellular lipid content was evaluated by the Sulfo-Phospho-Vanillin assay. Samples were incubated with 95% sulfuric acid at 95 °C for 20 min, quickly cooled, and assessed spectrophotometrically at 535 nm. Afterward, a solution of 0.2 mg/mL vanillin (#V1104, Sigma-Aldrich, St. Louis, MO, USA) in 17% aqueous phosphoric acid was added, incubated for 10 min in the dark, and re-evaluated at 535 nm. A mix of triglycerides (#17810, Sigma-Aldrich, St. Louis, MO, USA) was used to obtain a standard curve [111].

To evaluate the acetyl-CoA concentration, the PicoProbe acetyl-CoA assay kit (#ab87546 Abcam, Waltham, Boston, MA, USA) was employed, following the manufacturer's instructions.

The activity of 3-ketoacyl-ACP reductase was assayed as a marker of fatty acids β-oxidation. It was spectrophotometrically evaluated at 340 nm, following NADH oxidation in the presence of acetoacetyl-CoA. The reaction mix contained 100 mM sodium phosphate (pH 6.0), 0.2 mM NADH, and 0.1 mM acetoacetyl-CoA.

### 4.19 Evaluation of oxidative stress and its damages: ROS and hydrogen peroxide production; malondialdehyde, 4-hydroxynoneal, 3-nitrotyrosine, and 8-hydroxy 2 deoxyguanosine concentrations

To assess ROS production using a cytofluorimeter, cells were stained with 2',7'-dichlorodihydrofluorescein diacetate (H2DCFDA) (ThermoFisher, Waltham, MA, USA) for 20 minutes at 37 °C. H2DCFDA is non-fluorescent but is cleaved to 2',7'-dichlorofluorescein (H2DCF) inside the cell. In the presence of oxidants, H2DCF is converted to the fluorescent DCF. Samples were analyzed using a CyAn ADP cytometer (Beckman Coulter, Brea, CA, USA) equipped with a 15-mW 488-nm argon ion laser. A plot of all physical parameters (forward scatter (FSC) versus side scatter (SSC)) was used to set the gate that delimited debris and aggregates. Ten thousand cells per sample were analyzed.

$H_2O_2$ content was determined using the Fluorometric Hydrogen Peroxide Assay Kit (#ab102500 Abcam, Waltham, MA, USA), following the manufacturer's instructions.

Malondialdehyde (MDA) concentration was assessed to evaluate lipid peroxidation damage using the thiobarbituric acid reactive substances (TBARS) assay. This test is based on the reaction of thiobarbituric acid (TBA) with MDA, a breakdown product of lipid peroxides. The TBARS solution contained 26 mM thiobarbituric acid (#T5500, Sigma-Aldrich, St. Louis, MO, USA) and 15% trichloroacetic acid (TCA) in 0.25 N HCl. To evaluate the basal MDA concentration, 50 µg of total proteins dissolved in 300 µL of Milli-Q water were added to 600 µL of TBARS solution. The mix was incubated at 95 °C for 60 min, the samples were then centrifuged at 14,000 rpm for 2 min, and the supernatant was analyzed spectrophotometrically at 532 nm [111], [112].

4-hydroxynoneal (4-HNE), another lipid peroxidation marker, was evaluated by the Lipid Peroxidation 4-HNE Assay Kit (#ab238538, Abcam, Cambridge, UK) following the manufacturer's instructions.

3-nitrotyrosine, a marker of protein oxidative damage, was assayed by employing an ELISA Kit (#ab116691, Abcam, Cambridge, UK) following the manufacturer's instructions.

8-hydroxy-2'-deoxyguanosine (8-OHdG), a marker of DNA oxidative damage, was assayed by an ELISA Kit (#ab201734, Abcam Cambridge, UK) following the manufacturer's instructions.

### 4.20 Antioxidant defenses evaluation: catalase, glutathione reductase, G6PD, H6PD, and ALDH activity

20 µg of total protein was used for all assays, and data were normalized on the sample protein content.

Glutathione reductase (GR) activity was assayed spectrophotometrically at 340 nm following the oxidation of NADPH. The assay medium contained 100 mM Tris-HCl (pH 7.4), 1 mM EDTA, 5 mM GSSG, and 0.2 mM NADPH [104].

Catalase activity was spectrophotometrically assayed following the $H_2O_2$ decomposition at 240 nm. The assay mix contained 50 mM phosphate buffer (pH 7.0) and 5 mM $H_2O_2$ [111].

Glucose-6-phosphate dehydrogenase (G6PD) and hexose 6-phosphate dehydrogenase (H6PD) activity were assayed spectrophotometrically at 340 nm following NADP reduction. The assay mix contained Tris-HCl (pH 7.4), 0.5 mM NADP, and, respectively, 10 mM glucose-6-phosphate for G6PD or glucose for H6PD dosage [121].

ALDH activity was measured spectrophotometrically at 340 nm following the $NAD^+$ oxidation. The assay mix contained 100 mM sodium pyrophosphate (pH 9.0) (#221368, Sigma-Aldrich, St. Louis, MO, USA), 10 mM $NAD^+$ (#N0632, Sigma-Aldrich, St. Louis, MO, USA), and 10 mM acetaldehyde (#402788, Sigma-Aldrich, St. Louis, MO, USA).

The general antioxidant defenses and the relative level of scavengers were evaluated by the Total Antioxidant Capacity Assay Kit (#MAK187, Sigma-Aldrich, St. Louis, MO, USA), following the manufacturer's instructions.

### 4.21 Western Blot analyses

For Western Blot (WB) analysis, 30 µg of protein was loaded for each sample to perform denaturing electrophoresis (SDS-PAGE) using 4-20% gradient gels (BioRad, Hercules, CA, USA). The primary antibodies used are listed in Table 3, all diluted at a 1:1,000 ratio in PBS containing 0.15% Tween (PBSt).

| Name | Brand | Code |
|---|---|---|
| AKT | Cell Signaling (Danvers, MA, USA) | #2966S |
| Atg12 | Cell Signaling (Danvers, MA, USA) | #4180P |
| Atg16L1 | Cell Signaling (Danvers, MA, USA) | #8089P |
| Atg7 | Cell Signaling (Danvers, MA, USA) | #8558P |
| ATP synthase β subunit | Sigma-Aldrich (St. Louis, MO, USA) | #HPA001520 |
| Beclin1 | Cell Signaling (Danvers, MA, USA) | #3495P |
| CLUH | Bethyl Lab. Inc. (Montgomery, Texas, USA) | #A301-764A |
| DRP1 | ThermoFisher (Waltham, MA, USA) | #DRP1-101AP |
| FIS1 | Abcam (Waltham, Boston, MA, USA) | #ab229969 |
| FOXO3 | Cell Signaling (Danvers, MA, USA) | #2497S |
| G6PD | Abcam (Waltham, Boston, MA, USA) | #ab124738 |
| H6PD | Abcam (Waltham, Boston, MA, USA) | #ab170895 |
| LC3 | Novus Biologicals (Littleton, CO, USA) | #NB100-2220 |
| MFN2 | ThermoFisher (Waltham, MA, USA) | #PA5-72811 |
| MTCO2 | Abcam (Waltham, Boston, MA, USA) | #ab79393 |
| ND1 | Abcam (Waltham, Boston, MA, USA) | #ab181848 |
| OPA1 | Sigma-Aldrich (St. Louis, MO, USA) | #HPA036926 |
| Parkin | ThermoFisher (Waltham, MA, USA) | #PA5-13399 |
| phosphorylated-AKT | Cell Signaling (Danvers, MA, USA) | #4060S |
| phosphorylated-FOXO3 | Merck Millipore (Burlington, MA, USA) | #sab5701786 |
| phosphorylated-PTEN | Cell Signaling (Danvers, MA, USA) | #91885 |
| phosphorylated-γ-H2AX | Merck Millipore (Burlington, MA, USA) | #05-636 |
| Pink1 | ThermoFisher (Waltham, MA, USA) | #PA1-4515 |
| PTEN | Cell Signaling (Danvers, MA, USA) | #95545S |
| SDHB | Abcam (Waltham, Boston, MA, USA) | #ab84622 |
| TOM20 | Cell Signaling (Danvers, MA, USA) | #42406S |
| UCP2 | Santa Cruz Biotechnology (Dallas, TX, USA) | #sc-6525 |
| β-Actin | Santa Cruz Biotechnology (Dallas, TX, USA) | #sc-1616 |

Table 3 Primary antibodies used for WB analysis

Specific secondary antibodies (Sigma-Aldrich, St. Louis, MO, USA) were employed, all diluted at a 1:10,000 ratio in PBSt. Bands were detected, and their optical density was analyzed using an enhanced chemiluminescence substrate (ECL, BioRad, Hercules, CA, USA), a chemiluminescence system (Alliance 6.7 WL 20M, UVITEC, Cambridge, UK), and the UV1D software (UVITEC, Cambridge, UK). All bands of interest were normalized to β-Actin levels (used as housekeeping protein) detected on the same membrane.

### 4.22 Iron content evaluation

Iron intracellular content was determined using the Colorimetric Iron Assay Kit (#ab83366, Abcam, Waltham, MA, USA), following the manufacturer's instructions.

### 4.23 Statistical analyses

Data were analyzed using Prism 8 Software (GraphPad Software, Inc., La Jolla, CA, USA), appropriately using unpaired t-test, one-way ANOVA, or two-way ANOVA. One-way ANOVA and two-way ANOVA were followed by Tukey's or Sidak's multiple comparison test, respectively. All data are expressed as mean ± standard deviation (SD) and are representative of at least three independent experiments. SD are shown in figures as error bars. An error with a probability of $p < 0.05$ was considered statistically significant.

# 5 Results

## 5.1 Mitochondrial functional defect in Fanconi Anemia

### 5.1.1 Confirming known metabolic dysregulation on cellular models

As a preliminary step, I validated the data in the literature concerning metabolic alterations in FA using the same cell lines employed in all subsequent experiments. Specifically, I aimed to confirm the electron transport defect between complexes I and III and the resulting alteration in the cellular energy state.

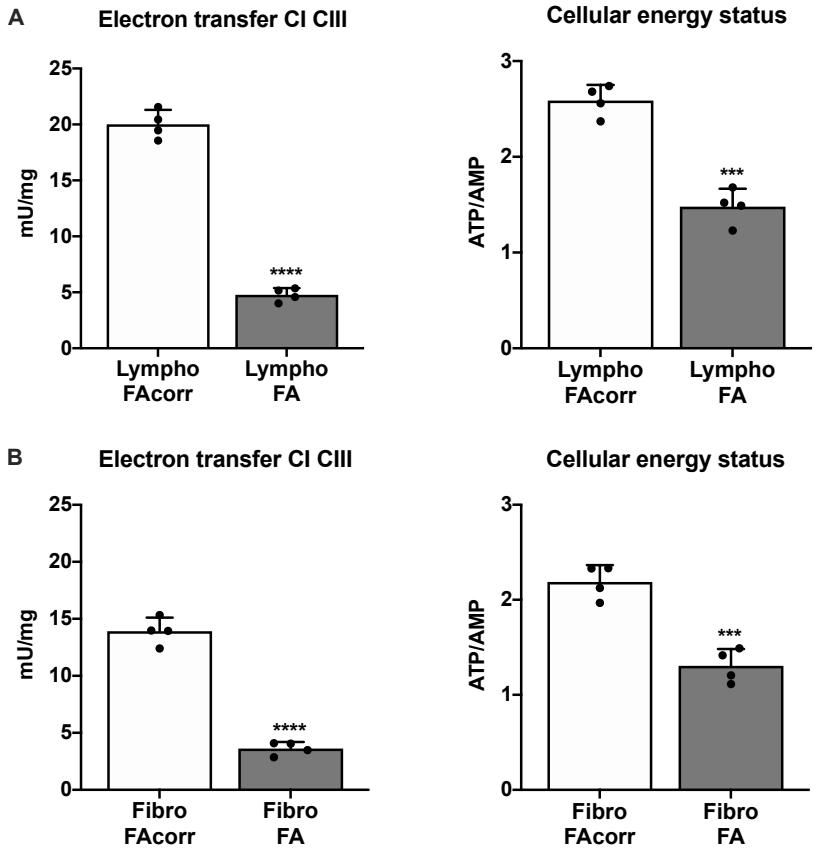


Figure 9 Electron transfer and cellular energy status in lymphoblasts and fibroblasts cell lines with and without FANCA mutation. Electron transfer between complexes I and III and ATP/AMP ratio as a marker of the cellular energy status in FAcorr and FA lymphoblasts (A) and fibroblasts (B). Each graph is representative of at least four independent experiments; FA and FAcorr represent four different lymphoblast (A) or fibroblast (B) cell lines. Data are expressed as mean ± SD. Statistical analysis was performed with an unpaired t-test. *** and **** represent $p < 0.001$ and 0.0001 between FA and FAcorr cell lines.

I validated the existing literature data in both lymphoblasts (Figure 9A) and fibroblasts (Figure 9B). Indeed, both cell lines exhibited a significant reduction in electron transport between complexes I and III, along with a substantial decrease in cellular energy status, as quantified by the ATP to AMP ratio.

### 5.1.2 Comprehensive Analyses of Metabolic Alterations in FA

Once these data were validated, I aimed to delve deeper into the study of the metabolic defect in FA, starting by assessing the oxygen consumption rate (OCR) and ATP synthesis of these cellular lines.

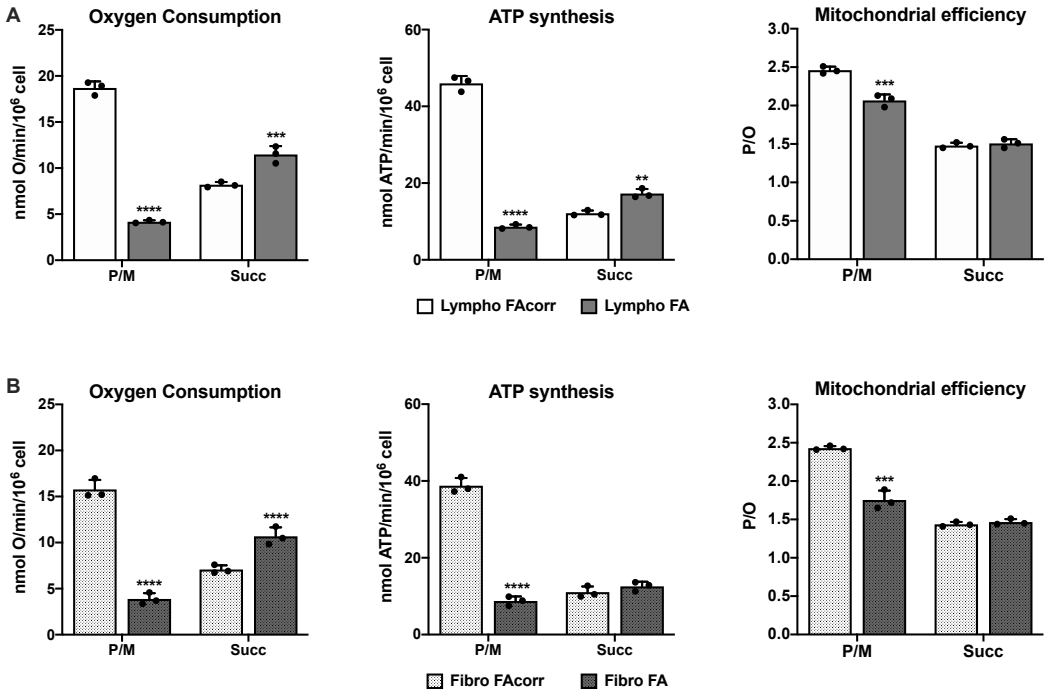


Figure 10 Mitochondrial metabolism in lymphoblasts and fibroblasts cell lines with and without FANCA mutation. Oxygen consumption rate (OCR), ATP synthesis through $F_oF_1$ ATP synthase, and P/O ratio as a marker of mitochondrial efficiency in FAcorr and FA lymphoblasts (A) and fibroblasts (B). All the experiments were performed with the addition of pyruvate and malate (P/M) or succinate (Succ) to activate, respectively, the pathway composed of respiratory complexes I, III, and IV or II, III, and IV. Each graph is representative of at least four independent experiments; FA and FAcorr represent four different lymphoblast (A) or fibroblast (B) cell lines. Data are expressed as mean ± SD. Statistical analysis was performed with an unpaired t-test. *, **, ***, and **** represent $p < 0.05$, 0.01, 0.001, or 0.0001 between FA and FAcorr cell lines.

Data in Figure 10 shows how the OCR is significantly lower for FANCA-mutated cells compared to their respective controls in lymphoblast (A) and fibroblast (B) cell lines. This observation occurred after the administration of pyruvate and malate, which selectively activate the pathway involving complexes I, III, and IV. Following the administration of succinate, which activates the pathway involving complexes II, III, and IV, mutated cells, when compared to their respective controls, showed a significant albeit minor increase in oxygen consumption, likely as an attempt to compensate for the reduction observed for the pathway led by complex I. The same trend is also observable for ATP synthesis, which is significantly diminished in both lymphoblast and fibroblast with the FANCA mutation following the administration of pyruvate and malate. An increase in ATP synthesis can be observed in mutated cells after succinate administration, although this increase is statistically significant only for lymphoblasts. Mitochondrial efficiency, represented by the P/O ratio, is significantly lower for all cells with FANCA mutation following the administration

of pyruvate and malate. However, there is no change in the P/O ratio after succinate administration. This observation suggests that the ETC is uncoupled just when considering the pathway involving complexes I, III, and IV, providing a motivation for the data presented in Figure 9. These insights shed light on the intricate metabolic alterations associated with FANCA mutations, offering valuable clues for further investigation into the pathophysiology of Fanconi Anemia.

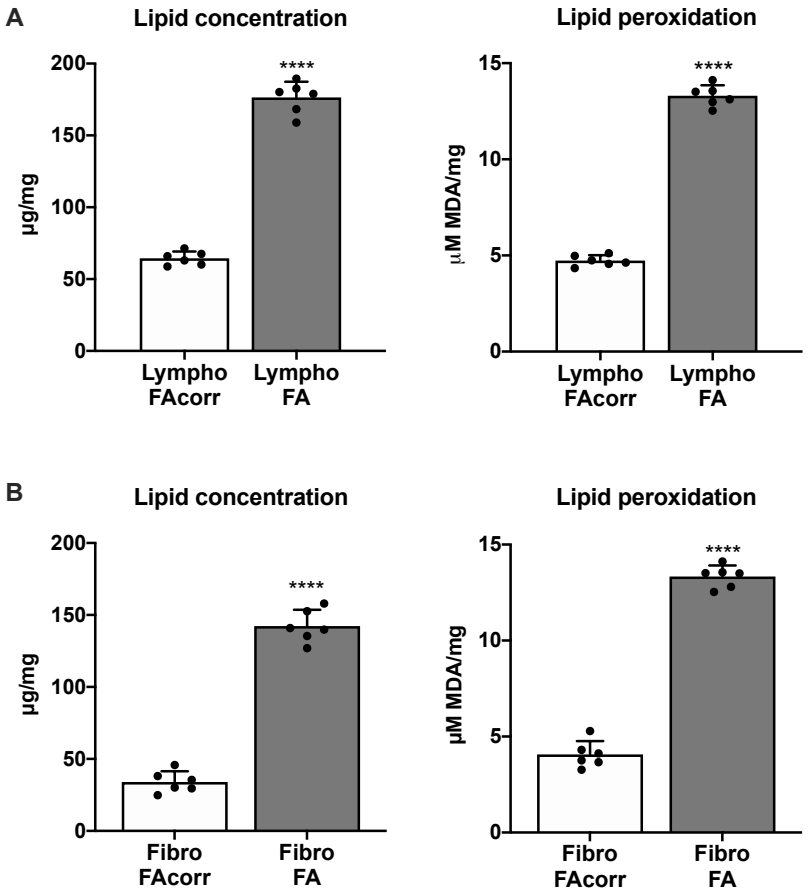


Figure 11 Lipid concentration and peroxidation in lymphoblasts and fibroblasts cell lines with and without FANCA mutation. Lipid concentration and malondialdehyde (MDA) as a marker of lipid peroxidation damage in FAcorr and FA lymphoblasts (A) and fibroblasts (B). Each graph is representative of at least four independent experiments; FA and FAcorr represent four different lymphoblast (A) or fibroblast (B) cell lines. Data are expressed as mean ± SD. Statistical analysis was performed with an unpaired t-test. **** represents a $p < 0.0001$ between FA and FAcorr cell lines.

In both FA lymphoblasts (Figure 11A) and fibroblasts (Figure 11B), we observe a significant increase in both intracellular lipid concentration (left panels) and MDA as a marker of lipid peroxidation when compared to their respective control cells. These findings underscore a substantial metabolic aberration in FA cells, shedding light on the intricate interplay between lipid metabolism and oxidative stress in this genetic disorder. The higher lipid accumulation and elevated peroxidation levels highlight FA cells' challenges in maintaining redox balance. To better comprehend the extent of the redox imbalance issue in these

cells, I also explored the enzymatic activity of catalase and glutathione reductase, two of the primary cellular antioxidant enzymes.

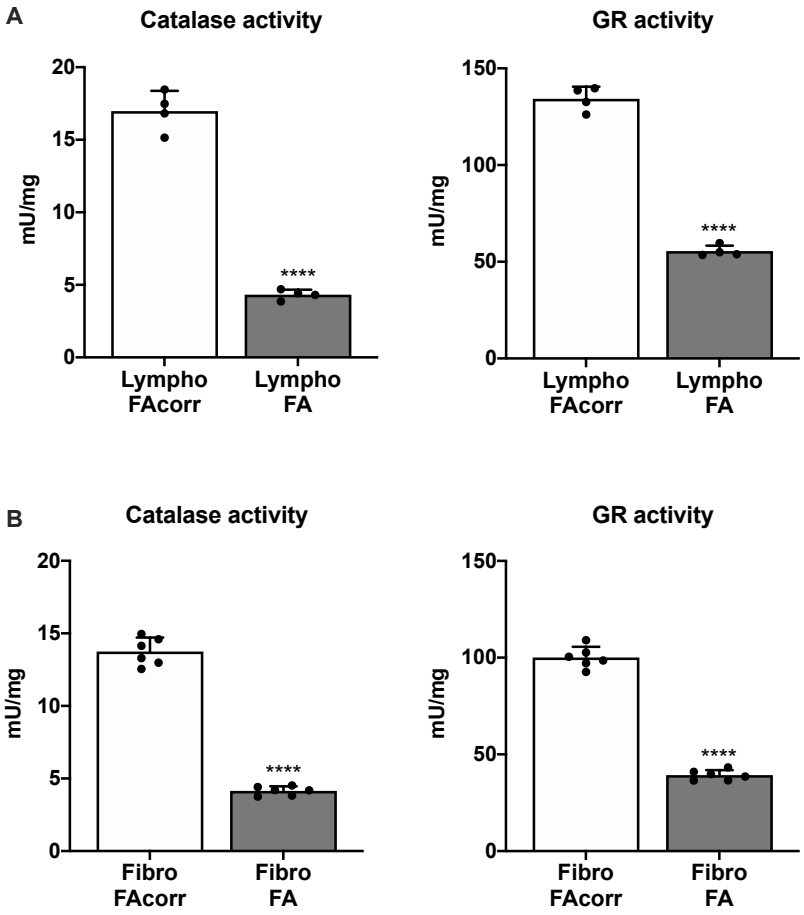


Figure 12 Antioxidant activity in lymphoblasts and fibroblasts cell lines with and without FANCA mutation. Catalase and glutathione reductase (GR) enzymatic activity as markers of antioxidant activity in FAcorr and FA lymphoblasts (A) and fibroblasts (B). Each graph is representative of at least four independent experiments; FA and FAcorr represent four different lymphoblast (A) or fibroblast (B) cell lines. Data are expressed as mean ± SD. Statistical analysis was performed with an unpaired t-test. **** represents a $p < 0.0001$ between FA and FAcorr cell lines.

The results of these analyses (Figure 12) revealed both for lymphoblasts (A) and fibroblasts (B) that the mutated cells, both catalase and glutathione reductase, exhibited significantly lower activity levels compared to their respective controls. This marked reduction in the enzymatic defenses against oxidative stress further accentuates the compromised antioxidative capacity of FA cells. These findings raise critical questions about the cellular mechanisms at play and emphasize the urgency of exploring potential therapeutic interventions to boost antioxidant defenses in FA patients. Besides highlighting the extent of metabolic damage in FA, all these preliminary analyses demonstrate that the lymphoblasts and fibroblast cell lines are robust models for studying this condition. The consistent results obtained from both lymphoblast and fibroblast cell lines indicate that these cell types may serve as suitable alternatives depending on experimental requirements.

### 5.2 FAcorr cell lines as controls: comparison with healthy donor cells

Since the FAcorr lines, both for lymphoblasts and fibroblasts, were generated by inserting the functional FANCA gene into cells initially derived from FA patients, I wanted to ensure they were a suitable control for the cellular model used in this thesis. I did this by comparing key metabolic parameters between healthy donors' (HD) cells and FAcorr lymphoblasts and fibroblasts. I began by checking for significant differences in oxygen consumption, ATP synthesis, and mitochondrial efficiency.

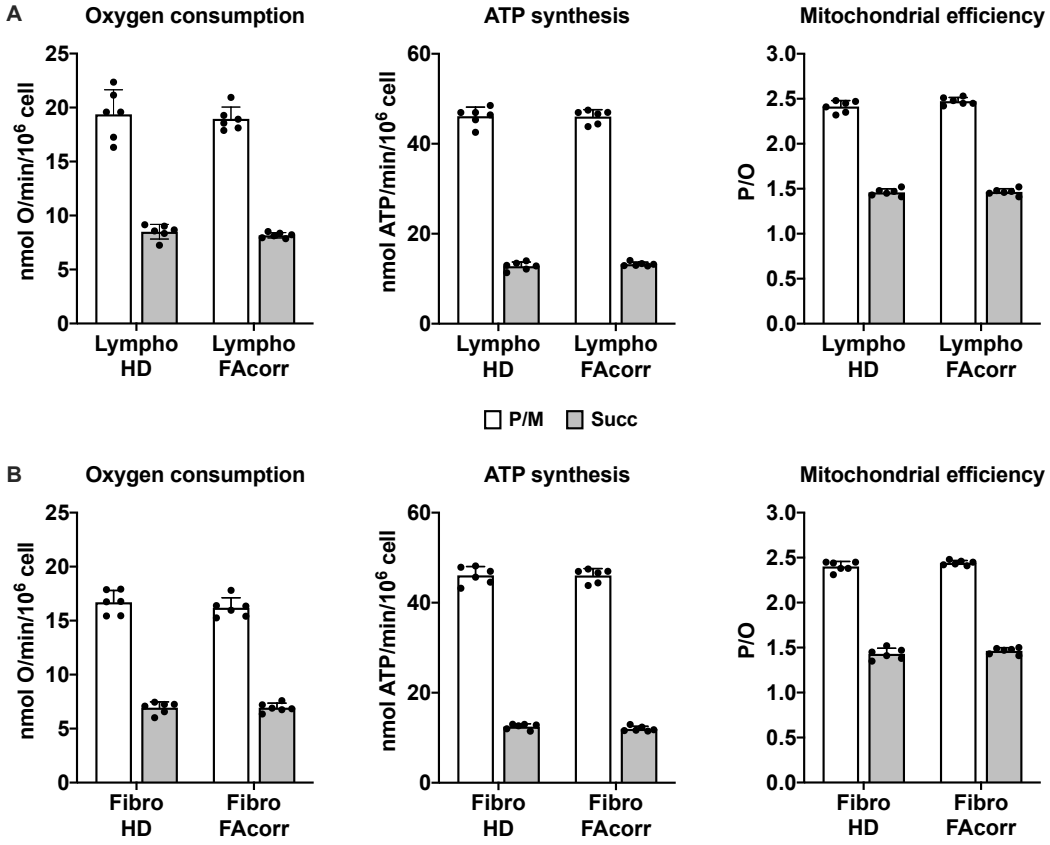


Figure 13 Comparison of OxPhos parameters between healthy donor-derived vs FA-corr lymphoblasts and fibroblasts cell lines. In healthy donor (HD) vs FAcorr lymphoblasts cell lines (A) or healthy donor (HD) vs FAcorr fibroblasts cell lines (B) were tested: Oxygen Consumption Rate (OCR) using pyruvate plus malate (P/M) or succinate (Succ); ATP synthesis through $F_oF_1$ ATP synthase in the presence of P/M or Succ; P/O ratio as an OxPhos efficiency marker using P/M or Succ. Data are reported as mean ± SD, and each graph is representative of 6 independent experiments. Statistical significance was tested with a one-way ANOVA, and no significant differences were observed.

The data shown in Figure 13 demonstrate no differences between HD and FAcorr cells in the evaluated parameters, both for lymphoblasts (A) and fibroblasts (B), whether using pyruvate and malate or succinate as metabolic substrates.

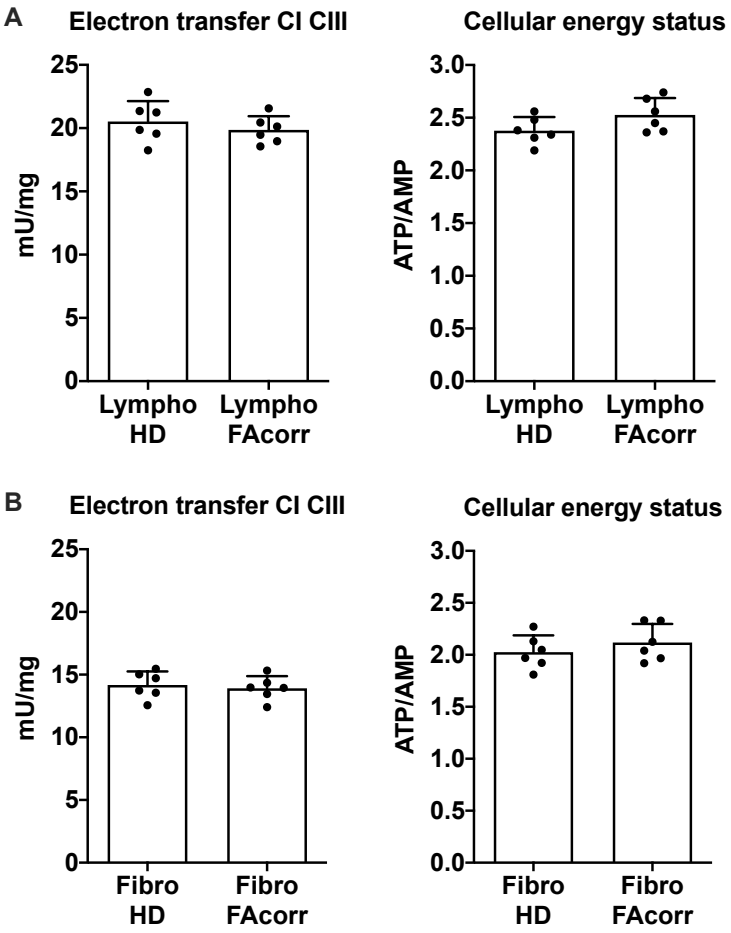


Figure 14 Comparison of electron transport activity between I and III respiratory complexes and cellular energy status between healthy donor-derived vs FA-corr lymphoblasts and fibroblasts cell lines. In healthy donor (HD) vs. FA-corr lymphoblasts cell lines (A) or healthy donor (HD) vs FA-corr fibroblasts cell lines (B) were tested: the electron transfer between respiratory chain's complexes I and III and the ATP/AMP ratio, representing the cellular energy status. Data are reported as mean ± SD, and each graph is representative of 6 independent experiments. Statistical significance was tested with a one-way ANOVA, and no significant differences were observed.

Figure 14 demonstrates no differences between HD and FAcorr cells (A for lymphoblasts and B for fibroblasts) even in terms of electron transport between complex I and III of the respiratory chain, one of the characteristic metabolic defects of FA. There are also no differences in the ATP to AMP ratio, which is a marker for the cellular energy status. I then wanted to verify if there were any differences in the activity of two of the main antioxidant enzymes, catalase (CAT) and glutathione reductase (GR).

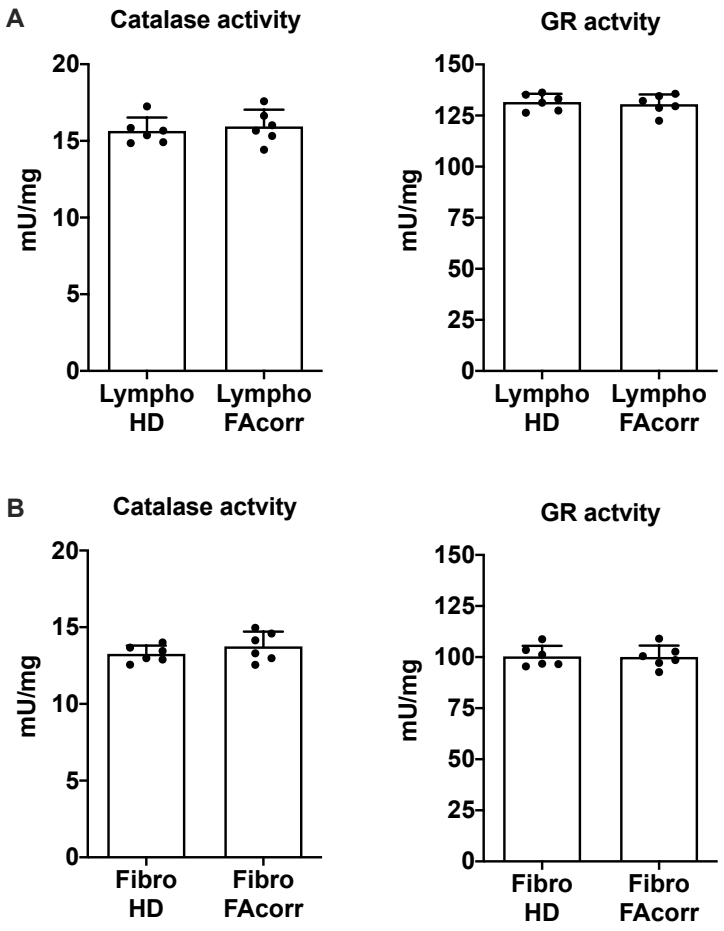


Figure 15 Comparison of antioxidant activity between healthy donor-derived vs FA-corr lymphoblasts and fibroblasts cell lines. Healthy donor (HD) vs. FA-corr lymphoblasts cell lines (A) or healthy donor (HD) vs FA-corr fibroblasts cell lines (B) were tested for catalase (CAT) and glutathione reductase (GR) activities. Data are reported as mean ± SD, and each graph is representative of 6 independent experiments. Statistical significance was tested with a one-way ANOVA, and no significant differences were observed.

Figure 15 shows no significant differences regarding CAT and GR activities between HD and FAcorr cells, neither in lymphoblasts (A) nor fibroblasts (B). The last thing I wanted to check was the potential differences in lipid accumulation and lipid peroxidation.

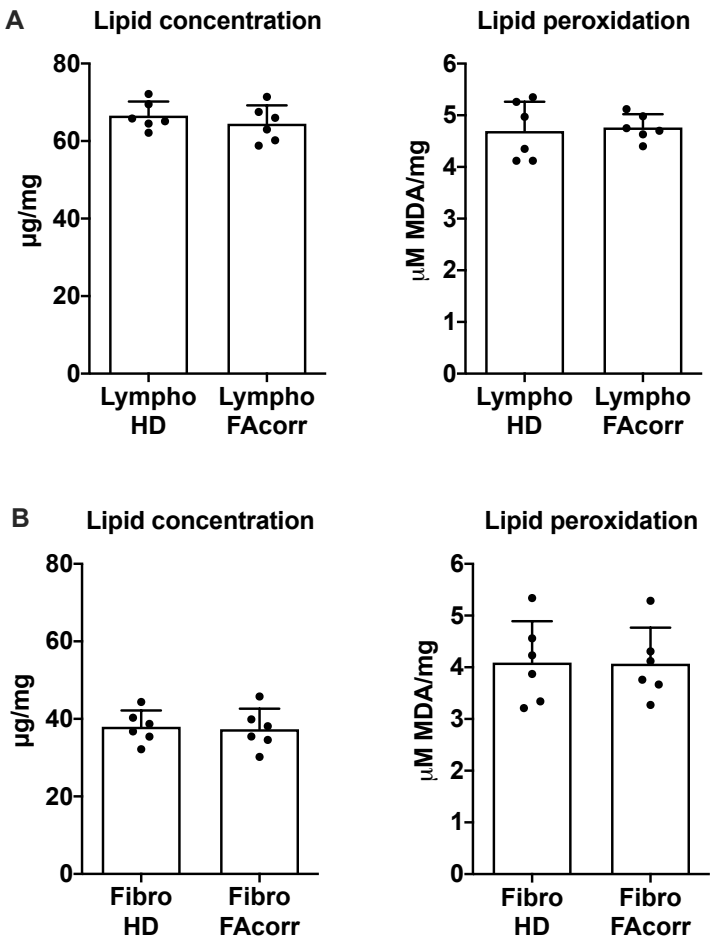


Figure 16 Comparison of lipid concentration and peroxidation in healthy donor-derived vs FA-corr lymphoblasts and fibroblasts cell lines. Healthy donor (HD) vs. FA-corr lymphoblasts cell lines (A) or healthy donor (HD) vs FA-corr fibroblasts cell lines (B) were tested for their lipid intracellular concentration and malondialdehyde (MDA) concentration as a marker of lipid peroxidation. Data are reported as mean ± SD, and each graph is representative of 6 independent experiments. Statistical significance was tested with a one-way ANOVA, and no significant differences were observed.

The data in Figure 16 demonstrate that even in the case of intracellular lipid concentration and malondialdehyde (MDA, used as a marker of lipid peroxidation), there are no significant differences between HD and FAcorr cells, both in lymphoblasts (A) and fibroblasts (B).
The data presented in this section of the thesis demonstrate that lymphoblasts and fibroblasts FAcorr, despite being generated in the laboratory from cells initially derived from patients, serve as a reliable control for my experiments.

### 5.3 Comparative analysis of bone marrow- and peripheral blood-derived cells in Fanconi Anemia patients and healthy donors

The primary metabolic defect in FA is linked to oxidative phosphorylation and, consequently, aerobic respiration. However, the leading causes of morbidity and mortality in patients are bone marrow failure and aplastic anemia. The bone marrow niche is typically a hypoxic microenvironment where cellular anaerobic respiration predominates over aerobic respiration. To better characterize the mitochondrial dysfunctions in FA and determine whether the metabolic defect is already present in the bone marrow to understand the timing of onset, I further investigated the primary FA metabolic defects. I compared mononucleated cells (MNCs) isolated from bone marrow (BM) and peripheral blood (PB) samples obtained from both FA patients (FA) and healthy donors (HD).

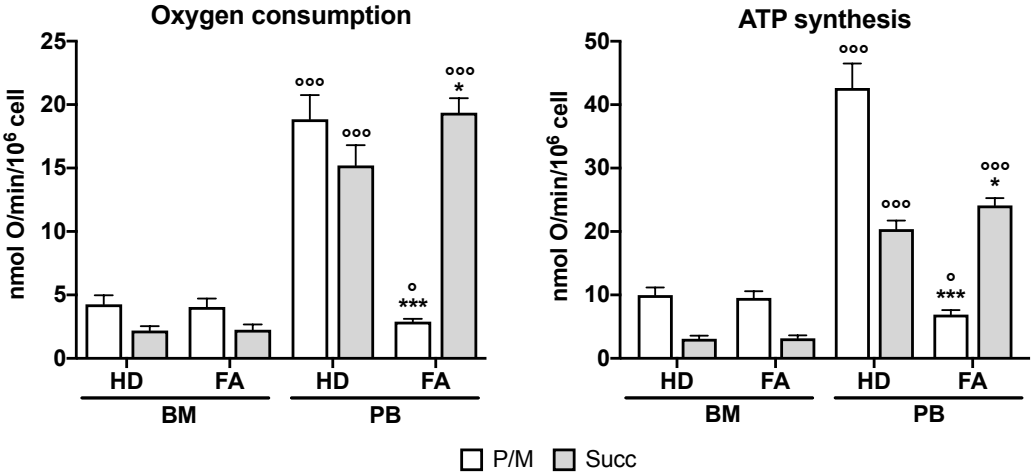


Figure 17 Comparison of mitochondrial metabolism in MNCs isolated from BM and PB of FA patients and healthy donors. All experiments were performed on MNCs isolated from BM and PB from FA patients (n = 8) and healthy donors (n = 7). Oxygen consumption rate (OCR) and ATP synthesis through $F_o$-$F_1$ ATP synthase in the presence of pyruvate and malate (P/M, white columns) or succinate (Succ, grey columns) as markers of aerobic metabolism. All data are expressed as mean ± SD. * and *** represent a significant difference for $p < 0.05$ or 0.001 between FA- and HD-MNCs isolated from the same site. ° and °°° indicate a significant difference for $p < 0.05$, 0.01, or 0.001, respectively, between BM- and PB-MNCs in the same clinical condition.

The data shown in Figure 17 highlight that there are no significant differences in oxygen consumption rate (OCR) and ATP synthesis between HD and FA in the BM-derived samples, whether using pyruvate and malate (P/M) or succinate (Succ) as respiratory substrates. However, the metabolic defect becomes quite evident when considering the PB-derived samples, where there is a significant reduction in both OCR and ATP synthesis in FA compared to HD for P/M and a minor yet still significant increase for the same parameters in FA for Succ. Since FA cells cannot properly activate the mitochondrial metabolism through the pathway involving complexes I, III, and IV (P/M), they attempt to compensate through the pathway involving complexes II, III, and IV (Succ).

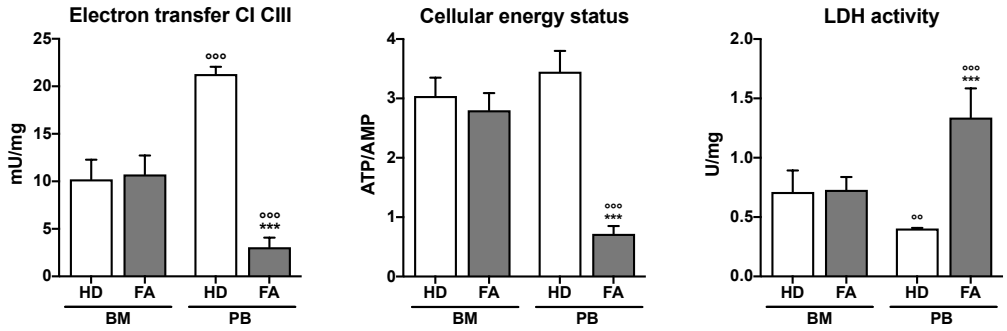


Figure 18 Comparison of electron transfer between respiratory complexes I and III, cellular energy status, and LDH activity in MNCs isolated from BM and PB of FA patients and healthy donors. All experiments were performed on MNCs isolated from BM and PB from FA patients (n = 8) and healthy donors (n = 7). Electron transfer between respiratory complexes I and III; ATP/AMP ratio, a marker of cellular energy status; lactate dehydrogenase activity (LDH), as a marker of anaerobic metabolism. All data are expressed as mean ± SD. *** represents a significant difference for $p < 0.001$ between FA- and HD-MNCs isolated from the same site. °° and °°° indicate a significant difference for $p < 0.01$ or 0.001, respectively, between BM- and PB-MNCs in the same clinical condition

As illustrated in the lower panels of Figure 18, there are no differences between HD and FA BM-derived samples in electron transport between complexes I and III of the respiratory chain, cellular energy state, or LDH enzyme activity. However, in PB-derived FA samples compared to HD, there is a significant reduction in electron transport between complexes I and III and cellular energy state, while LDH activity increases significantly.

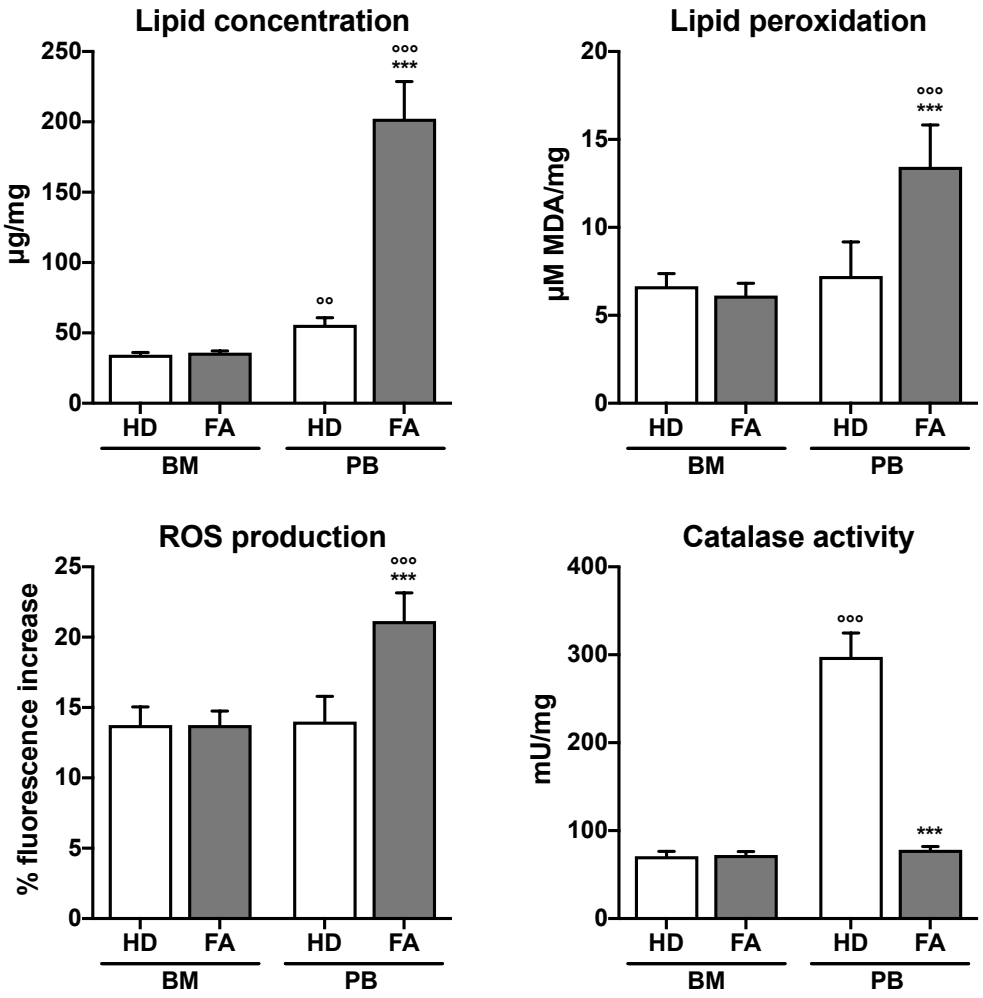


Figure 19 Comparison of lipid concentration, oxidative stress levels, and antioxidants in MNCs isolated from BM and PB of FA patients and healthy donors. All experiments were performed on MNCs isolated from BM and PB from FA patients (n = 8) and healthy donors (n = 7). Upper panels: intracellular lipid content and malondialdehyde (MDA) levels as a marker of lipid peroxidation damage. Lower panels: ROS production and catalase enzymatic activity as a marker of endogenous antioxidant defenses. All data are expressed as mean ± SD. *** indicates a significant difference for $p < 0.001$ between FA- and HD-MNCs isolated from the same site. °° or °°° indicate a significant difference for $p < 0.01$ or 0.001 between BM- and PB-MNCs in the same clinical condition.

I also evaluated other metabolic parameters typically altered in FA within the same samples, which included intracellular lipid accumulation, the level of lipid peroxidation, ROS production, and catalase activity (a key antioxidant enzyme in cells). As shown in Figure 19, the data again emphasize that there are no differences in any of these parameters between BM-derived samples from HD and FA patients. However, a significant increase is observed when comparing PB-derived samples from FA patients to their HD counterparts in terms of lipid concentration, malondialdehyde concentration (MDA, as a marker of lipid peroxidation), and ROS production. On the other hand, catalase activity appears to have significantly decreased to the point of reaching levels comparable to those in BM cells, indicating the impaired ability of FA cells to activate antioxidant defenses even in the presence of oxidative stress.

### 5.4 Timing of metabolic damage manifestation in FA cells

All the data presented in this section so far confirm the various metabolic defects in FA cells, demonstrating that these defects are not present in the bone marrow but only in peripheral blood when aerobic metabolism is activated by the cells in response to changes in oxygen concentration in their environment. So, I wanted to investigate this aspect further and pinpoint the exact timing at which the metabolic damages become evident by culturing MNCs derived from the bone marrow of both FA patients and HD for 72 hours. These cells were cultured under hypoxic (3% [$O_2$]) and normoxic (20% [$O_2$]) conditions to mimic the oxygen concentrations found in the bone marrow niche and the bloodstream, respectively.

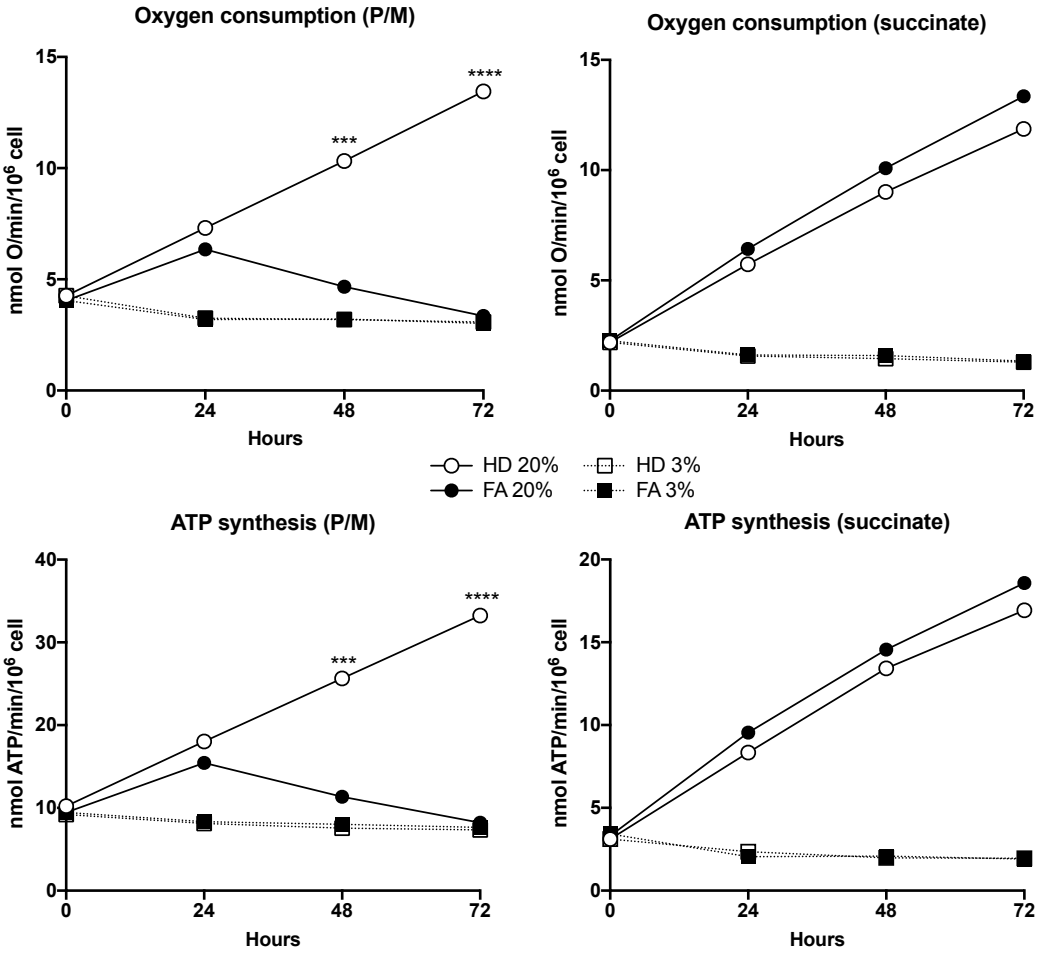


Figure 20 Modifications of mitochondrial metabolism in HD and FA BM-MNCs cultured in hypoxic or normoxic conditions. All data reported in this figure are obtained from FA or HD BM-MNCs stimulated with PHA and grown in 3% or 20% oxygen for 72 h. White circles represent HD BM-MNCs (n = 8), and black circles represent FA BM-MNCs (n = 6) cultured in 20% oxygen. White squares represent HD BM-MNCs (n = 8), and black squares represent FA BM-MNCs (n = 6) cultured in 3% oxygen. Upper panels: oxygen consumption rate in the presence of pyruvate and malate or succinate. Lower panels: ATP synthesis through $F_o$-$F_1$ ATP synthase in the presence of pyruvate and malate or succinate, respectively. All data are expressed as mean ± SD. *** or **** indicate a significant difference for $p < 0.001$ or 0.0001 between HD BM-MNCs and FA-MNCs cultured at 20% oxygen at the same time point; there were no significant differences between HD BM-MNCs and FA-MNCs cultured at 3% oxygen at the same time point.

In Figure 20, the samples cultured in 20% oxygen are represented as circles (black for FA and white for HD), and the samples cultured in 3% oxygen are represented as squares (black for FA and white for HD). The upper panels represent the oxygen consumption rate (OCR, P/M on the left and Succ on the right), while the lower panels represent ATP synthesis (P/M on the left and Succ on the right). The data in the left panels, OCR, and ATP synthesis measurements using P/M as a respiratory substrate show that samples cultured in hypoxia conditions exhibit a similar trend over all the 72 hours of the experiments for HD and FA (white and black squares). For samples cultured under normoxia conditions, however, the measurements follow a similar trend for the first 24 hours but show significant differences at the 48- and 72-hour time points. While HD samples continue to increase both OCR and ATP synthesis progressively, FA samples initially attempt to activate aerobic metabolism for the first 24 hours. Still, both parameters decrease significantly, reaching the level of cells cultured at 3% oxygen at 72 hours, demonstrating the inability of FA cells to activate mitochondrial metabolism through the pathway involving complexes I, III, and IV. Regarding OCR and ATP synthesis measured using succinate as the respiratory substrate (right panels), thus activating the oxidative phosphorylation pathway composed of complexes II, III, and IV, both cells cultured in 3% and those cultured in 20% oxygen exhibit similar trends between HD and FA. A slight, non-significant increase in the FA cultured in 20% oxygen compared to the HD cultured in the same conditions confirms the compensatory attempt observed earlier.

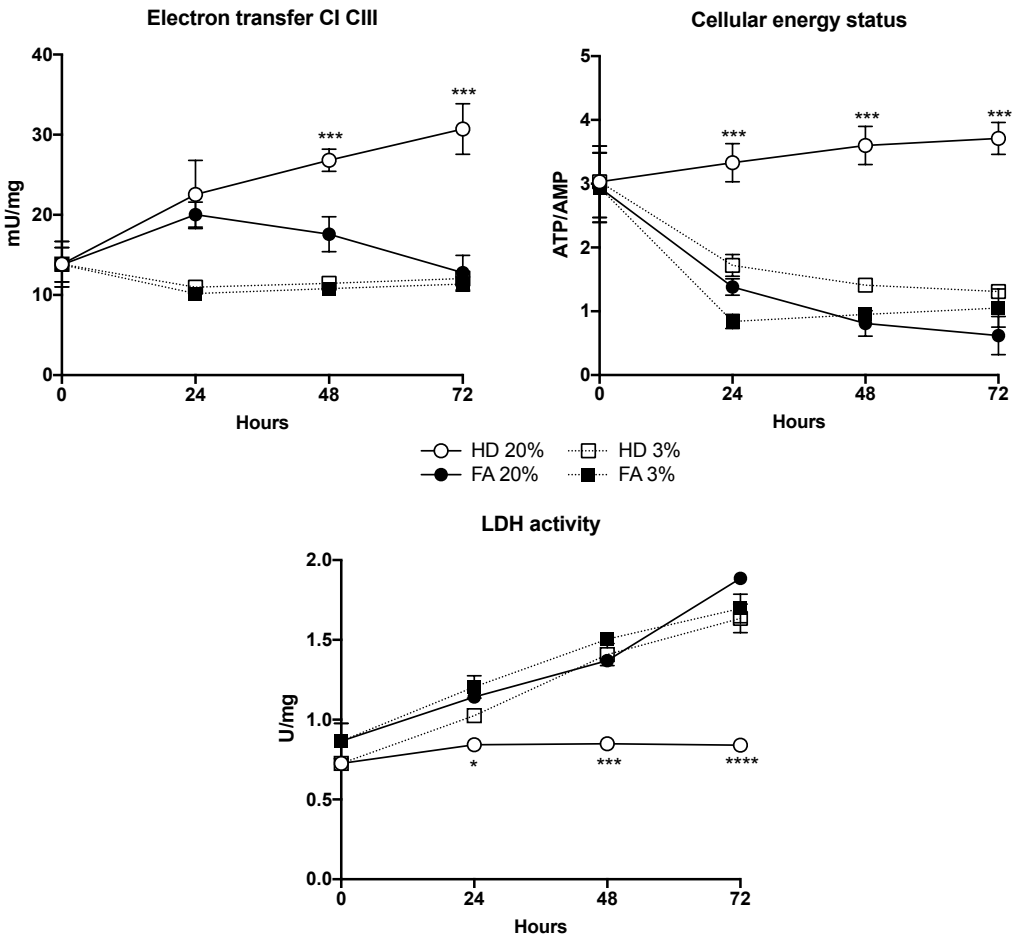


Figure 21 Modifications of electron transfer between respiratory complexes I and III, cellular energy status, and LDH activity in HD and FA BM-MNCs cultured in hypoxic or normoxic conditions. All data reported in this figure are obtained from FA or HD BM-MNCs stimulated with PHA and grown in 3% or 20% oxygen for 72 h. White circles represent HD BM-MNCs (n = 8), and black circles represent FA BM-MNCs (n = 6) cultured in 20% oxygen. White squares represent HD BM-MNCs (n = 8), and black squares represent FA BM-MNCs (n = 6) cultured in 3% oxygen. Upper panels: electron transfer between respiratory complexes I and III, ATP/AMP ratio as a marker of cellular energy status. Lower panel: LDH enzymatic activity as a marker of anaerobic metabolism. All data are expressed as mean ± SD. *, ***, and **** indicate a significant difference for $p < 0.05$, 0.001, or 0.0001 between HD BM-MNCs and FA-MNCs cultured at 20% oxygen at the same time point; there were no significant differences between HD BM-MNCs and FA-MNCs cultured at 3% oxygen at the same time point.

Regarding the electron transfer between complexes I and III, shown in the first panel of Figure 21, we can see how the measurements of FA and HD cultivated in 3% oxygen overlap once again, while for cells grown in 20% oxygen, there is a similar trend to what was measured for OCR and ATP synthesis: while HD cells progressively increase electron transfer between complexes I and III for all the 72 hours of the experiments, FA cells show an initial increase for the first 24 hours, but electron transfer decreases in the subsequent 48 hours, reaching the levels of cells cultivated in hypoxia. Cellular energy status, represented by the ATP/AMP ratio, appears to be similar or with non-significant differences between HD and FA cells cultivated in 3% oxygen. However, for cells grown in 20% oxygen, there is a slight increasing trend for HD cells and a progressive and significant decrease in

FA cells. LDH activity progressively increases over 72 hours for all cells cultivated in 3% oxygen as well as for FA cells cultivated in 20% oxygen, indicating their preference for anaerobic metabolism to compensate for inefficient mitochondrial metabolism. In contrast, in HD cells grown in normoxia conditions, where mitochondrial metabolism functions properly, LDH activity does not increase and remains constant over time.

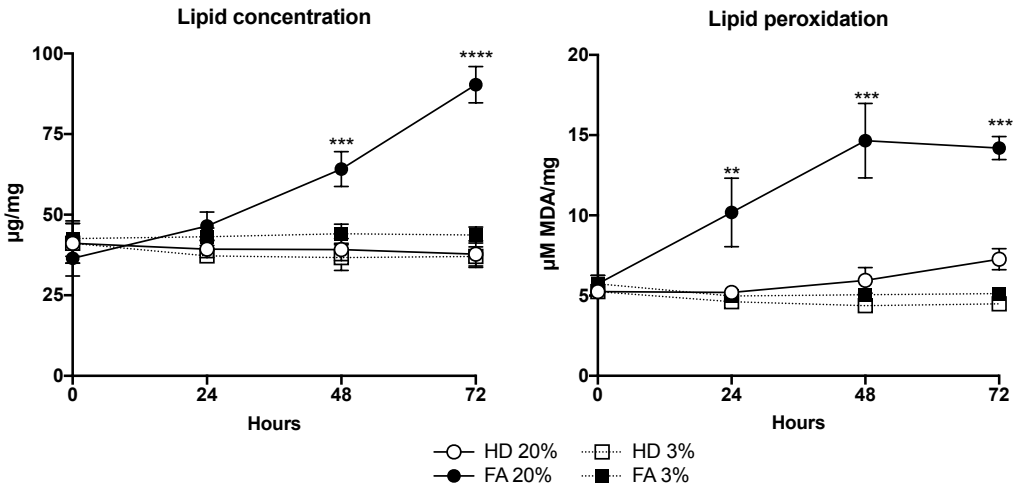


Figure 22 Modifications of lipid accumulation and peroxidation in HD and FA BM-MNCs cultured in hypoxic or normoxic conditions. All data reported in this figure are obtained from FA or HD BM-MNCs stimulated with PHA and grown in 3% or 20% oxygen for 72 h. White circles represent HD BM-MNCs (n = 8), and black circles represent FA BM-MNCs (n = 6) cultured in 20% oxygen. White squares represent HD BM-MNCs (n = 8), and black squares represent FA BM-MNCs (n = 6) cultured in 3% oxygen. Lipid intracellular concentration and malondialdehyde (MDA) as a marker of lipid peroxidation damage. All data are expressed as mean ± SD. **, ***, and **** indicate a significant difference for $p < 0.01$, 0.001, or 0.0001 between HD BM-MNCs and FA-MNCs cultured at 20% oxygen at the same time point; there were no significant differences between HD BM-MNCs and FA-MNCs cultured at 3% oxygen at the same time point.

As for intracellular lipid concentration and MDA levels, which serve as markers of lipid peroxidation, Figure 22 shows that all the curves virtually overlap for 72 hours, except for the FA cells cultivated at 20% oxygen, where both lipid accumulation and MDA levels are significantly higher.

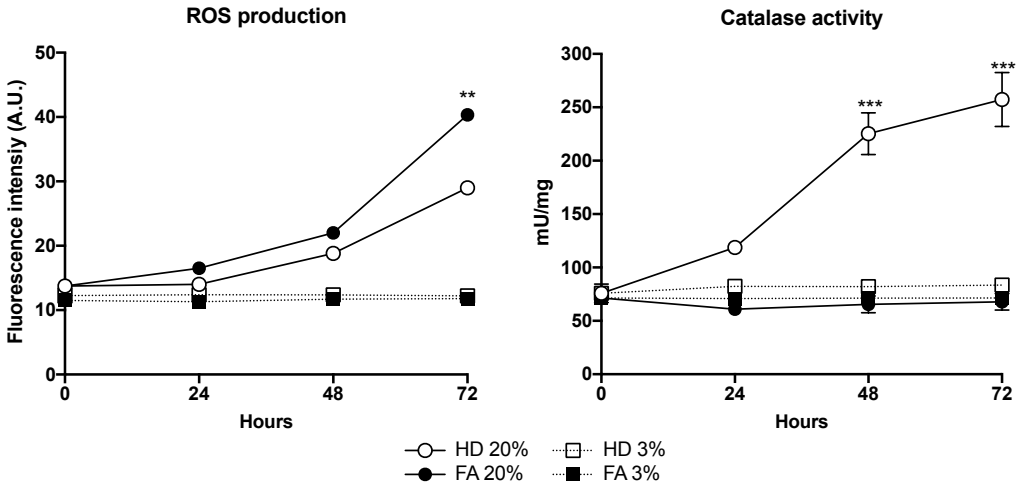


Figure 23 Modifications of ROS production and antioxidant defenses in HD and FA BM-MNCs cultured in hypoxic or normoxic conditions. All data reported in this figure are obtained from FA or HD BM-MNCs stimulated with PHA and grown in 3% or 20% oxygen for 72 h. White circles represent HD BM-MNCs (n = 8), and black circles represent FA BM-MNCs (n = 6) cultured in 20% oxygen. White squares represent HD BM-MNCs (n = 8), and black squares represent FA BM-MNCs (n = 6) cultured in 3% oxygen. ROS production, a marker of oxidative stress levels, and catalase enzymatic activity, a marker of cellular antioxidant defenses. All data are expressed as mean ± SD. ** and *** indicate a significant difference for $p < 0.01$ or 0.001 between HD BM-MNCs and FA-MNCs cultured at 20% oxygen at the same time point; there were no significant differences between HD BM-MNCs and FA-MNCs cultured at 3% oxygen at the same time point.

To measure oxidative stress, I measured ROS production. In the first panel of Figure 23, data show how this parameter remains constant and at low levels for both FA and HD at 3% oxygen. In comparison, it increases for both FA and HD cultivated in 20% oxygen, albeit more significantly for FA cells, which at 72 hours show a significant difference also compared to the HD counterpart. Concurrently with ROS production, catalase enzymatic activity remains constant over time for all cells cultured at 3% oxygen. Similarly, HD cells cultured at 20% oxygen increase catalase activity over time in response to increased ROS production. FA cells cultured at 20% oxygen, on the other hand, despite their significant increase in ROS production over time, are unable to increase catalase activity, which remains comparable to the activity measured for cells at 3% oxygen throughout the 72-hour duration of the experiments. All the data presented in sections 3.3 and 3.4 have been published in E. Cappelli *et al.*, “The passage from bone marrow niche to bloodstream triggers the metabolic impairment in Fanconi Anemia mononuclear cells,” *Redox Biol*, vol. 36, 2020 DOI: 10.1016/j.redox.2020.101618.

### 5.5 OxPhos complexes

To comprehend the underlying causes of the altered energy metabolism in cells with the FANCA gene mutation, I hypothesized that there might be an impaired or altered expression within the respiratory chain complexes protein subunits. To address this question, I conducted protein expression analyses using Western blotting (WB) on both lymphoblasts and fibroblasts, with and without the FANCA mutation. WBs were performed against ND1, a complex I subunit (encoded by mitochondrial DNA (mtDNA)), SDHB, a complex II subunit (encoded by nuclear DNA), MTCO2, a complex IV subunit (mtDNA encoded), and the β-subunit of ATP synthase's $F_o$ moiety (encoded by nuclear DNA). Considering the uncoupling of the respiratory chain, as demonstrated in section 3.1, I also assessed the expression levels of UCP2.

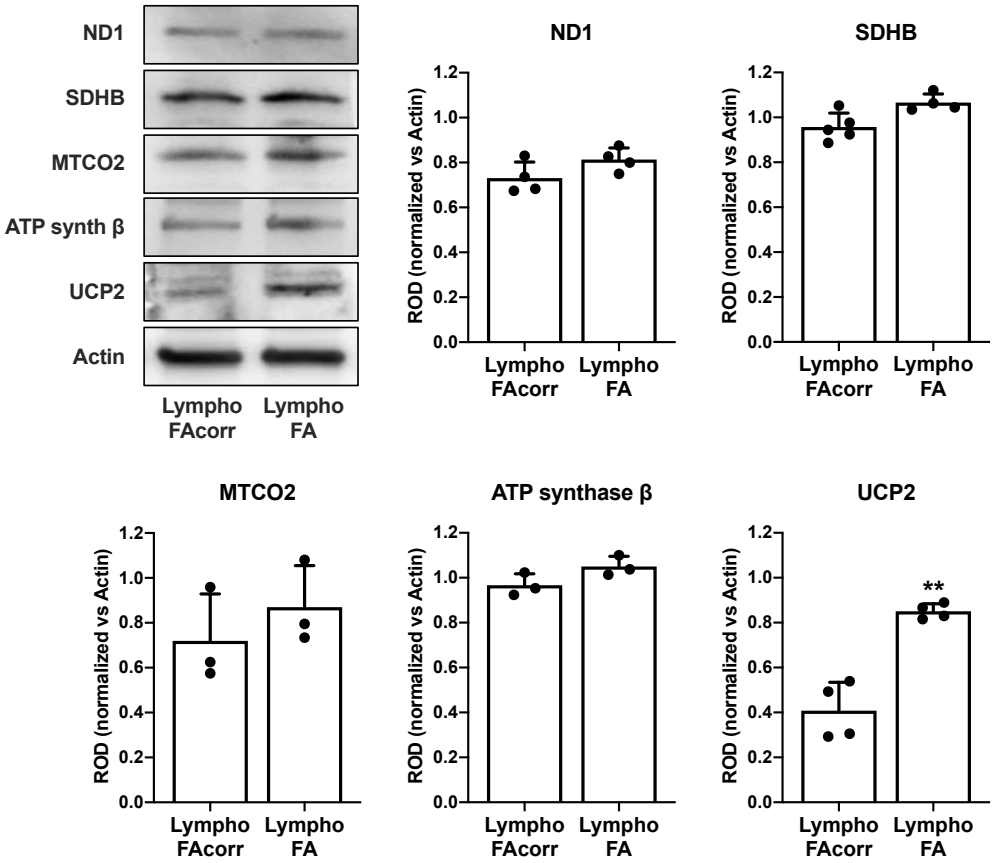


Figure 24 OxPhos subunits and UCP2 expression levels in FA and FAcorr lymphoblasts. WB signals of ND1 (Complex I), SDHB (Complex II), MTCO2 (Complex III), and ATP synthase β subunit; WB signal of uncoupling protein 2 (UCP2) in lymphoblasts cell lines mutated or not for the FANCA gene. Protein expression levels (densitometric analysis) were normalized on the Actin signal (housekeeping) revealed on the same membrane. Data are reported in histograms as mean ± SD, and each panel and graph is representative of at least 3 independent experiments. Statistical significance was tested opportunely with an unpaired t-test; ** represents a significant difference for $p < 0.01$ between FA and FAcorr cells.

Data did not show significant differences in the expression levels of any analyzed subunits either in lymphoblasts (Figure 24) or fibroblasts (Figure 25). However, UCP2 expression

levels were higher in both lymphoblasts and fibroblasts with the FANCA mutation than their respective controls. The increased expression of an uncoupling protein could offer a potential explanation for the uncoupling of the respiratory chain and, consequently, the metabolic defect observed in FA. However, this higher expression alone cannot be considered the sole factor contributing to FA metabolic dysfunctions.

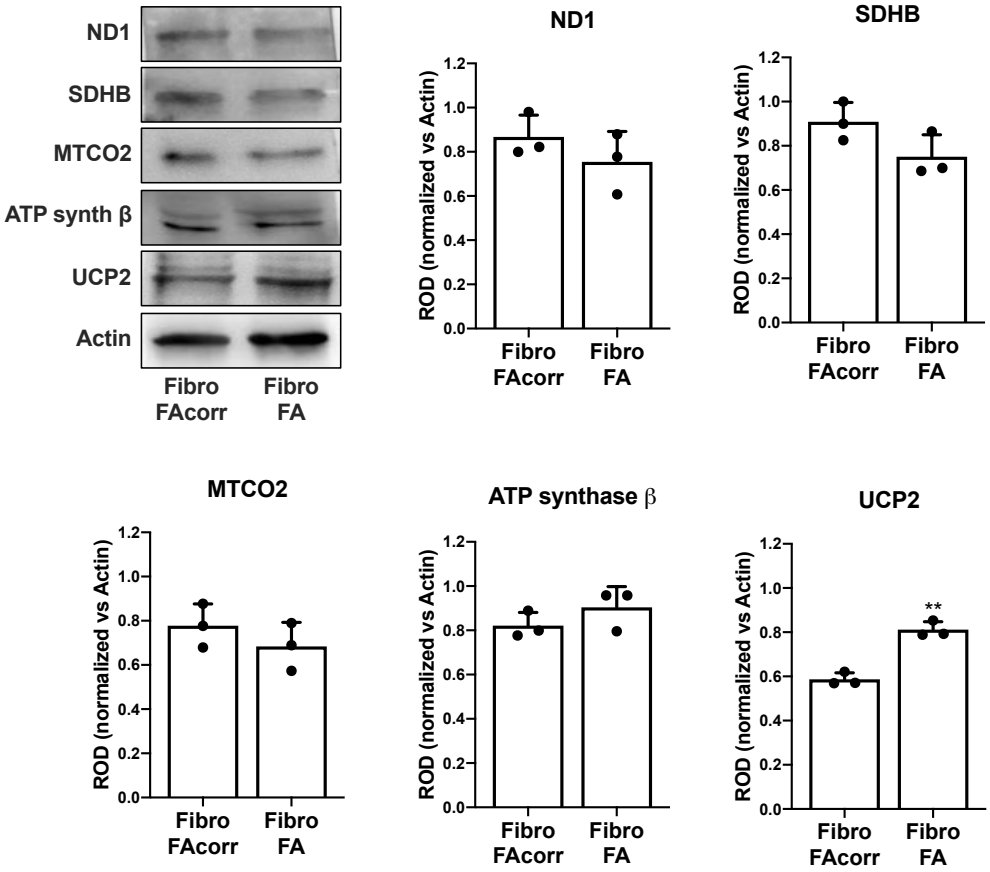


Figure 25 OxPhos subunits and UCP2 expression levels in FA and FAcorr fibroblasts. WB signals of ND1 (Complex I), SDHB (Complex II), MTCO2 (Complex III), and ATP synthase β subunit; WB signal of uncoupling protein 2 (UCP2) in fibroblasts cell lines mutated or not for the FANCA gene. Protein expression levels (densitometric analysis) were normalized on the Actin signal (housekeeping) revealed on the same membrane. Data are reported in histograms as mean ± SD, and each panel and graph is representative of at least 3 independent experiments. Statistical significance was tested opportunely with an unpaired t-test; ** represents a significant difference for $p < 0.01$ between FA and FAcorr cells.

### 5.6 Mitochondrial morphological defects

Given the absence of alterations in the expression of respiratory complex subunits, I began considering whether the problem could involve mitochondrial morphology. I performed an electron microscopy analysis on FA lymphoblasts (Figure 26A), FAcorr lymphoblasts (Figure 26B), FA fibroblasts (Figure 26C), and FAcorr fibroblasts (Figure 26D). This analysis enabled the visualization of mitochondrial morphology, highlighting swollen mitochondria with a disorganized inner membrane and mitochondrial cristae in both lymphoblasts and fibroblasts with the FANCA mutations (right panels) when compared to the FAcorr counterparts (left panels).

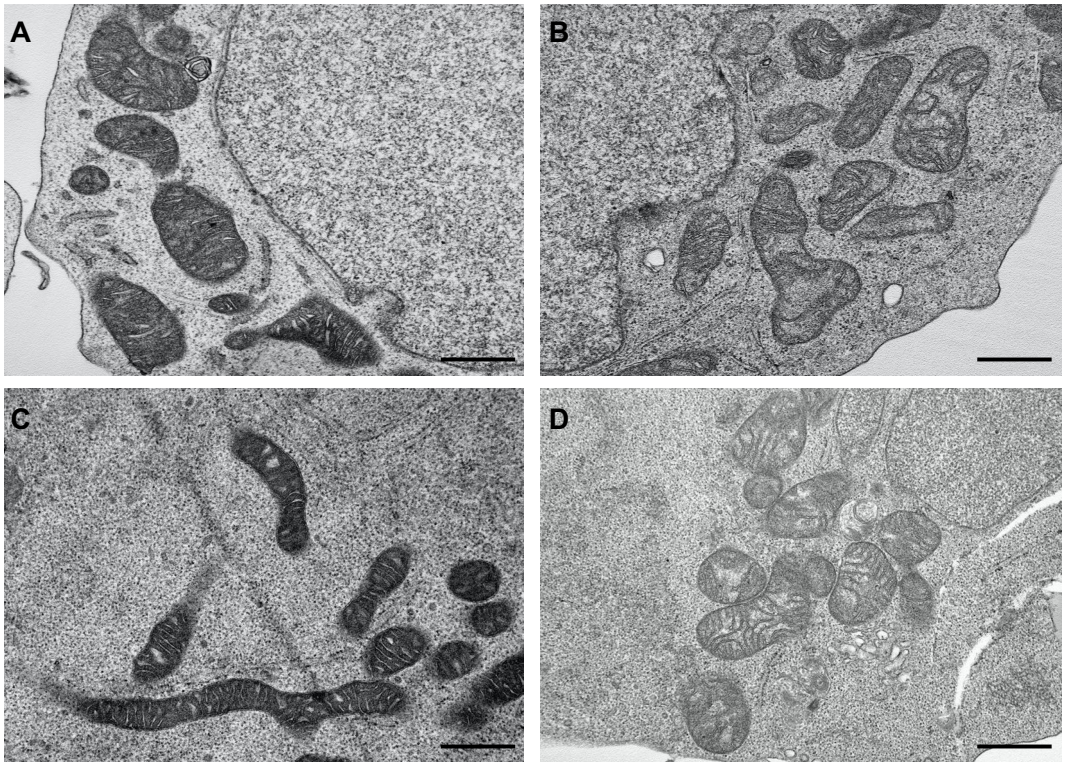


Figure 26 Mitochondrial structure in lymphoblasts and fibroblasts mutated or not for the FANCA gene. Representative electron microscopy of (A) FAcorr lymphoblasts (B) FA lymphoblasts (C) FAcorr fibroblasts (D) FA fibroblasts. The black scale bar corresponds to 1 μm.

This analysis has also highlighted another aspect: how the mitochondria in FAcorr cells, especially fibroblasts, were much more organized in forming a mitochondrial network, a feature entirely absent in FA cells, where mitochondria appear as individual entities, lacking organization. This also led me to hypothesize an issue with mitochondrial dynamics processes, which I wanted to explore further. Therefore, I assessed the expression levels of key proteins involved in these processes using WB. These proteins included CLUH, an mRNA-binding protein involved in mitochondrial biogenesis, DRP1 implicated in fission, and OPA1 and MFN2 associated with mitochondrial fusion. As shown in Figure 27 no significant differences were found in CLUH, OPA1, and MFN2 expression levels. However, the expression of DRP1 resulted significantly higher both for FA lymphoblasts (A) and FA fibroblasts (B) when compared to their respective controls. This finding suggests an imbalance in mitochondrial dynamics processes in FA, leading to a prevalence of fission over fusion, resulting in mitochondrial network fragmentation and reduced OxPhos efficiency.

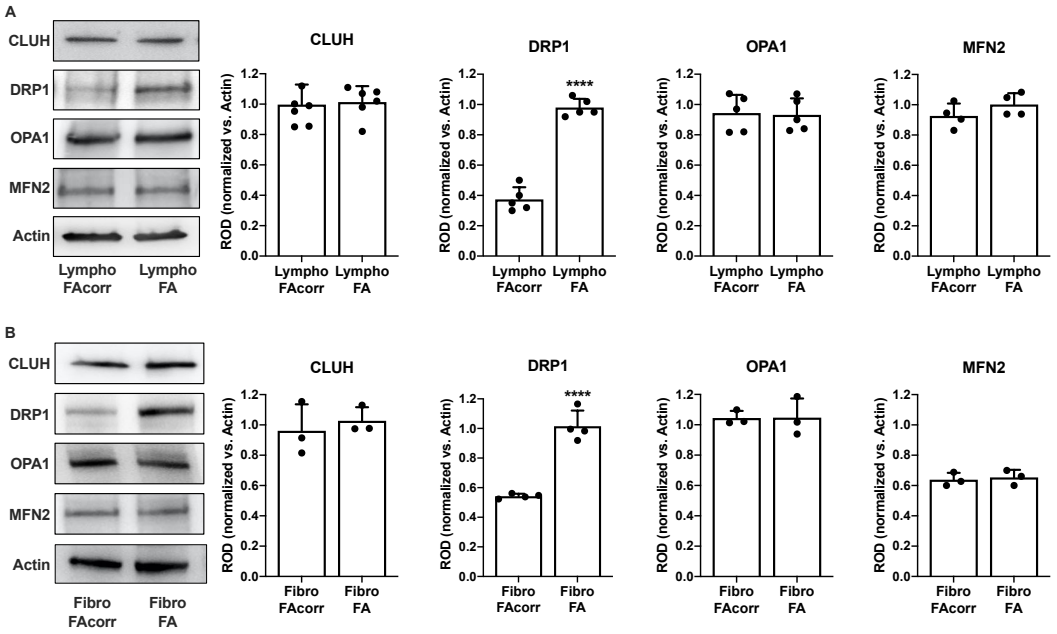


Figure 27 Mitochondrial dynamics makers expression levels in FA and FAcorr lymphoblasts and fibroblasts. WB signals of CLUH (mitochondrial biogenesis), DRP1 (mitochondrial fission), OPA1, MFN2 (mitochondrial fusion), and Actin (housekeeping protein) in lymphoblasts (A) and fibroblasts (B) cell lines mutated or not for the FANCA gene. Protein expression levels (densitometric analysis) were normalized on the Actin signal revealed on the same membrane. Data are reported in histograms as mean ± SD, and each panel and graph is representative of at least 3 independent experiments. Statistical significance was tested opportunely with an unpaired t-test; **** represents a significant difference for $p < 0.0001$ between FA and FAcorr cells.

I performed a confocal microscopy analysis to confirm mitochondrial network fragmentation in FA cells, as shown in Figure 28. FAcorr and FA fibroblasts were stained in green with an antibody against TOM20, a mitochondrial import receptor subunit located in the outer mitochondrial membrane, and in blue with DAPI to visualize cells' nuclei. The distribution of the mitochondrial network in fibroblasts was subsequently classified as elongated or intermediate/short.

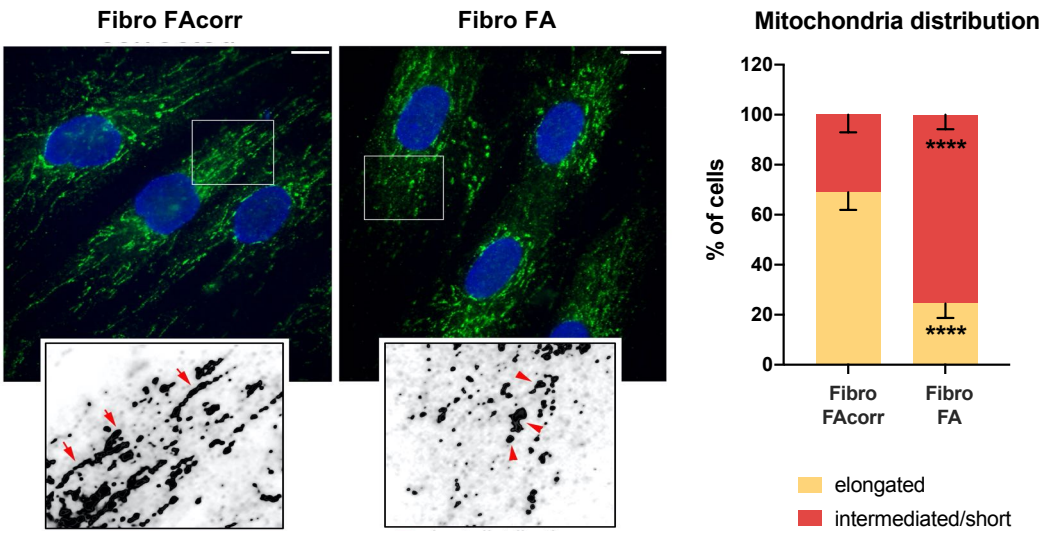


Figure 28 Mitochondrial network distribution. Confocal microscopy analysis of FAcorr and FA fibroblasts stained with antibodies against TOM20 (green) to mark mitochondrial reticulum and DAPI (blue) to mark nuclei. White scale bars correspond to 10 μm. The higher magnification images correspond to the area enclosed by the white squares and are examples of mitochondrial network distribution within the cells. Fibroblasts were scored depending on the morphology of most of their mitochondrial population as elongated or intermediated/short, and the results are reported in the histogram on the right. Data are reported as mean ± SD and are representative of at least three independent experiments. Statistical significance was tested with an unpaired t-test; **** represents a significant difference for $p < 0.0001$ between FA cells and FAcorr cells.

As illustrated in the right-hand graph of Figure 28, in fibroblasts with the FA mutation, the percentage of mitochondria exhibiting an intermediate/short distribution reaches nearly 80%, significantly higher compared to the FAcorr counterpart, where the elongated mitochondria approach almost 70%. This result confirms the unbalanced mitochondrial dynamics in FA and the consequent mitochondrial network fragmentation, offering a potential explanation for the inefficient OxPhos FANCA mutated cells.

### 5.6.1 Treatment with P110, a specific inhibitor of DRP1.

Given that in FANCA mutated cells, a prevalence of mitochondrial fission leads to mitochondrial network fragmentation probably due to the significant increase in DRP1 expression, as demonstrated in section 5.6, I opted to experiment with P110, a specific DRP1 inhibitor. My objective was to attempt to mitigate mitochondrial reticulum disruption and enhance OxPhos' efficiency. After treating both FA lymphoblasts and FA fibroblasts

for 24h with 1 μM of P110, I assessed its effects by considering DRP1 and UCP2 expression levels.

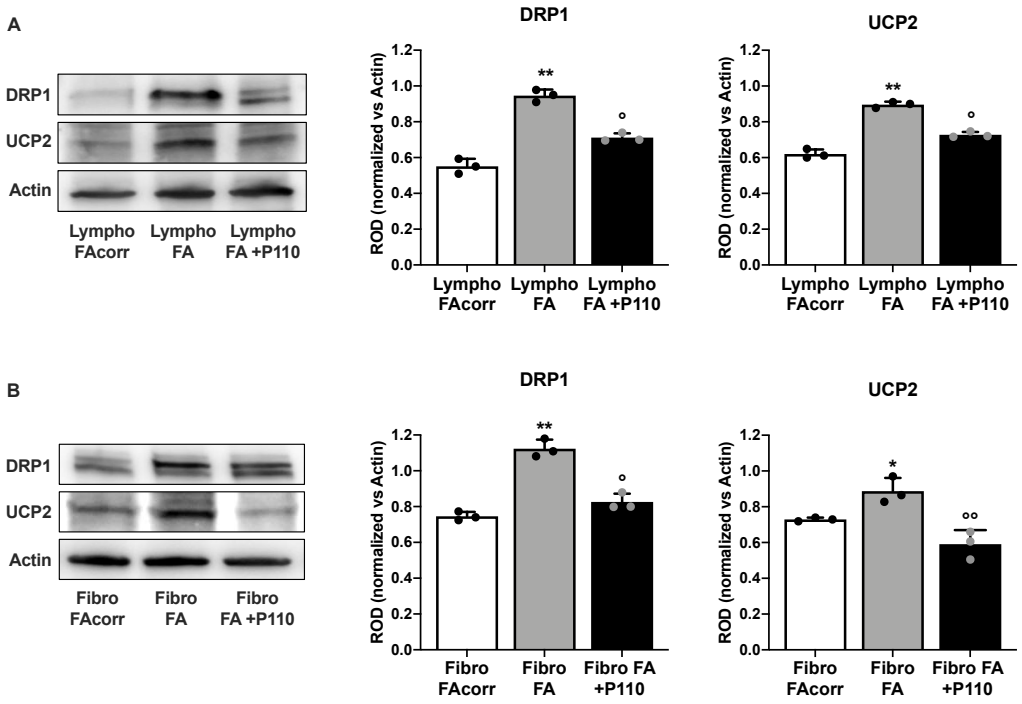


Figure 29 P110 treatment effects on DRP1 and UCP2 expression levels. WB signals of DRP1 (mitochondrial fission), UCP2 (uncoupling protein 2), and Actin (housekeeping protein) in lymphoblasts (A) and fibroblasts (B) cell lines mutated or not for the FANCA gene. Protein expression levels (densitometric analysis) were normalized on the Actin signal revealed on the same membrane. Data are reported in histograms as mean ± SD, and each panel and graph is representative of at least 3 independent experiments. Statistical significance was tested opportunely with a one-way ANOVA test; * and ** represent a significant difference for $p < 0.05$ and 0.01 between FA and FAcorr cells; ° and °° represent a significant difference for $p < 0.05$ and 0.01 between P110-treated FA cells and the untreated ones.

As shown in Figure 29, following the treatment with P110 in both lymphoblasts (A) and fibroblasts (B), the expression level of DRP1 is reduced compared to their respective untreated cells, and it results comparable to the FAcorr counterpart. Moreover, UCP2 expression levels were also found to be significantly reduced in both cellular models following P110 treatment.

Once again, I tried to correlate DRP1 expression levels with the integrity of the mitochondrial network by conducting a confocal microscopy analysis. FAcorr and FA fibroblasts, as well as FA fibroblasts treated with P110 for 24h, were incubated with an antibody against TOM20 (red) to visualize mitochondrial reticulum and DAPI (blue) to mark nuclei. Again, the distribution of the mitochondrial network was classified as elongated or intermediate/short, as shown in Figure 30.

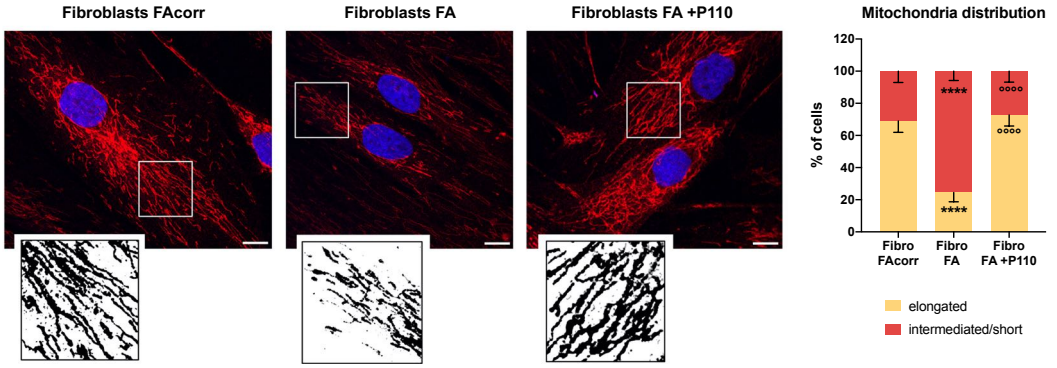


Figure 30 P110 treatment effect on mitochondrial network distribution. Confocal microscopy analysis of FAcorr, FA, and P110 treated FA fibroblasts stained with antibodies against TOM20 (red) to mark mitochondrial reticulum and DAPI (blue) to label nuclei. White scale bars correspond to 10 µm. The higher magnification images correspond to the area enclosed by the white squares and are examples of mitochondrial network distribution within the cells. Fibroblasts were scored depending on the morphology of most of their mitochondrial population as elongated or intermediated/short, and the results are reported in the histogram on the right. Data are reported as mean ± SD and are representative of at least three independent experiments. Statistical significance was tested with a one-way ANOVA test; **** represents a significant difference for $p < 0.0001$ between FA and FAcorr cells; °°°° represents a significant difference for $p < 0.0001$ between P110-treated FA cells and the untreated ones.

As illustrated in the right-hand graph of Figure 30, the results demonstrate that the treatment with P110 on FANCA mutant cells restores the percentage of mitochondria with elongated morphology to the levels observed in FAcorr cells.

Finally, I tested the biochemical parameters that had shown alterations in previous analyses to determine whether the P110 treatment and the consequent restoration of the mitochondrial network would positively impact cellular energy metabolism. Specifically, I tested ATP synthesis, OCR, mitochondrial efficiency, electron transport between complexes I and III, lipid content, and lipid peroxidation damage, as shown in Figure 31 for lymphoblasts and Figure 32 for fibroblasts. For both cell types, the P110 treatment significantly increased ATP synthesis levels and oxygen consumption, as well as mitochondrial efficiency (P/O ratio) following the administration of pyruvate and malate (which selectively activate the pathway involving complexes I, III, and IV). At the same time, P110-treated cells exhibit reduced oxygen consumption following activation of the pathway involving complexes II, III, and IV with succinate and a slight but not significant decrease in ATP synthesis, which, in any case, leads to an improvement in mitochondrial efficiency for this pathway as well which is no longer required to compensate for an energy deficit.

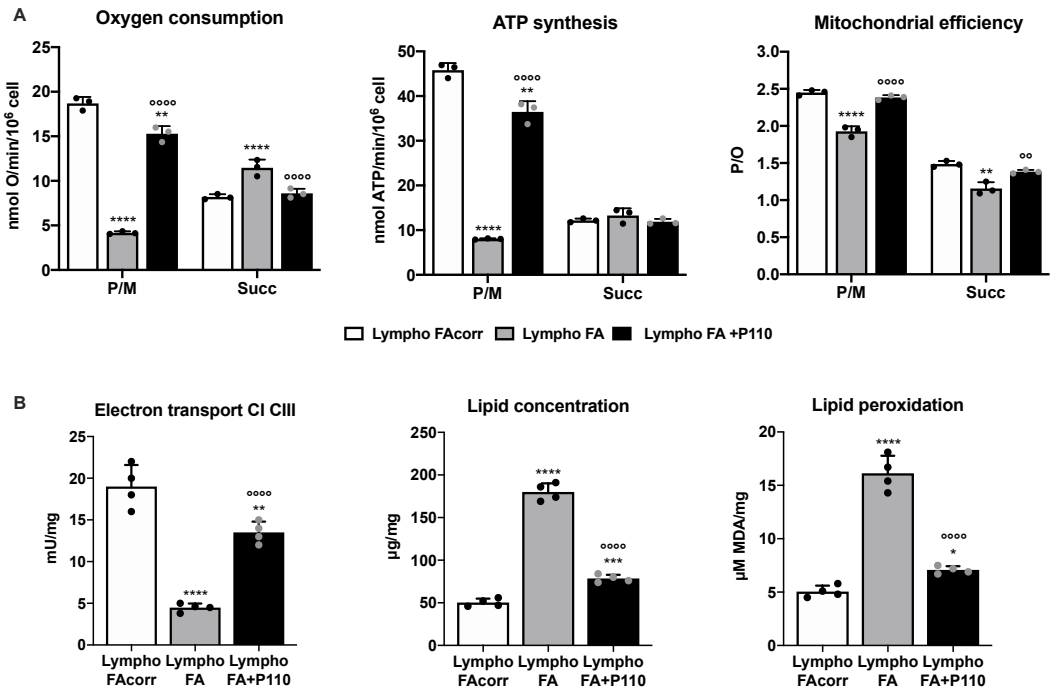


Figure 31 P110 treatment effects on energy and lipid metabolism of lymphoblasts cell lines mutated or not for the FANCA gene and FA lymphoblasts P110-treated. ATP synthesis, oxygen consumption rate (OCR), and P/O value (as mitochondrial efficiency marker) were obtained after stimulation with pyruvate and malate (P/M) or succinate (succ); electron transport between respiratory complexes I and III (CI-CIII); cellular lipid content; malondialdehyde (MDA) level (as lipid peroxidation damage marker). All data are reported as mean ± SD, and each graph is representative of at least 3 independent experiments. Statistical significance was tested opportunely with a one-way ANOVA test; *, **, ***, and **** represent a significant difference for $p < 0.05$, 0.01, 0.001, and 0.0001 between FA and FAcorr cells; °° and °°°° represent a significant difference for $p < 0.01$ and 0.0001 between P110-treated FA cells and the untreated ones.

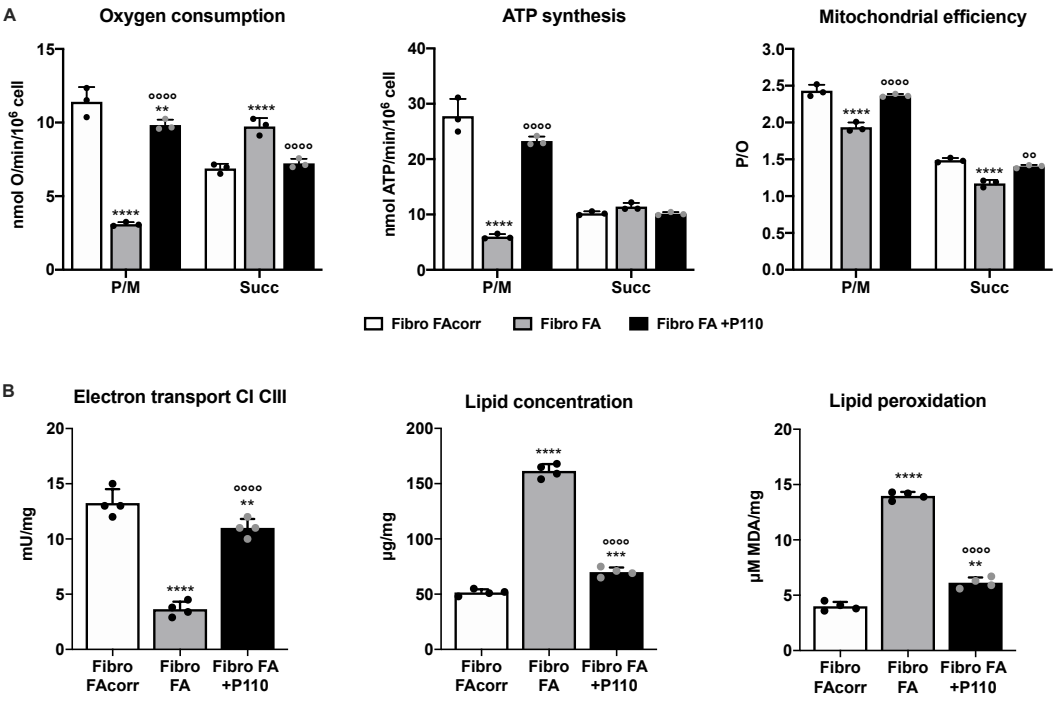


Figure 32 P110 treatment effects on energy and lipid metabolism of fibroblast cell lines mutated or not for the FANCA gene and FA fibroblast P110-treated. ATP synthesis, oxygen consumption rate (OCR), and P/O value (as mitochondrial efficiency marker) were obtained after stimulation with pyruvate and malate (P/M) or succinate (succ); electron transport between respiratory complexes I and III (CI-CIII); cellular lipid content; malondialdehyde (MDA) level (as lipid peroxidation damage marker). All data are reported as mean ± SD, and each graph is representative of at least 3 independent experiments. Statistical significance was tested opportunely with a one-way ANOVA test; *, **, ***, and **** represent a significant difference for $p < 0.05$, 0.01, 0.001, and 0.0001 between FA and FAcorr cells; °° and °°°° represent a significant difference for $p < 0.01$ and 0.0001 between P110-treated FA cells and the untreated ones.

The electron transport between complex I and III also shows a significant improvement following the treatment with P110, both for lymphoblasts (Figure 31) and fibroblasts (Figure 32), as well as the lipid content and lipid peroxidation damage, represented by MDA, which are significantly reduced. These data demonstrate that improving mitochondrial network morphology and dynamics significantly impacts mitochondria and OxPhos functionality, opening new therapeutic perspectives.

### 5.7 Autophagy and Mitophagy

Given the mitochondrial dynamics imbalance toward fission and subsequent disruption of the mitochondrial network in FA, as described in the previous paragraph, increased removal of damaged or dysfunctional mitochondria could be expected in FA cells compared to FAcorr. However, literature reports alterations in autophagy and mitophagy processes in FA. For this reason, I also wanted to investigate autophagy and mitophagy in my cellular models, analyzing the expression levels of some key proteins involved in these processes using WB. For autophagy, I evaluated the expression levels of Beclin1 (an autophagy activator, as shown in Figure 4), Atg7, Atg12, Atg16L1, and LC3, autophagy effectors.

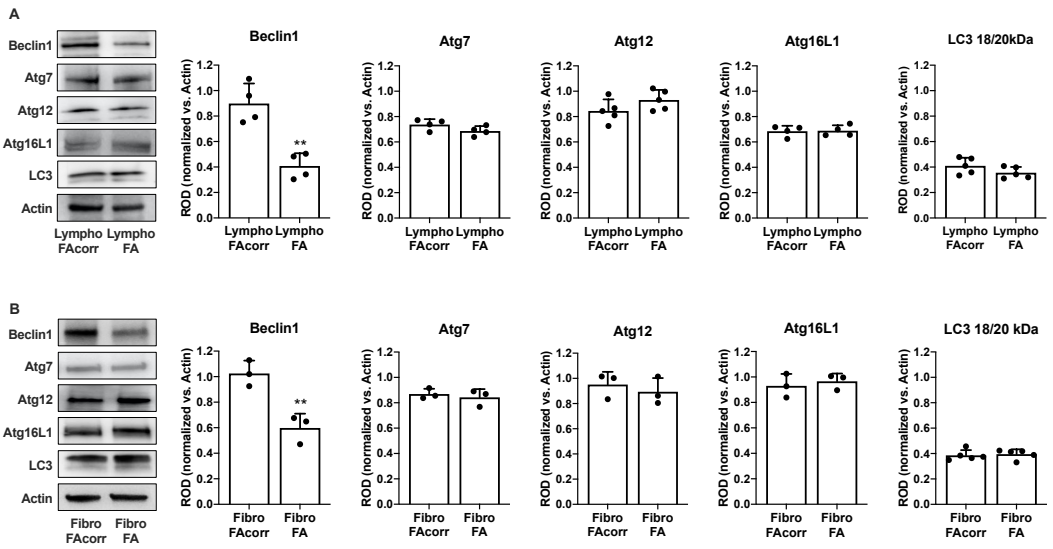


Figure 33 Autophagy makers expression levels in FA and FAcorr lymphoblasts and fibroblasts. WB signals of Beclin1, Atg7, Atg12, Atg16L1, LC3, and Actin (housekeeping protein) in lymphoblasts (A) and fibroblasts (B) cell lines mutated or not for the FANCA gene. The LC3 graphs represent the ratio between the 18 kDa active form and the 20 kDa inactive form of the protein. All protein expression levels (densitometric analysis) were normalized on the Actin signal revealed on the same membrane. Data are reported in histograms as mean ± SD, and each panel and graph is representative of at least 3 independent experiments. Statistical significance was tested opportunely with an unpaired t-test; ** represents a significant difference for $p < 0.01$ between FA and FAcorr cells.

As shown in Figure 33 data reveals that none of the autophagy effector proteins analyzed exhibit differences in expression levels when comparing FA and FAcorr, both in lymphoblasts (A) and fibroblasts (B). However, there is a significant reduction in Beclin1 expression, both in lymphoblasts (A) and fibroblasts (B).

Considering mitophagy, the proteins analyzed by WB were Pink1, a kinase that recognizes and tags non-functional mitochondria, and Parkin, an E3 ubiquitin ligase involved in mitochondria polyubiquitination.

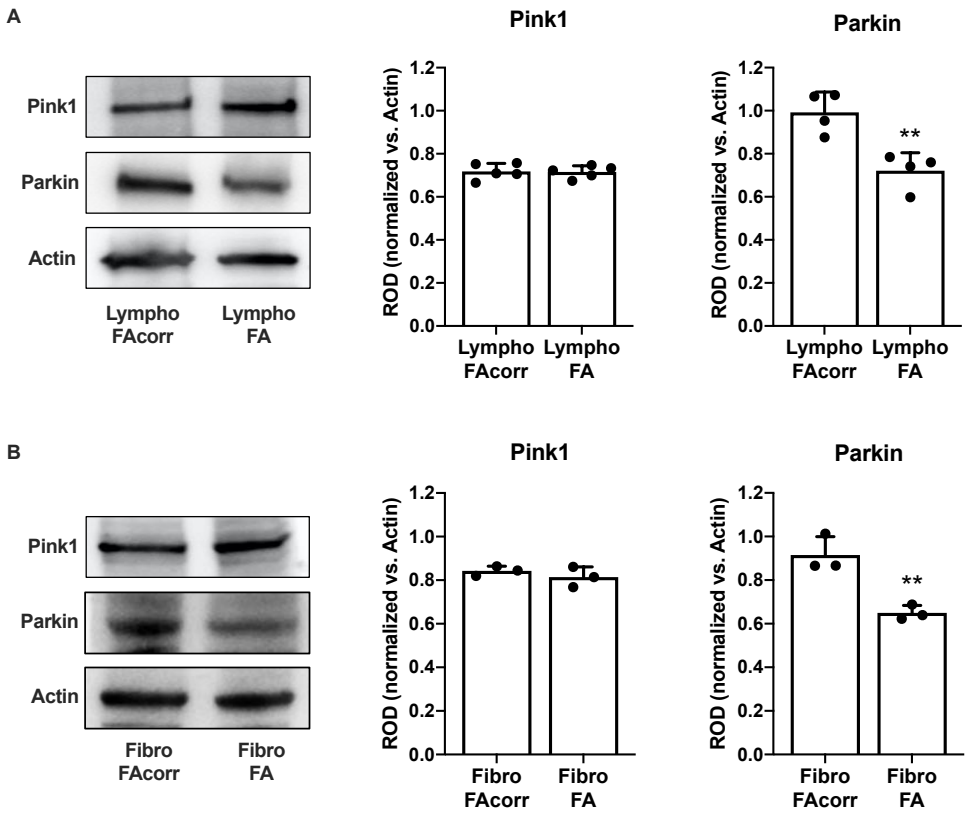


Figure 34 Mitophagy makers expression levels in FA and FAcorr lymphoblasts and fibroblasts. WB signals of Pink1, Parkin, and Actin (housekeeping protein) in lymphoblasts (A) and fibroblasts (B) cell lines mutated or not for the FANCA gene. Protein expression levels (densitometric analysis) were normalized on the Actin signal revealed on the same membrane. Data are reported in histograms as mean ± SD, and each panel and graph is representative of at least 3 independent experiments. Statistical significance was tested opportunely with an unpaired t-test; ** represents a significant difference for $p < 0.01$ between FA and FAcorr cells.

As depicted in Figure 34, the expression levels of Pink1 do not exhibit significant differences, neither in lymphoblasts (A) nor fibroblasts (B). Conversely, Parkin was significantly less expressed in both cell types when comparing FANCA mutant cells with their respective FAcorr cells.

All the data contained in sections 3.5, 3.6, and 3.7 were published in N. Bertola *et al.*, "Altered Mitochondrial Dynamic in Lymphoblasts and Fibroblasts Mutated for FANCA-A Gene: The Central Role of DRP1," *Int J Mol Sci*, vol. 24, no. 7, 2023, DOI: 10.3390/ijms24076557.

## 5.8 A multidrug approach to modulate the mitochondrial metabolism impairment and relative oxidative stress in Fanconi Anemia Complementation Group A.

Among the molecular defects leading FA cells to their dysfunctional state, the increase in oxidative stress caused by the defective electron transport between the first and third respiratory chain complexes is the most detrimental because FA cells cannot effectively counterbalance this oxidative stress with endogenous antioxidant defenses. The dysfunctional mitochondrial metabolism also results in acetyl-CoA accumulation in FA cells, which promotes lipid droplet formation and accumulation, exacerbating the existing mitochondrial dysfunction. These metabolic impairments are also associated with clinical effects such as insulin resistance, obesity, and dyslipidemia, frequently observed in FA patients.

In this part of my thesis, I aimed to investigate the impact of various drugs targeting these metabolic pathways to assess the interconnection between mitochondrial function, oxidative stress, and lipid metabolism. Specifically, I treated FA lymphoblasts with quercetin, an antioxidant molecule, 4-methylene-2-octyl-5-oxotetrahydrofuran-3-carboxylic acid (C75), a fatty acid synthesis inhibitor, and rapamycin, an mTOR (mammalian Target of Rapamycin) inhibitor, as mTOR is involved in mitochondrial metabolism modulation. I used these molecules either alone or in combination.

### 5.8.1 Cell proliferation and cell death

I evaluated the effect on cell proliferation and cell death of the three molecules alone or in combination on FA lymphoblasts using FAcorr lymphoblasts as a control.

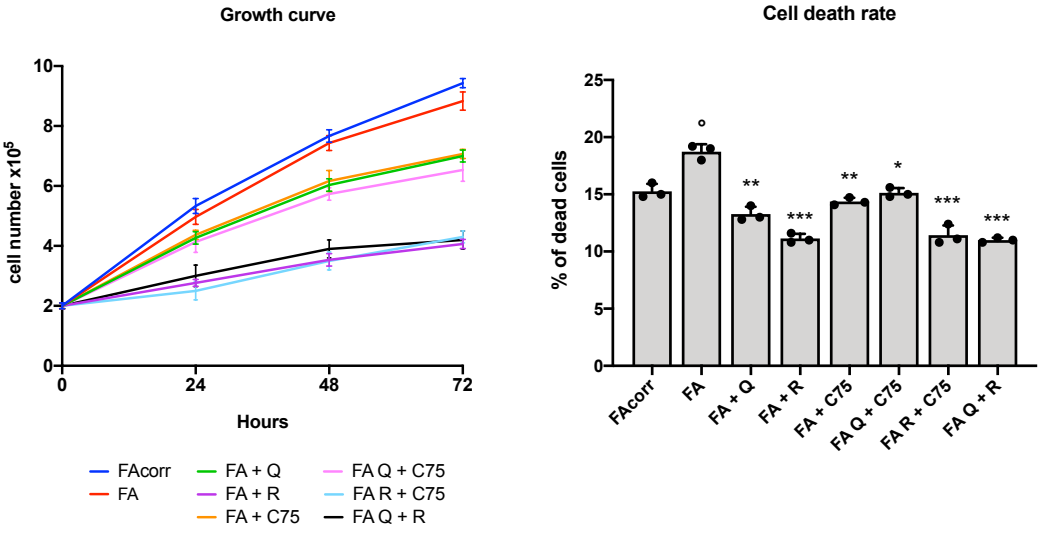


Figure 35 Cell growth and death rate of FA lymphoblasts treated with quercetin, rapamycin, C75 and their combinations. Cell growth curve (left panel) and percentage of dead cells after 48h of treatments (right panel) (Q = quercetin only; R = rapamycin only; C75 = C75 only; Q + C75 = quercetin and C75 combination; R + C75 = rapamycin and C75 combination; Q + R = quercetin and rapamycin combination). Each graph is representative of four independent experiments; FA and FAcorr represent four different lymphoblast cell lines. Data are expressed as mean ± SD. Statistical analysis was performed with a one-way ANOVA followed by the Tukey

multiple comparison test. ° represents a $p < 0.05$ between FA and FAcorr cell lines; *, **, or *** represent respectively $p < 0.05$, 0.01, or 0.001 between treated and untreated FA cells.

Despite the underlying genetic defect, FA lymphoblastoid cell lines exhibit a viability rate comparable to their corrected counterparts, as illustrated in the left panel of Figure 35. All drug treatments lead to a cell growth deceleration, with the most pronounced growth rate reduction for rapamycin, both alone and in combination with quercetin or C75. All the other treatments and combinations induce a milder slowdown (Figure 35). Despite the diminished cell growth rate, none of the treatments provoke a higher cell death rate compared to untreated FA cells, but they significantly reduce it, as illustrated in the right panel of Figure 35.

### 5.8.2 Quercetin, Rapamycin, and C75 effects on FA mitochondrial metabolism

Once it was confirmed that the treatments with these molecules do not have a negative impact on cellular viability, I wanted to see their effects on mitochondrial metabolism. I assessed OCR, ATP synthesis, P/O ratio, electron transport between the first and third complex of the respiratory chain, and mitochondrial membrane potential.

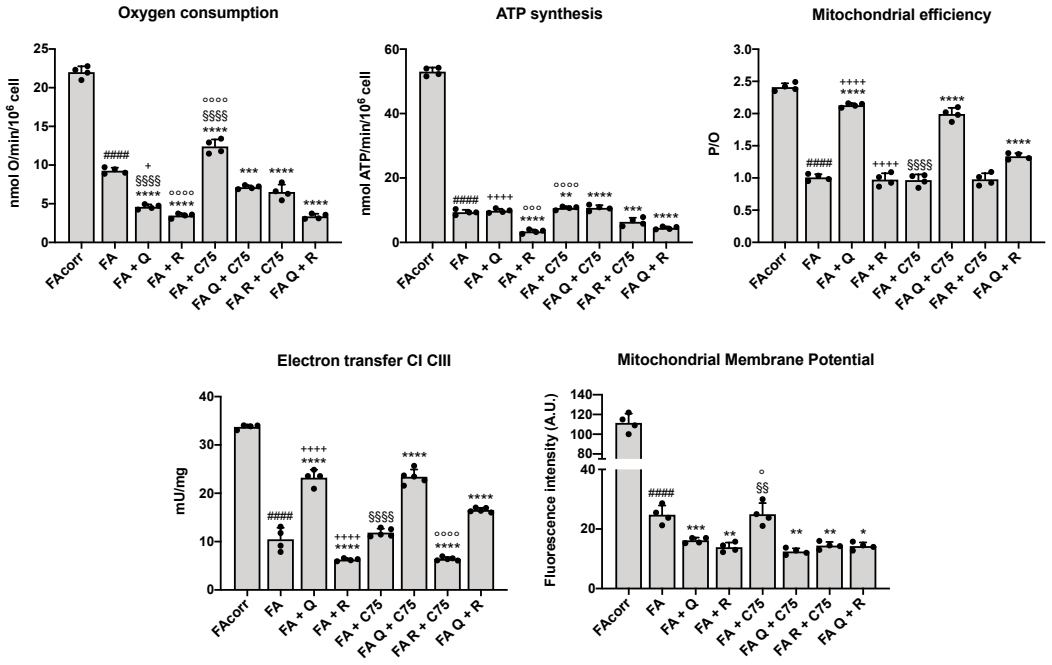


Figure 36 Aerobic metabolism of FA lymphoblasts treated with quercetin, rapamycin, C75 and their combinations. Oxygen consumption rate (OCR), ATP synthesis through FoF1-ATP synthase, P/O ratio as a marker for mitochondrial efficiency, electron transport between I and III respiratory complexes, and mitochondrial membrane potential measured by cytofluorimetric analysis (Q = quercetin only; R = rapamycin only; C75 = C75 only; Q + C75 = quercetin and C75 combination; R + C75 = rapamycin and C75 combination; Q + R = quercetin and rapamycin combination). All the experiments were conducted after 48 hours of treatment. Each graph represents four independent experiments; FA and FAcorr represent four different lymphoblast cell lines. Data are expressed as mean ± SD. Statistical analysis was performed with a one-way ANOVA followed by the Tukey multiple comparison test. #### represents a $p < 0.0001$ between FA and FAcorr cell lines; **, ***, or **** represent respectively $p < 0.01$, 0.001, or 0.0001 between treated and untreated FA cells; + or ++++ represent respectively

a p < 0.05, or 0.0001 between treatment with quercetin or rapamycin alone and quercetin/rapamycin combination; §§ or §§§§ represent respectively p < 0.01, or 0.0001 between treatment with quercetin or C75 alone and quercetin/C75 combination; °, °°°, or °°°° represent respectively a p < 0.05, 0.001, or 0.0001 between treatment with rapamycin or C75 alone and rapamycin/C75 combination.

As shown in Figure 36, several notable effects were observed in FA cells following quercetin treatment, starting with the partial recovery of the electron transport between Complexes I and III. Additionally, quercetin treatment led to a concurrent reduction of OCR and mitochondrial membrane potential (MMP) compared to the untreated samples. Intriguingly, despite the reduced mitochondrial activity, residual oxidative phosphorylation (P/O value) efficiency increased, reaching levels similar to those observed in FAcorr cells. So, quercetin treatment caused a slowdown of aerobic metabolism while simultaneously enhancing both electron transport and energy production efficiency. C75 treatment's primary effects are the enhanced OCR and MMP. This improvement might be attributed to the increased availability of acetyl-CoA, as this molecule is a fatty acid synthesis inhibitor. However, C75 did not improve electron transport between Complexes I and III or ATP synthesis, and cells maintained an uncoupled state similar to that observed in untreated samples. Rapamycin is a negative regulator of aerobic metabolism: indeed, its impact on FA cells was to reduce further Complexes I/III electron transport, OCR, MMP, and ATP synthesis, but without improving OxPhos efficiency. Quercetin, when combined with C75, maintains the effect already observed with rapamycin treatment alone, while in combination with rapamycin, it partially reduces the improvement in the P/O ratio given by rapamycin alone. The combination of C75 and rapamycin, on the other hand, worsens all parameters compared to untreated cells, except for the P/O ratio, which remains unchanged.

### 5.8.3 Quercetin, Rapamycin, and C75 effects on FA anaerobic metabolism and cellular energy status

Mitochondrial aerobic metabolism alteration or reduction is often linked to a metabolic shift towards anaerobic glucose catabolism. Consequently, to assess whether the decrease in OxPhos associated with treatment led to an increase in anaerobic glycolysis, I examined parameters such as glucose consumption, lactate release, and the resultant glycolysis rate.

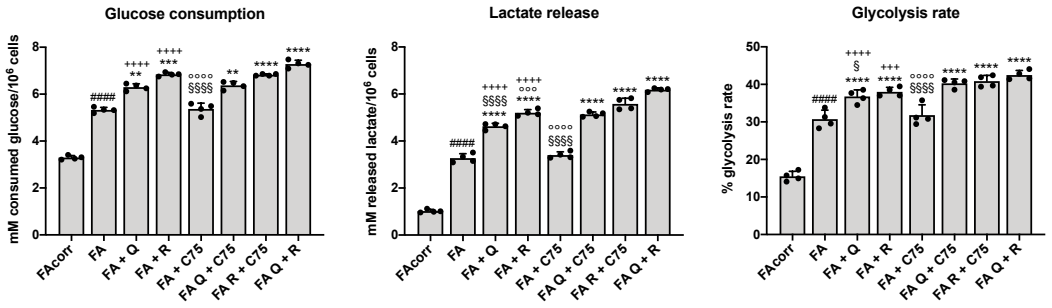


Figure 37 Anaerobic metabolism of FA lymphoblasts treated with quercetin, rapamycin, C75 and their combinations. Glucose consumption, lactate release in growth medium, and glycolysis rate calculated as ratio between real and theoretical lactate release, the latter corresponding to twice the concentration of consumed glucose (Q = quercetin only; R = rapamycin only; C75 = C75 only; Q + C75 = quercetin and C75 combination; R

+ C75 = rapamycin and C75 combination; Q + R = quercetin and rapamycin combination). All the experiments were conducted after 48 hours of treatment. Each graph represents four independent experiments; FA and FAcorr represent four different lymphoblast cell lines. Data are expressed as mean ± SD. Statistical analysis was performed with a one-way ANOVA followed by the Tukey multiple comparison test. #### represents a $p < 0.0001$ between FA and FAcorr cell lines; **, ***, or **** represent respectively $p < 0.01$, 0.001, or 0.0001 between treated and untreated FA cells; +++ or ++++ represent respectively a $p < 0.001$, or 0.0001 between treatment with quercetin or rapamycin alone and quercetin/rapamycin combination; § or §§§§ represent respectively a $p < 0.05$, or 0.0001 between treatment with quercetin or C75 alone and quercetin/C75 combination; °°° or °°°° represent respectively a $p < 0.001$ or 0.0001 between treatment with rapamycin or C75 alone and rapamycin/C75 combination.

The data, as depicted in Figure 37, indicate that both quercetin and rapamycin treatments can induce an increase in all these parameters in FA cells, while C75 administration did not produce any effects on the glycolysis flux. No treatment combination altered the outcomes observed for the individual treatments except for quercetin and rapamycin, which caused a further increase in the glycolysis rate compared to the single treatments, attributable to glucose consumption and lactate release enhancement.

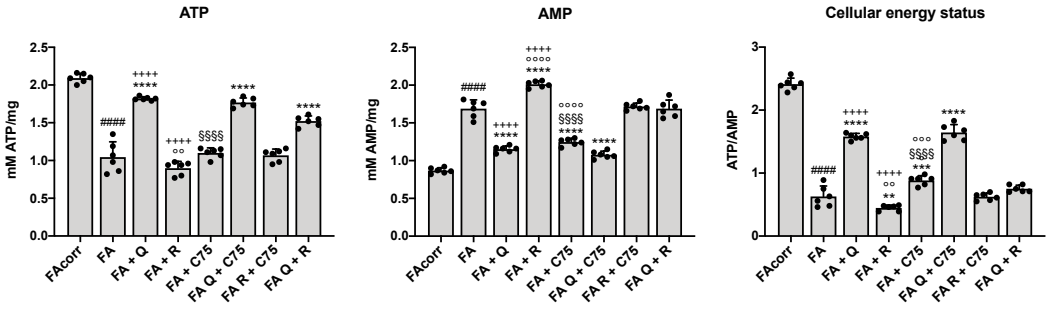


Figure 38 ATP and AMP intracellular content and consequent energy status of FA lymphoblasts treated with quercetin, rapamycin, C75, and their combinations. Intracellular ATP concentration, intracellular AMP concentration, ATP/AMP ratio as a marker of cellular energy status (Q = quercetin only; R = rapamycin only; C75 = C75 only; Q + C75 = quercetin and C75 combination; R + C75 = rapamycin and C75 combination; Q + R = quercetin and rapamycin combination). All the experiments were conducted after 48 hours of treatment. Each graph represents four independent experiments; FA and FAcorr represent four different lymphoblast cell lines. Data are expressed as mean ± SD. Statistical analysis was performed with a one-way ANOVA followed by the Tukey multiple comparison test. #### represents a $p < 0.0001$ between FA and FAcorr cell lines; **, ***, or **** represent respectively $p < 0.01$, 0.001, or 0.0001 between treated and untreated FA cells; ++++ represents a $p < 0.0001$ between treatment with quercetin or rapamycin alone and quercetin/rapamycin combination; §§§§ represents $p < 0.0001$ between treatment with quercetin or C75 alone and quercetin/C75 combination; °°, or °°°° represent a $p < 0.001$, or 0.0001 respectively between treatment with rapamycin or C75 alone and rapamycin/C75 combination.

As shown in Figure 38, only quercetin treatment, alone or in combination with C75 or rapamycin, significantly increases cellular ATP content, bringing it to levels comparable to control cells. As for AMP levels, only quercetin, C75, or the combination of the two leads to a significant decrease in intracellular content comparable to that of FAcorr cells. The overall cellular energy state, represented by the ATP/AMP ratio, is significantly improved only by quercetin, whether used alone or combined with C75. No other treatment or combination exhibits significant effects on these parameters.

### 5.8.4 Quercetin, Rapamycin, and C75 effects on FA lipid metabolism

In FA cells, there is an increased presence of acetyl-CoA, causing lipid droplet accumulation. Considering the inability of these cells to detoxify oxidative stress, this increased presence of lipid droplets raises lipoperoxidation probability, further exacerbating oxidative stress. Thus, in this section, I assessed acetyl-CoA content, 3-ketoacyl-ACP reductase activity (a marker of fatty acid synthesis—FAS), and lipid content in FA lymphoblasts after quercetin, C75, and rapamycin treatments.

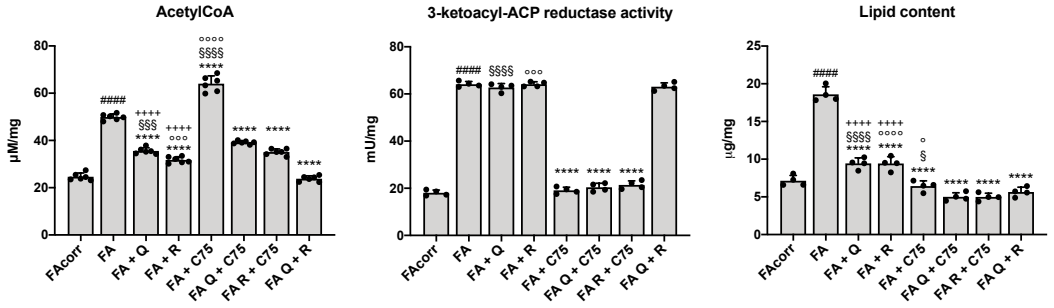


Figure 39 Fatty acid synthesis and accumulation of FA lymphoblasts treated with quercetin, rapamycin, C75 and their combinations. Acetyl-CoA intracellular accumulation, 3-ketoacyl-ACP reductase activity as a marker of fatty acid synthesis (FAS) and intracellular lipid accumulation (Q = quercetin only; R = rapamycin only; C75 = C75 only; Q + C75 = quercetin and C75 combination; R + C75 = rapamycin and C75 combination; Q + R = quercetin and rapamycin combination). All the experiments were conducted after 48 hours of treatment. Each graph represents four independent experiments; FA and FAcorr represent four different lymphoblast cell lines. Data are expressed as mean ± SD. Statistical analysis was performed with a one-way ANOVA followed by the Tukey multiple comparison test. #### represents a $p < 0.0001$ between FA and FAcorr cell lines; **** represents $p < 0.0001$ between treated and untreated FA cells; ++++ represents a $p < 0.0001$ between treatment with quercetin or rapamycin alone and quercetin/rapamycin combination; §, §§§, or §§§§ represent respectively a $p < 0.05$, 0.001, or 0.0001 between treatment with quercetin or C75 alone and quercetin/C75 combination; °, °°° or °°°° represent respectively a $p < 0.05$, 0.001 or 0.0001 between treatment with rapamycin or C75 alone and rapamycin/C75 combination.

As shown in Figure 39 quercetin and rapamycin treatments reduced acetyl-CoA and lipid content without impacting 3-ketoacyl-ACP reductase activity. Therefore, their effects could be attributed to the OxPhos impairment (Figure 36) and the increased reliance on anaerobic glycolysis (Figure 37), which results in a higher conversion of pyruvate into lactate rather than acetyl-CoA. Treatment with C75 decreased the 3-ketoacyl-ACP reductase activity and reduced lipid content. However, FAS inhibition by C75 was associated with acetyl-CoA accumulation.

An additive effect was observed when C75 was combined with quercetin or rapamycin. These combinations further decreased acetyl-CoA levels and 3-ketoacyl-ACP reductase activity, leading to a more pronounced reduction in lipid content. The combination of quercetin and rapamycin caused a significant decrease in acetyl-CoA and lipid content compared to the individual treatments, even though it did not affect FAS activity.

### 5.8.5 Quercetin, Rapamycin, and C75 effects on FA oxidative stress and antioxidant defenses

FA cells are characterized by an accumulation of reactive oxygen species (ROS) and associated damage due to the dysfunctional aerobic metabolism and the defective electron transport between Complexes I and III combined to a limited adaptive antioxidant response. For these reasons, I wanted to investigate how quercetin, rapamycin, and C75 treatments could impact the production of ROS, hydrogen peroxide, and malondialdehyde (MDA, a marker of lipid peroxidation), as well as the production of antioxidant (AO) defenses.

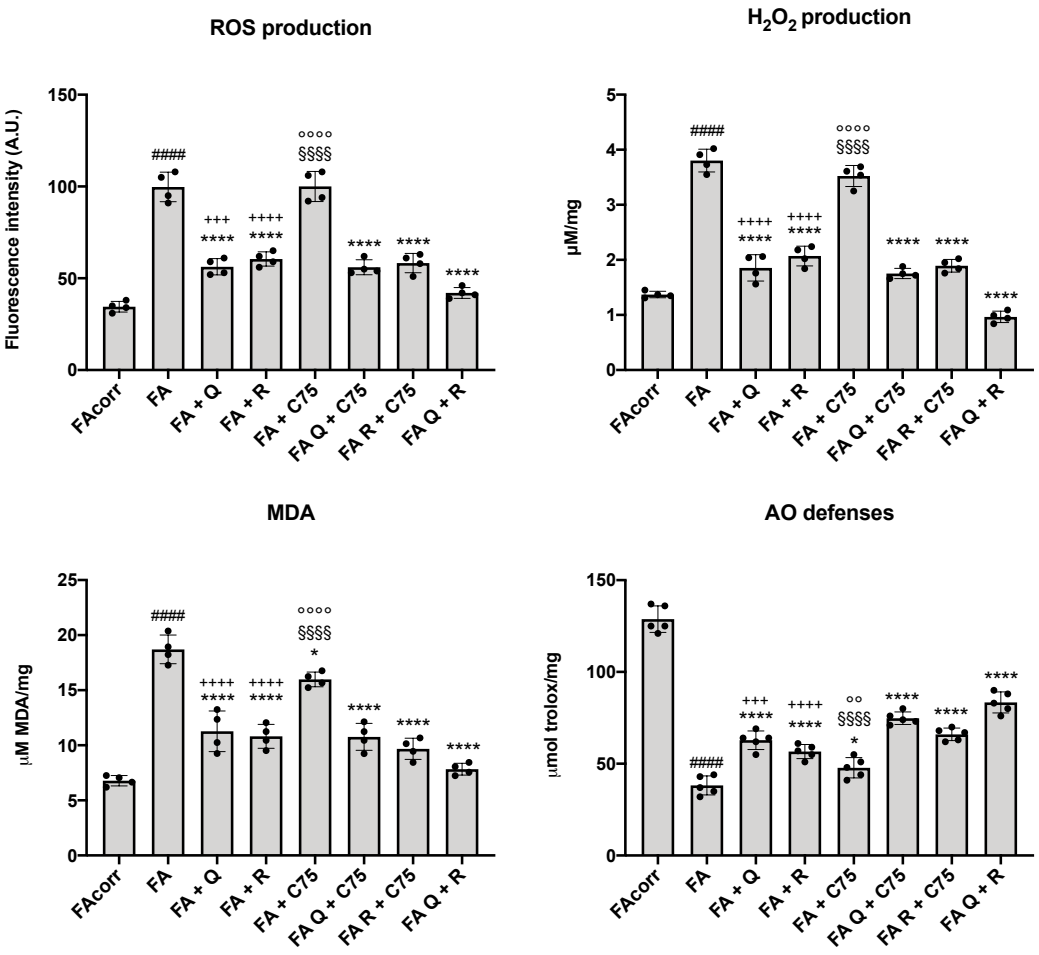


Figure 40 Oxidative stress production and antioxidant defenses of FA lymphoblasts treated with quercetin, rapamycin, C75, and their combinations. ROS production, hydrogen peroxide ($H_2O_2$) production, malondialdehyde (MDA) intracellular content as a marker for lipid peroxidation, total cellular antioxidant defenses (Q = quercetin only; R = rapamycin only; C75 = C75 only; Q + C75 = quercetin and C75 combination; R + C75 = rapamycin and C75 combination; Q + R = quercetin and rapamycin combination). All the experiments were conducted after 48 hours of treatment. Each graph represents four independent experiments; FA and FAcorr represent four different lymphoblast cell lines. Data are expressed as mean ± SD. Statistical analysis was performed with a one-way ANOVA followed by the Tukey multiple comparison test. #### represents a $p < 0.0001$ between FA and FAcorr cell lines; **** represents $p < 0.0001$ between treated and untreated FA cells; +++ or ++++ represents respectively a $p < 0.001$ or 0.0001 between treatment with quercetin or rapamycin alone and quercetin/rapamycin combination; §§§§ represents $p < 0.0001$ between treatment with quercetin or C75 alone and quercetin/C75 combination; °°, or °°°° represent a $p < 0.001$, or 0.0001 respectively between treatment with rapamycin or C75 alone and rapamycin/C75 combination.

Treatment with quercetin and rapamycin led to a significant decrease in ROS and $H_2O_2$ production and a reduction in MDA accumulation. Additionally, both drugs induced a minor but significant increase in AO defenses. In contrast, C75 did not influence oxidative stress production, but it decreased lipid peroxidation and enhanced AO capacity in FA cells, likely associated with lipid accumulation reduction.

A more pronounced positive effect on oxidative stress production and AO defenses was observed only with the quercetin and rapamycin combination. However, when C75 was combined with quercetin or rapamycin, a more substantial MDA reduction and an AO defense improvement were observed when compared to the effects of C75 treatment alone.

### 5.8.6 Hydroxyurea

To assess the potential of quercetin, rapamycin, C75, and their combinations in mitigating damages and DNA double-strand breaks induced by hydroxyurea (HU), cells were preincubated with these drugs for 24 hours, exposed to HU for 3 hours, and then maintained in culture for an additional 48 hours.

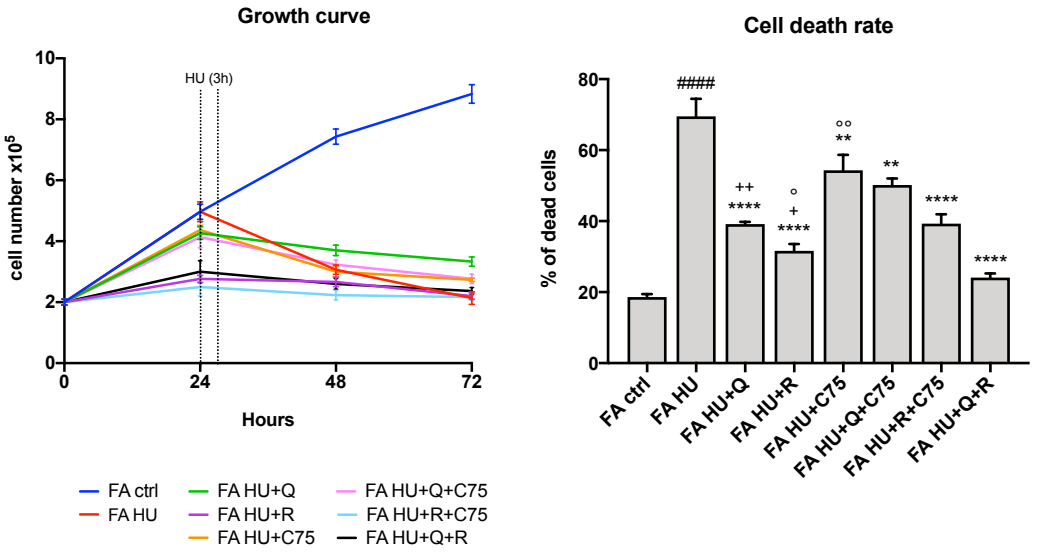


Figure 41 Effects of quercetin, rapamycin, C75 and their combinations on FA lymphoblasts treated with hydroxyurea to induce DNA double-strand breaks. Cell growth curves (left panel) and dead cell percentages (right panel) (Q = quercetin only; R = rapamycin only; C75 = C75 only; Q + C75 = quercetin and C75 combination; R + C75 = rapamycin and C75 combination; Q + R = quercetin and rapamycin combination). All the experiments were conducted after 48 hours of treatment. Each graph represents four independent experiments; FA and FAcorr represent four different lymphoblast cell lines. Data are expressed as mean ± SD. Statistical analysis was performed with a one-way ANOVA followed by the Tukey multiple comparison test. #### represents a $p < 0.0001$ between FA and FAcorr cell lines; ** or **** represent respectively $p < 0.01$ or 0.0001 between treated and untreated FA cells; + or ++ represent respectively a $p < 0.05$ or 0.01 between treatment with quercetin or rapamycin alone and quercetin/rapamycin combination; °, or °° represent a $p < 0.05$, or 0.01 respectively between treatment with rapamycin or C75 alone and rapamycin/C75 combination.

The results (Figure 41, left panel) indicate that all treatments reduce the rate of HU-induced decline in the growth of FA cells, although they do not completely reverse it. Additionally,

there is a reduction in cellular death (Figure 41, right panel). Specifically, quercetin, rapamycin, and their combination exhibit the most significant protective effects, while C75 seems to be somewhat less effective, although it still significantly reduces the percentage of dead cells.

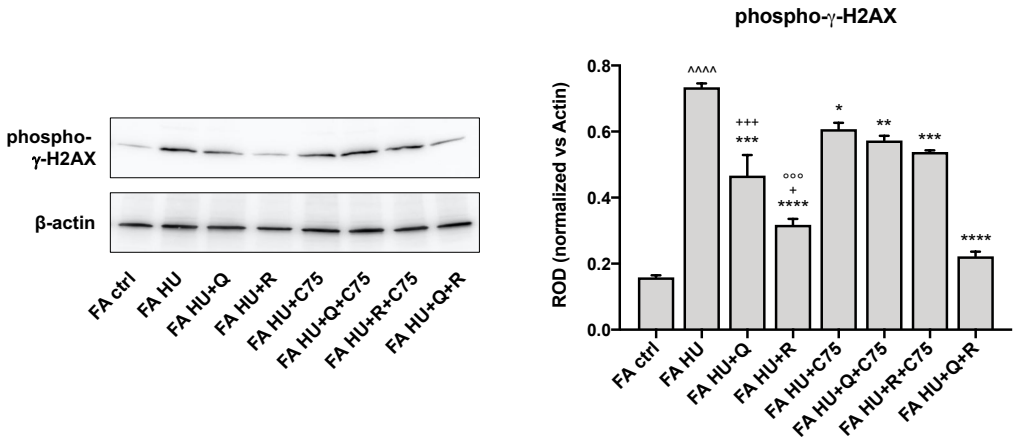


Figure 42 Effects of quercetin, rapamycin, C75 and their combinations on DNA double-strand breaks induced by hydroxyurea. WB signals against phospho-γ-H2AX and β actin used as a housekeeping protein (left) and densitometric analysis of WB signals (right) (Q = quercetin only; R = rapamycin only; C75 = C75 only; Q + C75 = quercetin and C75 combination; R + C75 = rapamycin and C75 combination; Q + R = quercetin and rapamycin combination). The experiments were conducted after 48 hours of treatment. Each graph represents four independent experiments; FA and FAcorr represent four different lymphoblast cell lines. Data are expressed as mean ± SD. Statistical analysis was performed with a one-way ANOVA followed by the Tukey multiple comparison test. ^^^^ represents a $p < 0.0001$ between FA cell lines treated with HU (FA HU) and untreated (FA ctrl); *, **, *** or **** represent respectively $p < 0.05$, 0.01, 0.001 or 0.0001 between treated and untreated FA HU cells; + or +++ represent respectively a $p < 0.05$ or 0.001 between treatment with quercetin or rapamycin alone and quercetin/rapamycin combination; °°° represents a $p < 0.001$ between treatment with rapamycin or C75 alone and rapamycin/C75 combination.

Furthermore, I assessed through western blot analysis the expression of phosphorylated γ-H2AX, which serves as a marker for DNA double-strand breaks. The data (Figure 42) show a very similar trend to what was observed for cell death. Specifically, the combination of quercetin and rapamycin proves to be the most effective treatment in reducing DNA double-strand breaks, although both compounds individually already exhibit a notable protective role against DNA damage. Conversely, the protective effects of rapamycin are partially diminished when combined with C75, while C75 alone exerts a relatively mild yet significant positive effect.

All the data presented in section 3.8 were published in E. Cappelli *et al.*, "A Multidrug Approach to Modulate the Mitochondrial Metabolism Impairment and Relative Oxidative Stress in Fanconi Anemia Complementation Group A" *Metabolites*, vol. 12, no. 1, 2022, DOI: 10.3390/metabo12010006.

## 5.9 Effects of deacetylase inhibition on the activation of the antioxidant response and aerobic metabolism in cellular models of Fanconi Anemia

FA cells are characterized by high oxidative stress production, which would not be an issue if their antioxidant defenses could effectively counterbalance it. Unfortunately, this is not the case, as cells with FANCA mutation appear unable to activate their endogenous antioxidant systems properly, thus failing to counteract the high production of oxidative stress effectively. This inability creates an environment where elevated oxidative stress becomes an additional source of DNA and ICL damage, thereby establishing a detrimental feedback loop.

Gene expression is controlled through diverse chromatin changes, among which acetylation holds a central role. It governs transcriptional regulation by influencing chromatin accessibility to transcription and DNA repair proteins. The balance between the activities of deacetylase (HDAC) and acetyltransferase (HAT) enzymes determines chromatin acetylation status. Histone acetylation promotes increased gene expression, whereas its counterpart, deacetylation, produces the opposite result. Furthermore, acetylation constitutes a fundamental post-translational modification that plays a crucial role in determining the functions and locations of specific proteins. Histone deacetylase inhibitors (HDACi) have applications in disorders spanning from chronic inflammatory disorders to cancers and neurodegenerative diseases.

The role of chromatin modifications in FA cells is an area that remains relatively unexplored. Renaud and colleagues' research reveals that FA cells' chromatin is in a hypoacetylated state, which facilitates the localization of 53BP1, a mammalian protein involved in repairing DNA double-strand breaks through a process called non-homologous DNA end-joining (NHEJ), to the sites where these breaks occur. By using HDACi, the detrimental effects of NHEJ are mitigated. This inhibition prevents the binding of the 53BP1 protein to DNA double-strand breaks, thereby allowing unrestricted access for homologous recombination proteins involved in repairing the breaks through an alternative mechanism. I, therefore, aimed to analyze how various types of HDACi could impact defective antioxidant responses and energy metabolism in my cellular models. Specifically, for the experiments presented in this section of my thesis, I employed Valproic acid, beta-hydroxybutyrate, and EX527. Valproic acid (VPA) is used for treating seizures and bipolar disorder and functions as an HDACi specific for both class I (HDAC1, 2, 3, and 8) and class IIa (HDAC4, 5, 7, and 9), demonstrating anti-cancer properties. β-hydroxybutyrate (OHB) is a specific class I HDACi (HDAC1 and HDAC2), triggers the transcription of catalase and mitochondria superoxide dismutase genes through upregulation of FoxO3A and MT2 genes, which are associated with oxidative stress resistance. EX527 is a sirtuin 1 (SIRT1) and (to a lesser extent) sirtuin 6 (SIRT6) inhibitor, both belonging to class III deacetylases involved in regulating stress response and mitochondrial biogenesis.

### 5.9.1 HDACi treatment effects on FA antioxidant defenses

I started testing the effects of HDACi on the expression and activity of the key cellular antioxidant enzymes, catalase (CAT) and glutathione reductase (GR), in my lymphoblast cell lines.

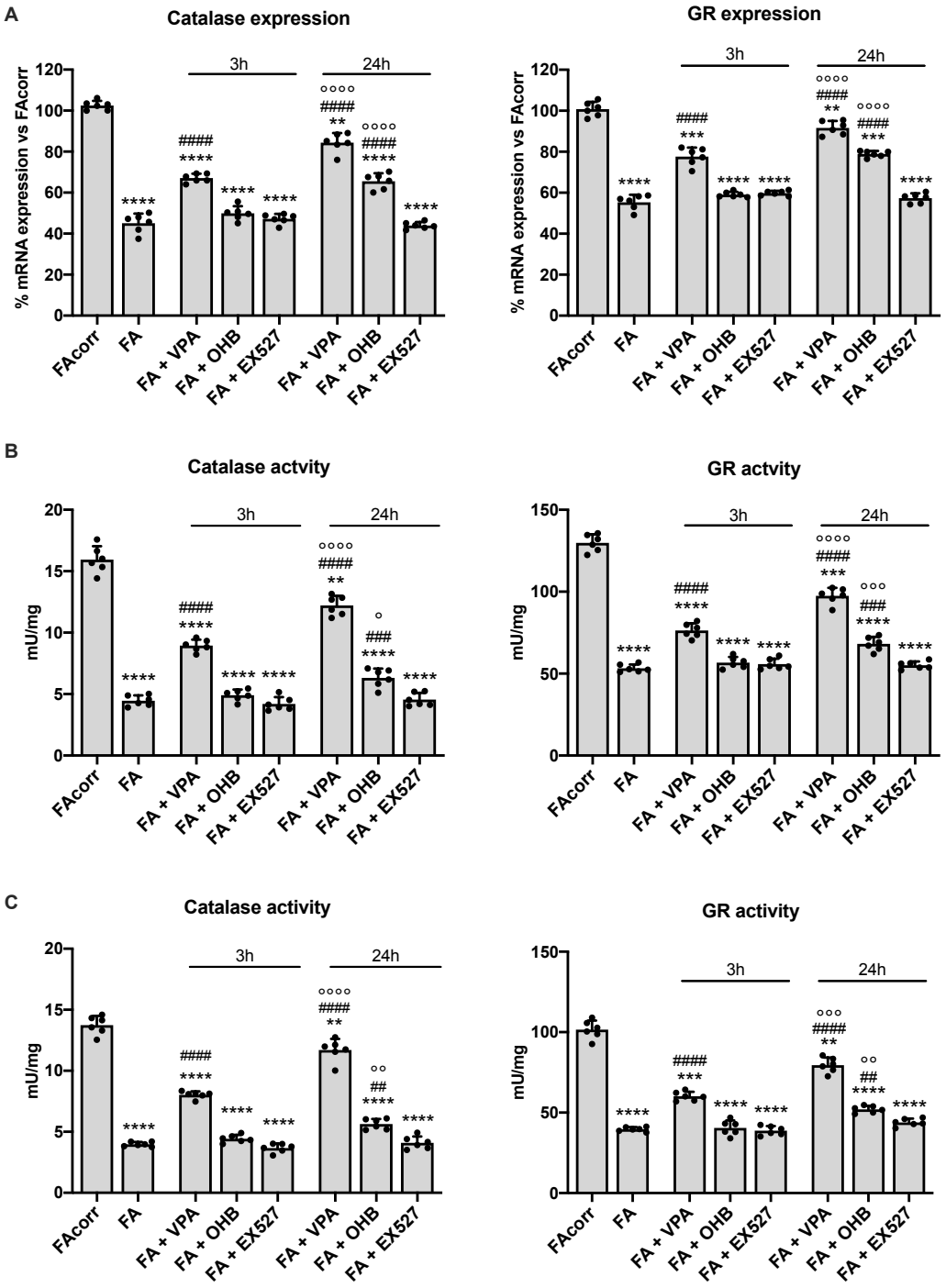


Figure 43 Catalase and glutathione reductase expression and activity in FA lymphoblasts and fibroblasts treated with VPA, OHB, and EX527. (A) CAT and GR gene expression; (B) CAT and GR reductase activity in lymphoblasts; (C) CAT and GR activity in fibroblasts. In each panel, HDACi effects were evaluated after 3 and 24 hours from their addition. Data are reported as mean ± SD, and each graph is representative of 6 independent experiments. Statistical significance was tested with a one-way ANOVA test; **, ***, and **** represent a significant

difference for $p < 0.01$, 0.001, or 0.0001, respectively, between FA and FAcorr cells. ##, ###, and #### represent a significant difference for $p < 0.01$, 0.001, or 0.0001, respectively, between treated and untreated FA cells, °, °°, °°°, and °°°° represent a significant difference for $p < 0.05$, 0.01, 0.001, or 0.0001 respectively between the same treatment after 3 and 24 hours.

The data presented in Figure 43 illustrate that both mRNA expression (A) and enzyme activity (B for lymphoblasts and C for fibroblasts) are significantly lower in FA cells compared to their FAcorr counterparts for both CAT and GR. The effects of HDACi treatments on cells with the FANCA mutation significantly differ depending on the molecule used, but the effect of all the molecules is comparable between lymphoblasts and fibroblasts. In fact, treatment with EX527 shows no effect on the expression or activity of these antioxidant enzymes for both lymphoblasts (Figure 43B) and fibroblasts (Figure 43C). OHB, after 24h but not 3h of treatment, leads to an increase in the mRNA expression but not in the activity of both CAT and GR. VPA is the only molecule that significantly improves both the expression and activity of these enzymes, already at 3h of treatment and to a greater extent after 24h.

### 5.9.2 HDACi treatment effects on FA energetic and lipid metabolisms

Given the results obtained in the previous section, I wanted to verify whether the improvement in CAT and GR expression and activity corresponded to an improvement in the functionality and efficiency of oxidative phosphorylation.

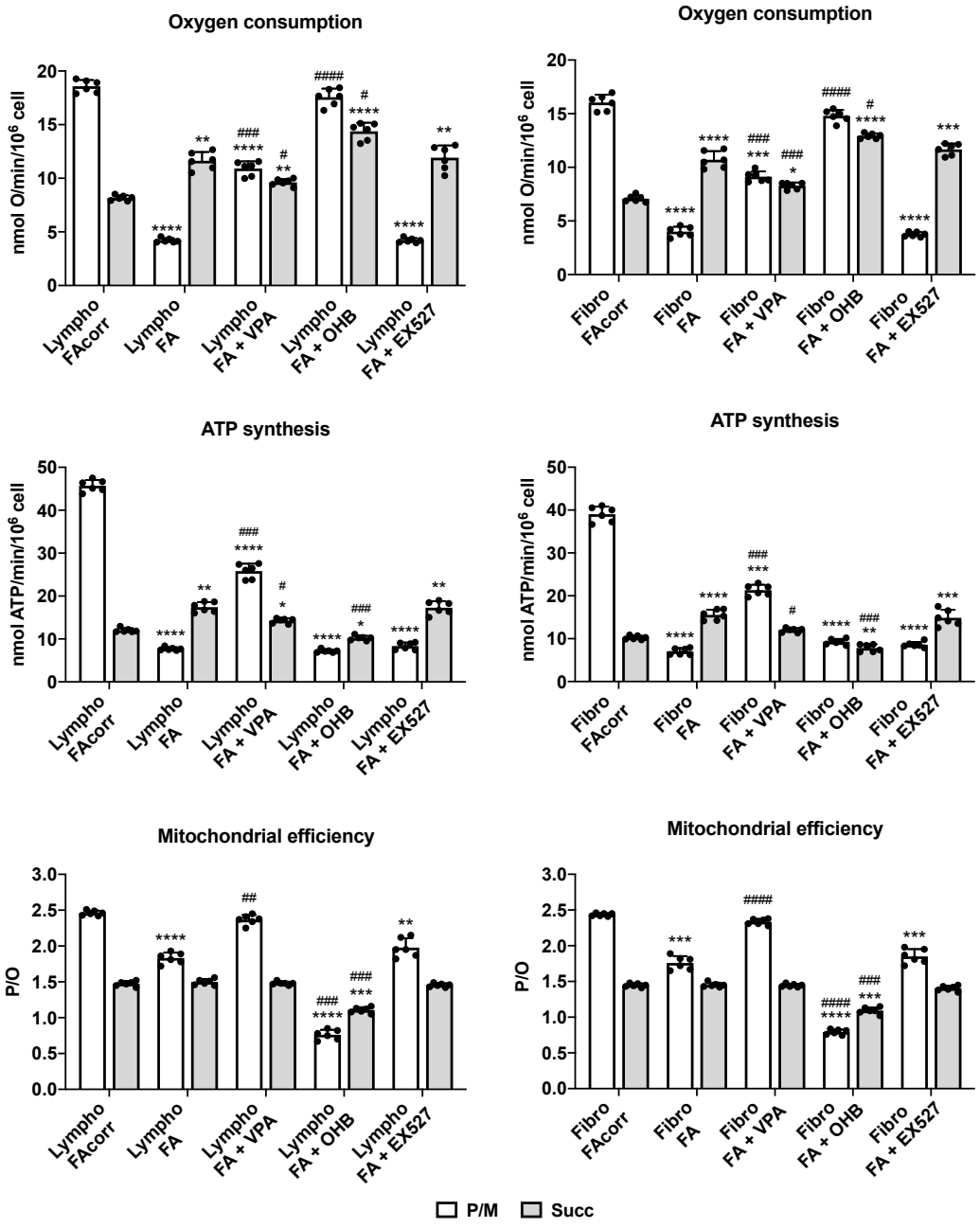


Figure 44 VPA, OHB, and EX527 effects on oxidative phosphorylation in FA lymphoblasts and fibroblasts. Oxygen consumption rate, ATP synthesis, and P/O ratio as an OxPhos efficiency marker in lymphoblasts (left) and fibroblasts (right). For all the panels, pyruvate plus malate (P/M, white columns) and succinate (Succ, grey columns) were used as respiratory substrates, and HDACi effects were evaluated after 24 hours from their addition. Data are reported as mean ± SD, and each graph is representative of at least 5 independent experiments. Statistical significance was tested with a one-way ANOVA test; *, **, ***, and **** represent a significant difference for $p < 0.05$, 0.01, 0.001, or 0.0001, respectively, between FA (treated or not) and FAcorr cells. #, ##, ###, and #### represent a significant difference for $p < 0.05$, 0.01, 0.001, or 0.0001, respectively, between treated and untreated FA cells.

The data shown in Figure 44 for lymphoblasts (left) and fibroblasts (right) confirm that for both cell lines, when stimulated with pyruvate and malate, the pathway composed by complexes I, III, and IV exhibits a significant reduction in oxygen consumption, ATP

synthesis, and mitochondrial metabolism efficiency (P/O) in FANCA mutant cells compared to the FAcorr counterpart. Similarly, it is once again confirmed that when stimulated with succinate, FA cells, compared to FAcorr ones, attempt to compensate for the deficit in the first pathway with an increase in OCR and ATP synthesis, which does not affect the P/O ratio. Regarding the HDACi treatments, I decided to limit the treatment duration to 24 hours as it has been shown to be the most effective timing in improving antioxidant defenses in the previous experiment. For both lymphoblasts and fibroblasts, VPA is the only treatment that improves all three considered parameters in all the experimental conditions: the significant increase in both OCR and ATP synthesis resulted in a restoration of mitochondrial efficiency for the P/M-stimulated pathway. Moreover, VPA brings OCR and ATP synthesis values for the succinate-stimulated pathway to be comparable to those of FAcorr cells without affecting the P/O ratio. Conversely, for both lymphoblasts and fibroblasts, treatment with OHB significantly worsens mitochondrial efficiency for both pathways composed of complexes I, III, and IV and complexes II, III, and IV. This is due to a significant increase in oxygen consumption not associated with an increase in ATP synthesis. Finally, we can observe that treatment with EX527 does not influence any considered parameters for either cell type. Thus, the data shown in Figure 44 confirm that the increase in cellular antioxidant defenses shown in Figure 43 following VPA treatment corresponds to improved oxidative phosphorylation and mitochondrial respiratory chain coupling.

I then assessed how these treatments affected two other parameters typically altered in FA: the electron transfer between the I and III complexes of the respiratory chain and the cellular energy status represented by the ATP/AMP ratio.

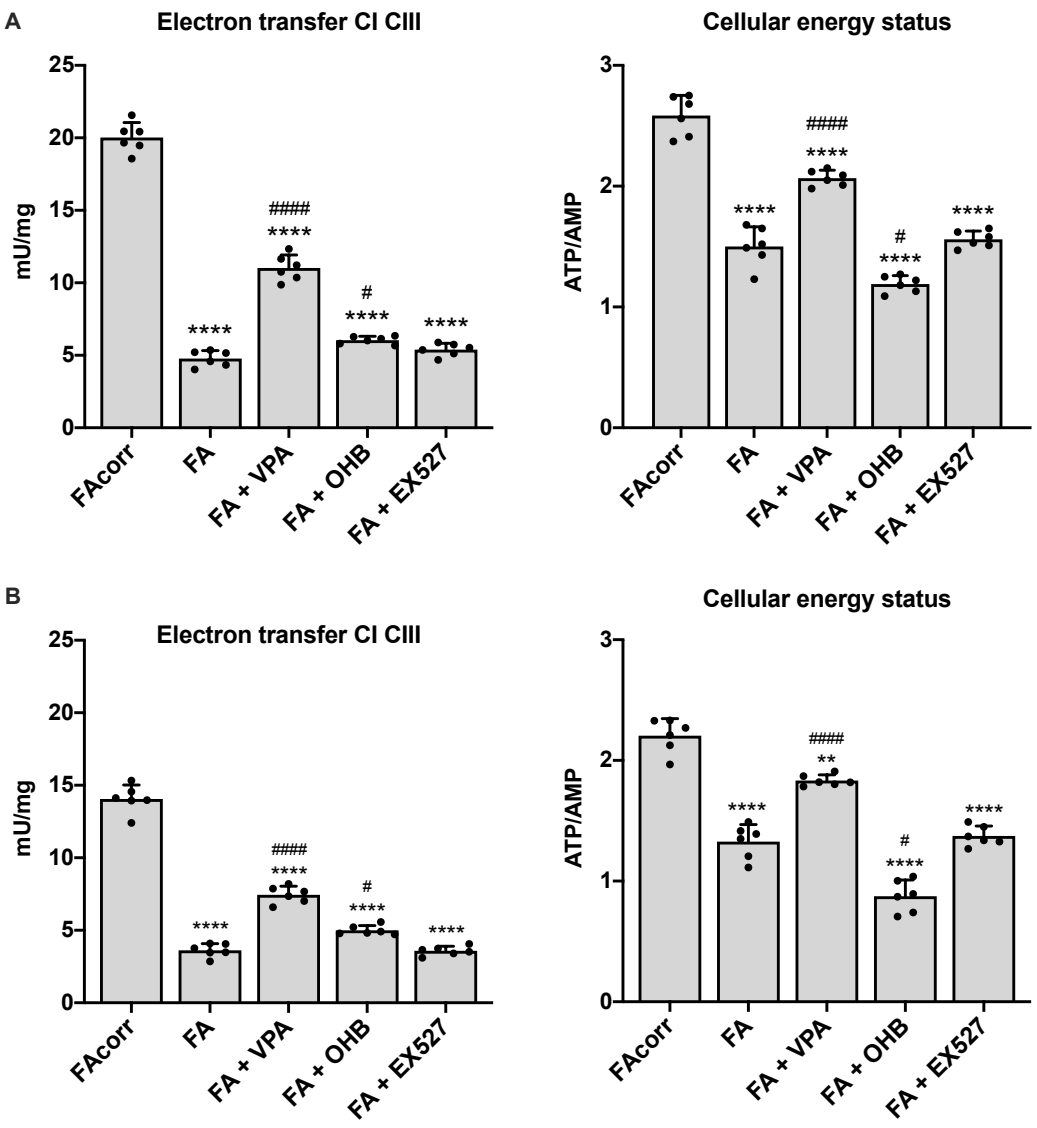


Figure 45 VPA, OHB, and EX527 effects on the electron transport between the first and the third respiratory chain's complexes and cellular energy status in FA lymphoblasts and fibroblasts. (A) Electron transport between I and III complexes and ATP/AMP ratio in lymphoblasts. (B) Electron transport between I and III complexes and ATP/AMP ratio in fibroblasts. HDACi effects were evaluated 24 hours after their addition for all the panels. Data are reported as mean ± SD, and each graph is representative of 6 independent experiments. Statistical significance was tested with a one-way ANOVA test; ** or **** represent a significant difference for $p < 0.01$ or 0.0001 between FA and FAcorr cells. # or #### represent a significant difference for $p < 0.05$ or 0.0001 between treated and untreated FA cells.

The data shown in Figure 45A for lymphoblasts and Figure 45B for fibroblasts demonstrate that, in line with the data already presented in Figure 43 and Figure 44, only treatment with VPA significantly improves both electron transfer between the I and III complexes and the ATP/AMP ratio in FA cells, although it does not restore them to the levels seen in FAcorr cells. Treatments with OHB and EX527 do not affect electron transfer between the I and III complexes, while the ATP/AMP ratio is negatively modulated by OHB treatment and remains unchanged after treatment with EX527.

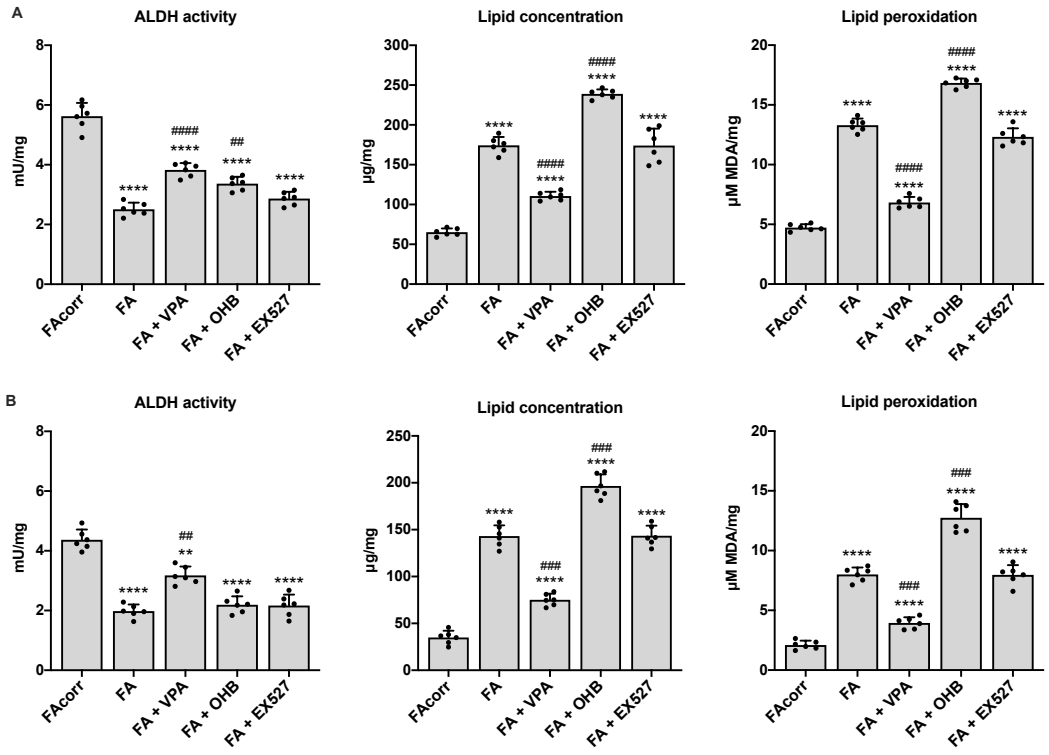


Figure 46 VPA, OHB, and EX527 effects on ALDH activity and lipid accumulation and peroxidation in FA lymphoblasts and fibroblasts. (A) ALDH activity, lipid concentration, and MDA as a marker for lipid peroxidation in lymphoblasts. (B) ALDH activity, lipid concentration, and MDA as a marker for lipid peroxidation in fibroblasts. HDACi effects were evaluated 24 hours after their addition for all the panels. Data are reported as mean ± SD, and each graph is representative of 6 independent experiments. Statistical significance was tested with a one-way ANOVA test; ** and **** represent a significant difference for $p < 0.01$ or 0.0001 between FA and FAcorr cells. ##, ###, and #### represent a significant difference for $p < 0.01$, 0.001, or 0.0001, respectively, between treated and untreated FA cells.

Furthermore, as shown in Figure 46, the activity of ALDH, an enzyme involved in aldehyde detoxification, significantly increases in FA cells treated with VPA and OHB for lymphoblasts (Figure 46A), but only after VPA treatment for fibroblasts (Figure 46B). VPA treatment is also the only one among the tested treatments to significantly reduce both lipid accumulation and malondialdehyde levels (a marker of lipid peroxidation) for both lymphoblasts (A) and fibroblasts (B).

### 5.9.3 HDACi effects on FA cell survival

VPA treatment is also the only one to improve the survival of FA lymphoblasts to mitomycin (MMC), as shown in Figure 47.

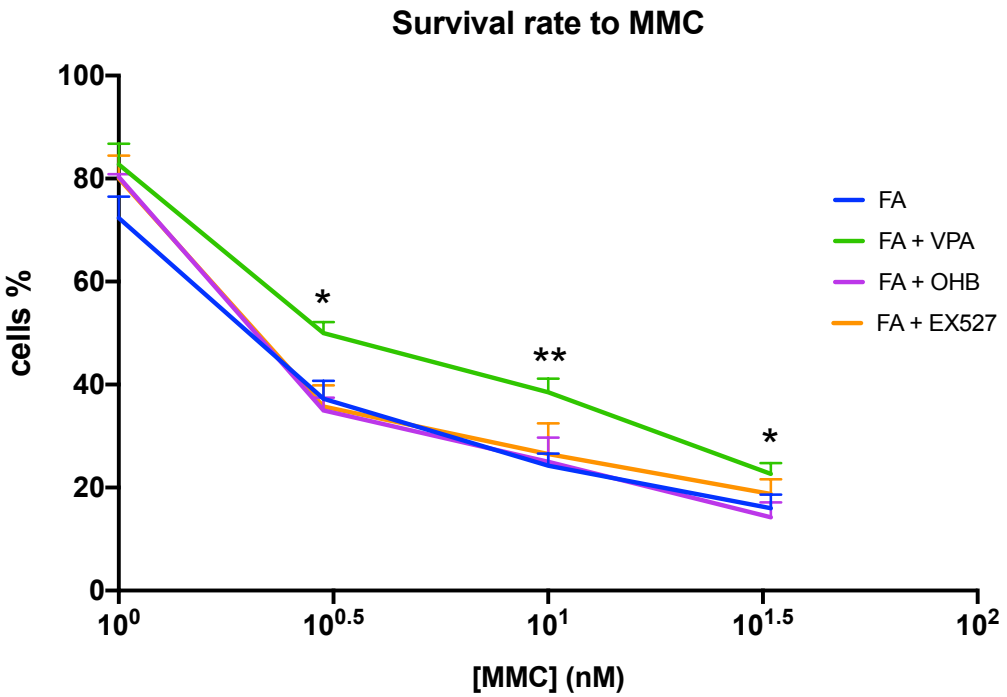


Figure 47 VPA, OHB, or EX527 effects on FA lymphoblasts survival to mitomycin. The graph shows the survival rate of FA lymphoblasts to mitomycin (MMC) after treatment with HDACi. Data are reported as mean ± SD, and the graph is representative of 6 independent experiments. Statistical significance was tested with a one-way ANOVA test; * and ** represent a significant difference for $p < 0.05$ or 0.01 between treated and untreated FA cells.

### 5.9.4 VPA effects on FA mitochondrial dynamics

As previously demonstrated in this thesis (3.6), FA cells present a fragmented mitochondrial network due to imbalanced mitochondrial dynamics, where fission predominates over the fusion process. Considering that VPA treatment has improved not only antioxidant defense expression and activity but also the efficiency of oxidative phosphorylation and coupling of the respiratory chain, I wanted to verify its effect on mitochondrial dynamics and the integrity of the mitochondrial network in FA fibroblasts.

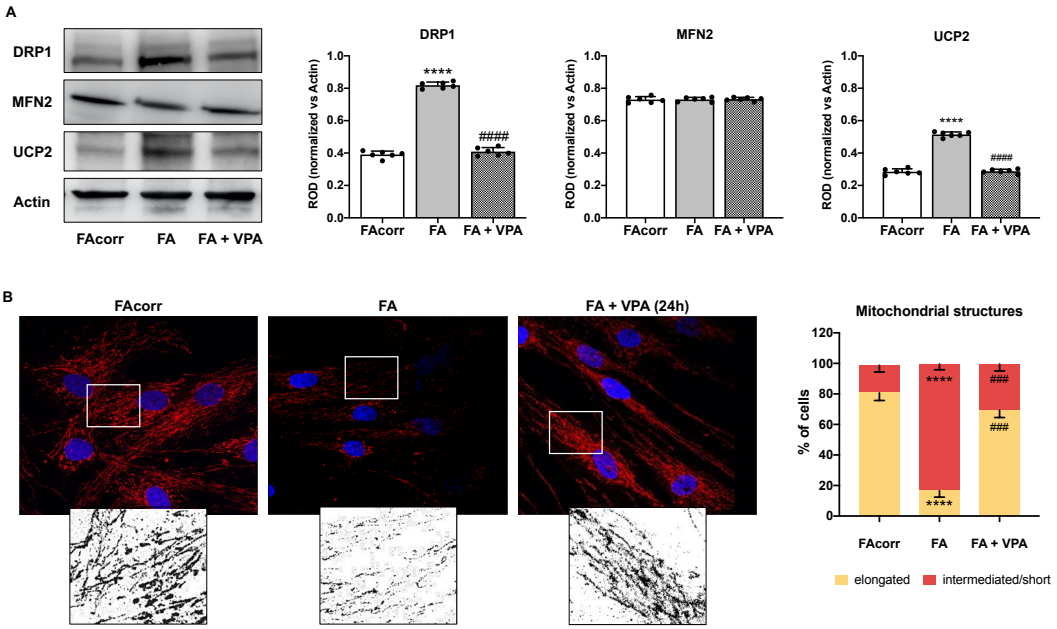


Figure 48 Effect of VPA treatment on mitochondrial dynamics and uncoupling protein 2 expression in FA primary fibroblasts. (A) Western blot signals (left) and relative densitometry analysis (right) of key mitochondrial proteins, including DRP1 (associated with mitochondrial fission), MFN2 (linked to mitochondrial fusion), UCP2 (Uncoupling Protein 2), and Actin (used as a housekeeping protein for signal normalization) in FAcorr and FA primary fibroblasts, with or without VPA treatment for 24 hours. Each signal was normalized on actin revealed on the same membrane. (B) Confocal images of FAcorr and FA fibroblasts stained with an antibody against TOM20 (in red) and DAPI (in blue) to visualize the mitochondrial reticulum and cell nuclei, respectively. White scale bars correspond to 10 µm. The white squares correspond to the higher magnification inserts and provide an example of mitochondrial network distribution. The data presented in the histogram on the right are expressed as mean values ± SD. Each panel shown is representative of a minimum of 6 independent experiments. Statistical significance was determined using a one-way ANOVA. **** represents a significant difference for $p < 0.0001$ between FAcorr and FA cells, while ### and #### indicate significant differences, respectively, for $p < 0.001$ or 0.0001, between untreated and VPA-treated FA fibroblasts.

The results shown in Figure 48A demonstrate that FA, compared to FAcorr fibroblasts, exhibit significantly higher expression of DRP1, an essential protein involved in mitochondrial fission, and the uncoupling protein UCP2. For both proteins, 24h of VPA treatment restores the expression levels of FA cells to the FAcorr level. I also assessed the expression levels of MFN2, a protein involved in mitochondrial fusion, and there are no differences in its expression between FAcorr, FA, or FA + VPA fibroblasts, confirming once again the imbalance towards fission in FA cell dynamics. These findings were also confirmed using confocal microscopy (Figure 48B). FAcorr, FA, and FA + VPA fibroblasts were labeled with TOM20 (in red) and DAPI (in blue) to highlight mitochondria and cell nuclei, respectively. The results, as illustrated in the right-hand graph of Figure 48B, demonstrate that the treatment with VPA on FANCA-mutated cells restores the percentage of mitochondria with elongated morphology, thus the mitochondrial network organization, to the levels observed for FAcorr cells.

### 5.9.5 HDACi combined with oxidative insult on FA antioxidant defenses and energy metabolism

Since cellular antioxidant defenses increase in response to oxidative insult, I wanted to test the effects of HDACi on my cellular models after treatment with hydrogen peroxide. In all the subsequent experiments, I pre-treated FA and FAcorr lymphoblasts and fibroblasts with 0.5 mM $H_2O_2$ to induce oxidative damage. Subsequently, I repeated the treatments with the HDACi for 24 hours.

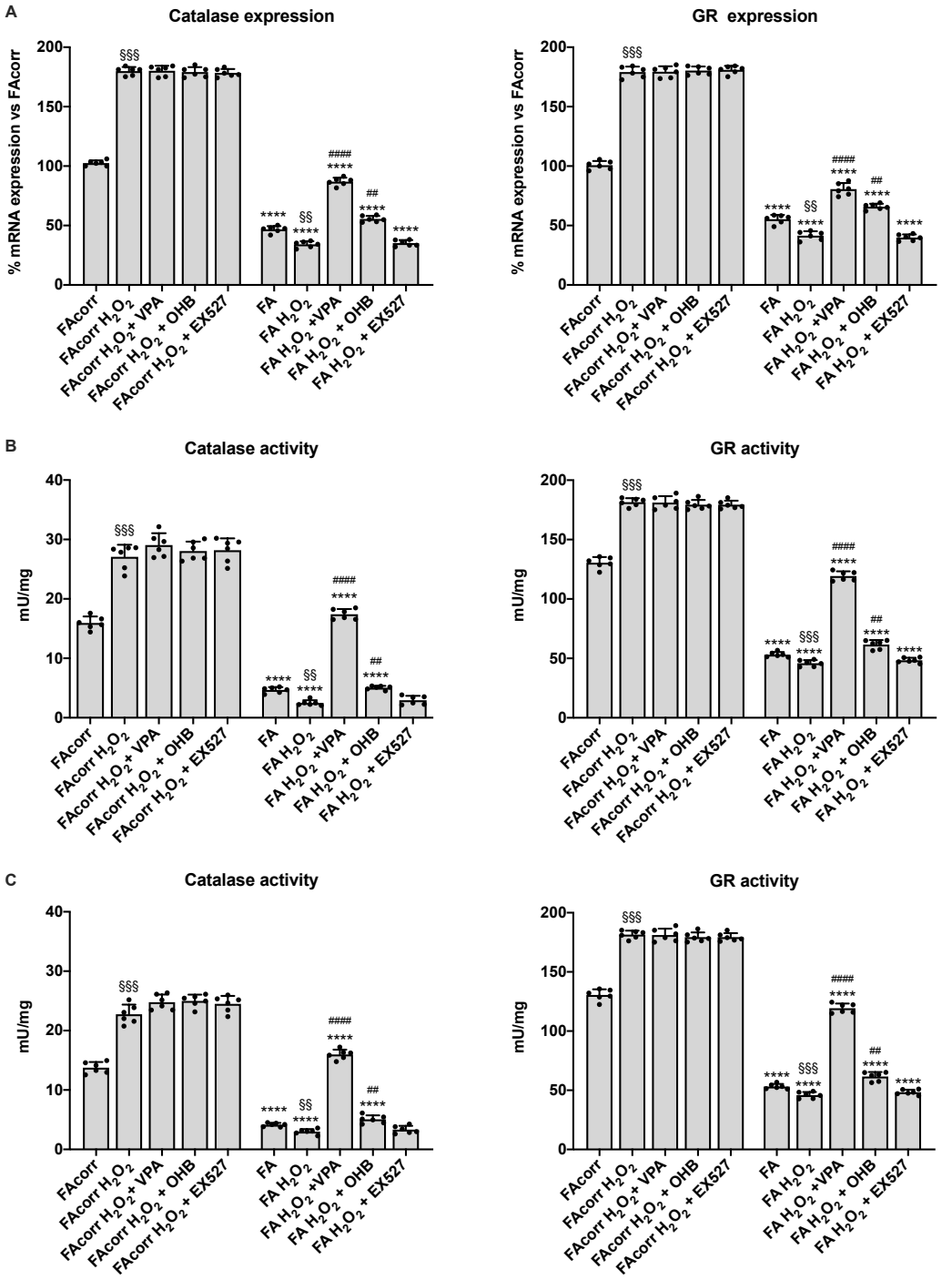


Figure 49 Catalase and glutathione reductase expression and activity in FA lymphoblasts and fibroblasts treated with VPA, OHB, and EX527 after hydrogen peroxide addition. (A) CAT and GR gene expression; (B) CAT and

GR reductase activity in lymphoblasts; (C) CAT and GR activity in fibroblasts. In each experiment represented in these graphs, 0.5 mM of $H_2O_2$ were used to induce oxidative stress. HDACi effects were evaluated 24 hours after their addition. Data are reported as mean ± SD, and each graph is representative of 6 independent experiments. Statistical significance was tested with a one-way ANOVA test; **** represents a significant difference for $p < 0.0001$ between FA and FAcorr cells in the same treatment condition. ##, and #### represent a significant difference for $p < 0.01$ or 0.0001 respectively between HDACi-treated and untreated samples, §, §§ and §§§ represent a significant difference respectively for $p < 0.05$, 0.01, or 0.001 between $H_2O_2$-treated and untreated samples.

Results indicate that FAcorr cells (both lymphoblast and fibroblasts) exhibited increased expression and activity of CAT and GR after $H_2O_2$ treatment (Figure 49). Moreover, this increase persisted without further improvement upon adding VPA, OHB, or EX527, suggesting that FAcorr cells autonomously trigger an adaptive response to oxidative stress. Conversely, both FA lymphoblasts and fibroblasts exposed to $H_2O_2$ show a further decline in CAT and GR expression and activity, likely due to oxidative damage accumulation. However, VPA treatment enhanced CAT and GR expression and activity even in a pro-oxidant environment. OHB treatment also resulted in a modest increase in antioxidant defenses, while EX527 exhibited no significant effect.

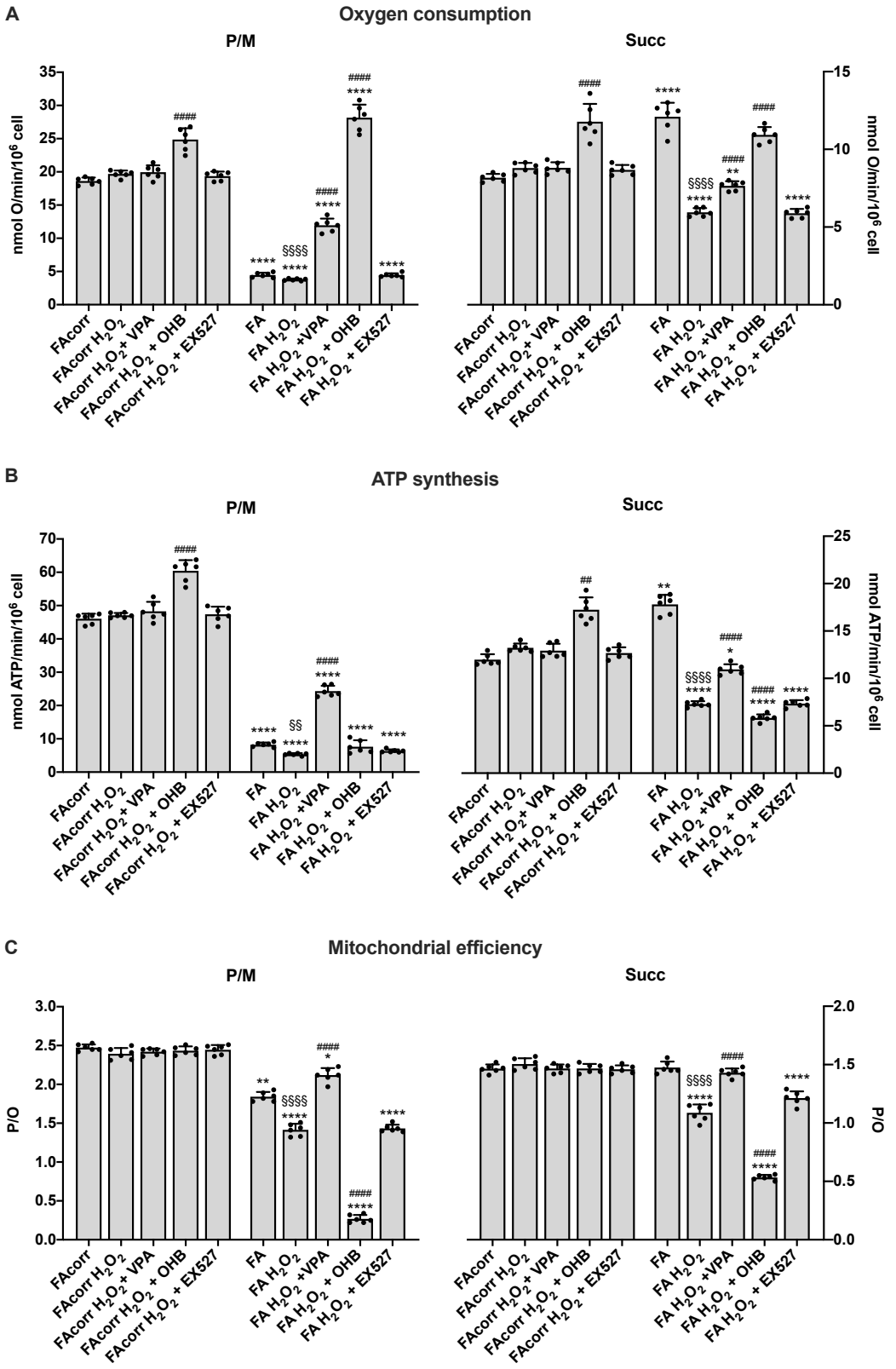


Figure 50 HDACi effects on mitochondrial metabolism in FA and FAcorr lymphoblasts after hydrogen peroxide addition. (A) Oxygen consumption rate (OCR); (B) ATP synthesis through FoF1 ATP synthase; (C) P/O ratio as a mitochondrial efficiency marker. All the experiments represented on the panels on the left were done in the presence of pyruvate plus malate, while all the experiments represented on the panels on the right were done in the presence of succinate as a respiratory substrate. In each experiment represented in these graphs, 0.5 mM of $H_2O_2$ were used to induce oxidative stress. HDACi effects were evaluated 24 hours after their addition. Data are

reported as mean ± SD, and each graph is representative of 6 independent experiments. Statistical significance was tested with a one-way ANOVA test; *, **, and **** represent respectively a significant difference for $p < 0.05$, 0.01, or 0.0001 between FA and FAcorr cells in the same treatment condition. ## and #### represent a significant difference for $p < 0.01$ or 0.0001 between HDACi-treated and untreated samples, §§ and §§§§ represent a significant difference for $p < 0.01$ or 0.0001 between $H_2O_2$-treated and untreated samples.

Regarding energy metabolism, $H_2O_2$ addition to FAcorr cells, either with or without HDACi treatments, does not produce any significant effect, neither for lymphoblasts (Figure 50) nor fibroblasts (Figure 51). Notably, only OHB is causing a coupled increase in OCR and ATP synthesis, likely attributable to the respiratory boost induced by this substrate in OxPhos activity. In cells with FANCA mutation, adding $H_2O_2$ worsened the metabolic defect, reducing OCR, ATP synthesis, and mitochondrial efficiency (P/O) for both P/M and succinate. As already observed under basal conditions (section 3.9.1), for both lymphoblasts (Figure 50) and fibroblasts (Figure 51) after the exposure to $H_2O_2$, treatment with EX527 had no effect, while treatment with OHB improved OCR without enhancing ATP synthesis, resulting in a deterioration of respiratory chain coupling for both P/M and succinate. Treatment with VPA was the only one capable of significantly improving OCR and ATP synthesis for both lymphoblasts and fibroblasts, leading to enhanced mitochondrial efficiency for both P/M and succinate.

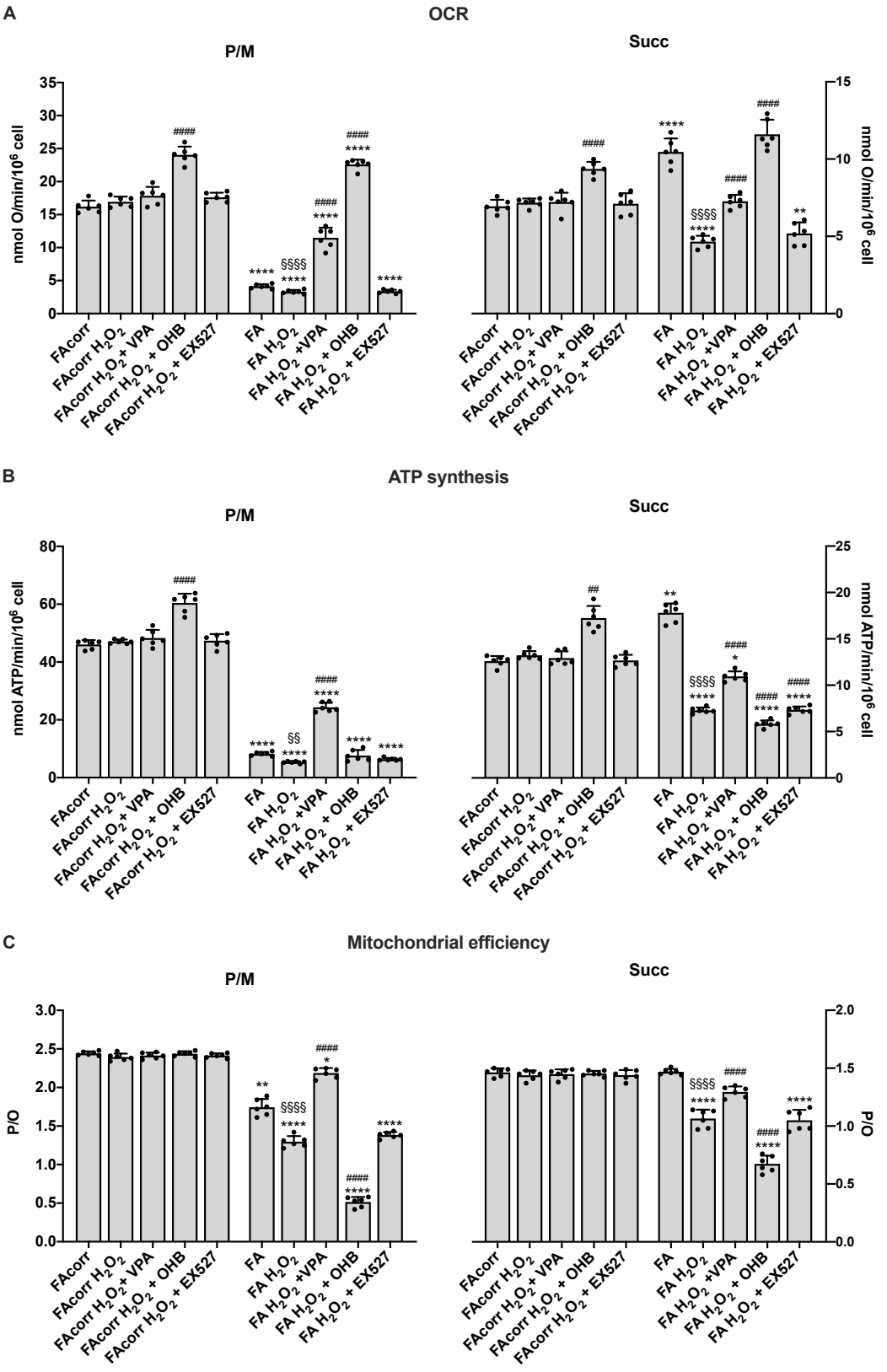


Figure 51 HDACi effects on mitochondrial metabolism in FA and FAcorr fibroblasts after hydrogen peroxide addition. (A) Oxygen consumption rate (OCR); (B) ATP synthesis through FoF1 ATP synthase; (C) P/O ratio as a mitochondrial efficiency marker. All the experiments represented on the panels on the left were done in the presence of pyruvate plus malate, while all the experiments represented on the panels on the right were done in the presence of succinate as a respiratory substrate. In each experiment represented in these graphs, 0.5 mM of

$H_2O_2$ were used to induce oxidative stress. HDACi effects were evaluated 24 hours after their addition. Data are reported as mean ± SD, and each graph is representative of 6 independent experiments. Statistical significance was tested with a one-way ANOVA test; *, **, and **** represent respectively a significant difference for $p < 0.05$, 0.01, or 0.0001 between FA and FAcorr cells in the same treatment condition. ## and #### represent a significant difference for $p < 0.01$ or 0.0001 between HDACi-treated and untreated samples, §§ and §§§§ represent a significant difference for $p < 0.05$ or 0.0001 between $H_2O_2$-treated and untreated samples.

Similarly, concerning the electron transfer between Complex I and III of the respiratory chain, the addition of $H_2O_2$, either alone or with HDACi treatments, does not affect FAcorr control cells (Figure 52A for lymphoblasts and Figure 52B for fibroblasts). However, $H_2O_2$ worsens the electron transfer in cells with the FANCA mutation. Once again, the only treatment to significantly improve this parameter is VPA, both for lymphoblasts (Figure 52A) and fibroblasts (Figure 52B).

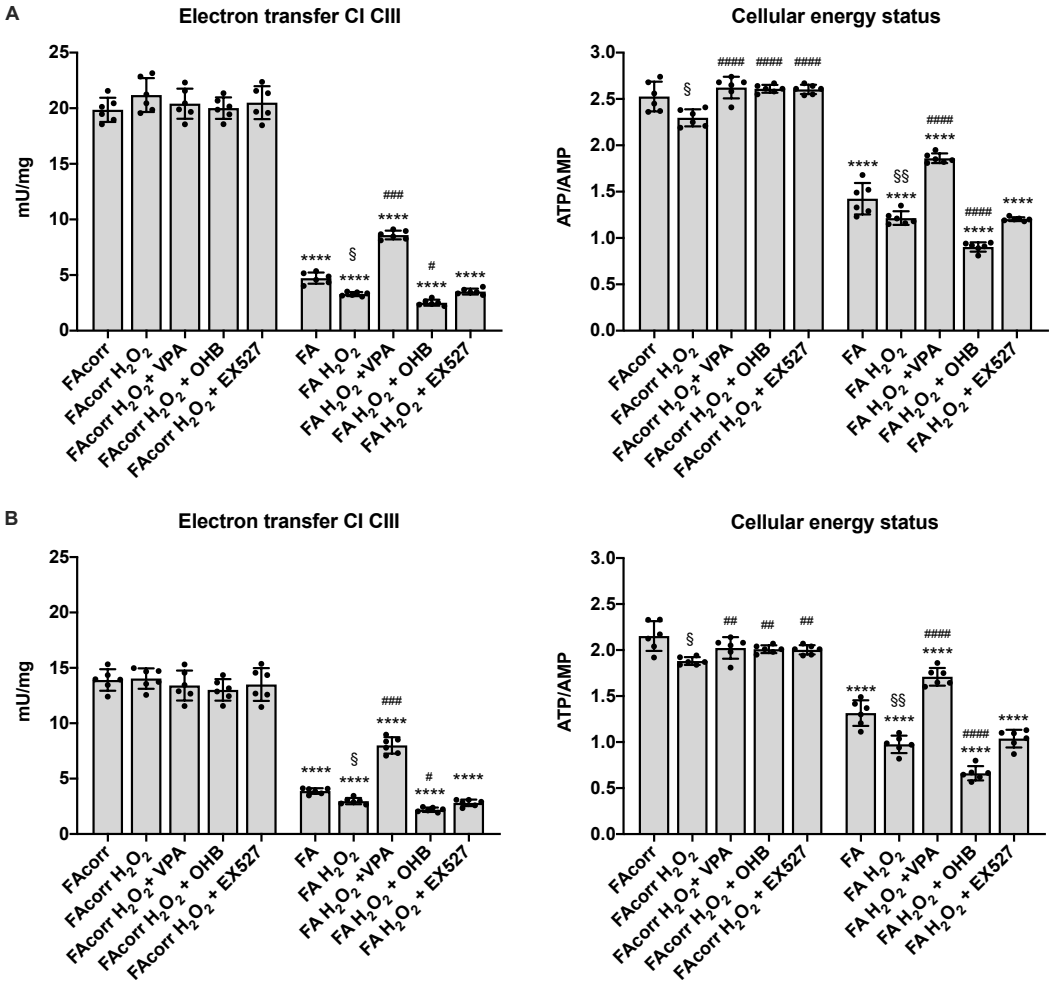


Figure 52 Electron transfer between the I and III respiratory complexes and cellular energy status in FA and FAcorr lymphoblasts and fibroblasts after hydrogen peroxide addition. (A) Electron transfer between the I and III respiratory complexes and cellular energy status in FA and FAcorr lymphoblasts (B) Electron transfer between the I and III respiratory complexes and cellular energy status in FA and FAcorr fibroblasts. In each experiment represented in these graphs, 0.5 mM of $H_2O_2$ were used to induce oxidative stress. HDACi effects were evaluated 24 hours after their addition. Data are reported as mean ± SD, and each graph is representative of 6 independent experiments. Statistical significance was tested with a one-way ANOVA test; **** represents a significant difference for $p < 0.0001$ between FA and FAcorr cells in the same treatment condition. #, ##, ###, and ####

represent a significant difference respectively for $p < 0.05$, 0.01, 0.001 or 0.0001 between HDACi-treated and untreated samples, § and §§ represent a significant difference for $p < 0.05$ or 0.01 between $H_2O_2$-treated and untreated samples.

Cellular energy status, represented by the ATP/AMP ratio, deteriorates following the addition of $H_2O_2$ for both FAcorr cells, where increased energy expenditure is likely due to enhanced synthesis and activity of antioxidant defenses, and FA cells, where this effect does not occur. All HDACi treatments improve cellular energy status for FAcorr cells, while in the case of FANCA cells, the only treatment that improves this parameter is once again VPA; EX527 has no effect, while OHB further worsens the ATP/AMP ratio (Figure 52A for lymphoblasts and Figure 52B for fibroblasts). The last parameters I reassessed after adding $H_2O_2$ were ALDH activity, lipid accumulation, and lipid peroxidation damage (MDA).

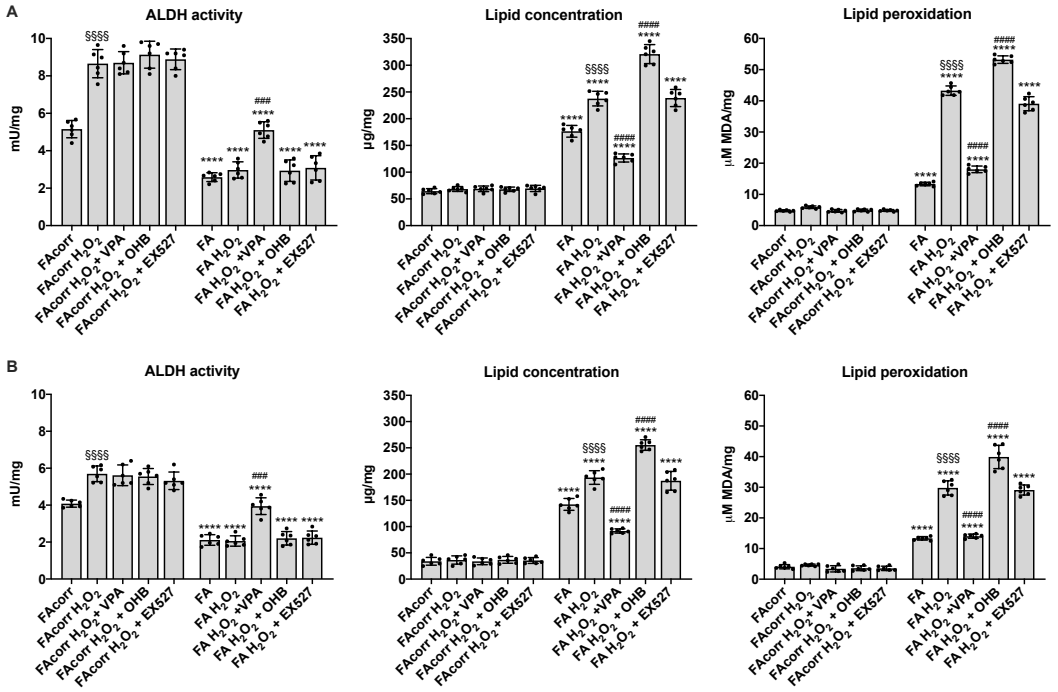


Figure 53 ALDH activity and lipid concentration and peroxidation in FA and FAcorr lymphoblasts and fibroblasts after hydrogen peroxide addition. (A) ALDH activity, lipid concentration, and MDA as a marker of lipid peroxidation in FA and FAcorr lymphoblasts (B) ALDH activity, lipid concentration and MDA as a marker of lipid peroxidation in FA and FAcorr fibroblasts. In each experiment represented in these graphs, 0.5 mM of $H_2O_2$ were used to induce oxidative stress. HDACi effects were evaluated 24 hours after their addition. Data are reported as mean ± SD, and each graph is representative of 6 independent experiments. Statistical significance was tested with a one-way ANOVA test; **** represents a significant difference for $p < 0.0001$ between FA and FAcorr cells in the same treatment condition. ### and #### represent a significant difference for $p < 0.001$ or 0.0001 between HDACi-treated and untreated samples, §§§§ represents a significant difference for $p < 0.0001$ between $H_2O_2$-treated and untreated samples.

Regarding ALDH activity, for FAcorr cells (Figure 53A for lymphoblasts and Figure 53B for fibroblasts), the oxidative insult, with or without HDACi treatments, increases the enzyme activity, while for FA cells, only the addition of VPA improves its response; $H_2O_2$ alone, as well as treatments with OHB and EX527, are unable to stimulate the cells to activate even this enzyme involved in aldehyde detoxification. As for lipid accumulation and lipid

peroxidation damage, we can see from the graphs in Figure 53A for lymphoblasts and Figure 53B for fibroblasts that both parameters follow the same trend for all cells and conditions analyzed. Indeed, FAcorr cells do not undergo any increase in any condition, while FA cells, which already have a higher basal concentration of both lipids and MDA, undergo a significant increase for these two parameters, which do not change after the addition of EX527, further worsen after the addition of OHB, and improve only after VPA treatment, which brings both lipid and MDA concentrations to values similar to untreated FA cells.

All the data presented in section 3.9 were published in N. Bertola *et al.*, “Effects of Deacetylase Inhibition on the Activation of the Antioxidant Response and Aerobic Metabolism in Cellular Models of Fanconi Anemia,” *Antioxidants*, vol. 12, no. 5, 2023, DOI: 10.3390/antiox12051100.

### 5.10 miRNA

microRNAs (miRNAs) are short, non-coding RNA molecules, typically 22 nucleotides long, known for their pivotal roles in regulating various biological and pathological processes [122]. They are estimated to influence the activity of up to 30% of human genes, mainly by modulating messenger RNA (mRNA) translation or degradation. Moreover, the variable expression levels of miRNAs make them promising candidates as disease-specific biomarkers. The significant advances in the miRNomics fields have facilitated the identification of miRNAs involved in cancer and disease development, leading to the concept of "miRNA signature" for diagnostics, disease progression, prognosis, and response to treatment [123], [124].

However, the application of 'omics' techniques in studying FA has been somewhat limited, with few reports focusing on gene microarrays, proteomic, metabolomic, and lipidomic. Regarding miRNAs, while limited studies have explored this area, they have yielded noteworthy findings. Therefore, in this part of my thesis, I investigated the role of miRNAs in Fanconi Anemia, building upon the insights provided by Degan et al. in 2019 [125], as miRNAs appear to play a crucial regulatory role in FA, shedding light on unknown regulatory mechanisms. Continued research into the role of miRNAs in FA is essential for achieving a comprehensive understanding of the disease's molecular regulation and complexity.

#### 5.10.1 miRNA29A

From the bioinformatic analyses conducted in collaboration with Dr. Degan and Dr. Regis, miRNA29A emerged as one of the most promising targets in FA, as it is also involved in regulating numerous metabolic pathways. I then tested the expression levels of miRNA29A in the cell lines used as a model for this thesis, which I later transfected.

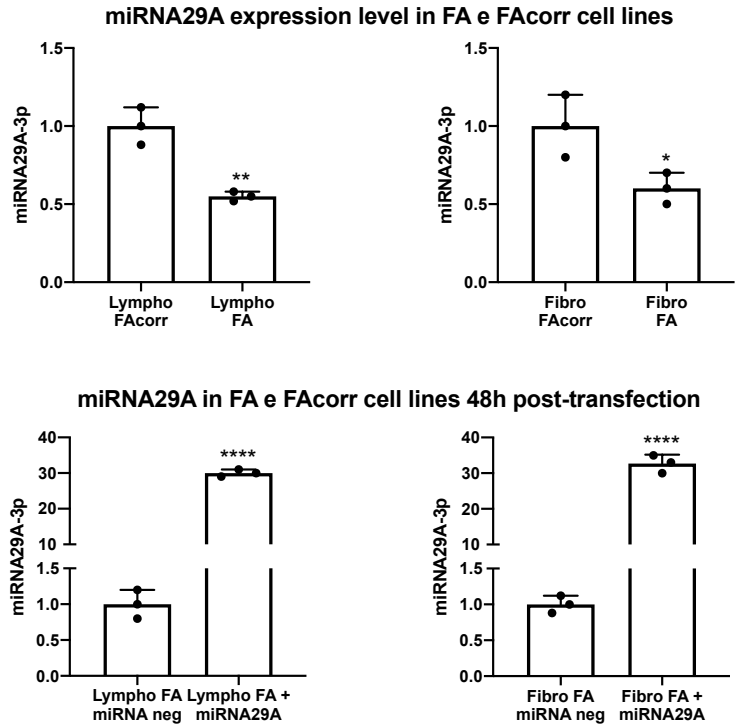


Figure 54 miRNA29A expression levels in FA and FAcorr lymphoblasts and fibroblasts before and 48 hours after miRNA29A transfection. Upper panels: basal miRNA29A expression levels; lower panels: miRNA29A expression levels 48h after FA cells miRNA29A transfection. Data are presented as mean ± SD and are representative of at least 5 independent experiments. Statistical significance was tested with an unpaired t-test. *, **, and *** represent statistical significance at $p < 0.05$, 0.01, or 0.0001, respectively.

The upper panel of Figure 54 shows how the basal levels of miRNA29A in FA cells, in both lymphoblasts and fibroblasts, are significantly lower than their respective corrected cells. After 48 hours of transfection with miRNA29A (lower panels), miRNA29A expression in FA cells increases to be 30 times higher than cells transfected with the empty plasmid. After confirming the effectiveness of miRNA29A transfection, I wanted to test the major metabolic parameters affected in FA to see how this transfection would impact them, starting with OCR, ATP synthesis, and mitochondrial efficiency.

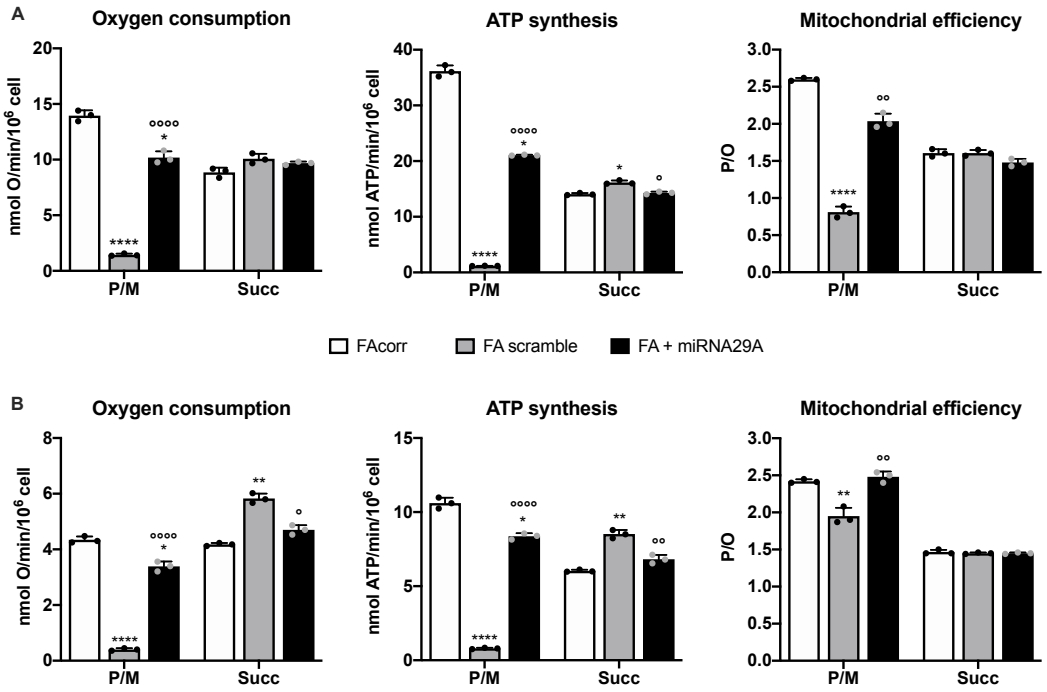


Figure 55 miRNA29A effects on mitochondrial metabolism in FA and FAcorr lymphoblasts and fibroblasts. (A) Oxygen consumption rate (OCR), ATP synthesis through $F_oF_1$ ATP synthase, and P/O ratio as a mitochondrial efficiency marker in lymphoblasts cell lines. (B) Oxygen consumption rate (OCR), ATP synthesis through $F_oF_1$ ATP synthase, and P/O ratio as a mitochondrial efficiency marker in fibroblast cell lines. All the experiments were done with pyruvate plus malate or succinate as respiratory substrates. Data are reported as mean ± SD, and each graph is representative of at least 3 independent experiments. Statistical significance was tested with a one-way ANOVA test; *, **, and **** represent respectively a significant difference for $p < 0.05$, 0.01, or 0.0001 between FA or FA + miRNA29A cells and FAcorr. ; °, °°, and °°°° represent respectively a significant difference for $p < 0.05$, 0.01, or 0.0001 between FA cells with and without miRNA.

Data presented in Figure 55 shows that, for both lymphoblasts (A) and fibroblasts (B), miRNA29A transfection significantly increases the levels of all analyzed parameters in experiments conducted with P/M as the respiratory substrate. This increase is more pronounced for fibroblasts (B), whose energy efficiency (P/O ratio) is completely restored. Regarding experiments with Succinate, we can see that for both cell types, OCR and ATP synthesis values decrease after transfection, returning virtually to the levels measured for corrected cells. This decrease, however, does not significantly affect the mitochondrial efficiency of this metabolic pathway.

Considering the significant improvement in mitochondrial metabolism following miRNA29A transfection, I evaluated other parameters typically altered in FA, such as electron transport between Complex I and Complex III of the respiratory chain, cellular energy status, and lipid peroxidation damages.

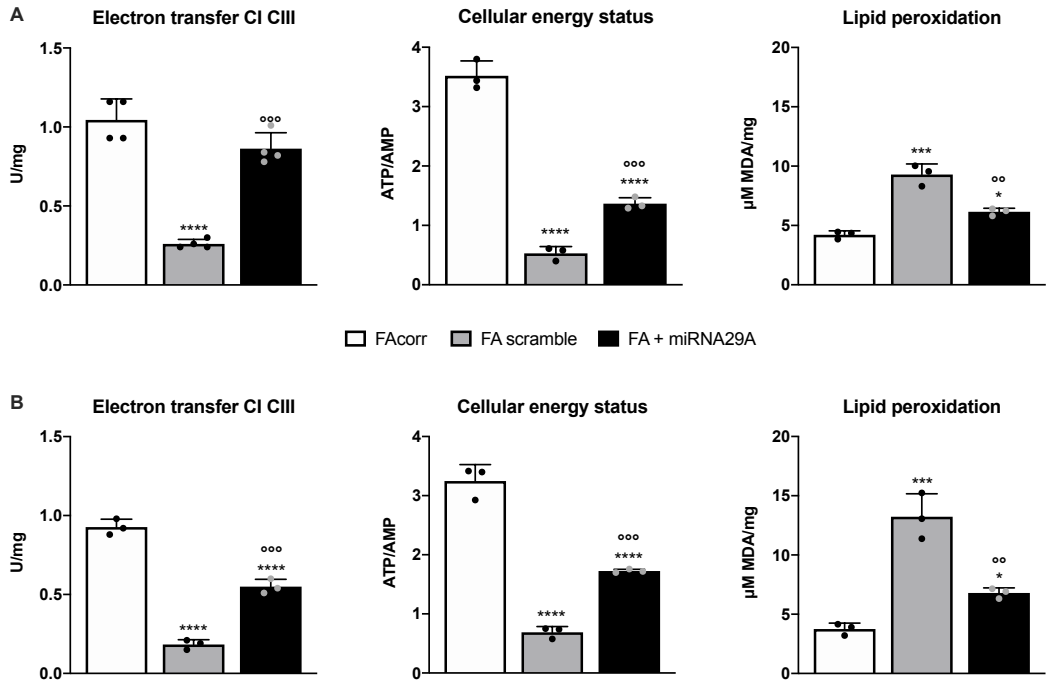


Figure 56 miRNA29A effects on electron transport between complexes I and III, cellular energy status, and lipid peroxidation in FA and FAcorr lymphoblasts and fibroblasts. (A) Electron transport between Complex I and Complex III of the respiratory chain, ATP/AMP ratio as a marker of cellular energy status, and malondialdehyde (MDA) as a marker of lipid peroxidation damage in lymphoblasts cell lines. (B) Electron transport between Complex I and Complex III of the respiratory chain, ATP/AMP ratio as a marker of cellular energy status, and malondialdehyde (MDA) as a marker of lipid peroxidation damage in fibroblast cell lines. Data are reported as mean ± SD, and each graph is representative of at least 3 independent experiments. Statistical significance was tested with a one-way ANOVA test; *, ***, and **** represent respectively a significant difference for $p < 0.05$, 0.001, or 0.0001 between FA or FA + miRNA29A cells and FAcorr. ; °° and °°° represent respectively a significant difference for $p < 0.01$, or 0.001 between FA cells with and without miRNA.

The data shown in Figure 56 indicate that both lymphoblasts (A) and fibroblasts (B) transfected cells have a significant improvement in electron transport between Complex I and Complex III of the respiratory chain compared to FA cells, although the improvement is more pronounced in lymphoblasts (A). Cellular energy status, represented by the ATP/AMP ratio, is also improved in transfected cells compared to FA cells. MDA levels, which represent lipid peroxidation damage in the cell, decrease significantly in transfected cells, although they do not return to the levels of cells with the functional FANCA gene. Finally, I wanted to assess whether DRP1 expression levels, the main protein involved in mitochondrial fission, improved following transfection, as reduced mitochondrial fragmentation could explain the improved efficiency of mitochondrial metabolism.

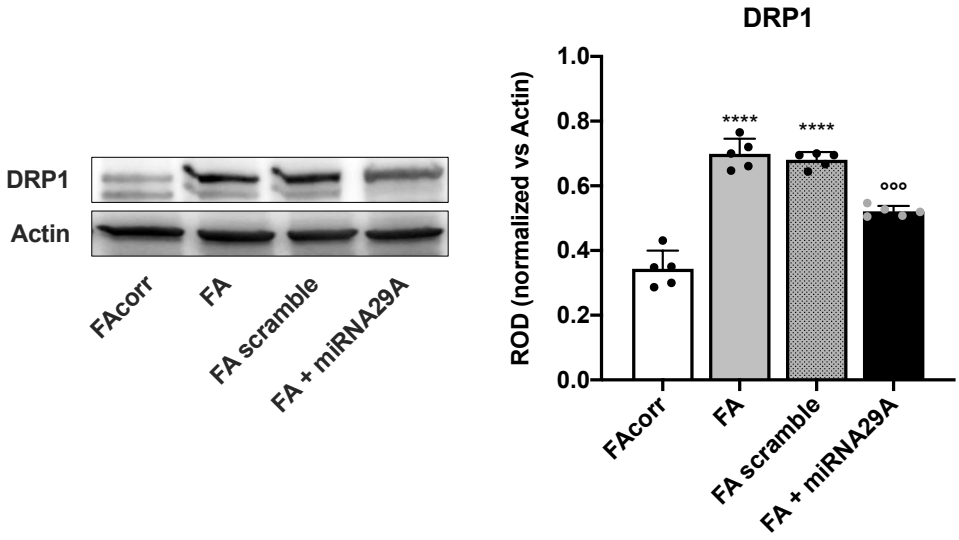


Figure 57 miRNA29A transfection effects on mitochondrial fission maker expression levels in FA lymphoblasts. WB signals of DRP1 and Actin (housekeeping protein) in lymphoblast cell lines are charged in WB as follows: FAcorr, FA, FA transfected with the empty plasmid and miRNA29A. Protein expression levels (densitometric analysis) were normalized on the Actin signal revealed on the same membrane. Data are reported in the histogram as mean ± SD, and both WB signals and graph are representative of 5 independent experiments. Statistical significance was tested opportunely with an unpaired t-test; **** represents a significant difference for $p < 0.0001$ between FA or FA scramble and FAcorr cells; °°° represents a significant difference for $p < 0.001$ between FA cells transfected or not with miRNA29A.

As shown in Figure 57, transfection of FA cells with miRNA29A significantly reduces DRP1 expression levels compared to non-transfected FA cells, thereby reducing mitochondrial network fragmentation and providing a possible explanation for aerobic metabolism improvement.

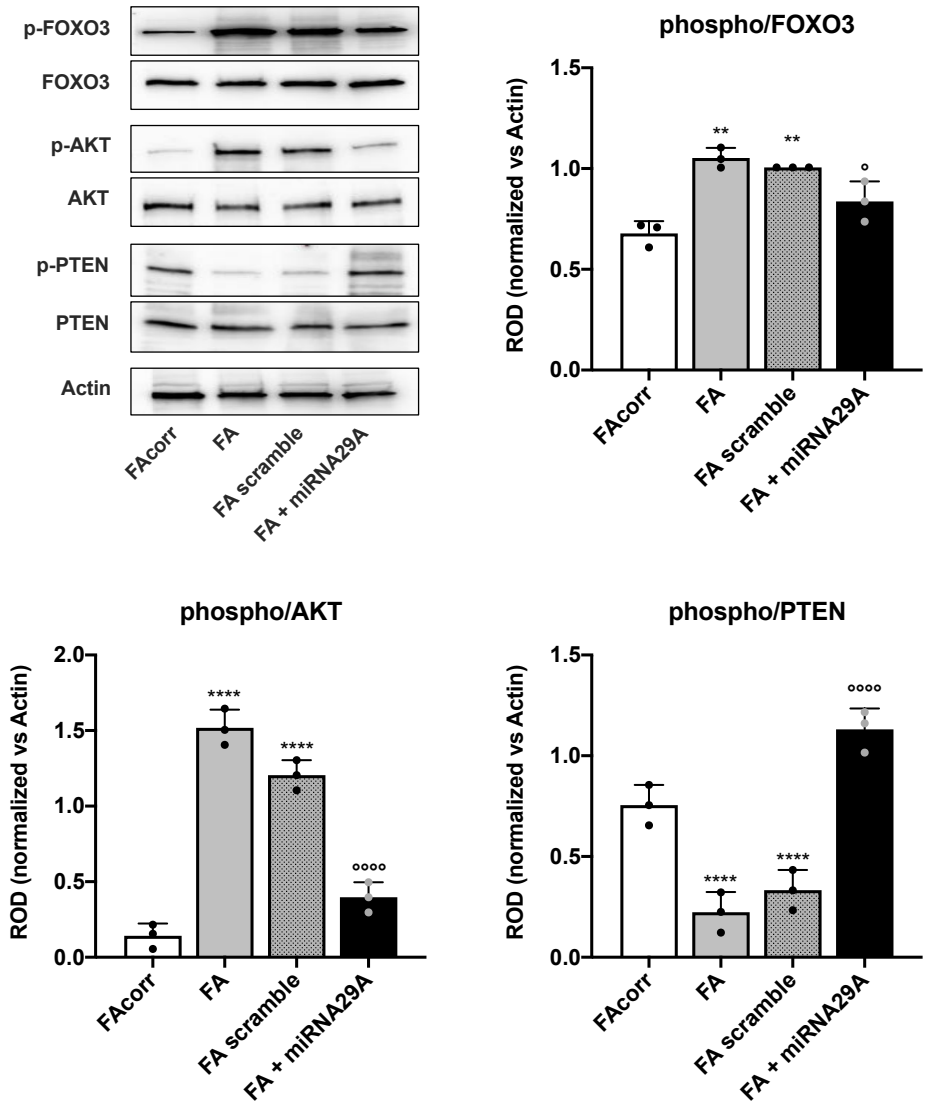


Figure 58 miRNA29A transfection effects on various protein expression levels in FA and FAcorr lymphoblasts. WB signals of phospho-FOXO3, total FOXO3, phospho-AKT, total AKT, phospho-PTEN, total PTEN, and Actin (housekeeping protein) in lymphoblast cell lines charged in WB as follows: FAcorr, FA, FA transfected with the empty plasmid, or with miRNA29A. Protein expression levels (densitometric analysis) were normalized on the Actin signal revealed on the same membrane. Data are reported in the histogram as active proteins, namely the ratio between phosphorylated and total proteins revealed on the same membrane. Data are reported as mean ± SD, and both WB signals and graphs are representative of at least 3 independent experiments. Statistical significance was tested with a one-way ANOVA test; ** or **** represent a significant difference for $p < 0.01$ and 0.0001 between FA or FA scramble and FAcorr cells; ° or °°°° represent a significant difference for $p < 0.05$ and 0.001 between FA cells transfected or not with miRNA29A.

As shown in Figure 58, the data demonstrate no significant differences in the expression levels of the analyzed active proteins between FA cells and FA scramble cells, which were transfected with an empty plasmid. However, miRNA29A transfection significantly decreases the expression levels of active FOXO3 and AKT (phospho/tot), bringing them closer to the levels observed in FAcorr cells. Levels of activated PTEN, instead, increase significantly after transfection, to the extent that they exceed those in FAcorr cells.

### 5.11 FA and inflammation

FA exhibits a complex interplay with inflammation and oxidative stress. FA patients frequently endure chronic inflammation triggered by increased oxidative stress production due to mitochondrial respiratory chain defects, which are extensively discussed in this thesis. The imbalance between oxidative stress production and antioxidant defenses exacerbates the accumulation of DNA damage that FA patients are unable to repair due to defective DNA ICLs repair system. This heightened inflammation can further escalate ROS production and DNA damage, creating a detrimental cycle. Elevated inflammation can enhance oxidative stress levels, and, in turn, oxidative stress can fuel inflammation. This results in a vicious cycle that perpetuates the progression of the disease. Understanding this multifaceted interplay is crucial for developing targeted therapies that not only address the genetic defects but also manage the associated inflammatory complications and oxidative stress in FA patients.

So, I wanted to conduct analyses comparing cell lines with FANCA mutation, FANCC mutation, and their respective isogenic lines corrected with functional FANCA or FANCC genes. I also treated these cell lines with various antioxidant drugs, comparing them with the effects of P110, which we have already analyzed in detail in section 3.6.1. In particular, I used a TNFα inhibitor, an IL1 inhibitor, an NLRP3 inhibitor, and a TGFβ inhibitor. TNFα (Tumor Necrosis Factor α) is a cytokine produced by various cells in the body, including immune cells like macrophages and T-cells. It plays a central role in the immune response, particularly in the inflammatory process. It can trigger inflammation to combat infections and injuries. Abnormal or excessive TNFα production is associated with chronic inflammatory conditions like rheumatoid arthritis and inflammatory bowel disease. IL1 (Interleukin 1) is a proinflammatory cytokine produced by immune cells, including monocytes and macrophages. It plays a crucial role in the regulation of immune responses and inflammation. It is involved in fever induction, activation of immune cells, and the inflammatory response to infections. Dysregulation of IL1 signaling is associated with autoimmune diseases and autoinflammatory syndromes. NLRP3 (NOD-Like Receptor Pyrin Domain Containing 3) is a protein receptor involved in the innate immune response. It forms a part of the multiprotein complex NLRP3 inflammasome. Activation of NLRP3 is a critical step in initiating inflammation and immune responses. Dysregulation of NLRP3 activation can lead to autoinflammatory diseases like cryopyrin-associated periodic syndromes (CAPS). TGFβ (Transforming Growth Factor β) is a multifunctional cytokine that regulates cell growth, differentiation, and immune responses. It is crucial in tissue development, wound healing, and immune tolerance. It can have both anti- and pro-inflammatory effects depending on the context. Dysregulation of TGFβ signaling is implicated in fibrotic diseases and cancer progression. These molecules were chosen as targets in this context because they are essential regulators of the immune system and inflammation, and their functions are intricately linked to various physiological and pathological processes in the body.

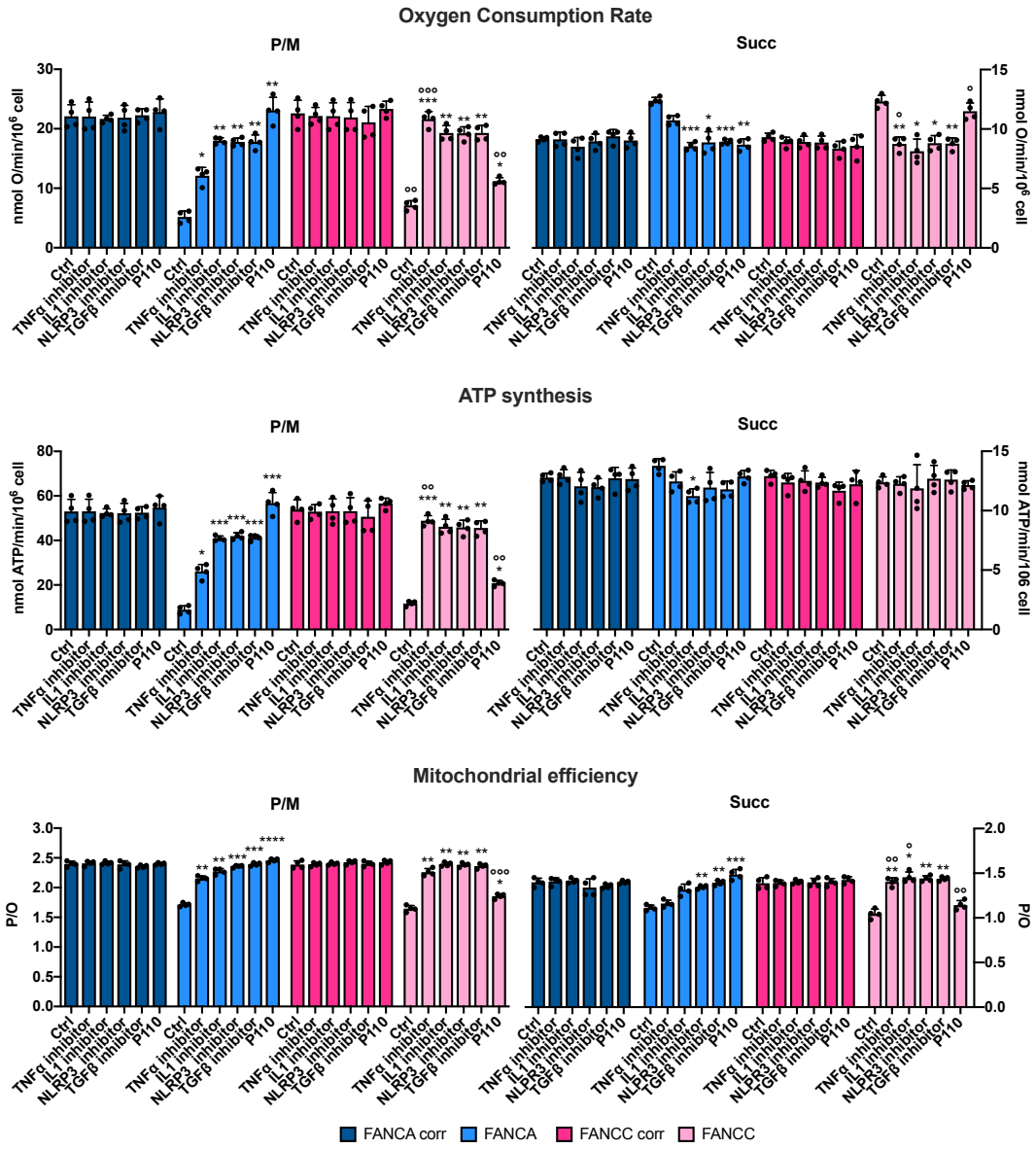


Figure 59 Effect of various anti-inflammatory molecules on the mitochondrial metabolism of FANCA and FANCC mutated or corrected lymphoblast cell lines. TNFα inhibitor, IL1 inhibitor, NLRP3 inhibitor, TGFβ inhibitor, and P110 effects on (A) oxygen consumption rate, (B) ATP synthesis through FoF1 ATP synthase, and (C) P/O ratio as a marker of mitochondrial efficiency on FANCA corr (blue) FANCA (light blue) FANCC corr (magenta) and FANCC (pink) lymphoblast cell lines. All the experiments represented on the left panels were performed with the addition of pyruvate plus malate (P/M), while all the experiments represented on the right panels with the addition of succinate (Succ) as the respiratory substrate to stimulate the pathway composed of respiratory complexes I, III, and IV or II, III, and IV. Data are reported as mean ± SD, and each graph is representative of at least three independent experiments. Statistical significance was tested with a one-way ANOVA test; *, **, ***, and **** represent $p < 0.05$, 0.01, 0.001, or 0.0001 between treated and untreated cells; °, °°, and °°° represent $p < 0.05$, 0.01, or 0.001 between FANCA and FANCC cells in the same clinical condition.

The data related to oxidative phosphorylation shown in Figure 59 reveal that both for cell lines with FANCA and FANCC mutations, there is a significant reduction in OCR, ATP synthesis, and mitochondrial efficiency (P/O ratio) when stimulated with P/M. There's also a compensatory increase in the succinate-stimulated pathway, especially notable for OCR, although this doesn't translate into coupling with ATP synthase. No treatment affected any

parameter for both FANCA- and FANCC-corrected cell lines, while for the mutated cell lines, the effects of the various treatments differ for the different mutations. While for FANCA, the TNFα inhibitor is the least effective overall, with a significant effect on all considered parameters, P110 proves to be the most effective, restoring mitochondrial efficiency for both respiratory substrates. However, this isn't the case for FANCC-mutated cell lines. In this scenario, P110 is the least effective on various parameters, while IL1, NLRP3, and TGFβ inhibitors bring oxidative phosphorylation back to an efficient state, with OCR and ATP synthesis values closer to those of FANCC-corrected cells. Finally, I evaluated the effect of these molecules on cellular energy status and malondialdehyde (MDA) as a marker of lipid peroxidation.

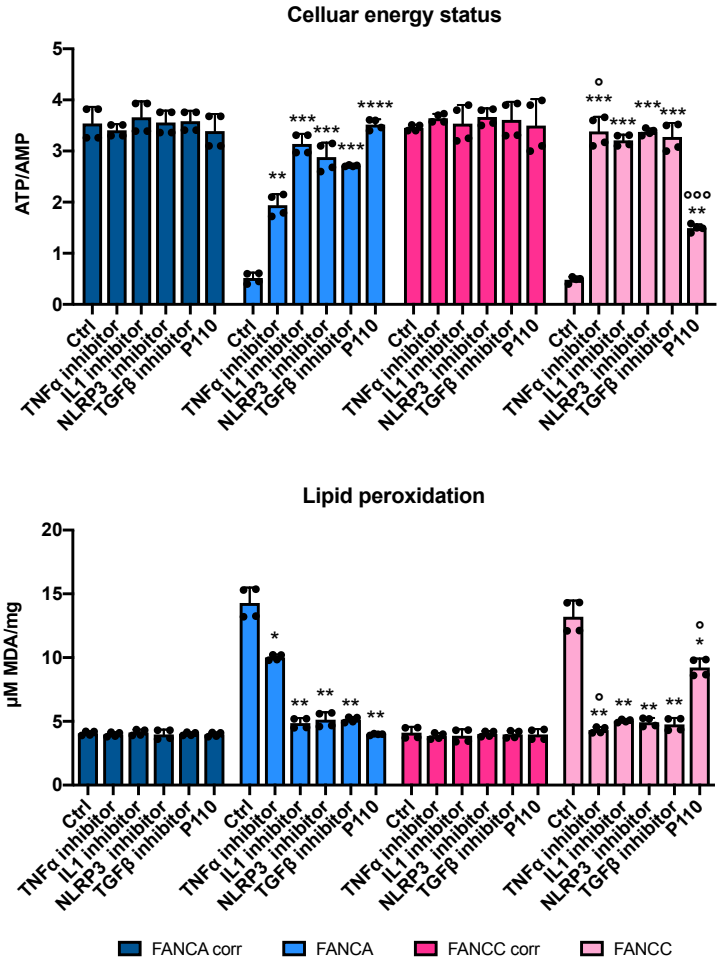


Figure 60 Effect of various anti-inflammatory molecules on the mitochondrial metabolism of FANCA and FANCC mutated or corrected lymphoblast cell lines. TNFα inhibitor, IL1 inhibitor, NLRP3 inhibitor, TGFβ inhibitor, and P110 effects on ATP/AMP ratio as a marker of the cellular energy status and malondialdehyde (MDA) as a marker of lipid peroxidation damage on FANCA corr (blue) FANCA (light blue) FANCC corr (magenta) and FANCC (pink) lymphoblast cell lines. Data are reported as mean ± SD, and each graph is representative of at least three independent experiments. Statistical significance was tested with a one-way ANOVA test; *, **, ***, and **** represent $p < 0.05$, 0.01, 0.001, or 0.0001 between treated and untreated cells; ° and °°° represent $p < 0.05$ or 0.001 between FANCA and FANCC cells in the same clinical condition.

The data shown in Figure 60 reveal a significant reduction in cellular energy status (ATP/AMP ratio) for both FANCA and FANCC mutations and a significant increase in the MDA level. Regarding the effect of the molecules, the situation aligns with what was previously observed for oxidative phosphorylation in the preceding figure. In fact, no treatment has any effects on the corrected cell lines. However, concerning the FANCA cell lines, the TNFα inhibitor is the least effective in increasing ATP/AMP ratio and decreasing MDA levels, although with a significant effect on both parameters, while P110 proves to be the most effective. In FANCC cell lines, P110 is the least effective, while TNFα, IL1, NLRP3, and TGFβ inhibitors restore cellular energy ratio and lipid peroxidation to values closer to those of FANCC-corrected cells.

These preliminary data further emphasize how Fanconi Anemia is a heterogeneous, multifactorial, and complex disease. Despite causing common metabolic and molecular issues, the heterogeneity of FANC gene mutations makes this condition's clinical management extremely complex.

### 5.12 Fanconi Anemia-related Head and Neck Squamous Cell Carcinoma

HNSCC is the most common solid tumor in FA patients and presents with distinct characteristics compared to the general population; for instance, the onset is increased by 500-800-fold, is more aggressive, and develops at a younger age, even without exposure to the major risk factors. Undoubtedly, these issues are partly attributed to the defect in the ICL repair system secondary to the mutation in FANC genes. However, considering the results presented in the previous sections of this thesis, which highlight the central role of metabolic dysfunctions among the factors driving the pathogenesis and progression of FA, I questioned whether and to what extent these metabolic factors could influence the onset and aggressiveness of FA-related HNSCC. In the experiments reported in this thesis section, I employed the OHSU-S91 cell lines (with FANCA mutation) and OHSU-FAcorr cell lines (with the FANCA functional gene inserted) to test this hypothesis.

#### 5.12.1 Energy metabolism

I started by testing the oxygen consumption rate, the ATP synthesis, and the mitochondrial efficiency (P/O ratio).

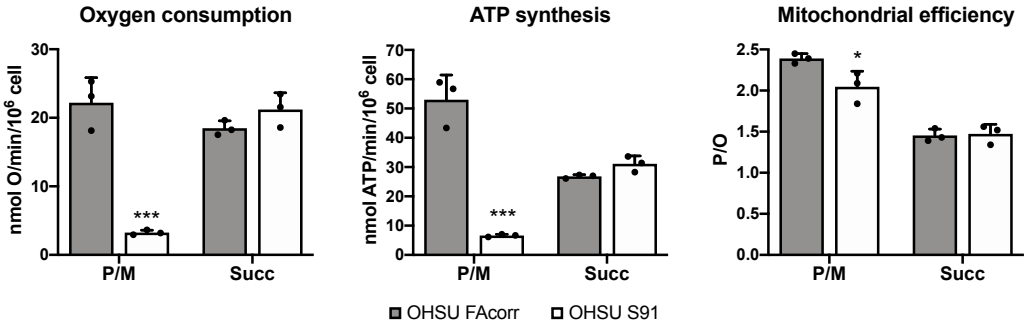


Figure 61 Energy metabolism of HNSSC cell lines mutated (OHSU S91) or not (OHSU FAcorr) for the FANCA gene. ATP synthesis, oxygen consumption rate (OCR), and P/O value (as mitochondrial efficiency marker) were obtained after stimulation with pyruvate and malate (P/M) or succinate (succ). All data are reported as mean ± SD, and each graph is representative of at least 3 independent experiments. Statistical significance was tested opportunely with a one-way ANOVA test; *** represents a significant difference for $p < 0.001$ between FA and FAcorr cells.

As previously demonstrated for lymphoblasts and fibroblasts in section 3.1, the results shown in Figure 61 illustrate that OHSU-S91 cells (with FANCA gene mutation), compared to OHSU-FAcorr control cells, exhibit significantly reduced ATP synthesis and oxygen consumption rate (OCR) when the pathway composed of complexes I, III, and IV is stimulated using pyruvate plus malate. This leads to a decrease in mitochondrial efficiency (P/O ratio) and, therefore, uncoupling of the respiratory chain. Notably, when stimulating the pathway involving complexes II, III, and IV with succinate, OHSU-S91 cells, compared to their control cells, attempt to compensate for the deficit in the first pathway, albeit to a non-significant extent, while mitochondrial efficiency remains unaffected. Given the similarities in the data obtained compared to those previously obtained from the other cell lines with the FANCA mutation, I also assessed whether this metabolic defect could be

attributed to the electron transport issue between the first and third complexes of the respiratory chain, characteristic of FA.

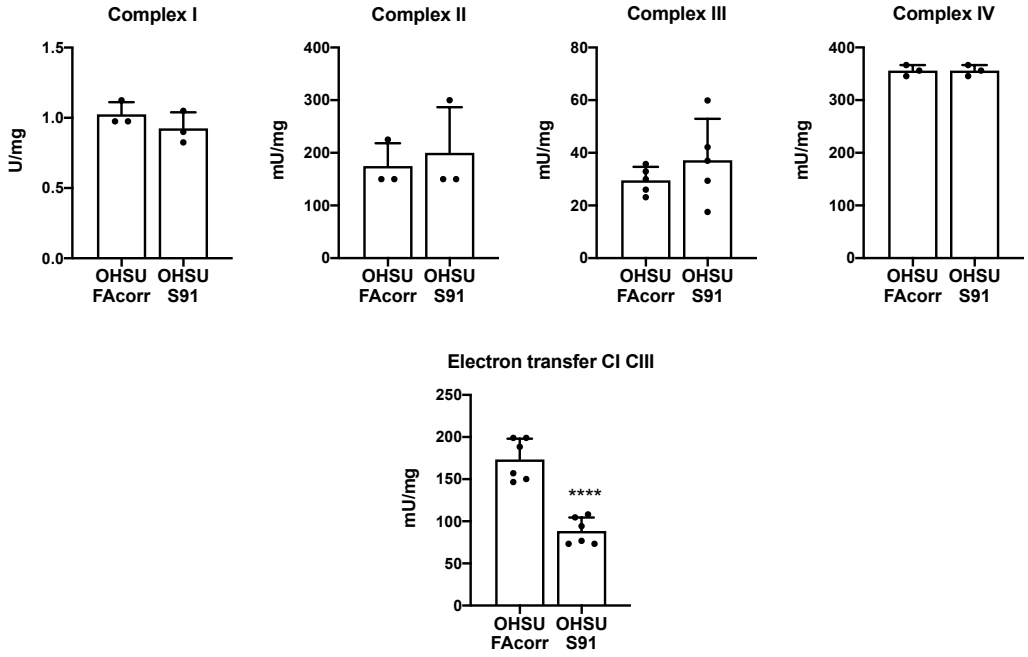


Figure 62 Mitochondrial respiratory complexes activity and electron transport between complexes I and III of HNSSC cell lines mutated (OHSU S91) or not (OHSU FAcorr) for the FANCA gene. Activity of Complex I, II, III, and IV; electron transfer between I and III complexes. All data are reported as mean ± SD, and each graph is representative of at least 3 independent experiments. Statistical significance was tested opportunely with an unpaired t-test; **** represents a significant difference for $p < 0.0001$ between FA and FAcorr HNSCC cells.

The results shown in Figure 62 demonstrate that, by quantifying the four respiratory complexes' activity, none show significant differences in activity between FANCA mutated cells and FAcorr cells (upper panels). However, a non-significant increase in the activity of complexes II and III can be observed, which is analogous to the increase in the activity of the pathway composed of complexes II, III, and IV observed for ATP synthesis and oxygen consumption and reported in Figure 61. As in the case of lymphoblasts and fibroblasts, the decrease in electron transport between the I and III complexes of the respiratory chain is significant, explaining the significant OxPhos reduction when cells are stimulated to use the pathway composed by complexes I, III, and IV.

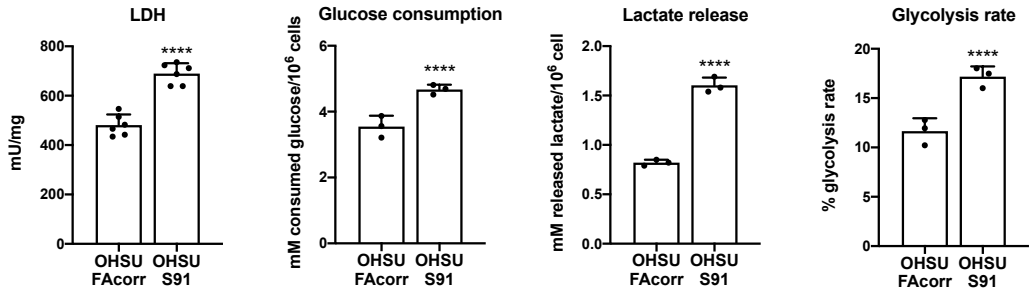


Figure 63 Lactic fermentation of HNSSC cell lines mutated (OHSU S91) or not (OHSU FAcorr) for the FANCA gene. Lactate dehydrogenase (LDH) activity. Glucose consumption. Lactate release in the growth medium. Lactic

fermentation yield. All data are reported as mean ± SD, and each graph is representative of at least 3 independent experiments. Statistical significance was tested opportunely with an unpaired t-test; **** represents a significant difference for $p < 0.0001$ between FA and FAcorr HNSCC cells.

In Figure 63, we can observe a significant increase in LDH activity in OHSU S91 compared to OHSU FAcorr. Lactate dehydrogenase is the enzyme that converts pyruvate derived from glycolysis into lactic acid in the absence of oxygen. Similarly, glucose consumption, lactate release, and lactic fermentation yield are significantly increased in OHSU S91 compared to their control counterparts. All these data suggest, as already demonstrated for fibroblasts and lymphoblasts, that the FANCA mutation leads to a metabolic shift towards lactic fermentation and anaerobic metabolism due to impaired oxidative phosphorylation.

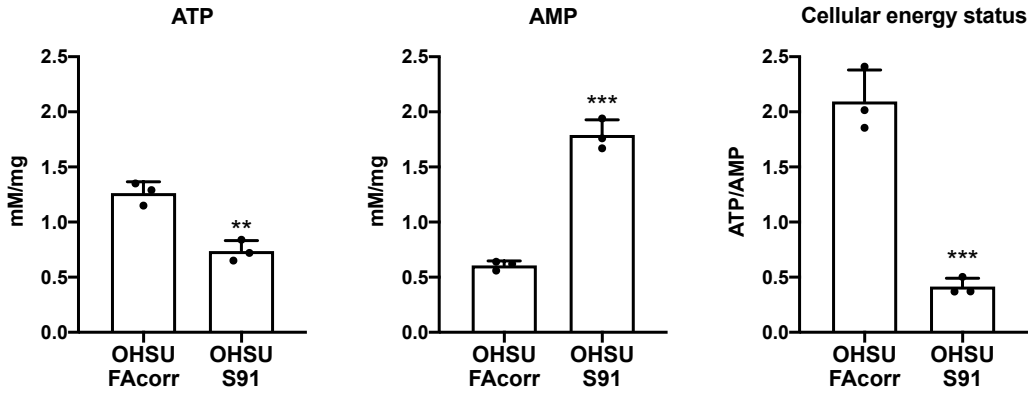


Figure 64 ATP and AMP intracellular concentrations and cellular energy status in HNSSC cell lines mutated (OHSU S91) or not (OHSU FAcorr) for the FANCA gene. Intracellular ATP content. Intracellular AMP content. ATP/AMP ratio as a marker of cellular energy status. Data are reported as mean ± SD, and each graph is representative of at least 3 independent experiments. Statistical significance was tested with an unpaired t-test. ** or *** represent respectively $p < 0.01$ or 0.001 between FA and FAcorr HNSCC cells.

However, due to the lower efficiency of energy production in anaerobic metabolism, this attempt to compensate for ATP production is insufficient. As shown in the data presented in Figure 64, the OHSU S91 cells, compared to the FAcorr control cell line, exhibit a significant reduction in intracellular ATP content and an even more pronounced increase in AMP content. This results in an altered and significantly reduced cellular energy state for the cells with the FANCA mutation. Consequently, these cells lack the necessary biochemical energy to respond to environmental changes or even perform essential functions.

Considering that tumor cells often undergo changes in their metabolism, as other than supporting energy production, they utilize a significant number of metabolic intermediates as building blocks to sustain enhanced proliferation, I assessed the OHSU cell lines' energy substrate affinity to understand whether the FANCA gene mutation could further impact the metabolism of these cell lines. To achieve this, I re-evaluated OCR and ATP synthesis in the presence of BPTES, Etomoxir, and UK5099 to inhibit, respectively, the utilization of glutamine, fatty acids, and pyruvate, as also shown in the left panel of Figure 65.

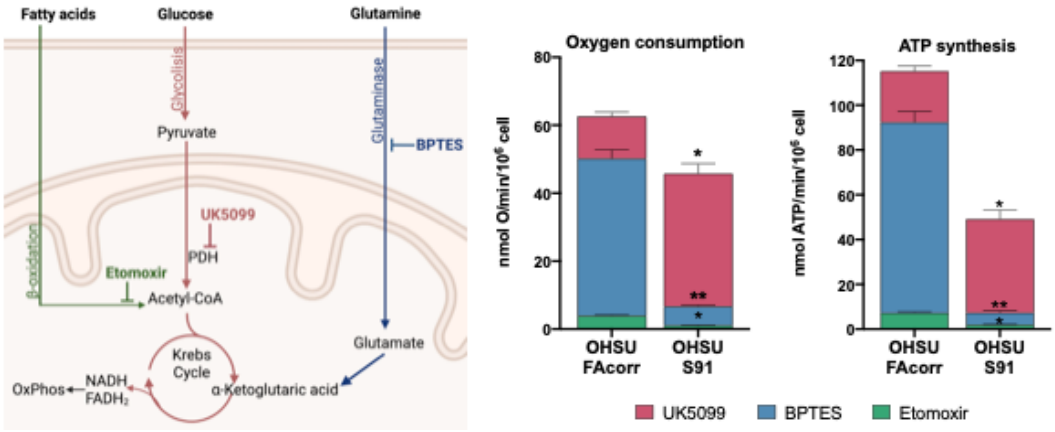


Figure 65 Respiratory substrates affinity in HNSSC cell lines mutated (OHSU S91) or not (OHSU FAcorr) for the FANCA gene. On the left is a graphic schematic representation of the targets of the inhibitors used to assess the respiratory substrate's affinity for mitochondrial metabolism (BPTES is a glutaminase inhibitor, etomoxir prevents the transport of fatty acids to the mitochondrion, inhibiting β-oxidation, and UK5099 is a Pyruvate Dehydrogenase (PDH) inhibitor). On the right, the OCR and ATP synthesis through FoF1 ATP-synthase considering their affinity for glucose (inhibited by UK5099, Bordeaux), glutamine (inhibited by BPTES, Blue), and fatty acids (inhibited by Etomoxir, green). Data are reported as mean ± SD, and each graph is representative of at least 3 independent experiments. Statistical significance was tested with two-way ANOVA. * and ** represent a $p < 0.05$ and 0.01, respectively, between OHSU S91 cells and OHSU FAcorr cells used as control.

The data from Figure 65 corroborate those from Figure 61, demonstrating that OHSU S91 cells exhibit lower oxidative phosphorylation activity (OCR and ATP synthesis) compared to the OHSU FAcorr cells used as controls. Additionally, notable differences between the two cell lines are observed in their utilization of respiratory substrates. In OHSU FAcorr cells, both OCR and ATP synthesis are primarily supported by glutamine, followed by glucose, with a minor contribution from fatty acids. On the other hand, in OHSU S91 cells, a significant portion of energy production relies on glucose, and there's a significant reduction in the utilization of both glutamine and fatty acids as respiratory substrates.

### 5.12.2 Mitochondrial dynamics

I wanted to verify the expression of the respiratory chain subunits previously analyzed in lymphoblasts and fibroblasts in section 3.5. This was done through Western blotting to determine if the issues with oxidative phosphorylation could be attributed to any differential expression of these subunits, specifically ND1 (Complex I), SDHB (Complex II), MTCO2 (Complex III), and ATP synthase β subunit.

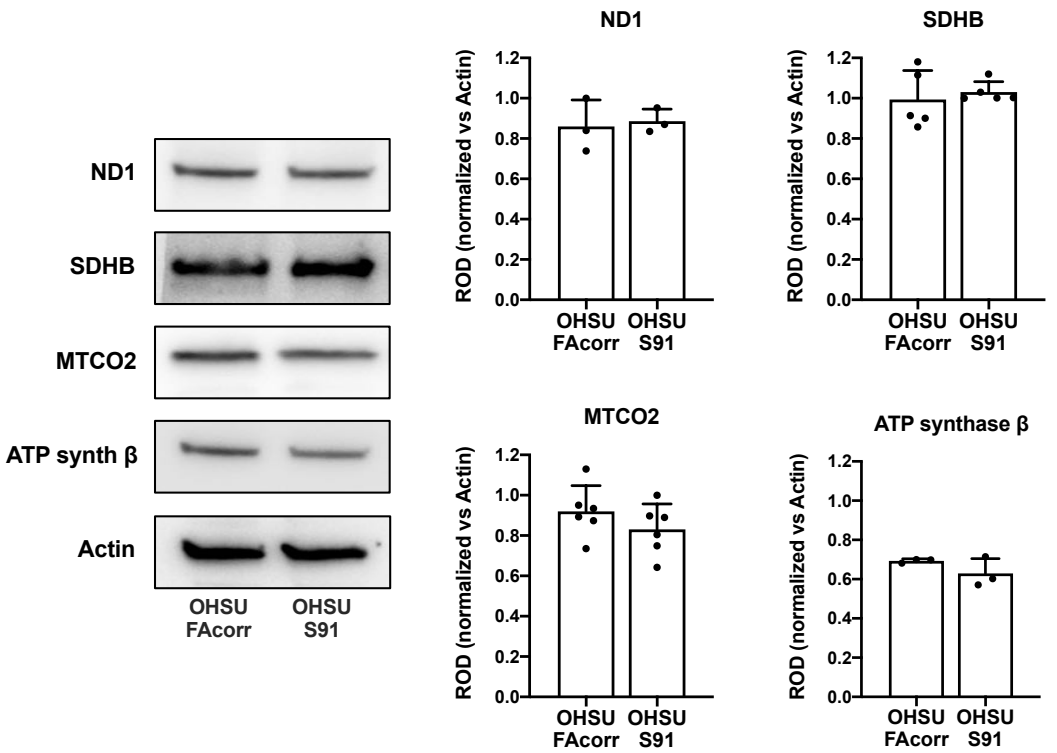


Figure 66 OxPhos proteins subunit expression in OHSU FAcorr and OHSU S91 cell lines. WB signals of OxPhos subunits (namely ND1 (Complex I), SDHB (Complex II), MTCO2 (Complex IV), and β-subunit of ATP synthase), and β-Actin, used as the housekeeping protein. Each signal is representative of at least 3 independent experiments. On the right, the densitometric analysis of WB signals normalized versus the housekeeping signal revealed on the same membrane. Data are reported as mean ± SD of Relative Optical Density (ROD), and each graph is representative of at least 3 independent experiments. Statistical significance was tested opportunely with the unpaired t-test, and no significant differences were observed between OHSU S91 cells and the OHSU FAcorr cell lines.

The data presented in Figure 66 demonstrate that, like in lymphoblasts and fibroblasts, there are no significant differences in the expression levels of the analyzed respiratory complex subunits between OHSU cell lines with and without the FANCA mutation. I then proceeded with my analyses by examining markers of mitochondrial biogenesis and dynamics, specifically CLUH (mitochondrial biogenesis), DRP1 (mitochondrial fission), OPA1, and MFN2 (mitochondrial fusion).

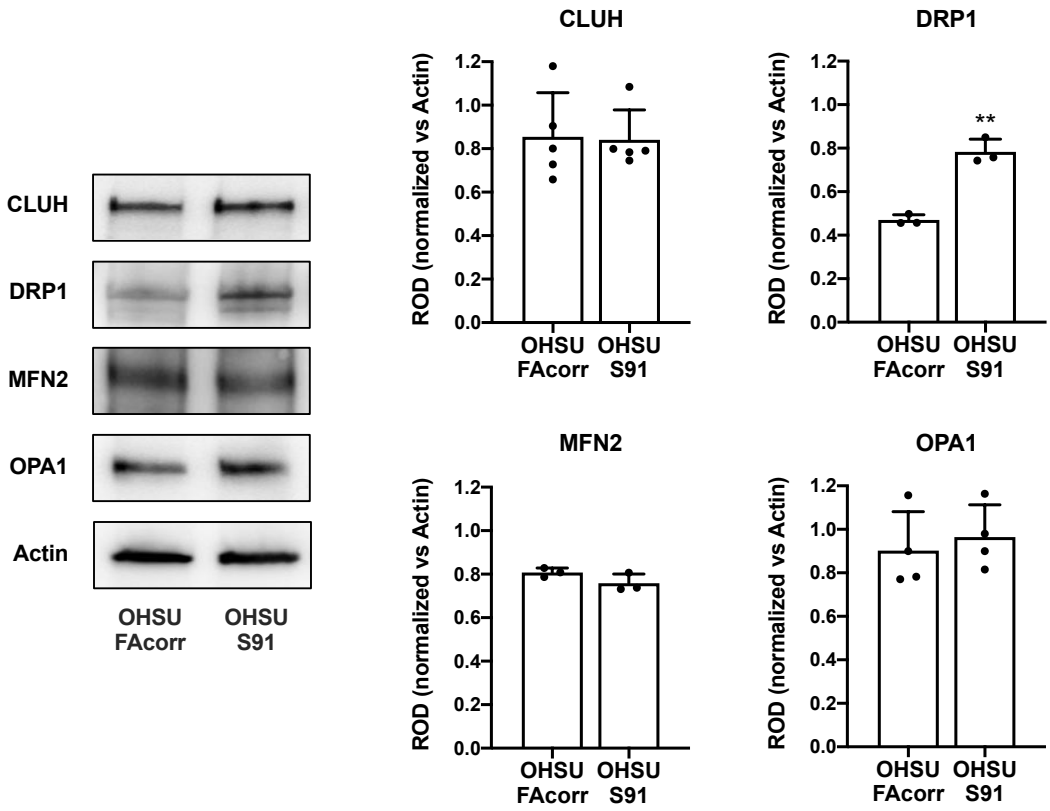


Figure 67 Mitochondrial dynamic proteins expression in OHSU FAcorr and OHSU S91. WB signals of CLUH (mitochondria dynamic regulator), DRP1 (mitochondrial fission marker), MFN2, OPA1 (mitochondrial fusion markers), and β-Actin (housekeeping protein). Each WB signal is representative of at least 3 independent experiments. On the right, the densitometric analysis of the WB signals normalized versus the housekeeping protein revealed on the same membrane. Data are reported as mean ± SD of ROD, and each graph is representative of at least 3 independent experiments. Statistical significance was tested with an unpaired t-test. ** represents a $p < 0.01$ between the OHSU S91 cells and the OHSU FAcorr cells used as control.

The data (Figure 67) show that there are no significant differences when comparing the expression levels of biogenesis markers (CLUH) and mitochondrial fusion markers (MFN2 and OPA1) between FANCA mutated and corrected OHSU. However, the expression levels of DRP1, a marker of mitochondrial fission, are significantly increased in OHSU S91 compared to OHSU FAcorr, highlighting how the FANCA mutation leads to an imbalance in mitochondrial dynamics towards fission and, consequently, to the disruption of the mitochondrial network.

To investigate potential differences in the expression levels of proteins involved in autophagy and mitophagy processes between OHSU FAcorr and OHSU S91, I analyzed in WB the expression levels of Beclin1, Atg7, Atg12, Atg16L1, and LC3 (autophagy) as well as Pink1 and Parkin (mitophagy).

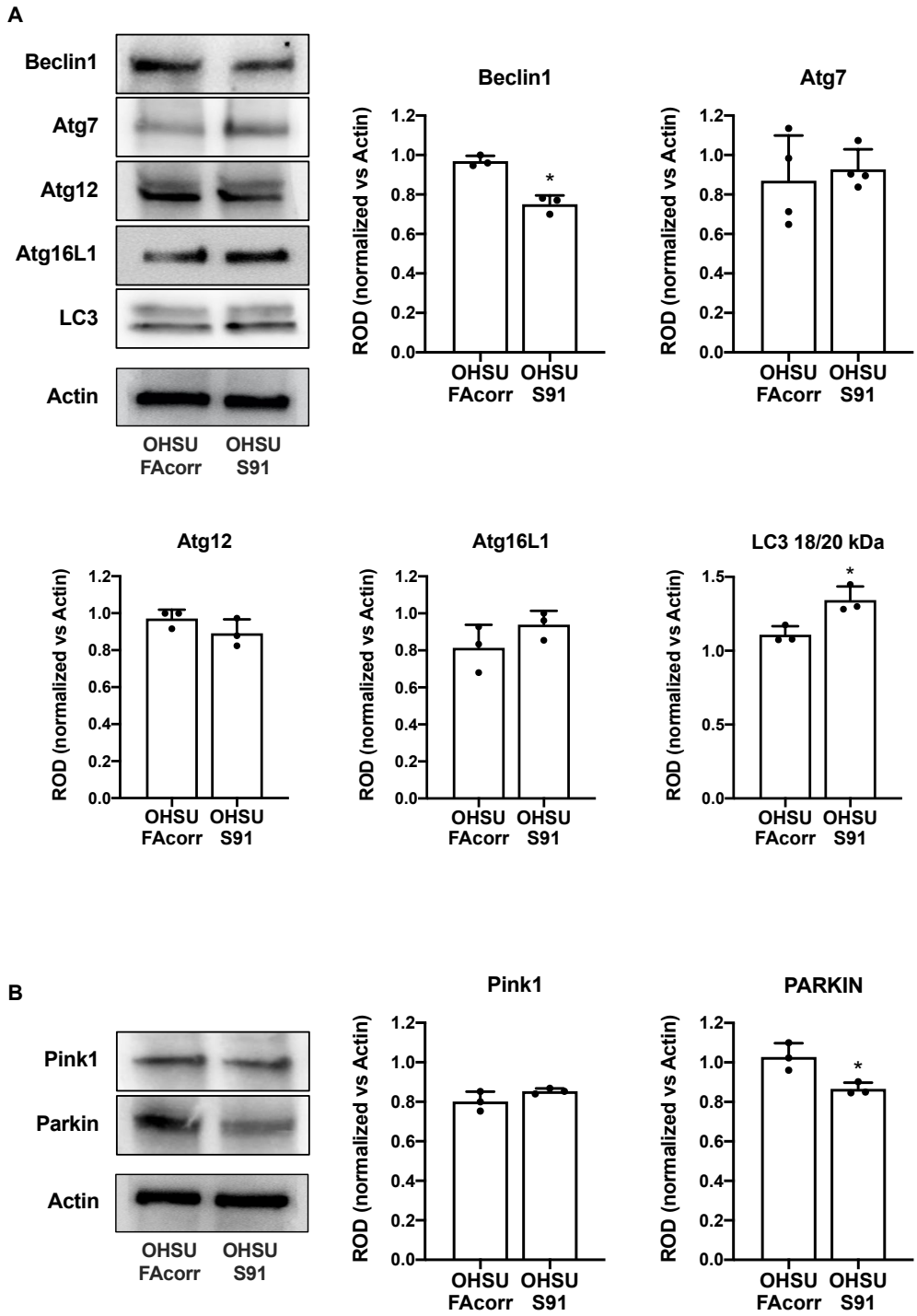


Figure 68 Autophagy and mitophagy proteins expression in OHSU FAcorr and OHSU S91. WB signals of Beclin1, Atg7, Atg12, Atg16L1, LC3 (autophagy markers), Pink1 and Parkin (mitophagy markers), and β-Actin (housekeeping). On the right, densitometric analysis of WB signals normalized versus β-Actin revealed on the same membrane. Data are reported as mean ± SD and are representative of at least 3 independent experiments. Statistical significance was tested with an unpaired t-test. * represents a $p < 0.05$ between OHSU S91 cells and the OHSU FAcorr cells used as control.

Concerning autophagy (as shown in Figure 68A), the data show a significant reduction in the expression levels of Beclin1, which is an initiator protein involved in the autophagy process, comparing the OHSU S91 with the OHSU FAcorr cell lines. Additionally, the

OHSU S91 cell line, when compared with its corrected counterpart, displays a significant increase in the ratio between the cleaved (active) and the un-cleaved (inactive) form of LC3, an effector protein commonly associated with both autophagy and mitophagy pathways. Conversely, there were no notable differences between the two cell lines in relation to any of the three Atg family effector proteins analyzed (Atg7, 12, 16L1). Considering the markers related explicitly to the process of mitophagy (Figure 68B), there are no significant differences between the two lines regarding Pink1 expression levels, the protein targeting damaged mitochondria. However, there is a significant reduction in Parkin expression in the line with the FANCA mutation compared to its corrected counterpart. These findings could suggest that the genetic mutation enables the recognition of damaged mitochondria but not their proper removal from the cell.

### 5.12.3 Antioxidant defense and oxidative damage

FA cells are characterized by high oxidative stress production and subsequent oxidative damage, as demonstrated in section 3.1. Therefore, in this thesis section, I tested whether HNSCC cells with FANCA mutation also exhibited such damages by measuring malondialdehyde (MDA), a lipid peroxidation marker, in my cellular lines.

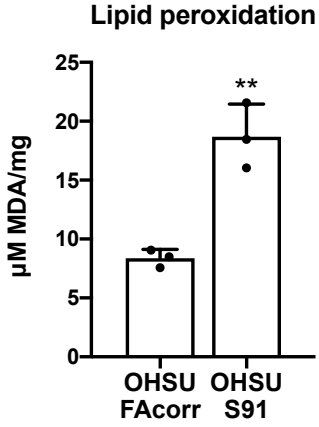


Figure 69 Lipid peroxidation in OHSU FAcorr and OHSU S91 cell lines. Malondialdehyde (MDA) level as a marker of lipid peroxidation. Data are reported as mean ± SD, and the graph is representative of at least 3 independent experiments. Statistical significance was tested with an unpaired t-test. ** represents a $p < 0.01$ between OHSU S91 and OHSU FAcorr cell lines used as control.

Data show (Figure 69) that the OHSU S91 cell line, when compared to the OHSU FAcorr cell line used as a control, exhibits a 2.5-fold increase in MDA levels.

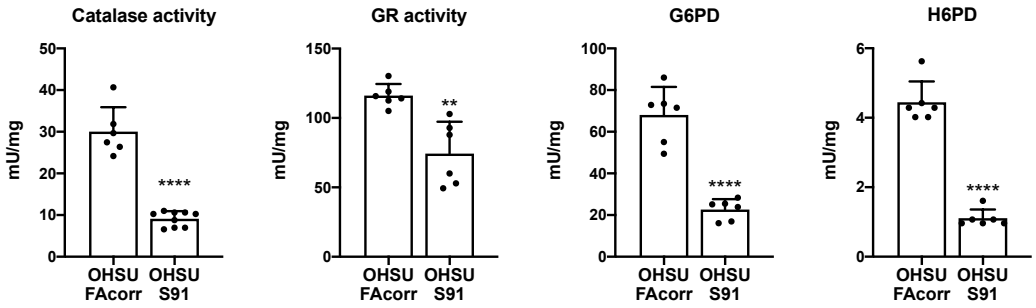


Figure 70 Enzymatic antioxidant defense activities in OHSU FAcorr and OHSU S91 cell lines. Catalase activity. Glutathione reductase (GR) activity. Glucose-6-phosphate dehydrogenase (G6PD) activity. Hexose-6-phosphate dehydrogenase (H6PD) activity. Data are reported as mean ± SD, and each graph is representative of at least 3 independent experiments. Statistical significance was tested with an unpaired t-test. **, and **** represent respectively a $p < 0.01$ and 0.0001 between OHSU S91 cells and the OHSU FAcorr cells used as control.

However, testing the activity levels of antioxidant enzymes, the results (Figure 70) demonstrate a significant reduction in activity (approximately 60%) for catalase, G6PD, and H6PD and a 40% reduction for glutathione reductase (GR) activity in the mutated cells compared to the correct cells.

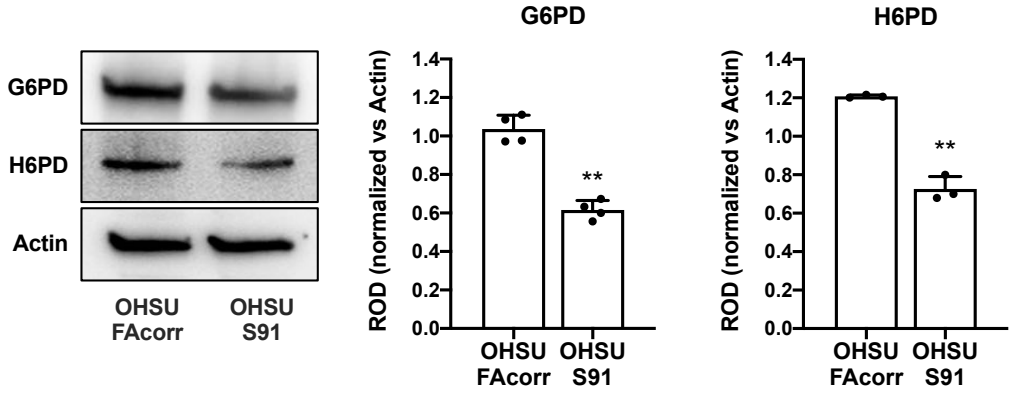


Figure 71 Expression levels of G6PD and H6PD. Glucose-6-phosphate-dehydrogenase, hexose-6-phosphate dehydrogenase, and β-actin WB signals. On the right, the densitometric analysis normalized versus β-Actin revealed on the same membrane. Data are reported as mean ± SD, and each signal and graph are representative of at least 3 independent experiments. Statistical significance was tested with an unpaired t-test. ** represent a $p < 0.01$ between OHSU S91 cells and OHSU FAcorr used as control.

A Western blot analysis has also revealed that the decrease in G6PD and H6PD activity is correlated with a reduced expression of these proteins in the FANCA cells compared to the control (Figure 71). Overall, the data presented in this section demonstrate that, despite the increased lipid peroxidation damage in FANCA-mutated cells, they are still unable to express or activate antioxidant pathways more effectively to counteract this oxidative stress, which consequently leads to the accumulation of damage within the cell.

### 5.12.4 Cell morphology and proliferation and DNA damage

To determine whether the FANCA gene mutation could affect the morphology and growth rate of HNSCC cells, I assessed these parameters in my cellular models.

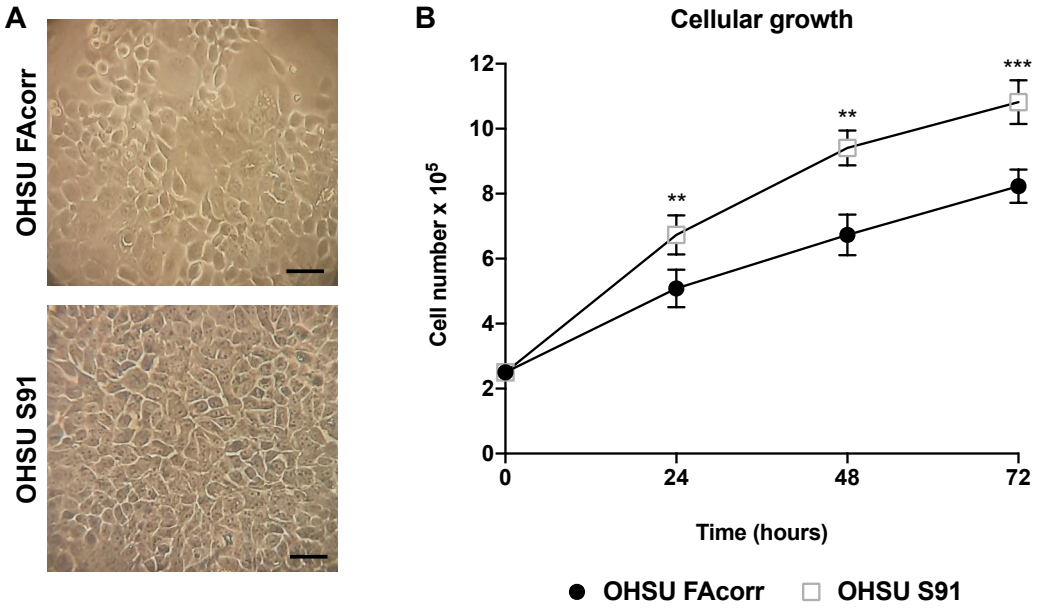


Figure 72 Morphology and growth curve of OHSU FAcorr and OHSU S91. On the left is an example of OHSU FAcorr and OHSU S91 morphology, as observed at the transmitted light microscope. The scale bar corresponds to 50 µm. Each panel is representative of at least five fields of three independent experiments. On the right, the growth curves of OHSU FAcorr and OHSU S91 cell lines, monitored for 72 h, every 24 h. Data are reported as mean ± SD, and the graph is representative of at least 3 independent experiments. Statistical significance was tested with a two-way ANOVA test. ** or *** represent respectively a $p < 0.01$ and 0.001, between OHSU S91 and OHSU FAcorr cell used as control.

Figure 72A displays optical microscope images of the two cell lines (OHSU FAcorr in the upper panel and OHSU S91 in the lower panel), which do not show any significant macroscopic morphological differences. However, the growth rate, monitored over 72 hours post-plating (as shown in Figure 72B), is significantly higher in the OHSU S91 line than the OHSU FAcorr line, even as early as the 24-hour mark. This finding is consistent with extensive clinical data reported in the literature regarding the heightened aggressiveness of HNSCC in FA patients. Finally, I aimed to ascertain whether the FANCA mutation led to double-strand DNA damage accumulation in HNSCC cell lines. To achieve this, I examined the expression of phosphorylated-γ-H2AX (p-γ-H2AX) in the presence or absence of hydroxyurea, a molecule that promotes DNA damage.

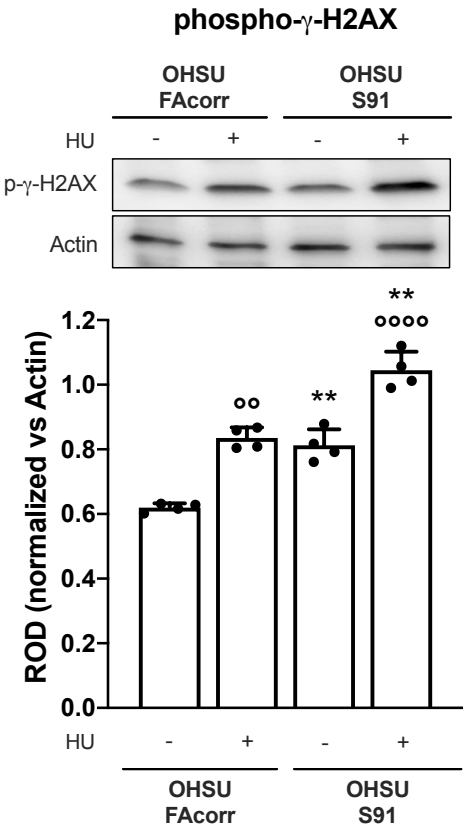


Figure 73 Evaluation of DNA double-breaks in the absence or presence of hydroxyurea in OHSU FAcorr and OHSU S91 cell lines. WB signal of phosphorylated-γ-H2AX (H2AX), a marker of DNA damage accumulation, with or without hydroxyurea (HU) (upper panel), and the relative densitometric analysis normalized versus β-Actin used as housekeeping (lower panel). Data are reported as mean ± SD, and each graph is representative of at least 3 independent experiments. Statistical significance was tested with a two-way ANOVA test. ** represents a $p < 0.01$ between OHSU S91 and OHSU FAcorr cells used as control; °° or °°°° represent a $p < 0.01$ or 0.0001 between HU-treated and untreated cells.

Figure 73 illustrates how the OHSU S91 cell line already exhibits a significantly higher expression of p-γ-H2AX, indicating DNA damage, compared to the control OHSU FAcorr line even before treatment with HU (I vs. III column in the histogram). Following HU treatment, the level of DNA damage in OHSU FAcorr cells becomes comparable to that of FANCA-mutated cells before treatment, after which OHSU S91 displays the highest level of DNA damage, significantly increased compared to all other conditions.

All the data presented in section 3.12 were published in N. Bertola *et al.*, "Mutated FANCA Gene Role in the Modulation of Energy Metabolism and Mitochondrial Dynamics in Head and Neck Squamous Cell Carcinoma" *Cells*, vol. 11, no. 15, 2022, DOI: 10.3390/cells11152353.

## 5.13 Comparing Metabolic Defects in Fanconi Anemia and Shwachman-Diamond Syndrome

FA and Shwachman-Diamond Syndrome (SDS) are two rare genetic disorders that, despite their distinct characteristics, exhibit striking similarities in their effects on hematopoiesis and overall health. Both conditions can lead to bone marrow dysfunction, resulting in various hematologic complications. These disorders' common thread is their ability to disrupt physiological blood cell production. Consequently, patients with FA or SDS require treatments such as hematopoietic stem cell transplantation to address these hematologic issues. While FA and SDS differ in their genetic origins (FANC genes in FA and SBDS gene in SDS) and clinical presentations, they serve as important reminders of the intricate interplay between genetics and hematopoiesis [126]. Recognizing these similarities can facilitate early diagnosis and the development of targeted therapies for affected individuals. Furthermore, it has been demonstrated that patients with SDS exhibit a defect in mitochondrial metabolism [127]. To this end, I conducted metabolic analyses on primary cells from SDS patients, aiming to unravel the shared pathophysiology and potentially identify common therapeutic strategies with FA. As illustrated in this paragraph, the preliminary results reveal a significant deficit in metabolic parameters in primary cells from SDS patients, mirroring what was observed in FA cells. The analyses primarily focus on comparing primary cells from SDS patients with those from healthy donors, both before and after treatment with two antioxidant molecules: DMSO, which, according to literature, acts as a scavenger molecule at low concentrations, and N-acetylcysteine (NAC), one of the most potent known antioxidants. This comparative investigation aims to shed light on the impact of these antioxidants on the metabolic profiles of primary cells from SDS patients, potentially uncovering therapeutic avenues for this rare condition. Moreover, this comparative approach holds promise for advancing research and the development of targeted therapies for these rare diseases, ultimately enhancing the quality of life for affected patients. Understanding the similarities between FA and SDS represents a crucial step in combating these complex genetic disorders. The data presented in this section were obtained through the collaboration of Dr. D'Amico and Dr. Gervasoni from the Tettamanti Centre, Fondazione IRCCS San Gerardo dei Tintori in Monza, who kindly provided us with the samples.

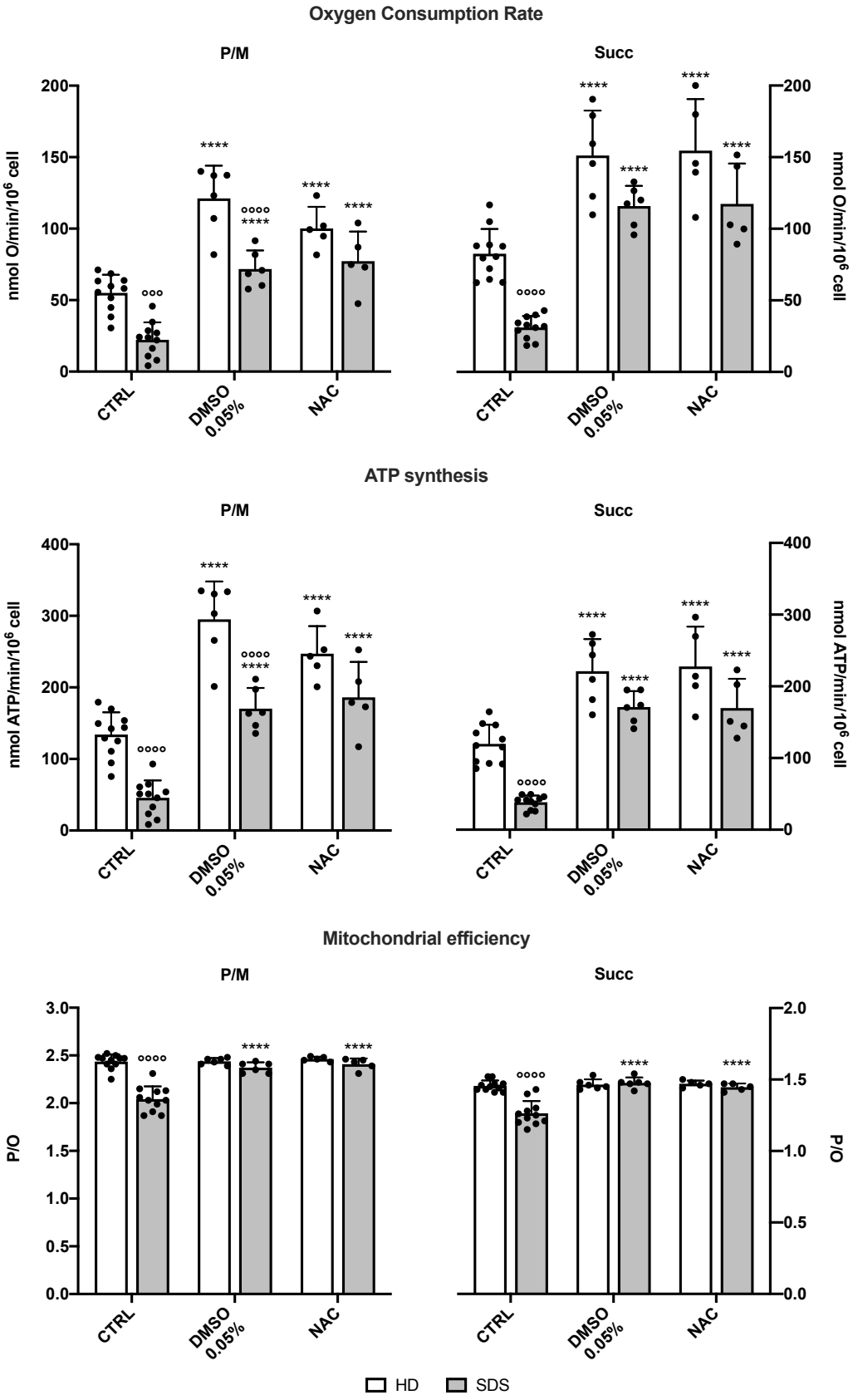


Figure 74 Effects of DMSO and NAC on mitochondrial metabolism of SDS patients and healthy donors. DMSO 0.05% and NAC effects on (A) oxygen consumption rate (OCR), (B) ATP synthesis through FoF1 ATP synthase, and (C) P/O ratio as a marker of mitochondrial efficiency on SDS patients (grey columns) and healthy donors

(HD, white columns). All the experiments represented on the left panels were performed with the addition of pyruvate plus malate (P/M), while all the experiments represented on the right panels with the addition of succinate (Succ) as respiratory substrate to stimulate respectively the pathway composed of respiratory complexes I, III, and IV or II, III, and IV. Data are reported as mean ± SD, and each graph is representative of at least three independent experiments. Statistical significance was tested with a one-way ANOVA test; **** represents a $p < 0.0001$ between treated and untreated cells in the same clinical conditions; °°° and °°°° represent a $p < 0.001$ or 0.0001 between HD and SDS patients undergone the same treatment.

In Figure 74, we can observe that the OCR and ATP synthesis values are significantly lower in untreated SDS cells than untreated HD cells, whether using pyruvate plus malate (P/M) or succinate (Succ) as respiratory substrates. This translates into a low P/O ratio for the patient-derived cells, indicating mitochondrial metabolism inefficiency for both substrates used. Both DMSO and NAC treatments significantly improve both OCR and ATP synthesis for both SDS- and HD-derived cells, with no significant differences between the two treatments. This increase does not impact the mitochondrial efficiency of the HD-derived cells but restores the P/O ratio for SDS patients, whether using P/M or Succ. The substantial difference between SDS and FA cells appears to be the affected metabolic pathway. In FA, decreased values for OCR and ATP synthesis, associated with the uncoupling of the respiratory chain from ATP synthase (altered P/O ratio), were evident only after the use of P/M, thus following the activation of the pathway composed of respiratory complexes I, III, and IV. There is an additional metabolic defect in SDS cells due to the pathway of respiratory complexes II, III, and IV, which Succ stimulates. These data suggest that the metabolic defect cannot be limited to the electron transport between complexes I and III like in FA but has to be located at a point common to both electron transport pathways, causing uncoupling with ATP synthase in both cases. For this reason, I tested the activity of all the complexes in the respiratory chain (data not shown), revealing a defect in complex IV activity (Figure 75). I also assessed the cellular energy state.

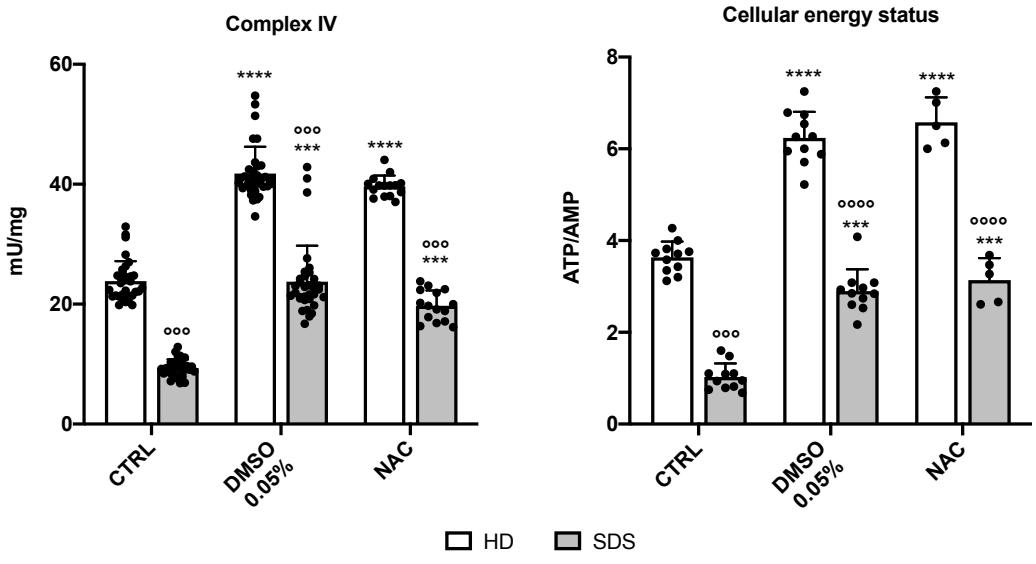


Figure 75 Effects of DMSO and NAC on respiratory complex IV and cellular energy status of SDS patients and healthy donors' primary cells. DMSO 0.05% and NAC effects on complex IV activity and ATP/AMP ratio as a

marker of cellular energy status on SDS patients (grey columns, n=11) and healthy donors (HD, white columns, n =11) primary cells. Data are reported as mean ± SD, and each graph is representative of at least three independent experiments. Statistical significance was tested with a one-way ANOVA test. *** and **** represent a p < 0.001 or 0.0001 between treated and untreated cells in the same clinical conditions; °°° and °°°° represent a p < 0.001 or 0.0001 between HD and SDS patients undergone the same treatment.

The data in Figure 75 demonstrate a significant reduction in complex IV activity and the cellular energy state in cells derived from SDS patients compared to the HD-derived. Treatments with antioxidants, as for the oxidative phosphorylation itself, do not show significant differences between the two treatments, but both molecules significantly improve both the activity of complex IV and the cellular energy state for both SDS- and HD-derived cells. I then measured the levels of lipid peroxidation damage, oxidative stress, and the activity of some of the main cellular antioxidant enzymes.

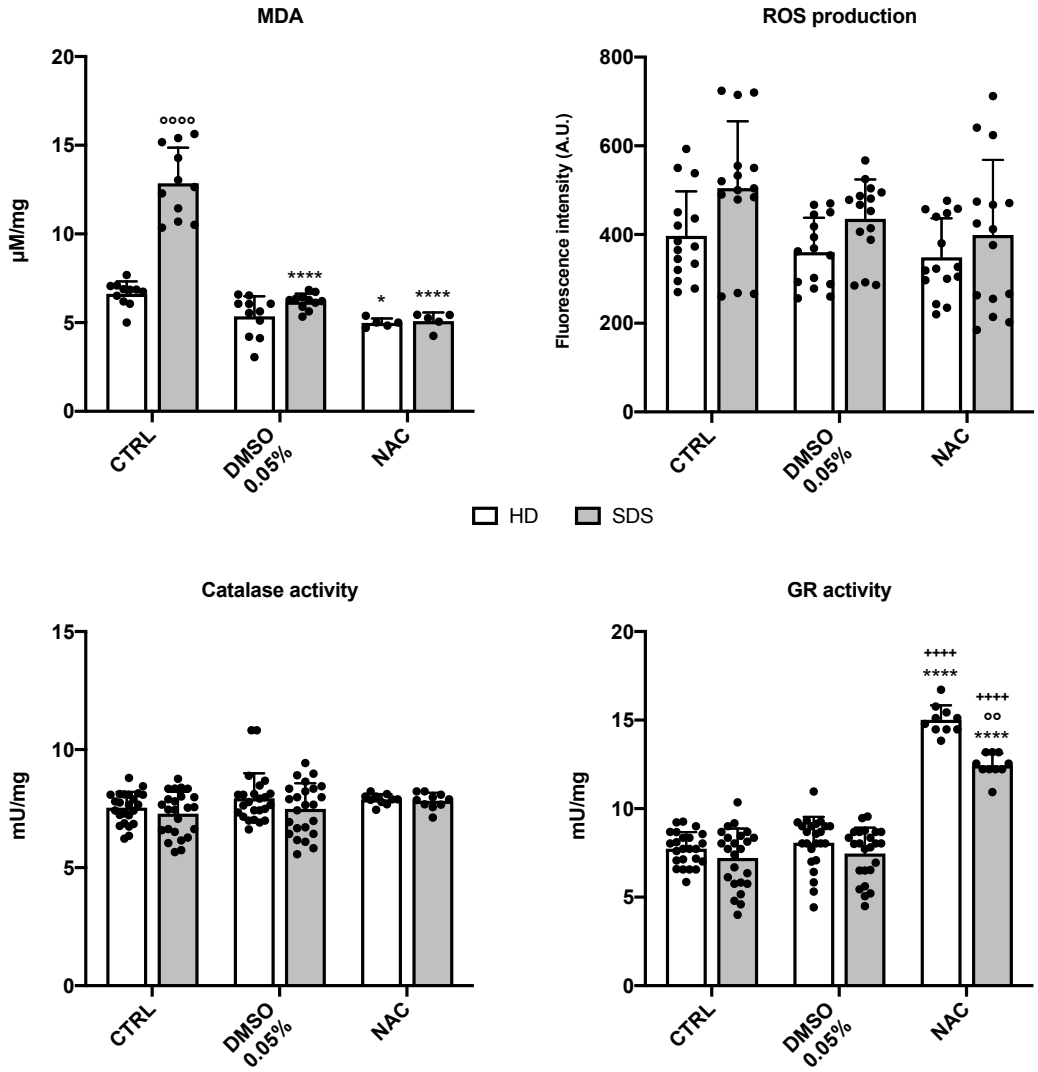


Figure 76 Effects of DMSO and NAC on oxidative stress and antioxidant activity of SDS patients and healthy donors' primary cells. DMSO 0.05% and NAC effects on malondialdehyde (MDA) as a marker of lipid peroxidation damage, reactive oxygen species (ROS) production as markers of oxidative stress; catalase and glutathione reductase activity as markers of antioxidant defenses on SDS patients (grey columns, n=11) and healthy donors (HD, white columns, n=11) primary cells. Data are reported as mean ± SD, and each graph is representative of

at least three independent experiments. Statistical significance was tested with a one-way ANOVA test; * and **** represent a $p < 0.05$ or 0.0001 between treated and untreated cells in the same clinical conditions; °° and °°°° represent a $p < 0.01$ or 0.0001 between HD and SDS patients undergone the same treatment; ++++ represents a $p<0.0001$ between DMSO and NAC treatments.

The data presented in Figure 76 show how the levels of malondialdehyde (MDA), used as a marker for lipid peroxidation damage, are significantly higher in SDS than in HD-derived cells. However, both treatments can prevent this damage, bringing MDA levels back to those of HD-derived cells without significantly affecting HD-derived cells. Although there is a trend of increased ROS production in SDS- compared to HD-derived cells, there are no significant differences. Similarly, the treatments do not have a significant impact on this parameter. As for the antioxidant defenses, catalase enzymatic activity does not appear to differ between the two cell types and does not show significant differences after either of the treatments. This is also true for glutathione reductase (GR) enzymatic activity, which, however, is significantly increased in both cell types following treatment with NAC. The last metabolic parameters I wanted to assess are related to anaerobic metabolism. In particular, I evaluated glucose consumption, lactate release into the culture medium, LDH enzymatic activity, and lactate fermentation yield.

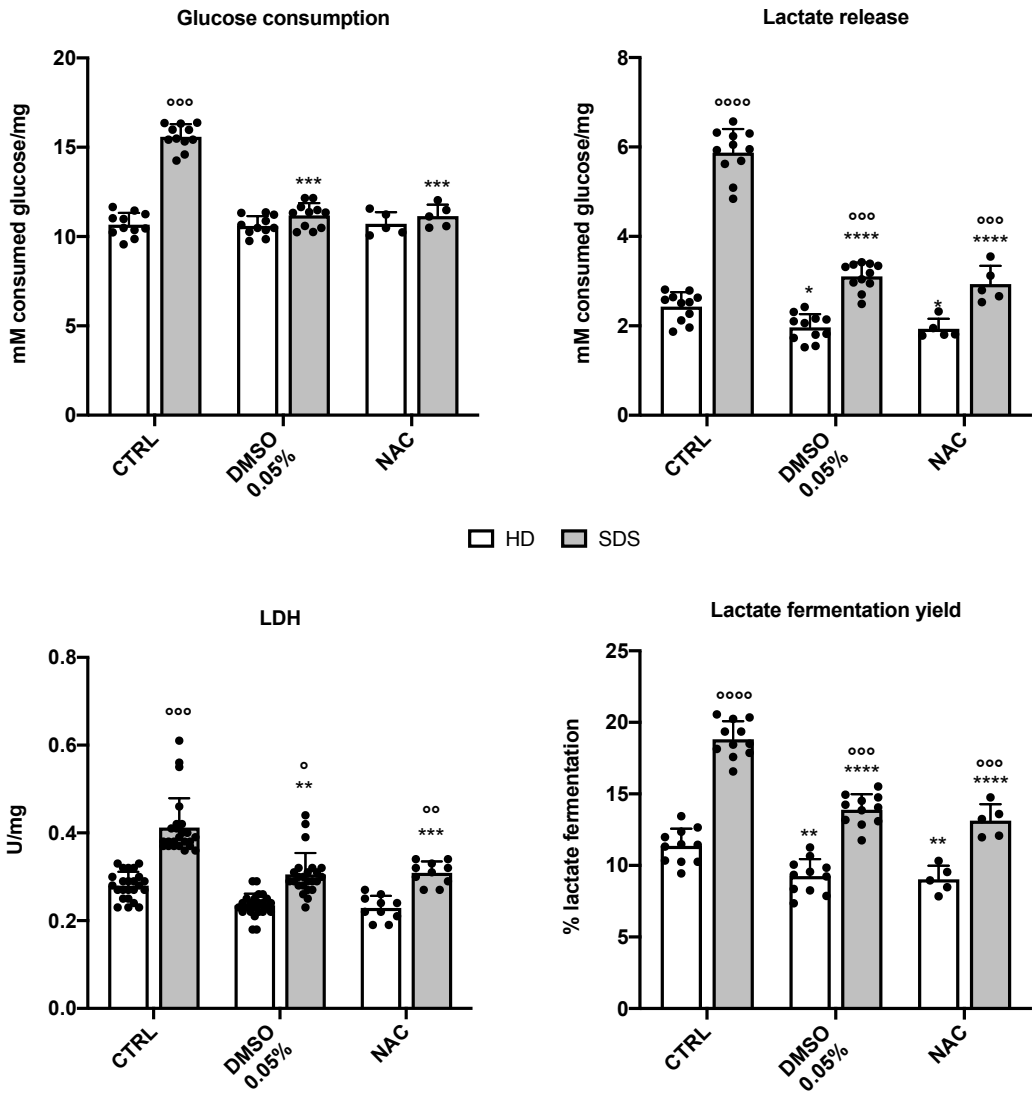


Figure 77 Effects of DMSO and NAC on the anaerobic metabolism of SDS patients and healthy donors' primary cells. DMSO 0.05% and NAC effects on glucose consumption, lactate release, LDH activity, and lactate fermentation yield as markers of anaerobic metabolism on SDS patients (grey columns, n=11) and healthy donors (HD, white columns, n=11) primary cells. Data are reported as mean ± SD, and each graph is representative of at least three independent experiments. Statistical significance was tested with a one-way ANOVA test; *, **, ***, and **** represent a $p < 0.05$, 0.01, 0.001, or 0.0001 between treated and untreated cells in the same clinical conditions; °, °°, °°° and °°°° represent a $p < 0.05$, 0.01, 0.001 or 0.0001 between HD and SDS patients undergone the same treatment.

The data shown in Figure 77 indicate that all parameters considered as markers of anaerobic metabolism are significantly higher in SDS- compared to the HD-derived cells. Both treatments equally reduce all parameters in SDS-derived cells without significantly affecting HD cells. I then conducted several experiments to assess the effect of DMSO and NAC on intracellular damage, particularly concerning lipid peroxidation, DNA oxidation, and protein oxidation.

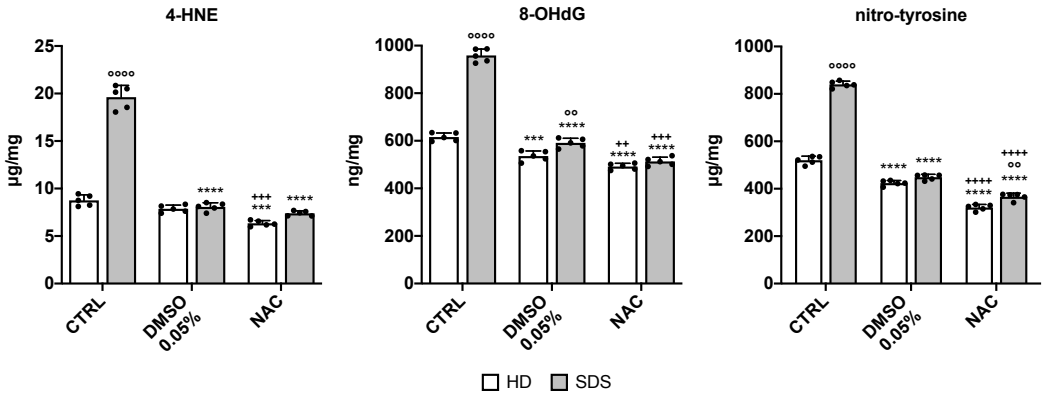


Figure 78 Effects of DMSO and NAC on intracellular damage of SDS patients and healthy donors' primary cells. DMSO 0.05% and NAC effects on 4-HNE (4-hydroxynonenal) as a marker of lipid peroxidation, 8-OHdG (8-hydroxy-2′-deoxyguanosine) as a marker of DNA oxidation, and 3-nitro-tyrosine as a marker of protein damage in SDS patients (grey columns, n=5) and healthy donors (HD, white columns, n=5) primary cells. Data are reported as mean ± SD, and each graph is representative of at least three independent experiments. Statistical significance was tested with a one-way ANOVA test; *** and **** represent a $p < 0.001$ or 0.0001 between treated and untreated cells in the same clinical conditions; °° and °°°° represent a $p < 0.01$ or 0.0001 between HD and SDS patients undergone the same treatment; ++, +++, and ++++ represent a $p < 0.01$, 0.001, or 0.0001 between DMSO and NAC treatments.

In Figure 78, the results of the experiments evaluating 4-HNE as a marker for lipid peroxidation, 8-OHdG as a marker of DNA oxidation, and nitro-tyrosine as a marker of protein damage are displayed. The results indicate that all the considered markers of oxidative damage are significantly higher in cells derived from SDS compared to cells derived from HD. SDS-cell treatments with antioxidants restore all markers to a similar level as cells from HD, which remain unaffected by the treatments.

In summary, all the data presented in this section so far demonstrate that cells derived from SDS patients have a metabolic defect similar to that in FA. However, in SDS, this defect is caused by a deficiency in complex IV of the mitochondrial respiratory chain, affecting both electron transport pathways. Both diseases share metabolic similarities, such as the uncoupling of the respiratory chain from ATP synthase, resulting in decreased cellular energy status and a metabolic shift towards anaerobic metabolism. Both diseases also share the accumulation of oxidative damage, and SDS showed a milder deficiency in antioxidant enzyme activity, involving only glutathione reductase but not catalase, compared to FA. These data also show no significant differences in the positive effect on metabolism produced by NAC or low doses of the scavenger DMSO.

To investigate whether the metabolic defect in cells derived from SDS patients could also be caused by issues in mitochondrial dynamics, in subsequent experiments, I examined the expression levels of some proteins involved in mitochondrial dynamics, using only the treatment with low doses of DMSO which has proven to be equally effective as the NAC treatment.

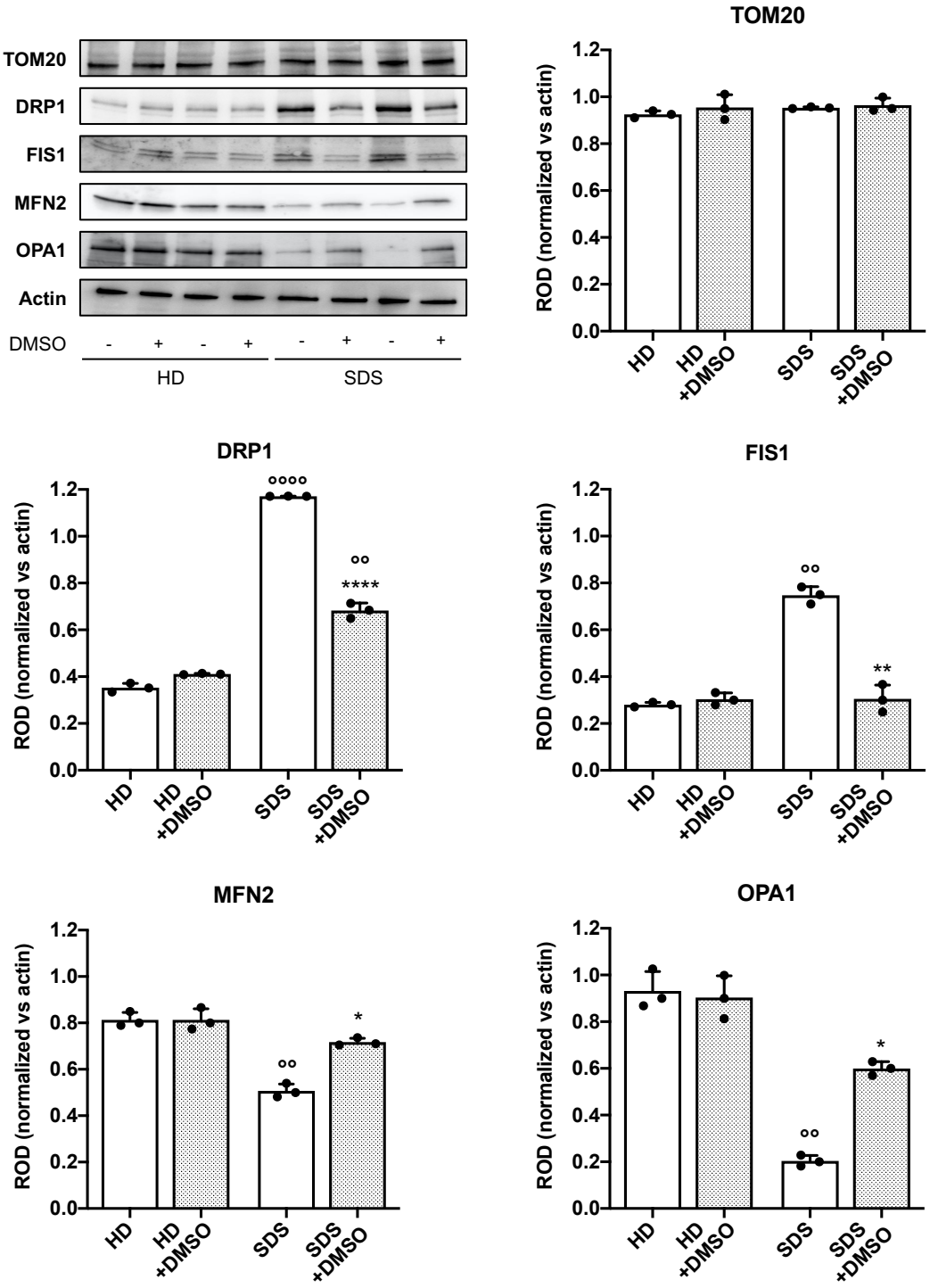


Figure 79 DMSO treatment effects on mitochondrial dynamic markers expression levels concentration of SDS patients and healthy donors' primary cells. WB signals of DPR1 and FIS1 as mitochondrial fission markers, TOM20 as a mitochondrial mass marker, MFN2 and OPA1 as mitochondrial fusion markers, and Actin as housekeeping protein in SDS patients (n=4) and healthy donors (HD=4) primary cells. Protein expression levels (densitometric analysis) were normalized on the Actin signal revealed on the same membrane. Data are reported as mean ± SD, and both WB signals and graphs are representative of at least 3 independent experiments. Statistical significance was tested with a one-way ANOVA test; *, **, or **** represent a significant difference for $p < 0.05$, 0.01, and 0.0001 between treated and untreated cells in the same clinical conditions; °° and °°°° represent a $p < 0.001$ or 0.0001 between HD and SDS patients undergone the same treatment.

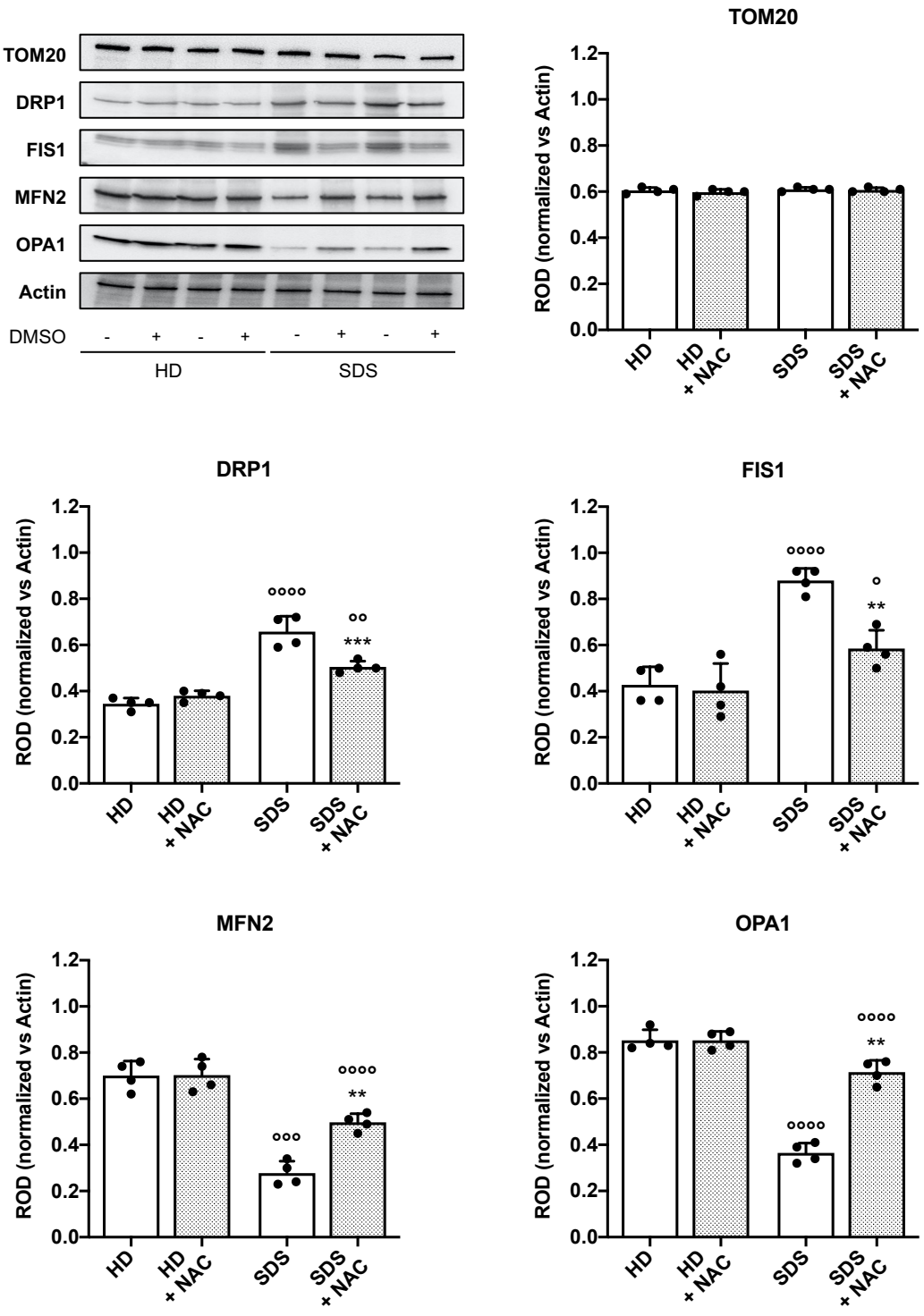


Figure 80 NAC treatment effects on mitochondrial dynamic markers expression levels of SDS patients and healthy donors' primary cells. WB signals of DPR1 and FIS1 as mitochondrial fission markers, TOM20 as a mitochondrial mass marker, MFN2 and OPA1 as mitochondrial fusion markers, and Actin as housekeeping protein in SDS patients (n=4) and healthy donors (HD=4) primary cells. Protein expression levels (densitometric analysis) were normalized on the Actin signal revealed on the same membrane. Data are reported as mean ± SD, and both WB signals and graphs are representative of at least 3 independent experiments. Statistical significance was tested with a one-way ANOVA test; ** and *** represent a significant difference for $p < 0.01$ or 0.001 between treated and untreated cells in the same clinical conditions; °, °°, °°°, and °°°° represent a $p < 0.05$, 0.01, 0.001 or 0.0001 between HD and SDS patients undergone the same treatment.

As the data in Figure 79 and Figure 80 demonstrates, there are significant issues in SDS-derived cells' mitochondrial dynamics compared to HD-derived cells. Indeed, the proteins involved in mitochondrial fission (DRP1 and FIS1) are significantly more expressed in SDS than in HD-derived cells. Furthermore, the proteins involved in mitochondrial fusion (MFN2 and OPA1) are significantly less expressed, without any differences in TOM20 expression, a marker for mitochondrial mass. For all the proteins analyzed, both the treatments with DMSO (Figure 79) and NAC (Figure 80) do not influence expression in HD-derived cells but partially restore the expression levels of all altered proteins in SDS-derived cells, significantly decreasing the expression of proteins involved in fission and increasing the levels of those involved in fusion in SDS patients. All these data highlight substantial issues in mitochondrial dynamics in SDS-derived cells, with altered protein expression related to fission and fusion processes. Treatments with DMSO and NAC both partially restore these protein levels in SDS-derived cells, bringing them closer to those observed in HD-derived cells. Notably, the mitochondrial dynamics issue in SDS cells appears to be even more severe than that observed in FA cells, as in SDS, it involves both increased fission and reduced mitochondrial fusion, whereas, in FA, the defect is primarily limited to enhanced fission.

### 5.13.1 Implications of iron metabolism in SDS metabolic defect

Iron metabolism plays a crucial role in cellular functions, and its dysregulation can have significant health implications. Iron metabolism can be particularly relevant in SDS, primarily characterized by hematologic issues such as bone marrow failure and neutropenia. One aspect to consider is that the bone marrow is a major site for iron storage and utilization in the body. In SDS, there are bone marrow abnormalities, and the regulation of iron within the marrow might be disrupted. This could potentially lead to iron imbalance, affecting hematopoiesis and exacerbating anemia, which is a common symptom in SDS patients. Furthermore, iron is also essential for various enzymatic processes and the functioning of mitochondria. Given the mitochondrial defects observed in SDS, alterations in iron metabolism could further impact mitochondrial function, potentially contributing to the metabolic abnormalities in these patients. While the direct link between iron metabolism and SDS is not extensively studied, it's plausible that iron dysregulation could be an additional factor complicating the already complex pathophysiology of SDS. Understanding these aspects can be valuable in developing comprehensive treatments for SDS patients. For these reasons, I wanted to investigate the $Fe^{3+}$ to $Fe^{2+}$ ratio in cells derived from SDS patients and HD before and after treatment with DMSO and NAC. $Fe^{2+}$ plays a vital role in biological systems, primarily as a component of heme groups in hemoglobin and myoglobin, which are responsible for transporting and storing oxygen in red blood cells and muscle tissues, respectively. It is also involved in various enzymatic reactions, including those related to electron transport chains in mitochondria. $Fe^{2+}$ can be oxidized to $Fe^{3+}$, which is less commonly involved in biological processes, less soluble, and less biologically active than $Fe^{2+}$. It is typically found in ferric ions bound to proteins and is essential for the

activity of some enzymes, such as cytochromes involved in electron transport. Overall, iron, in its different forms, plays a crucial role in oxygen transport, energy production, and various enzymatic reactions that are vital for maintaining cellular functions and overall health. Furthermore, an imbalance between the oxidized and reduced forms of iron can promote Fenton reactions, where ferrous iron ($Fe^{2+}$) oxidizes to ferric iron ($Fe^{3+}$), producing hydroxide ions ($OH^-$) and the hydroxyl radical (·OH). The hydroxyl radical is highly reactive and can contribute to cellular oxidative stress damaging, for example, DNA, proteins, and lipids.

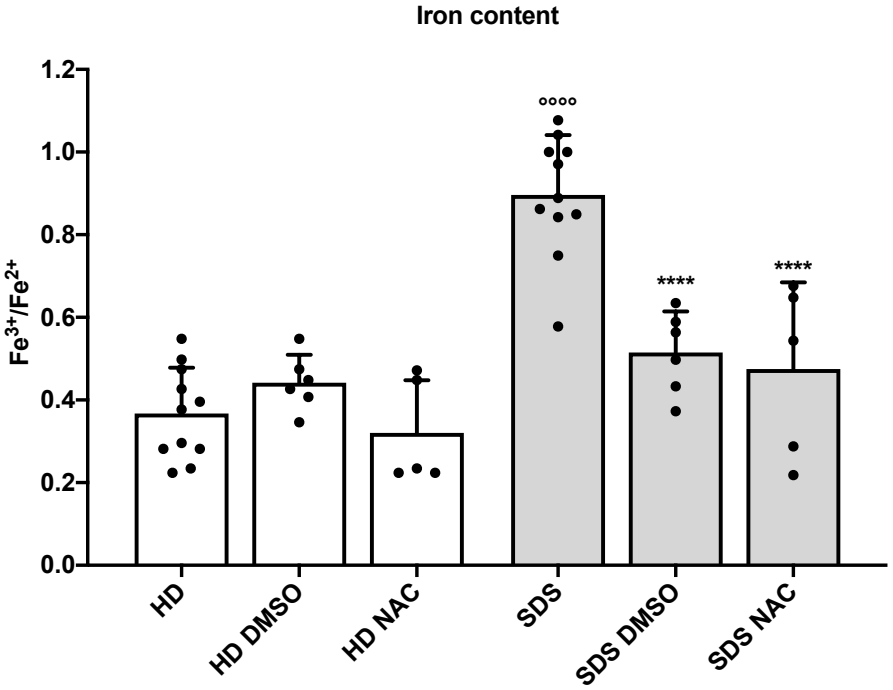


Figure 81 Effects of DMSO and NAC on $Fe^{3+}/Fe^{2+}$ content in SDS patients and healthy donors' primary cells. DMSO 0.05% and NAC effects on the $Fe^{3+}$ to $Fe^{2+}$ ratio in SDS patients (n=11) and healthy donors (HD, n=11) primary cells. Data are reported as mean ± SD, and each graph is representative of at least four independent experiments. Statistical significance was tested with a one-way ANOVA test; **** represents a $p < 0.0001$ between treated and untreated cells in the same clinical conditions; °°°° represents a $p < 0.0001$ between HD and SDS patients undergone the same treatment.

The data in Figure 81 shows that for cells derived from HD, the $Fe^{3+}$ to $Fe^{2+}$ ratio is not influenced by antioxidant treatments. However, this ratio is significantly higher in cells derived from SDS, and antioxidant treatment (with no significant differences between the two treatments) reduces this value significantly, though it does not bring it back to the level of HD-derived cells.

# 6 Discussion

Fanconi Anemia (FA) is a rare genetic disease caused by mutations in FANC genes, which encode proteins responsible for repairing DNA interstrand crosslinks (ICLs) [128]. This thesis focuses on the most common mutation affecting 60% of FA patients, which occurs in the FANCA gene [9]. A mutation in a FANC gene results in a defective DNA repair system, leading FA patients to accumulate a significant number of DNA mutations [128]. Although this molecular issue is the most extensively studied and highly relevant in the pathogenesis of FA patients, while exploring other molecular and biochemical aspects, one of the major defects in this condition involves mitochondrial metabolism, resulting in an inability to perform efficient oxidative phosphorylation (OxPhos) [32]. In addition, mitochondria show severe alterations in their internal structure with swollen and few cristae [107]. It is impossible to determine whether the problem arises from a structural mitochondrial alteration that subsequently affects mitochondrial functionality or if the malfunction disrupts the structure. However, it has been demonstrated, and confirmed in this thesis, that the dysfunctional OxPhos in FA is caused by a defective electron transport between Complexes I and III of the mitochondrial respiratory chain [36], [37]. Since the pathway involving respiratory Complexes I-III is primarily responsible for cellular ATP production, its malfunction reduces energy availability in FA cells [68]. This results in diminished cellular responsiveness to potential environmental changes and difficulty maintaining cellular homeostasis [129]. Besides maintaining cellular homeostasis, ATP is crucial for antioxidant defenses, especially in FA. Indeed, malfunctioning complexes I-III pathway increases reactive oxygen species (ROS) production, thus oxidative stress [68]. FA cells cannot activate an adaptive response as they cannot enhance intracellular antioxidant defense production. Conversely, as indicated by the data presented in this thesis, FA lymphoblasts and fibroblasts exhibit significantly lower antioxidant enzyme activity than control cells, even following severe oxidative insult, substantially increasing lipid peroxidation accumulation.

These data suggest that the pronounced increase in oxidative stress, especially within the mitochondria, may be one of the reasons why the mitochondria appear morphologically altered: ROS generated due to the impaired functionality of the respiratory chain can damage the inner mitochondrial membrane and compromise its structure. In the mitochondrion, the structure is tightly linked to organelle functionality, and the loss of internal structure results in a loss of functionality, creating a vicious cycle [68], [130], [131]. The lack of adaptive capacity in FA cells could be attributed to the energetic issue, as a cell requires a high energy amount to synthesize enzymes to respond to a homeostasis change. Given that the formation of each peptide bond necessitates four ATP molecules [68], FA cells likely do not have an adequate energy supply to produce enough antioxidant molecules and enzymes. As demonstrated, they only generate a minimal amount, which the data have shown to be insufficient to counterbalance the oxidative stress resulting from the malfunction of OxPhos.

These observations were made on cellular lines expressing the FANCA mutation and FA-patients PBMCs isolated from peripheral blood (PB), thus fully differentiated cells. Therefore, I wondered if this defect was already present in bone marrow (BM) cells or if it emerged during cell maturation. For this reason, the metabolic study was also extended to cells isolated from the bone marrow of patients. Upon analysis, the typical metabolic issues found in mature cells were not observed in these cells. One possible explanation could be attributed to the fact that bone marrow cells reside in a hypoxic niche with an oxygen tension of approximately 3%, reducing the possibility of using mitochondria as the principal energy source.

Moreover, a low aerobic metabolism is essential for a stem cell because by restricting the use of oxygen for fundamental cellular functions, the risk of oxygen forming reactive species and subsequently causing damage to both the cell's internal structure and, more importantly, its DNA is minimized, as the risk to transmit this damaged DNA to its progeny [132], [133]. However, when bone marrow cells leave the hypoxic niche, they should be able to activate the mitochondrial metabolism, adapting to the PB oxygen tension (20%). Investigating what happens when exposing BM-derived patients' cells from hypoxia to normoxia, I observed that BM-derived cells from FA patients and HD initially respond to changes in oxygen tension by activating aerobic respiration. Nevertheless, while cells from HD continue to use oxidative phosphorylation for energy production over time, FA cells, after 24 hours, shift their energetic metabolism back towards lactic fermentation and begin to exhibit the typical metabolic issues seen in mature cells. Exposure to higher oxygen concentrations activates mitochondria, which do not function appropriately in FA. Despite the cells attempting to compensate for their energy demand through anaerobic respiration partially, the malfunctioning mitochondria remain active, producing significant oxidative stress. These data demonstrate that the mitochondrial dysfunction in FA, which results in both the production of high levels of ROS and subsequent oxidative damage, as well as the inadequate production of ATP for maintaining cellular homeostasis, along with the inability of these cells to generate sufficient antioxidant defenses, is dormant in hematopoietic stem cells and becomes apparent only as these cells mature and leave the hypoxic marrow niche. Consequently, it can be assumed that this is mutation-dependent, although the exact mechanism is currently unknown.

At this point, I wondered what could be causing this functional OxPhos defect in FA cells, and the initial suspects were the respiratory chain's main components, the mitochondrial respiratory complexes and ATP synthase. Therefore, I analyzed the expression of some respiratory complexes and ATP synthase subunits to understand if the FANCA mutation led to their differential expression compared to control cells. The data demonstrate that my initial hypothesis is not confirmed, as both FA lymphoblasts and fibroblasts express at equal levels to control cells all the analyzed protein subunits of Complexes I, II, IV, and ATP

synthase. However, FA cells express significantly higher levels of the uncoupling protein 2 (UCP2), a protein responsible for uncoupling mitochondrial respiration from ATP production. This mechanism is typical in brown fat [38], which uses it to generate heat, and in cancer cells that use ROS produced as a pro-proliferative signal [43]. This protein should not be expressed at such high levels in the analyzed lymphoblasts and fibroblasts. In this case, uncoupling of oxygen consumption from ATP production is another cause of the elevated production of oxidative stress, which confirms the vicious cycle in which high levels of oxidative stress, caused by inefficient OxPhos, damage mitochondrial membranes, affecting mitochondrial morphology, which, in turn, exacerbates the functional defect. Structurally efficient mitochondria have a highly developed inner membrane, composing the mitochondrial cristae where the respiratory chain complexes and ATP synthase are located.

On the other hand, mitochondria with a swollen appearance and few cristae in the inner membrane are less functional and efficient, which precisely describes the mitochondria in FA cells, as shown by the electron microscopy images presented, suggesting that the functional mitochondrial defect in FA is linked to the morphological defect. However, the potential connection between FANC gene mutations and altered mitochondrial morphology remains unexplained as the direct correlation between altered mitochondrial morphology and Fanconi protein mutations remains to be elucidated.

Upon ultrastructural examination of mitochondria, I realized that other than issues with their internal structural organization, they also had problems with distribution and organization within the cell. So, I suspected an issue with mitochondrial dynamics processes, which allow mitochondria to change shape continuously, relative position to other organelles, and organization with other mitochondria [134], [135]. The fusion process enables mitochondria to form a mitochondrial network, increasing OxPhos efficiency [136]. In contrast, the fission process disaggregates the reticulum, following the cell's energy requirements and cycle. Moreover, mitochondrial fission is crucial for removing damaged mitochondria and properly distributing mitochondria to daughter cells [137]. The more balanced these processes are, the more prepared cells will respond to changes, damage, and stress [46], [50], [51].

Therefore, I evaluated the expression levels of specific proteins involved in mitochondrial dynamics processes: OPA1 and MFN2, markers of mitochondrial fusion; DRP1, a marker of mitochondrial fission; and CLUH, an RNA binding protein that regulates the entire process of dynamics upstream. The data show that the only significant difference is in DRP1 expression level, which is more expressed in both FA lymphoblasts and fibroblasts compared to their respective controls, suggesting that in FA cells, the balance of mitochondrial dynamics leans towards mitochondrial fission and the disaggregation of the mitochondrial network, a finding corroborated by confocal microscopy. The increased expression of DRP1 in FA may explain the poor OxPhos efficiency since isolated mitochondria are less efficient [138]. To confirm the role of DRP1 and the increased mitochondrial fission in the mitochondrial metabolism issue, I treated the cells with P110, a

specific DRP1 inhibitor. After treatment with this molecule, FA cells significantly improved OxPhos efficiency and mitochondrial network morphology. Thus, reducing DRP1's ability to induce mitochondrial fission and allowing the formation of a mitochondrial network helps the cell enhance its metabolic functions. This confirms that both the morphology of individual mitochondria and their mutual organization within the cell are crucial for OxPhos' efficiency, highlighting how the metabolic defect can have various complex causes [107]. However, it should be noted that the treatment with the DRP1 inhibitor, while significantly improving mitochondrial efficiency, does not restore it to the control cells' level, suggesting that the issue of mitochondrial network organization is undoubtedly significant but insufficient to explain FA mitochondrial metabolic problems.

Given the significant amount of damaged and malfunctioning mitochondria in FA, I wanted to understand if FA cells could distinguish them from functional mitochondria. Malfunctioning mitochondria inevitably produce substantial amounts of oxidative stress, and their physiological removal preserves the cell and its internal structures from the damage caused by this stress [139]. So, I studied some markers of autophagy and mitophagy processes, evaluating their expression levels. The data show no significant differences between FA lymphoblasts and fibroblasts and their respective controls for the autophagy markers analyzed. However, there is a reduction in the expression of Beclin, a critical protein in autophagosome formation. This process occurs upstream of this pathway and is essential for removing damaged molecules and organelles [56], suggesting that FA cells can theoretically trigger autophagy. Still, with a reduced capacity to form autophagosomes, they may accumulate a large number of damaged molecules, such as misfolded proteins or poorly functioning mitochondria.

Furthermore, when studying the expression levels of the primary mitophagy markers, the specific autophagic process for removing damaged mitochondria, it was evident that PARKIN, an effector protein of the mitophagy process, is significantly less expressed in FA cells than in controls. Through Pink1, a protein that marks damaged or depolarized mitochondria, whose expression remains unaltered, FA cells can recognize these mitochondria. However, the reduced expression of PARKIN, which is responsible for directing them towards the autophagosome, coupled with the diminished ability to form the autophagosome itself, leads these cells to accumulate a significant quantity of damaged mitochondria, subsequently becoming a substantial source of oxidative stress [48], [67], [140].

Mitochondrial malfunction can also lead to fat accumulation. Indeed, when mitochondria are not functioning correctly, they are less efficient at breaking down and utilizing fatty acids for energy, causing excess fatty acids to accumulate within cells [68]. This is precisely the case in FA, where there is lipid droplet accumulation in the cytoplasm of lymphoblasts and fibroblasts, cells not intended for fat storage. Although these cells do not use fatty acids as an energy substrate, fatty acid synthesis cannot slow down, as it is the only way the cell

can recycle CoA, which is essential for the functioning of the Krebs cycle [68]. Per se, the accumulation of fats inside the cell is not problematic; however, due to the OxPhos malfunction, FA cells produce high levels of ROS, which, peroxiding the accumulated lipids in the cell, increases the membrane damage, becoming an additional source of oxidative stress.

Therefore, I wanted to test various molecules on my FA cellular models, which act on the aspects of FA metabolic dysfunction that have been analyzed and discussed. Specifically, I selected (i) quercetin, a potent antioxidant molecule that acts as a scavenger and can also slow down ATP synthase activity [141]. Slowing ATP synthase also slows the upstream respiratory chain, reducing FA ROS production [68]; (ii) C75, an inhibitor of fatty acid synthesis that is employed to limit lipid droplet accumulation in FA cells; (iii) Rapamycin, an mTOR inhibitor [142], chosen because it is a regulator of mitochondrial metabolism [143] and appears hyperphosphorylated in FA cell [144]. Since mTOR has a regulatory role, I hypothesized that negatively modulating it could slow down OxPhos, reduce oxidative stress, and improve mitochondrial dynamics. These molecules were used individually or in combination.

The results showed that treating the cellular models with C75 significantly reduced lipid accumulation in the cell cytoplasm without improving OxPhos. In other words, it reduces the cell's ability to undergo lipid peroxidation. Still, it does not reduce ROS production, which will find other targets within the cell, such as proteins or DNA. Rapamycin, by inhibiting mTOR, effectively reduces OxPhos and ROS production. However, it does not revert the defect in electron transport from Complex I to Complex III and does not help restore cellular energy status. This is also because, by slowing down OxPhos, the cell must rely almost entirely on lactic fermentation for energy production. However, lactic fermentation generates 2 ATP molecules for every glucose molecule, compared to the 36/38 produced by OxPhos [68]. The molecule that had the most overall positive effects is quercetin.

Thanks to its antioxidant scavenger action, it limits oxidative stress damage. Moreover, quercetin's effect on ATP synthase, which is slowed down, reduces the aerobic metabolism flux and the consequent risk of fatty acid accumulation and ROS production, reducing the need to increase the antioxidant response. All of this leads to a significant reduction in ATP consumption and improves the cell's energy status. Regarding the treatment combinations, there are no significant improvements compared to treatments with individual molecules, except in the case of the combination of quercetin and C75, where the benefits described for the single treatments are cumulative. This combination addresses most of the issues in FA mitochondrial metabolism. So, using these two molecules could ensure a longer cell lifespan, reduce the burden on the bone marrow of patients, and delay the onset of bone marrow aplasia.

Additionally, by reducing oxidative stress, this treatment reduces γ-H2AX phosphorylation, a marker of double-stranded DNA damage, the first link connecting FA mitochondrial

metabolism issues to the defect in the DNA repair system for interstrand crosslinks (ICLs). In other words, this data helps us understand how improving OxPhos dysfunction also helps address these cells' primary problem: the accumulation of DNA damage. In other words, by improving OxPhos dysfunction and thereby reducing oxidative stress, the likelihood of causing DNA damage that FA cells cannot fix is decreased.

At this point, the data have shown a high production of oxidative stress in FA, primarily due to mitochondrial dysfunction. However, we know that the reduced energy status caused by defective OxPhos is not the sole reason FA cells cannot respond to oxidative stress. In literature, another possible explanation is the hypo-deacetylation of genes related to the adaptive response to oxidative stress in FA [145], [146]. I treated the cells with different histone deacetylase inhibitors (HDACi) to target these pathways. I selected three molecules with distinct targets: valproic acid (VPA) acts on both class I and II histone deacetylases, beta-hydroxybutyrate (OHB) acts on class I histone deacetylase and has metabolic significance as it can be used as an intermediate by the Krebs cycle, and EX527 a SIRT1 inhibitor [147], [148], [149].

The data show that EX527 produced limited results in improving the expression and activity of antioxidant enzymes, mitochondrial function, cellular energy status, lipid peroxidation levels, and oxidative stress damage, suggesting that SIRT1 is not directly involved in these processes. The treatment with OHB showed limited results as it enhances antioxidant enzymes expression but increases the uncoupled OxPhos flux. In detail, I observed an improvement in the expression and activity of catalase and glutathione reductase, two of the primary cellular antioxidant enzymes. However, OHB also has a metabolic significance, as it can be converted into Acetyl-CoA, which is used in the Krebs cycle to supply the respiratory chain with NADH and $FADH_2$, stimulating their cellular utilization to produce ATP; this induces FA cells to rely more on OxPhos for energy production. However, the increase in oxygen consumption is not paralleled by a proportional increase in ATP production, resulting in more significant mitochondrial uncoupling. This uncoupling extends even to the pathway of the respiratory chain complexes II and III, typically coupled in FA, likely because the increased ROS production causes significant damage to the inner mitochondrial membrane.

Consequently, higher oxidative stress production is not compensated by the parallel increase in antioxidant defenses, also because cellular energy status does not improve. The treatment with VPA is the one that showed the best results on all examined parameters. It increased the expression and activity of catalase and glutathione reductase, improved OxPhos efficiency, and enhanced cellular energy status. Furthermore, it also improved electron transport between complexes I and III of the respiratory chain, addressing the underlying issue of dysfunctional mitochondrial metabolism in FA. VPA's action on the mitochondria is not a direct effect. Instead, improving antioxidant defense levels and cellular energy status reduces damage to the inner mitochondrial membranes,

setting up a positive feedback loop. Undamaged membranes favor coupling between the respiratory chain and ATP synthase, resulting in decreased ROS production better balanced by increased antioxidant defenses. This also reduces the need to recycle CoA, reducing lipid synthesis and, subsequently, lipid accumulation and lipid peroxidation damage in the cell.

Moreover, VPA treatment improved FA cells' survival following exposure to mitomycin, enhancing their ability to withstand DNA damage induction. VPA also negatively modulates DRP1 expression, improving mitochondrial dynamics equilibrium and network aggregation, further explaining the improved OxPhos efficiency. It similarly reduces UCP2 expression, justifying the enhanced uncoupling of the respiratory chain with ATP synthase and the subsequent reduction in oxidative stress production.

I then repeated the same experiments with the HDACi treatments while adding hydrogen peroxide to exacerbate oxidative damage to see how cells would respond to high oxidative stress. Results confirmed that FA cells cannot initiate an adaptive response to oxidative stress: while healthy cells physiologically increase their antioxidant defenses in $H_2O_2$ presence, FA cells cannot. Furthermore, the data obtained following treatment with HDACi reflects the data discussed earlier in the absence of $H_2O_2$, confirming that VPA is the only treatment capable of improving all parameters, even adding the oxidative insult. This underscores the pivotal role of hypoacetylation in the pathophysiology of FA.

All the data discussed so far allow us to characterize FA as a multifactorial disease in which there is damage to the DNA repair system and functional, structural, and organizational damage to the mitochondria. This leads to the uncoupling of the respiratory chain from ATP synthase, which decreases cellular energy status, lipid accumulation, and increased production of oxidative stress, leading to enhanced lipid peroxidation damage. This is exacerbated by the inability of these cells to activate their antioxidant defenses. Modulating these various metabolic aspects with different molecules improves the adaptability and functionality of these cells, thereby enhancing their health and survival. By increasing the lifespan of circulating cells, the bone marrow of patients would be required to do less work to replace them, giving it more time to replenish its pool of stem cells and thus delaying the onset of aplastic anemia in patients.

To understand the connection between the FANCA gene mutation and the metabolic defect, we analyzed the miRNome in FA cells and their corrected counterparts in collaboration with Dr. Degan (IRCCS Policlinico San Martino - Genova) and Dr. Regis (IRCCS Istituto Giannina Gaslini -Genova). This analysis identified the most promising candidate as miRNA29A, which is significantly less expressed in FA cells than controls. Furthermore, miRNA29A is involved in regulating energy metabolism [150]. I then transfected FA cells with miRNA29A, and once I confirmed the efficacy of the transfection, I evaluated the energy metabolism. The results show that transfection partially restores mitochondrial functionality, improving mitochondrial morphology and dynamics by reducing

the expression of DRP1 to levels similar to control cells. Electron transfer between Complex I and Complex III in the respiratory chain is enhanced by improving the structure and organization of mitochondria, increasing OxPhos efficiency, and improving cellular energy status. This, in turn, reduces oxidative stress and lipid peroxidation damage. These findings underscore the role of miRNA29A in regulating energy metabolism and once again suggest that mitochondrial dysfunction is a central issue in this disease. The ability to improve it through various approaches implies that there are multiple contributing factors. miRNA29A is also capable of modulating the phosphorylation of AKT and FOXO3. These two proteins are found to be hyperphosphorylated in FA and are related to both mitochondrial function and the ability to respond to oxidative stress [151]. In particular, data show that FA cells have hyperphosphorylated AKT, leading to hyperphosphorylation of FOXO3 and, simultaneously, low phosphorylation levels of PTEN, which inhibit AKT phosphorylation. Hyperphosphorylation of these two proteins causes mTOR's further hyperactivation [152] and a reduction in mitochondrial biogenesis [153], respectively. By transfecting cells with miRNA29A, we restore the phosphorylation levels of these proteins similarly to those of the control, thereby reducing the activation of the AKT-FOXO3 pathway and increasing the activation and inhibitory activity of PTEN. Thus, mitochondrial function was significantly improved by acting on apparently unrelated and distinct points.

Another aspect I was interested in investigating was the inflammation associated with FA. It is known that FA patients have high levels of proinflammatory interleukins in their plasma, such as IL1, TNF-α, and TGF-β [154], [155], [156], [157], [158]. I wanted to understand whether modulating inflammation could positively impact cellular energy metabolism, as a proinflammatory environment is usually pro-oxidative. The data from this thesis demonstrate a close association between oxidative stress and mitochondria's structural, organizational, and functional dysfunctions. In this case, I wanted to analyze lymphoblastoid cell lines with FANCA and FANCC mutations parallelly. These two mutations are the most common in patients, resulting in a similar clinical picture. In both cases, patients develop aplastic anemia and have a significantly higher risk of tumors, especially after bone marrow transplantation, due to the defect in DNA repair systems. These two different mutations lead to distinct cellular, molecular, and biochemical profiles: patients with FANCA mutations have high levels of TNF-α in their peripheral blood; in contrast, those with FANCC mutations have high levels of TGF-β. I wanted to investigate whether inhibiting these cytokines would yield different responses based on the genetic mutation.

Furthermore, I treated the samples with an IL1 inhibitor, a typical proinflammatory cytokine, and an NLRP3 inhibitor, a protein that regulates inflammasome activation. Lastly, I added P110 as a modulator of mitochondrial dynamics, whose response I had already extensively characterized, as an additional control to ensure the model worked correctly. The data show that cells with the FANCA mutation significantly improve mitochondrial function with

all the inhibitors analyzed. They respond less to TNF-α inhibition and more to IL1, TGF-β, NLRP3, and P110 inhibition, with P110 having the most pronounced effect. This suggests that in the case of FANCA, the TNF-α pathway is less relevant to the FA pathological process than the TGF-β or IL1 pathways. In the case of FANCC, the most significant improvement is indeed seen with TGF-β inhibition, and these cells respond less significantly to the inhibition of the other interleukins considered and even less to P110. In all cases, the improvement in oxidative phosphorylation efficiency is followed by an enhancement of cellular energy status and a reduction in lipid peroxidation. These data confirm that, despite the clinical similarity of patients with these different mutations, these cells' cellular and molecular behavior is diverse. Therefore, once the mechanism for FANCA is understood (which accounts for 60% of patients), and a therapeutic strategy is developed to support them, it would be essential to assess the differences between the other two most common mutations, FANCC and FANCG. These preliminary data from the comparison between the two mutations highlight the need for personalized therapy based on the type of genetic mutation for these patients.

In conclusion, this thesis explored the intricate landscape of Fanconi Anemia (FA), a rare genetic disorder traditionally characterized by its defective DNA repair system. While DNA repair remains a central focus in understanding the condition, this research reveals a more complex and interconnected network of metabolic dysfunctions that significantly influence the course of this disease. These metabolic alterations profoundly impact the lifespan of lymphocytes and, consequently, the timing of developing aplastic anemia, a leading cause of mortality in FA. Mitochondrial dysfunction, specifically defective OxPhos due to impaired electron transport between Complexes I and III of the respiratory chain, stands out as a central issue in FA. Furthermore, FA cells struggle with mitochondrial dynamics, favoring fission over fusion, which disrupts the reticulum and leads to increased oxidative stress and in performing autophagy and mitophagy correctly, exacerbating oxidative stress and DNA damage, adding another layer to the complexity of FA.

The data suggest the existence of a self-perpetuating cycle within FA cells, in which DNA damage can trigger systemic inflammation. This inflammation negatively impacts mitochondrial activity by uncoupling the respiratory chain from ATP synthesis, resulting in high production of oxidative stress, which damages mitochondrial structure, further promoting OxPhos uncoupling and ROS production. The high level of oxidative stress can also damage DNA, further promoting inflammation and perpetuating the cycle. The only viable strategy to extend the lifespan of circulating cells and delay the onset of aplastic anemia in FA patients is to address these metabolic alterations on multiple fronts. Specifically, to address these multifaceted issues, various treatment strategies were explored. A promising approach involved using P110, a molecule restoring mitochondrial dynamics, and quercetin, an antioxidant, which mitigated oxidative stress, enhanced mitochondrial efficiency, and improved cellular energy status.

Moreover, histone deacetylase inhibitors (HDACi), particularly valproic acid (VPA), demonstrated remarkable potential in restoring mitochondrial function and addressing hyperacetylation issues in FA cells. After a miRNome analysis, we also tested miRNA29A, which emerged as a promising candidate and partially restored mitochondrial functionality and enhanced energy metabolism in FA cells. Finally, the impact of different cytokine inhibitors was evaluated to address the proinflammatory environment associated with FA. Data suggest that the response to cytokine inhibition varies depending on the specific genetic mutation, highlighting the need for personalized therapies tailored to the type of mutation. By improving OxPhos coupling and efficiency, ROS production is decreased, and cellular energy status is enhanced, allowing a higher production of antioxidant defenses and better oxidative stress management. This enhancement in redox status ensures less lipid accumulation and peroxidation damage, reducing damage to mitochondrial membranes and DNA, thus establishing a virtuous cycle.

Additionally, the improved energy status and the reduced oxidative stress damaging mitochondria and DNA can decrease the cell cycle frequency, giving the cell the time to identify the necessary time to detect DNA damage through the Fanconi protein complex, even though it remains defective. The role of this complex is to identify interstrand crosslinks (ICLs) and recruit molecules responsible for repairing this type of damage. This will prevent the rapid accumulation of severe cellular dysfunctions and DNA damage, which FA cannot correctly manage due to defects in the DNA repair system. Notably, the approach proposed in this thesis does not directly address the defective DNA repair system, which may be a candidate for gene therapy in the future. Instead, it suggests immediate therapeutic strategies employing only molecules already in clinical use, thus a therapeutic maintenance approach to help patients manage mitochondrial and metabolic dysfunctions, oxidative stress, and inflammation. By mitigating these factors, the accumulation of DNA mutations is also reduced, enhancing patients' quality of life and delaying the onset of aplastic anemia and the need for a transplant, thereby increasing their life expectancy.

In summary, this study underscores the multifactorial nature of Fanconi Anemia and the complex interplay of genetic mutations, mitochondrial dysfunction, oxidative stress, and inflammation. By gaining a deeper understanding of these mechanisms and exploring targeted therapeutic interventions, we pave the way for potential personalized treatments to improve the health and survival of FA patients, delay the onset of bone marrow aplasia, and reduce the risk of associated complications. This research not only sheds light on the intricacies of FA but also points toward the promise of more effective treatment strategies in the future.

Another critical aspect in the pathogenesis of Fanconi anemia is the onset of HNSCC, which is 700 times more frequent in patients than in the healthy population [7], [94]. This increased likelihood is undoubtedly due to the accumulation of DNA mutations and the

ablation treatments patients must undergo to receive a bone marrow transplant [93], [95], [159]. It is known that tumor cells have significant metabolic alterations in non-FA patients [70], so I wondered if and how the genetic mutation of FA patients could also influence the pathogenesis of these tumors. If the metabolic characterization of FA cells were maintained in HNSCC-FA cells, we could open up new therapeutic targets. In summary, the data presented in this thesis demonstrate that HNSCC-FA has the same defect in oxidative phosphorylation already characterized in lymphoblasts and fibroblasts. This issue is again due to defective electron transport between complexes I and III of the respiratory chain. This leads to a compensatory metabolic switch towards increased utilization of lactic fermentation for energy production. This is accompanied by a simultaneous decrease in cellular energy status due to anaerobic respiration's lower energy production than aerobic respiration.

Furthermore, analyzing the preference for energy substrate utilization in ATP production through OxPhos reveals a shift from predominant glutamine utilization in control cells to predominantly glucose utilization in cells with the mutation. Subunit expression levels in the respiratory complexes do not show significant differences. Still, as observed in lymphoblasts and fibroblasts, the protein DRP1, a marker of mitochondrial fission, is overexpressed in FANCA mutant cells. This contributes to mitochondrial network fragmentation, further impairing OxPhos efficiency.

Analysis of the expression of autophagy and mitophagy proteins in HNSCC-FA cells yields similar results to those obtained in lymphoblasts and fibroblasts, indicating decreased Beclin1 and PARKIN expression, signifying inefficiencies in these processes and the accumulation of damaged mitochondria. Additionally, there is a significant increase in lipid peroxidation damage caused by the increased ROS production and the decreased activity of antioxidant enzymes in FANCA mutant cells compared to their corrected counterparts. Moreover, the mutated cells exhibit a significantly higher proliferative rate than control cells. Notably, the mutated cells are much more susceptible to DNA damage induction, highlighting the substantial contribution of defective DNA repair in the onset and progression of HNSCC in FA patients. This characterization aligns with the metabolic characteristics discussed earlier in lymphoblasts and fibroblasts, indicating that the genetic mutation significantly impacts the development of HNSCC with distinct metabolic features compared to non-FA head and neck squamous cell carcinomas.

These findings could open a new therapeutic perspective for non-FA patients with neoplasms acquiring FA mutations. For instance, in these cases, it could be beneficial to exacerbate dysfunctional mitochondrial metabolism, resembling that of tumor cells, by administering compounds such as dichloroacetic acid, which forces pyruvate to become acetyl-CoA or hydroxybutyrate. Both compounds push the use of OxPhos. Since this process is dysfunctional, it leads to very high levels of oxidative stress and the accumulation of lipid droplets, which become another source of oxidative damage. This oxidative stress and the consequent damage reduce the cell's ability to maintain

homeostatic balance (although altered compared to a healthy cell) and, thus, to survive. The discussed characterization of HNSCC-FA also highlights the complexity of finding an adequate therapeutic strategy for FA patients who develop this (or other) types of tumors, where all the individual cells have the genetic defect causing the described metabolic alterations. Currently, these patients undergo traditional chemotherapy and surgical ablation. However, subjecting these patients to conventional chemotherapy increases their likelihood of developing additional primary tumors and worsens their overall health. The presented characterization suggests that alternative therapeutic targets, more related to inflammation and suitable for non-FA patients, should be evaluated. Indeed, further investigations should expand this characterization to other types of tumors developed by FA patients and to non-FA tumors that acquire the mutation to assess appropriate therapeutic strategies for both patient groups. In conclusion, this research not only advances our understanding of the intricate interplay between FA, HNSCC, and metabolic dysfunction but also underscores the need for tailored therapeutic strategies that consider the unique characteristics of these tumors in FA patients with potential implications for other tumor types, opening to more personalized treatments for non-FA patients with cancer acquiring FA mutations. Further investigations are warranted to expand this characterization and explore innovative therapeutic options for both patient groups.

Over these years, we have also analyzed various other diseases from the perspective of energy metabolism that share with FA the development of aplastic anemia and mitochondrial dysfunction. My attention has been mainly focused on Schwachman-Diamond Syndrome (SDS), another rare genetic disease caused by a mutation in the SBDS gene that regulates ribosomal function [126]. In this case, the genetic mutation also appears to have nothing to do with mitochondria. However, literature reports indicate that SDS cells have dysfunctional mitochondria [160]. This suggests that the mitochondrial defect cannot cause both pathologies but is a consequence of different genetic mutations. In this case, the defect is not limited to electron transport between two respiratory complexes, as in the case of FA. Instead, it appears to involve all four complexes in the electron transport chain. This leads to dysfunctional mitochondria that cannot produce sufficient ATP.

In collaboration with Dr. D'Amico and Dr. Gervasoni (Tettamanti Center – Monza), who provided us with primary cells from SDS patients, we conducted a more detailed metabolic characterization of these cells, comparing them with those from healthy donors. We also treated these cells with NAC, a powerful antioxidant and precursor of glutathione, and with low doses of DMSO, which is already used in clinical settings at low concentrations and seems to have a scavenging function for oxidative stress [161]. The data show that in SDS, mitochondrial damage affects complex IV. Similar to what has been observed in FA, reducing oxidative stress in these cells helps recover complex IV functionality and oxidative phosphorylation. It also reduces the compensatory use of lactic fermentation and

diminishes oxidative damage to lipids, proteins, and DNA. In this case, it is possible to use the same reasoning applied to FA: reducing oxidative stress limits damage to the inner mitochondrial membrane, which is closely linked to mitochondrial function. This increase in ATP synthesis makes the cell more resilient. The data also reveal that low concentrations of DMSO have a comparable effect to NAC, demonstrating its role as a scavenger that reduces ROS before they can harm the cell. The most significant difference between the two pathologies is in their antioxidant response. While FA cells cannot activate an adaptive response, SDS cells do not face this issue, and their antioxidant defenses remain active, although insufficient to balance oxidative stress. In the case of SDS, mitochondrial dynamics appear to be imbalanced, even more so than in FA. This is evident by the increased expression of proteins involved in mitochondrial fission and the decreased expression of those involved in mitochondrial fusion. The use of antioxidants helps rebalance this situation and restore the expression of all these proteins to levels similar to healthy donors. It is essential to remember that only when mitochondria organize into a network does the efficiency of oxidative phosphorylation significantly increase.

Literature studies have shown that antioxidants also function as scavengers modulating the intracellular iron content [162], a critical component of hemoglobin, and the cytochromes that are part of the electron transport chain complexes [68]. However, iron is an ion present at the cellular level in both reduced and oxidized forms, and it can potentially lead to reactions that contribute to the accumulation of oxidative stress, such as Fenton's reactions [163], [164]. Therefore, I wanted to assess the ratio between $Fe^{3+}$ and $Fe^{2+}$ in SDS cells and how antioxidant treatment affected this ratio. The data reveal that the oxidized to reduced iron ratio is almost twice as high in SDS patients compared to healthy donors. Antioxidant treatment brings this ratio back to levels similar to healthy donors, which remain unaffected by the treatments. This data indicates mitochondrial damage because a poorly functioning mitochondrion will have a lower demand for cytochromes. Consequently, iron is utilized less, and unbound iron becomes a target for Fenton reactions, leading to cellular oxidative stress.

In conclusion, data presented in this thesis has provided valuable insights into the relationship between energy metabolism, mitochondrial dysfunction, and the development of aplastic anemia in the context of rare genetic diseases, specifically Fanconi Anemia (FA) and Schwachman-Diamond Syndrome (SDS). Despite originating from distinct genetic mutations, both FA and SDS exhibit commonalities in mitochondrial dysfunction, which has been the central focus of this thesis. These findings enhance our understanding of the intricate connections between mitochondrial dysfunction and rare genetic diseases, demonstrating the potential for antioxidant interventions to alleviate the associated mitochondrial impairments and oxidative stress, paving the way for further investigations and potential therapeutic approaches to benefit patients with these conditions.

## 7 Future Perspectives

The insights gained from the comprehensive examination of FA provide a solid foundation for future research aimed at improving therapeutic strategies and patient outcomes. Moving forward, several key areas of investigation deserve focus to address the complexity of this rare genetic disease:

1. Targeted therapies: building upon the identified metabolic dysfunctions and molecular mechanisms underlying FA, the development of targeted therapies tailored to specific metabolic abnormalities holds promise. Efforts should focus on elucidating novel therapeutic targets and designing interventions to restore mitochondrial function, mitigate oxidative stress, and enhance DNA repair mechanisms.
2. Mitochondrial restoration: Given the central role of mitochondrial dysfunctions in the disease pathogenesis, strategies aimed at restoring mitochondrial health represent a promising opportunity for future investigation. This may involve the development of mitochondrial-targeted therapies, modulation of mitochondrial dynamics, and optimization of cellular bioenergetics to alleviate oxidative stress and enhance cellular resilience.
3. Combination therapies: Considering the multifactorial nature of FA, combination therapies targeting multiple pathways may yield synergistic effects and improve treatment efficacy. Integration of conventional treatments with novel therapeutic modalities, including antioxidants, histone deacetylase inhibitors, and cytokine inhibitors, holds potential for optimizing patient outcomes and reducing treatment-related complications.
4. Personalized medicine: the heterogeneity observed in FA patients with different genetic mutations underscores the importance of personalized medicine approaches. Further research is warranted to delineate the genotype-phenotype correlations and identify biomarkers that can inform individualized treatment strategies. Integration of genomic, metabolomic, and proteomic data may facilitate the identification of patient-specific therapeutic interventions.
5. Translational research: bridging the gap between basic science discoveries and clinical applications is essential for translating research findings into tangible benefits for patients. Collaborative efforts between basic researchers, clinicians, and industry partners are needed to accelerate the development and clinical translation of promising therapeutic interventions.
6. Long-term follow-up studies: longitudinal studies are critical for evaluating the long-term efficacy and safety of emerging therapeutic modalities in FA patients. Comprehensive follow-up assessments should include monitoring of disease progression, treatment response, and potential adverse effects to inform clinical decision-making and refine treatment protocols.
7. Exploration of novel biomarkers: identification of reliable biomarkers for disease diagnosis, prognosis, and treatment response is crucial for guiding clinical management

and monitoring disease progression in FA patients. Continued exploration of novel biomarkers, including for example circulating miRNAs, metabolites, and mitochondrial DNA, may provide valuable insights into disease pathogenesis and facilitate early intervention strategies.

In summary, future research efforts in FA should focus on advancing our understanding of disease mechanisms, developing targeted therapeutic interventions, and translating scientific discoveries into clinical practice. By leveraging interdisciplinary approaches and collaborative networks, we can strive towards improving outcomes and quality of life for individuals affected by this rare genetic disease.

## 8 References


[1] S. Lobitz and E. Velleuer, “Guido Fanconi (1892–1979): a jack of all trades,” *Nature Reviews Cancer 2006 6:11*, vol. 6, no. 11, pp. 893–898, Oct. 2006, doi: 10.1038/nrc2009.

[2] A. Shimamura and B. P. Alter, “Pathophysiology and management of inherited bone marrow failure syndromes,” *Blood Rev*, vol. 24, no. 3, pp. 101–122, May 2010, doi: 10.1016/J.BLRE.2010.03.002.

[3] A. D. Auerbach, “Fanconi anemia and its diagnosis,” *Mutat Res*, vol. 668, no. 1–2, pp. 4–10, Jul. 2009, doi: 10.1016/J.MRFMMM.2009.01.013.

[4] G. C. Bagby, “The Genetic Basis of Fanconi Anemia,” *Curr Opin Hematol.*, vol. 10, no. 1, pp. 68–76, 2006, doi: 10.1097/00062752-200301000-00011.

[5] A. Butturini, R. Gale, P. Verlander, B. Adler-Brecher, A. Gillio, and A. Auerbach, “Hematologic Abnormalities in Fanconi Anemia: An International Fanconi Anemia Registry Study,” *Blood*, vol. 84, no. 5, pp. 1650–1655, Sep. 1994, doi: 10.1182/BLOOD.V84.5.1650.1650.

[6] A. M. Risitano, S. Marotta, R. Calzone, F. Grimaldi, and A. Zatterale, “Twenty years of the Italian Fanconi Anemia Registry: Where we stand and what remains to be learned,” *Haematologica*, vol. 101, no. 3, pp. 319–327, 2016, doi: 10.3324/haematol.2015.133520.

[7] D. I. Kutler *et al.*, “A 20-year perspective on the International Fanconi Anemia Registry (IFAR),” *Blood*, vol. 101, no. 4, pp. 1249–1256, Feb. 2003, doi: 10.1182/BLOOD-2002-07-2170.

[8] P. Río, S. Navarro, and J. A. Bueren, “From the Molecular Biology to the Gene Therapy of a DNA Repair Syndrome: Fanconi Anemia,” in *DNA Repair and Human Health*, InTech, 2011, pp. 349–372. [Online]. Available: www.intechopen.com

[9] P. S. Rosenberg, H. Tamary, and B. P. Alter, “How high are carrier frequencies of rare recessive syndromes? Contemporary estimates for Fanconi Anemia in the United States and Israel,” *Am J Med Genet A*, vol. 155, no. 8, pp. 1877–1883, Aug. 2011, doi: 10.1002/ajmg.a.34087.

[10] A. Hernández-Martínez, “Fanconi Anemia. Adult Head and Neck Cancer and Hematopoietic Mosaicism,” *Medicina Interna de Mexico*, vol. 34, no. 5, pp. 730–734, 2018, doi: 10.24245/mim.v34i5.1836.

[11] M. Grompe and A. D’Andrea, “Fanconi anemia and DNA repair.,” *Hum Mol Genet*, vol. 10, no. 20, pp. 2253–9, Oct. 2001, doi: 10.1093/hmg/10.20.2253.

[12] B. García De Teresa, A. Rodríguez, and S. Frias, “Chromosome instability in fanconi anemia: From breaks to phenotypic consequences,” *Genes (Basel)*, vol. 11, no. 1528, pp. 1–35, Dec. 2020, doi: 10.3390/genes11121528.

[13] A. T. Wang and A. Smogorzewska, “SnapShot: Fanconi anemia and associated proteins,” *Cell*, vol. 160, no. 1–2, pp. 354-354.e1, Jan. 2015, doi: 10.1016/J.CELL.2014.12.031.

[14] Fanconi Anemia Research Fund (FARF), “Fanconi Anemia: Guidelines for Diagnosis and Management,” no. 4th edition. 2014. [Online]. Available: https://www.fanconi.org/

[15] J. Bhandari, P. K. Thada, and Y. Puckett, “Fanconi Anemia,” *StatPearls Publishing*, Nov. 2021.

[16] D. C. Kimble *et al.*, “A comprehensive approach to identification of pathogenic FANCA variants in Fanconi anemia patients and their families,” *Hum Mutat*, vol. 39, no. 2, pp. 237–254, Feb. 2018, doi: 10.1002/HUMU.23366.

[17] J. A. Casado *et al.*, “A comprehensive strategy for the subtyping of patients with Fanconi anaemia: conclusions from the Spanish Fanconi Anemia Research Network,” *J Med Genet*, vol. 44, no. 4, pp. 241–249, Apr. 2007, doi: 10.1136/JMG.2006.044719.

[18] A. R. Meetei *et al.*, “X-linked inheritance of Fanconi anemia complementation group B,” *Nature Genetics 2004 36:11*, vol. 36, no. 11, pp. 1219–1224, Oct. 2004, doi: 10.1038/ng1458.

[19] A. T. Wang *et al.*, “A Dominant Mutation in Human RAD51 Reveals Its Function in DNA Interstrand Crosslink Repair Independent of Homologous Recombination,” *Mol Cell*, vol. 59, no. 3, pp. 478–490, Aug. 2015, doi: 10.1016/j.molcel.2015.07.009.

[20] J. Niraj, A. Färkkilä, and A. D. D’Andrea, “The Fanconi Anemia Pathway in Cancer,” *https://doi.org/10.1146/annurev-cancerbio-030617-050422*, vol. 3, no. 1, pp. 457–478, Mar. 2019, doi: 10.1146/ANNUREV-CANCERBIO-030617-050422.

[21] A. D. D’Andrea and M. Grompe, “The Fanconi anaemia/BRCA pathway,” *Nature Reviews Cancer 2003 3:1*, vol. 3, no. 1, pp. 23–34, Jan. 2003, doi: 10.1038/nrc970.

[22] V. Krishnan, L. S. Tay, and Y. Ito, “The Fanconi Anemia Pathway of DNA Repair and Human Cancer,” in *Advances in DNA Repair*, InTech, 2015, pp. 255–289. doi: 10.5772/59995.

[23] A. J. Deans and S. C. West, “DNA interstrand crosslink repair and cancer,” *Nat Rev Cancer*, vol. 11, no. 7, p. 467, Jul. 2011, doi: 10.1038/NRC3088.

[24] R. Che, J. Zhang, M. Nepal, B. Han, and P. Fei, “Multifaceted Fanconi Anemia Signaling,” *Trends in Genetics*, vol. 34, no. 3, pp. 171–183, Mar. 2018, doi: 10.1016/j.tig.2017.11.006.

[25] E. Gluckman and J. E. Wagner, “Hematopoietic stem cell transplantation in childhood inherited bone marrow failure syndrome,” *Bone Marrow Transplantation 2008 41:2*, vol. 41, no. 2, pp. 127–132, Dec. 2007, doi: 10.1038/sj.bmt.1705960.

[26] P. A. Mehta and C. Ebens, *Fanconi Anemia*, vol. updated in 2021. 1993. [Online]. Available: http://www.ncbi.nlm.nih.gov/pubmed/20598602

[27] Q. S. Zhang *et al.*, “Oxymetholone therapy of fanconi anemia suppresses osteopontin transcription and induces hematopoietic stem cell cycling,” *Stem Cell Reports*, vol. 4, no. 1, pp. 90–102, Jan. 2015, doi: 10.1016/j.stemcr.2014.10.014.

[28] P. A. Mehta *et al.*, “Quercetin: A Novel Targeted Chemoprevention for Patients with Fanconi Anemia (FA),” *Blood*, vol. 130, no. Supplement 1, pp. 1178–1178, Dec. 2017, doi: 10.1182/BLOOD.V130.SUPPL_1.1178.1178.

[29] J. Adair, J. Sevilla, C. Heredia, P. Becker, H.-P. Kiem, and J. Bueren, “Lessons Learned from Two Decades of Clinical Trial Experience in Gene Therapy for Fanconi Anemia,” *Curr Gene Ther*, vol. 16, no. 5, pp. 338–348, Feb. 2017, doi: 10.2174/1566523217666170119113029.

[30] F. J. Román-Rodríguez *et al.*, “NHEJ-Mediated Repair of CRISPR-Cas9-Induced DNA Breaks Efficiently Corrects Mutations in HSPCs from Patients with Fanconi Anemia,” *Cell Stem Cell*, vol. 25, no. 5, pp. 607-621.e7, Nov. 2019, doi: 10.1016/j.stem.2019.08.016.

[31] H. Montanuy *et al.*, “Gefitinib and afatinib show potential efficacy for fanconi anemia-related head and neck cancer,” *Clinical Cancer Research*, vol. 26, no. 12, pp. 3044–3057, 2020, doi: 10.1158/1078-0432.CCR-19-1625.

[32] S. Ravera, C. Dufour, P. Degan, and E. Cappelli, “Fanconi anemia: From DNA repair to metabolism,” *European Journal of Human Genetics*, vol. 26, no. 4. Nature Publishing Group, pp. 475–476, Apr. 01, 2018. doi: 10.1038/s41431-017-0046-6.

[33] D. L. Nelson and M. M. Cox, *Lehninger Principle of Biochemistry*, 7th ed., vol. 7th edition. W H Freeman & Co, 2017.

[34] P. D. Boyer, “A Research Journey with ATP Synthase,” *Journal of Biological Chemistry*, vol. 277, no. 42, pp. 39045–39061, Oct. 2002, doi: 10.1074/jbc.X200001200.

[35] P. C. Hinkle, “P/O ratios of mitochondrial oxidative phosphorylation,” *Biochim Biophys Acta Bioenerg*, vol. 1706, pp. 1–11, Jan. 2005, doi: 10.1016/j.bbabio.2004.09.004.

[36] S. Ravera *et al.*, “Mitochondrial respiratory Complex I defects in Fanconi anemia,” *Biochimie*, vol. 95, no. 10, pp. 1828–1837, Oct. 2013, doi: 10.1016/j.biochi.2013.06.006.

[37] E. Cappelli *et al.*, “Mitochondrial respiratory complex I defects in Fanconi anemia,” *Trends Mol Med*, vol. 19, no. 9, pp. 513–514, Sep. 2013, doi: 10.1016/j.molmed.2013.07.008.

[38] D. G. Nicholls, “Mitochondrial proton leaks and uncoupling proteins,” *Biochim Biophys Acta Bioenerg*, vol. 1862, no. 7, Jul. 2021, doi: 10.1016/J.BBABIO.2021.148428.

[39] M. Klingenberg, “UCP1 - A sophisticated energy valve,” *Biochimie*, vol. 134, pp. 19–27, Mar. 2017, doi: 10.1016/J.BIOCHI.2016.10.012.

[40] D. T. Hass and C. J. Barnstable, “Uncoupling proteins in the mitochondrial defense against oxidative stress,” *Prog Retin Eye Res*, vol. 83, Jul. 2021, doi: 10.1016/J.PRETEYERES.2021.100941.

[41] J. Hirschenson, E. Melgar-Bermudez, and R. J. Mailloux, “The Uncoupling Proteins: A Systematic Review on the Mechanism Used in the Prevention of Oxidative Stress,” *Antioxidants (Basel)*, vol. 11, no. 2, Feb. 2022, doi: 10.3390/ANTIOX11020322.

[42] A. Ardalan, M. D. Smith, and M. Jelokhani-Niaraki, “Uncoupling Proteins and Regulated Proton Leak in Mitochondria,” *Int J Mol Sci*, vol. 23, no. 3, Feb. 2022, doi: 10.3390/IJMS23031528.

[43] G. Baffy, “Uncoupling protein-2 and cancer,” *Mitochondrion*, vol. 10, no. 3, pp. 243–252, Apr. 2010, doi: 10.1016/J.MITO.2009.12.143.

[44] A. Sreedhar *et al.*, “UCP2 Overexpression Redirects Glucose into Anabolic Metabolic Pathways,” *Proteomics*, vol. 19, no. 4, Feb. 2019, doi: 10.1002/PMIC.201800353.

[45] A. Luby and M. C. Alves-Guerra, “UCP2 as a Cancer Target through Energy Metabolism and Oxidative Stress Control,” *International Journal of Molecular Sciences 2022, Vol. 23, Page 15077*, vol. 23, no. 23, p. 15077, Dec. 2022, doi: 10.3390/IJMS232315077.

[46] M. Giacomello, A. Pyakurel, C. Glytsou, and L. Scorrano, “The cell biology of mitochondrial membrane dynamics,” *Nat Rev Mol Cell Biol*, vol. 21, no. 4, pp. 204–224, Apr. 2020, doi: 10.1038/s41580-020-0210-7.

[47] R. Quintana-Cabrera and L. Scorrano, “Determinants and outcomes of mitochondrial dynamics,” *Mol Cell*, vol. 83, no. 6, pp. 857–876, Mar. 2023, doi: 10.1016/J.MOLCEL.2023.02.012.

[48] S.-M. Yoo and Y.-K. Jung, “A Molecular Approach to Mitophagy and Mitochondrial Dynamics,” *Mol. Cells*, vol. 41, no. 1, pp. 18–26, 2018, doi: 10.14348/molcells.2018.2277.

[49] N. M. B. Yapa, V. Lisnyak, B. Reljic, and M. T. Ryan, “Mitochondrial dynamics in health and disease,” *FEBS Lett*, vol. 595, no. 8, pp. 1184–1204, Apr. 2021, doi: 10.1002/1873-3468.14077.

[50] D. C. Chan, “Mitochondrial Dynamics and Its Involvement in Disease,” *Annu. Rev. Pathol. Mech. Dis. 2020*, vol. 15, pp. 235–259, 2019, doi: 10.1146/annurev-pathmechdis.

[51] T. Wai and T. Langer, “Mitochondrial Dynamics and Metabolic Regulation,” *Trends in Endocrinology and Metabolism*, vol. 27, no. 2, pp. 105–117, Feb. 2016, doi: 10.1016/j.tem.2015.12.001.

[52] E. Zacharioudakis and E. Gavathiotis, “Mitochondrial dynamics proteins as emerging drug targets,” *Trends Pharmacol Sci*, vol. 44, no. 2, pp. 112–127, Feb. 2023, doi: 10.1016/j.tips.2022.11.004.

[53] B. N. Whitley, E. A. Engelhart, and S. Hoppins, “Mitochondrial dynamics and their potential as a therapeutic target,” *Mitochondrion*, vol. 49, pp. 269–283, Nov. 2019, doi: 10.1016/j.mito.2019.06.002.

[54] G. Twig *et al.*, “Fission and selective fusion govern mitochondrial segregation and elimination by autophagy,” *EMBO J*, vol. 27, no. 2, pp. 433–446, Jan. 2008, doi: 10.1038/sj.emboj.7601963.

[55] D. Glick, S. Barth, and K. F. Macleod, “Autophagy: cellular and molecular mechanisms,” *J Pathol*, vol. 221, no. 1, pp. 3–12, May 2010, doi: 10.1002/PATH.2697.

[56] K. Prerna and V. K. Dubey, “Beclin1-mediated interplay between autophagy and apoptosis: New understanding,” *Int J Biol Macromol*, vol. 204, pp. 258–273, Apr. 2022, doi: 10.1016/j.ijbiomac.2022.02.005.

[57] E. Wirawan *et al.*, “Beclin1: A role in membrane dynamics and beyond,” *Autophagy*, vol. 8, no. 1, pp. 6–17, Jan. 2012, doi: 10.4161/auto.8.1.16645.

[58] I. Tanida, T. Ueno, and E. Kominami, “LC3 and Autophagy,” 2008, pp. 77–88. doi: 10.1007/978-1-59745-157-4_4.

[59] D. Glick, S. Barth, and K. F. Macleod, “Autophagy: Cellular and molecular mechanisms,” *Journal of Pathology*, vol. 221, no. 1, pp. 3–12, 2010, doi: 10.1002/path.2697.

[60] K. R. Parzych and D. J. Klionsky, “An Overview of Autophagy: Morphology, Mechanism, and Regulation,” *Antioxid Redox Signal*, vol. 20, no. 3, p. 460, Jan. 2014, doi: 10.1089/ARS.2013.5371.

[61] J. Yang, R. Zhou, and Z. Ma, “Autophagy and Energy Metabolism,” *Adv Exp Med Biol*, vol. 1206, pp. 329–357, 2019, doi: 10.1007/978-981-15-0602-4_16.

[62] K. H. Kim and M. S. Lee, “Autophagy--a key player in cellular and body metabolism,” *Nat Rev Endocrinol*, vol. 10, no. 6, pp. 322–337, 2014, doi: 10.1038/NRENDO.2014.35.

[63] E. White, E. C. Lattime, and J. Y. Guo, “Autophagy Regulates Stress Responses, Metabolism, and Anticancer Immunity,” *Trends Cancer*, vol. 7, no. 8, pp. 778–789, Aug. 2021, doi: 10.1016/J.TRECAN.2021.05.003.

[64] S. Saha, D. P. Panigrahi, S. Patil, and S. K. Bhutia, “Autophagy in health and disease: A comprehensive review,” *Biomed Pharmacother*, vol. 104, pp. 485–495, Aug. 2018, doi: 10.1016/J.BIOPHA.2018.05.007.

[65] A. M. K. Choi, S. W. Ryter, and B. Levine, “Autophagy in human health and disease,” *N Engl J Med*, vol. 368, no. 7, pp. 651–662, Feb. 2013, doi: 10.1056/NEJMRA1205406.

[66] M. Onishi, K. Yamano, M. Sato, N. Matsuda, and K. Okamoto, “Molecular mechanisms and physiological functions of mitophagy,” *EMBO J*, vol. 40, no. 3, Feb. 2021, doi: 10.15252/EMBJ.2020104705.

[67] A. Eiyama and K. Okamoto, “PINK1/Parkin-mediated mitophagy in mammalian cells,” *Curr Opin Cell Biol*, vol. 33, pp. 95–101, 2015, doi: 10.1016/j.ceb.2015.01.002.

[68] D. L. Nelson and M. M. Cox, *Lehninger Principle of Biochemistry*, 7th edition. New York: W. H. Freeman and Company, 2017.

[69] N. Bertola, P. Degan, E. Cappelli, and S. Ravera, “Mutated FANCA Gene Role in the Modulation of Energy Metabolism and Mitochondrial Dynamics in Head and Neck Squamous Cell Carcinoma,” *Cells*, vol. 11, no. 15, 2022, doi: 10.3390/cells11152353.

[70] I. Martínez-Reyes and N. S. Chandel, “Cancer metabolism: looking forward,” *Nat Rev Cancer*, vol. 21, no. 10, pp. 669–680, Oct. 2021, doi: 10.1038/S41568-021-00378-6.

[71] S. S. Mukhopadhyay, K. S. Leung, M. J. Hicks, P. J. Hastings, H. Youssoufian, and S. E. Plon, “Defective mitochondrial peroxiredoxin-3 results in sensitivity to oxidative stress in Fanconi anemia,” *J Cell Biol*, vol. 175, no. 2, pp. 225–235, Oct. 2006, doi: 10.1083/jcb.200607061.

[72] C. B. Jagadeesh K *et al.*, “Loss of Mitochondrial Localization of Human FANCG Causes Defective FANCJ Helicase,” *Mol Cell Biol*, vol. 40, no. 23, Nov. 2020, doi: 10.1128/MCB.00306-20.

[73] P. Fernandes *et al.*, “FANCD2 modulates the mitochondrial stress response to prevent common fragile site instability,” *Commun Biol*, vol. 4, no. 1, p. 127, Jan. 2021, doi: 10.1038/s42003-021-01647-8.

[74] F. Langevin, G. P. Crossan, I. V. Rosado, M. J. Arends, and K. J. Patel, “Fancd2 counteracts the toxic effects of naturally produced aldehydes in mice,” *Nature*, vol. 475, no. 7354, pp. 53–58, Jul. 2011, doi: 10.1038/nature10192.

[75] A. Solanki, A. Rajendran, S. Mohan, R. Raj, and B. R. Vundinti, “Mitochondrial DNA variations and mitochondrial dysfunction in Fanconi anemia,” *PLoS One*, vol. 15, no. 1, p. e0227603, Jan. 2020, doi: 10.1371/journal.pone.0227603.

[76] D. L. Longo and L. Q. M. Chow, “Head and Neck Cancer,” *New England Journal of Medicine*, vol. 382, no. 1, pp. 60–72, Jan. 2020, doi: 10.1056/NEJMRA1715715.

[77] C. R. Leemans, B. J. M. Braakhuis, and R. H. Brakenhoff, “The molecular biology of head and neck cancer,” *Nat Rev Cancer*, vol. 11, no. 1, pp. 9–22, Jan. 2011, doi: 10.1038/nrc2982.

[78] M. Hashibe *et al.*, “Alcohol Drinking in Never Users of Tobacco, Cigarette Smoking in Never Drinkers, and the Risk of Head and Neck Cancer: Pooled Analysis in the International Head and Neck Cancer Epidemiology Consortium,” *JNCI: Journal of the National Cancer Institute*, vol. 99, no. 10, pp. 777–789, May 2007, doi: 10.1093/JNCI/DJK179.

[79] M. L. Gillison *et al.*, “Distinct Risk Factor Profiles for Human Papillomavirus Type 16–Positive and Human Papillomavirus Type 16–Negative Head and Neck Cancers,” *JNCI: Journal of the National Cancer Institute*, vol. 100, no. 6, pp. 407–420, Mar. 2008, doi: 10.1093/JNCI/DJN025.

[80] D. E. Johnson, B. Burtness, C. R. Leemans, V. W. Y. Lui, J. E. Bauman, and J. R. Grandis, “Head and neck squamous cell carcinoma,” *Nature Reviews Disease Primers*, vol. 6, no. 92. 2020. doi: 10.1038/s41572-020-00224-3.

[81] K. Sakamoto *et al.*, “Down-regulation of keratin 4 and keratin 13 expression in oral squamous cell carcinoma and epithelial dysplasia: a clue for histopathogenesis,” *Histopathology*, vol. 58, no. 4, pp. 531–542, Mar. 2011, doi: 10.1111/j.1365-2559.2011.03759.x.

[82] C. H. Chung *et al.*, “Molecular classification of head and neck squamous cell carcinomas using patterns of gene expression,” *Cancer Cell*, vol. 5, no. 5, pp. 489–500, May 2004, doi: 10.1016/S1535-6108(04)00112-6.

[83] A. Buitrago-Perez, G. Garaulet, A. Vazquez-Carballo, J. Paramio, and R. Garcia-Escudero, “Molecular Signature of HPV-Induced Carcinogenesis: pRb, p53 and Gene Expression Profiling,” *Curr Genomics*, vol. 10, no. 1, pp. 26–34, Mar. 2009, doi: 10.2174/138920209787581235.

[84] Á. Buitrago-Pérez *et al.*, “A Humanized Mouse Model of HPV-Associated Pathology Driven by E7 Expression,” *PLoS One*, vol. 7, no. 7, p. e41743, Jul. 2012, doi: 10.1371/journal.pone.0041743.

[85] J. W. Park *et al.*, “Deficiencies in the Fanconi Anemia DNA Damage Response Pathway Increase Sensitivity to HPV-Associated Head and Neck Cancer,” *Cancer Res*, vol. 70, no. 23, pp. 9959–9968, Dec. 2010, doi: 10.1158/0008-5472.CAN-10-1291.

[86] S. Partlová *et al.*, “Distinct patterns of intratumoral immune cell infiltrates in patients with HPV-associated compared to non-virally induced head and neck squamous cell carcinoma,” *Oncoimmunology*, vol. 4, no. 1, p. e965570, Jan. 2015, doi: 10.4161/21624011.2014.965570.

[87] M. A. Gingerich *et al.*, “Comprehensive review of genetic factors contributing to head and neck squamous cell carcinoma development in low-risk, nontraditional patients,” *Head Neck*, vol. 40, no. 5, pp. 943–954, May 2018, doi: 10.1002/hed.25057.

[88] B. Peltanova, M. Raudenska, and M. Masarik, “Effect of tumor microenvironment on pathogenesis of the head and neck squamous cell carcinoma: a systematic review,” *Mol Cancer*, vol. 18, no. 1, p. 63, Dec. 2019, doi: 10.1186/s12943-019-0983-5.

[89] E. Muraro *et al.*, “Cetuximab in locally advanced head and neck squamous cell carcinoma: Biological mechanisms involved in efficacy, toxicity and resistance,” *Crit Rev Oncol Hematol*, vol. 164, p. 103424, Aug. 2021, doi: 10.1016/j.critrevonc.2021.103424.

[90] J. D. Cramer, B. Burtness, and R. L. Ferris, “Immunotherapy for head and neck cancer: Recent advances and future directions,” *Oral Oncol*, vol. 99, p. 104460, Dec. 2019, doi: 10.1016/j.oraloncology.2019.104460.

[91] B. P. Alter, “Cancer in Fanconi anemia, 1927-2001,” *Cancer*, vol. 97, no. 2, pp. 425–440, Jan. 2003, doi: 10.1002/cncr.11046.

[92] C. P. Furquim, A. Pivovar, J. M. Amenábar, C. Bonfim, and C. C. Torres-Pereira, “Oral cancer in Fanconi anemia: Review of 121 cases,” *Crit Rev Oncol Hematol*, vol. 125, no. July 2017, pp. 35–40, 2018, doi: 10.1016/j.critrevonc.2018.02.013.

[93] D. I. Kutler *et al.*, “Natural history and management of Fanconi anemia patients with head and neck cancer: A 10-year follow-up,” *Laryngoscope*, vol. 126, no. 4, pp. 870–879, Apr. 2016, doi: 10.1002/lary.25726.

[94] P. S. Rosenberg, M. H. Greene, and B. P. Alter, “Cancer incidence in persons with Fanconi anemia,” *Blood*, vol. 101, no. 3, pp. 822–826, Feb. 2003, doi: 10.1182/blood-2002-05-1498.

[95] P. S. Rosenberg, B. P. Alter, G. Socié, and E. Gluckman, “Secular trends in outcomes for fanconi anemia patients who receive transplants: Implications for future studies,” *Biology of Blood and Marrow Transplantation*, vol. 11, no. 9, pp. 672–679, Sep. 2005, doi: 10.1016/j.bbmt.2005.05.007.

[96] H. Archibald, K. Kalland, A. Kuehne, F. Ondrey, B. Roby, and L. Jakubowski, “Oral Premalignant and Malignant Lesions in Fanconi Anemia Patients,” *Laryngoscope*, vol. 133, no. 7, pp. 1745–1748, Jul. 2023, doi: 10.1002/lary.30370.

[97] A. L. H. Webster *et al.*, “Genomic signature of Fanconi anaemia DNA repair pathway deficiency in cancer,” *Nature*, vol. 612, no. 7940, pp. 495–502, Dec. 2022, doi: 10.1038/s41586-022-05253-4.

[98] D. I. Kutler *et al.*, “High incidence of head and neck squamous cell carcinoma in patients with Fanconi anemia,” *Archives of Otolaryngology - Head and Neck Surgery*, vol. 129, no. 1. pp. 106–112, 2003. doi: 10.1001/archotol.129.1.106.

[99] T. H. Beckham *et al.*, “Treatment modalities and outcomes of Fanconi anemia patients with head and neck squamous cell carcinoma: Series of 9 cases and review of the literature,” *Head Neck*, vol. 41, no. 5, pp. 1418–1426, May 2019, doi: 10.1002/hed.25577.

[100] R. H. Lee, H. Kang, S. S. Yom, A. Smogorzewska, D. E. Johnson, and J. R. Grandis, “Treatment of Fanconi Anemia–Associated Head and Neck Cancer: Opportunities to Improve Outcomes,” *Clinical Cancer Research*, vol. 27, no. 19, pp. 5168–5187, Oct. 2021, doi: 10.1158/1078-0432.CCR-21-1259.

[101] B. P. Alter, N. Giri, S. A. Savage, W. G. V. Quint, M. N. C. de Koning, and M. Schiffman, “Squamous cell carcinomas in patients with Fanconi anemia and dyskeratosis congenita: A search for human papillomavirus,” *Int J Cancer*, vol. 133, no. 6, pp. 1513–1515, Sep. 2013, doi: 10.1002/ijc.28157.

[102] Q.-S. Zhang *et al.*, “Metformin improves defective hematopoiesis and delays tumor formation in Fanconi anemia mice,” *Blood*, vol. 128, no. 24, pp. 2774–2784, Dec. 2016, doi: 10.1182/blood-2015-11-683490.

[103] M. R. Owen, E. Doran, and A. P. Halestrap, “Evidence that metformin exerts its anti-diabetic effects through inhibition of complex 1 of the mitochondrial respiratory chain.,” *Biochem J*, vol. 348 Pt 3, pp. 607–614, 2000, doi: 10.1042/0264-6021:3480607.

[104] S. Ravera *et al.*, “808-nm photobiomodulation affects the viability of a head and neck squamous carcinoma cellular model, acting on energy metabolism and oxidative stress production,” *Biomedicines*, vol. 9, no. 11, Nov. 2021, doi: 10.3390/biomedicines9111717.

[105] E. Cappelli *et al.*, “The passage from bone marrow niche to bloodstream triggers the metabolic impairment in Fanconi Anemia mononuclear cells,” *Redox Biol*, vol. 36, no. June, p. 101618, Sep. 2020, doi: 10.1016/j.redox.2020.101618.

[106] X. Qi, N. Qvit, Y. C. Su, and D. Mochly-Rosen, “A novel Drp1 inhibitor diminishes aberrant mitochondrial fission and neurotoxicity,” *J Cell Sci*, vol. 126, no. 3, pp. 789–802, Feb. 2013, doi: 10.1242/jcs.114439.

[107] N. Bertola *et al.*, “Altered Mitochondrial Dynamic in Lymphoblasts and Fibroblasts Mutated for FANCA-A Gene: The Central Role of DRP1,” *Int J Mol Sci*, vol. 24, no. 7, 2023, doi: 10.3390/ijms24076557.

[108] E. Cappelli *et al.*, “A Multidrug Approach to Modulate the Mitochondrial Metabolism Impairment and Relative Oxidative Stress in Fanconi Anemia Complementation Group A,” *Metabolites*, vol. 12, no. 6, 2022.

[109] R. Bottega *et al.*, “Two further patients with Warsaw breakage syndrome. Is a mild phenotype possible?,” *Mol Genet Genomic Med*, vol. 7, no. 5, May 2019, doi: 10.1002/MGG3.639.

[110] S. Bruno *et al.*, “N-(4-hydroxyphenyl)retinamide promotes apoptosis of resting and proliferating B-cell chronic lymphocytic leukemia cells and potentiates fludarabine and ABT-737 cytotoxicity,” *Leukemia*, vol. 26, no. 10, pp. 2260–2268, Oct. 2012, doi: 10.1038/LEU.2012.98.

[111] E. Cappelli *et al.*, “The passage from bone marrow niche to bloodstream triggers the metabolic impairment in Fanconi Anemia mononuclear cells,” *Redox Biol*, vol. 36, p. 101618, Sep. 2020, doi: 10.1016/j.redox.2020.101618.

[112] E. Cappelli *et al.*, “Defects in mitochondrial energetic function compels Fanconi Anaemia cells to glycolytic metabolism,” *Biochim Biophys Acta Mol Basis Dis*, vol. 1863, no. 6, pp. 1214–1221, Jun. 2017, doi: 10.1016/j.bbadis.2017.03.008.

[113] N. M. Vacanti *et al.*, “Regulation of substrate utilization by the mitochondrial pyruvate carrier,” *Mol Cell*, vol. 56, no. 3, pp. 425–435, 2014, doi: 10.1016/j.molcel.2014.09.024.

[114] R. S. O’Connor *et al.*, “The CPT1a inhibitor, etomoxir induces severe oxidative stress at commonly used concentrations,” *Sci Rep*, vol. 8, no. 1, Dec. 2018, doi: 10.1038/S41598-018-24676-6.

[115] Y. Zhong *et al.*, “Application of mitochondrial pyruvate carrier blocker UK5099 creates metabolic reprogram and greater stem-like properties in LnCap prostate cancer cells in vitro,” *Oncotarget*, vol. 6, no. 35, pp. 37758–37769, 2015, doi: 10.18632/ONCOTARGET.5386.

[116] S. C. Chandrasekharappa *et al.*, “Assessing the Spectrum of Germline Variation in Fanconi Anemia Genes among Patients with Head and Neck Carcinoma before Age 50 Settara,” *Cancer*, vol. 123, no. 20, pp. 3943–3954, Oct. 2017, doi: 10.1002/cncr.30802. Assessing.

[117] M. Columbaro *et al.*, “Treatment of FANCA cells with resveratrol and N-acetylcysteine: A comparative study,” *PLoS One*, vol. 9, no. 8, pp. 1–7, Aug. 2014, doi: 10.1371/journal.pone.0104857.

[118] G. López-Doménech *et al.*, “Miro proteins coordinate microtubule- and actin-dependent mitochondrial transport and distribution,” *EMBO J*, vol. 37, no. 3, pp. 321–336, Feb. 2018, doi: 10.15252/EMBJ.201696380.

[119] M. M. Bradford, “A rapid and sensitive method for the quantitation of microgram quantities of protein utilizing the principle of protein-dye binding,” *Anal Biochem*, vol. 72, no. 1–2, pp. 248–254, May 1976, doi: 10.1016/0003-2697(76)90527-3.

[120] S. Ravera *et al.*, “Sclareol modulates free radical production in the retinal rod outer segment by inhibiting the ectopic f1fo-atp synthase,” *Free Radic Biol Med*, vol. 160, pp. 368–375, Nov. 2020, doi: 10.1016/J.FREERADBIOMED.2020.08.014.

[121] A. Miceli *et al.*, “18F-fluorodeoxyglucose positron emission tomography tracks the heterogeneous brain susceptibility to the hyperglycemia-related redox stress,” *Int J Mol Sci*, vol. 21, no. 8154, pp. 1–14, Nov. 2020, doi: 10.3390/ijms21218154.

[122] H. oki Iwakawa and Y. Tomari, “The Functions of MicroRNAs: mRNA Decay and Translational Repression,” *Trends Cell Biol*, vol. 25, no. 11, pp. 651–665, Nov. 2015, doi: 10.1016/J.TCB.2015.07.011.

[123] Z. Ali Syeda, S. S. S. Langden, C. Munkhzul, M. Lee, and S. J. Song, “Regulatory Mechanism of MicroRNA Expression in Cancer,” *Int J Mol Sci*, vol. 21, no. 5, p. 1723, Mar. 2020, doi: 10.3390/ijms21051723.

[124] A. Vishnoi and S. Rani, “miRNA Biogenesis and Regulation of Diseases: An Updated Overview,” in *Methods in Molecular Biology*, vol. 2595, J. M. Walker, Ed., Springer, 2023. doi: 10.1007/978-1-0716-2823-2_1.

[125] P. Degan *et al.*, “A Global MicroRNA Profile in Fanconi Anemia: A Pilot Study,” *Metab Syndr Relat Disord*, vol. 17, no. 1, pp. 53–59, Feb. 2019, doi: 10.1089/met.2018.0085.

[126] A. S. Nelson and K. C. Myers, “Diagnosis, Treatment, and Molecular Pathology of Shwachman-Diamond Syndrome,” *Hematol Oncol Clin North Am*, vol. 32, no. 4, pp. 687–700, Aug. 2018, doi: 10.1016/J.HOC.2018.04.006.

[127] S. Ravera *et al.*, “Evaluation of energy metabolism and calcium homeostasis in cells affected by Shwachman-Diamond syndrome,” *Sci Rep*, vol. 6, no. May, pp. 1–12, May 2016, doi: 10.1038/srep25441.

[128] M. Grompe and A. D’Andrea, “Fanconi anemia and DNA repair,” *Hum Mol Genet*, vol. 10, no. 20, pp. 2253–2259, Oct. 2001, doi: 10.1093/hmg/10.20.2253.

[129] L. long Xie, F. Shi, Z. Tan, Y. Li, A. M. Bode, and Y. Cao, “Mitochondrial network structure homeostasis and cell death,” *Cancer Sci*, vol. 109, no. 12, pp. 3686–3694, 2018, doi: 10.1111/cas.13830.

[130] A. Lyakhovich, “Damaged mitochondria and overproduction of ROS in Fanconi anemia cells,” *Rare Diseases*, vol. 1, no. 1, p. e24048, Jan. 2013, doi: 10.4161/rdis.24048.

[131] A. M. Pisoschi and A. Pop, “The role of antioxidants in the chemistry of oxidative stress: A review,” *Eur J Med Chem*, vol. 97, pp. 55–74, Apr. 2015, doi: 10.1016/J.EJMECH.2015.04.040.

[132] F. Kocabas *et al.*, “Hypoxic metabolism in human hematopoietic stem cells,” *Cell Biosci*, vol. 5, no. 1, Jul. 2015, doi: 10.1186/S13578-015-0020-3.

[133] M. D. Filippi and S. Ghaffari, “Mitochondria in the maintenance of hematopoietic stem cells: new perspectives and opportunities,” *Blood*, vol. 133, no. 18, pp. 1943–1952, May 2019, doi: 10.1182/BLOOD-2018-10-808873.

[134] C. S. Palmer, L. D. Osellame, D. Stojanovski, and M. T. Ryan, “The regulation of mitochondrial morphology: intricate mechanisms and dynamic machinery.,” *Cell Signal*, vol. 23, no. 10, pp. 1534–1545, 2011, doi: 10.1016/j.cellsig.2011.05.021.

[135] B. Westermann, “Mitochondrial fusion and fission in cell life and death,” *Nat Rev Mol Cell Biol*, vol. 11, no. 12, pp. 872–884, 2010, doi: 10.1038/nrm3013.

[136] D. C. Chan, “Dissecting mitochondrial fusion,” *Dev Cell*, vol. 11, no. 5, pp. 592–594, 2006, [Online]. Available: http://www.ncbi.nlm.nih.gov/entrez/query.fcgi?cmd=Retrieve&db=PubMed&dopt=Citation&list_uids=17084350

[137] G. Twig *et al.*, “Fission and selective fusion govern mitochondrial segregation and elimination by autophagy.,” *EMBO J*, vol. 27, no. 2, pp. 433–446, 2008, doi: 10.1038/sj.emboj.7601963.

[138] S. Ravera *et al.*, “Mesenchymal stem cells from preterm to term newborns undergo a significant switch from anaerobic glycolysis to the oxidative phosphorylation,” *Cellular and Molecular Life Sciences*, vol. 75, no. 5, 2018, doi: 10.1007/s00018-017-2665-z.

[139] H. M. Ni, J. A. Williams, and W. X. Ding, “Mitochondrial dynamics and mitochondrial quality control,” *Redox Biol*, vol. 4, pp. 6–13, Apr. 2015, doi: 10.1016/J.REDOX.2014.11.006.

[140] P. Shyamsunder *et al.*, “Impaired mitophagy in Fanconi anemia is dependent on mitochondrial fission,” *Oncotarget*, vol. 7, no. 36, pp. 58065–58074, 2016, doi: 10.18632/oncotarget.11161.

[141] M. R. de Oliveira, S. M. Nabavi, N. Braidy, W. N. Setzer, T. Ahmed, and S. F. Nabavi, “Quercetin and the mitochondria: A mechanistic view,” *Biotechnol Adv*, vol. 34, no. 5, pp. 532–549, Sep. 2016, doi: 10.1016/J.BIOTECHADV.2015.12.014.

[142] D. Benjamin, M. Colombi, C. Moroni, and M. N. Hall, “Rapamycin passes the torch: a new generation of mTOR inhibitors,” *Nat Rev Drug Discov*, vol. 10, no. 11, pp. 868–880, Nov. 2011, doi: 10.1038/NRD3531.

[143] M. Morita *et al.*, “mTOR coordinates protein synthesis, mitochondrial activity and proliferation,” *Cell Cycle*, vol. 14, no. 4, pp. 473–480, Feb. 2015, doi: 10.4161/15384101.2014.991572.

[144] E. Abad *et al.*, “Identification of metabolic changes leading to cancer susceptibility in Fanconi anemia cells,” *Cancer Lett*, vol. 503, pp. 185–196, Apr. 2021, doi: 10.1016/J.CANLET.2020.12.010.

[145] N. Bertola *et al.*, “Effects of Deacetylase Inhibition on the Activation of the Antioxidant Response and Aerobic Metabolism in Cellular Models of Fanconi Anemia,” *Antioxidants*, vol. 12, no. 5, 2023, doi: 10.3390/antiox12051100.

[146] L. Verdone, M. Caserta, and E. Di Mauro, “Role of histone acetylation in the control of gene expression,” *Biochem Cell Biol*, vol. 83, no. 3, pp. 344–353, Jun. 2005, doi: 10.1139/O05-041.

[147] N. Gurvich, O. M. Tsygankova, J. L. Meinkoth, and P. S. Klein, “Histone deacetylase is a target of valproic acid-mediated cellular differentiation,” *Cancer Res*, vol. 64, no. 3, pp. 1079–1086, Feb. 2004, doi: 10.1158/0008-5472.CAN-03-0799.

[148] T. Shimazu *et al.*, “Suppression of oxidative stress by β-hydroxybutyrate, an endogenous histone deacetylase inhibitor,” *Science*, vol. 339, no. 6116, pp. 211–214, Jan. 2013, doi: 10.1126/SCIENCE.1227166.

[149] S. Broussy, H. Laaroussi, and M. Vidal, “Biochemical mechanism and biological effects of the inhibition of silent information regulator 1 (SIRT1) by EX-527 (SEN0014196 or selisistat),” *J Enzyme Inhib Med Chem*, vol. 35, no. 1, pp. 1124–1136, Jan. 2020, doi: 10.1080/14756366.2020.1758691.

[150] L. T. Dalgaard, A. E. Sørensen, A. A. Hardikar, and M. V. Joglekar, “The microRNA-29 family: role in metabolism and metabolic disease,” *Am J Physiol Cell Physiol*, vol. 323, no. 2, pp. C367–C377, Aug. 2022, doi: 10.1152/AJPCELL.00051.2022.

[151] T. Otsuki *et al.*, “Phosphorylation of Fanconi anemia protein, FANCA, is regulated by Akt kinase,” *Biochem Biophys Res Commun*, vol. 291, no. 3, pp. 628–634, 2002, doi: 10.1006/bbrc.2002.6504.

[152] C. Betz, D. Stracka, C. Prescianotto-Baschong, M. Frieden, N. Demaurex, and M. N. Hall, “Feature Article: mTOR complex 2-Akt signaling at mitochondria-associated endoplasmic reticulum membranes (MAM) regulates mitochondrial physiology.,”

*Proc Natl Acad Sci U S A*, vol. 110, no. 31, pp. 12526–12534, 2013, doi: 10.1073/pnas.1302455110.

[153] Z. Cheng, "FoxO transcription factors in mitochondrial homeostasis," *Biochemical Journal*, vol. 479, no. 4, pp. 525–536, Feb. 2022, doi: 10.1042/BCJ20210777.

[154] W. Du, O. Erden, and Q. Pang, "TNF-α signaling in Fanconi anemia," *Blood Cells Mol Dis*, vol. 52, no. 1, pp. 2–11, Jan. 2014, doi: 10.1016/J.BCMD.2013.06.005.

[155] H. Tummala and I. Dokal, "TGF-β Pathway Inhibition Signals New Hope for Fanconi Anemia," *Cell Stem Cell*, vol. 18, no. 5, pp. 567–568, May 2016, doi: 10.1016/J.STEM.2016.04.008.

[156] P. Río and J. A. Bueren, "TGF-β: a master regulator of the bone marrow failure puzzle in Fanconi anemia," *Stem Cell Investig*, vol. 3, no. NOV, Nov. 2016, doi: 10.21037/SCI.2016.09.17.

[157] K. Minton, "Inflammation: Inflammatory pathology of Fanconi anaemia," *Nat Rev Immunol*, vol. 16, no. 6, p. 336, Jun. 2016, doi: 10.1038/NRI.2016.60.

[158] G. C. Bagby, "Multifunctional Fanconi proteins, inflammation and the Fanconi phenotype," *EBioMedicine*, vol. 8, pp. 10–11, Jun. 2016, doi: 10.1016/J.EBIOM.2016.06.005.

[159] P. S. Rosenberg, G. Socié, B. P. Alter, and E. Gluckman, "Risk of head and neck squamous cell cancer and death in patients with Fanconi anemia who did and did not receive transplants," *Blood*, vol. 105, no. 1, pp. 67–73, Jan. 2005, doi: 10.1182/blood-2004-04-1652.

[160] S. Ravera *et al.*, "Evaluation of energy metabolism and calcium homeostasis in cells affected by Shwachman-Diamond syndrome," *Sci Rep*, vol. 6, May 2016, doi: 10.1038/SREP25441.

[161] C. Sanmartín-Suárez, R. Soto-Otero, I. Sánchez-Sellero, and E. Méndez-Álvarez, "Antioxidant properties of dimethyl sulfoxide and its viability as a solvent in the evaluation of neuroprotective antioxidants," *J Pharmacol Toxicol Methods*, vol. 63, no. 2, pp. 209–215, Mar. 2011, doi: 10.1016/J.VASCN.2010.10.004.

[162] M. Imam, S. Zhang, J. Ma, H. Wang, and F. Wang, "Antioxidants Mediate Both Iron Homeostasis and Oxidative Stress," *Nutrients*, vol. 9, no. 7, p. 671, Jun. 2017, doi: 10.3390/nu9070671.

[163] C. C. Winterbourn, "Toxicity of iron and hydrogen peroxide: the Fenton reaction," *Toxicol Lett*, vol. 82–83, pp. 969–974, Dec. 1995, doi: 10.1016/0378-4274(95)03532-X.

[164] W. H. Koppenol and R. H. Hider, "Iron and redox cycling. Do's and don'ts," *Free Radic Biol Med*, vol. 133, pp. 3–10, Mar. 2019, doi: 10.1016/j.freeradbiomed.2018.09.022.